

Development of an Atmospheric
Transport Model Simulating
Concentration and Deposition of
Reduced Nitrogen over the British Isles



Nicolas Fournier

Doctor of Philosophy
The University of Edinburgh
2002



Acknowledgements

I would like to thank my two excellent supervisors, Dr. Keith Weston and Dr. Mark Sutton. I could not describe briefly the intensity of their support and encouragement.

I would also like to thank people from the Centre of Ecology and Hydrology without whom the development of the model would have not been possible. In particular, Ulli Dragosits for the emissions data, Sim Tang for the measurements, Ron Smith for a wide range of input data and Tony Dore for his warmful and helpful advice. I can not forget too the support I had at the Institute for Meteorology from the italian fellows Vicente Pais and Massimo Vieno in the numerical modelling challenges. In addition, the NEG-TAP report (2001) has been of great help to assess the results of the model. Thanks must also go to the rest of the Institute for Meteorology who provided a nice and supportive atmosphere throughout my PhD.

The same can be said of my climbing partners Alex, Simon and Steve and also of the runners of the University and Carnethy : Keiths, Willie, Peter, James, Graham. My parents have been more than supportive throughout this expatriate experience and last but not least delicious thoughts sparkle in my mind when I think of my beautiful damselfly, Al.

Abstract

Ammonia is the principal atmospheric alkaline gas, emitted mainly from agricultural sources. Once emitted, either it is deposited close to the source, or it reacts with atmospheric acids to form ammonium aerosols, which can be transported over larger distances, before being deposited. This results in ammonia concentrations that are highly spatially variable, making it difficult to produce accurate concentration maps from measurements alone. In order to complement these measurements, numerical models are required. This provides the main impetus for this work, in which an existing atmospheric transport model, FRAME (Fine Resolution AMmonia Exchange), is improved and subsequently used to model the spatial pattern of reduced nitrogen concentrations and deposition over the British Isles.

Firstly, improvement in the model run-time was sought. By developing a parallel implementation using High Performance Fortran, a speed-up by a factor of 69 is achieved on a Cray *T3E* (128 processors). In addition, an alternative diffusion discretisation, the implicit Finite Volume method, is implemented, producing a speed-up of 34. Combined, these two approaches yield a speed-up of

2346. The results of this new version compare well with those of the previously validated sequential code. Secondly, attention is focused on the wet deposition process for reduced nitrogen, a common and recognised weakness of existing UK models. Here, in contrast with previous approaches, the directional orographic enhancement of precipitation and wet deposition from the seeder-feeder effect is investigated and then explicitly taken into account. Furthermore, a more realistic description of the wet deposition parameterisation is developed. Comparison with measurement data shows that these two considerations improve significantly the reduced nitrogen wet deposition results.

These and other developments of the model result in a robust and significantly improved tool for atmospheric reduced nitrogen predictions. Moreover, they provide a foundation for further use of the model in a variety of applications. The model is applied here to consider the transport and deposition of oxidised nitrogen and sulphur, to evaluate regional budgets of reduced nitrogen for the British Isles and to test scenarios for 2010.

Contents

1	Introduction	1
1.1	Ammonia in the atmosphere	4
1.2	Ammonia emissions	7
1.2.1	Ammonia sources	7
1.2.2	A detailed inventory of ammonia sources for UK	8
1.3	Atmospheric transport models	15
1.4	Objectives of this study	17
1.5	Summary	18
2	The FRAME model	20
2.1	Introduction	20
2.2	Components of FRAME	22
2.2.1	Sources and emissions	22
2.2.2	Meteorological input data	26
2.2.3	Diffusion process	28
2.2.4	Removal processes	34
2.2.5	Chemical processes	43

2.2.6	Sensitivity of FRAME to input parameters	45
2.3	Results of FRAME 1.1	47
2.3.1	Uncertainties of the measurement based estimates	48
2.3.2	Atmospheric budgets of N and S calculated with FRAME	
1.1	49
2.3.3	Comparison with measurements	51
2.4	Summary	66
3	Extension of FRAME to the British Isles and development of	
	numerical procedures	72
3.1	Introduction	72
3.2	Domain extension to the British Isles	73
3.2.1	Emissions	73
3.2.2	Boundary conditions	75
3.2.3	Meteorological and other input data	76
3.2.4	Modifications to allow UK budgets from the BI model	78
3.2.5	Results of FRAME 2.0	78
3.2.6	Conclusions	85
3.3	Parallelisation of the FRAME model	87
3.3.1	Optimisation of the code	88
3.3.2	Parallelisation of the code	89
3.3.3	High Performance Fortran	90
3.3.4	Computing platforms	92

3.3.5	Load-balance	93
3.3.6	Results	93
3.3.7	Conclusions regarding the development of a parallel version of FRAME	94
3.4	Numerical discretisation of the vertical diffusion in FRAME . . .	96
3.4.1	Finite Difference Method	97
3.4.2	Finite Element Method	97
3.4.3	Finite Volume Method	99
3.4.4	Results of FRAME 4.0 using the FVM	105
3.4.5	Conclusions regarding the implementation of a FVM in FRAME	108
3.5	Summary of the developments to extend the FRAME domain and improve numerical procedures	108
4	Development of the parameterisation of atmospheric processes in FRAME	110
4.1	Introduction	110
4.2	Parameterisation of wet deposition	111
4.2.1	Precipitation model	112
4.2.2	Application of the model to estimate the directional oro- graphic precipitation	115
4.2.3	Parameterisation of the scavenging coefficients in FRAME	116
4.2.4	Results of FRAME 4.1 with directional orographic rainfall	118

4.2.5	Discussion about the use of directional orographic rainfall in FRAME	122
4.3	Effect of the mixing layer depth on the precipitation scavenging	126
4.3.1	Introduction	126
4.3.2	Result of considering a variable height of the mixing layer	127
4.4	Conclusions concerning the parameterisation of wet deposition in FRAME	131
4.5	Treatment of oxidised nitrogen in FRAME	134
4.5.1	Introduction	134
4.5.2	Deposition velocities	135
4.5.3	NO _x emissions height	139
4.5.4	Conclusions concerning the NO _y treatment in FRAME	142
4.6	Treatment of SO ₂ sources height in FRAME	145
4.6.1	Introduction	145
4.6.2	Accounting for high-level SO ₂ emissions	146
4.6.3	Results of FRAME 4.6 considering high-level sources of SO ₂	147
4.6.4	Conclusions on using SO ₂ point sources in FRAME	152
4.7	Summary of development of the parameterisation of atmospheric processes in FRAME	155
5	Applications of the FRAME model	157
5.1	Introduction	157

5.2	Assessment of regional budgets of reduced nitrogen for the British Isles	158
5.2.1	Method of approach	158
5.2.2	Performance of the FRAME model	159
5.2.3	Regional budgets of reduced nitrogen	165
5.2.4	Conclusions concerning the assessment of regional NH _x budgets	168
5.3	2010 predictions for the UK	170
5.3.1	Introduction	170
5.3.2	2010 emissions	171
5.3.3	Results from FRAME 4.6 with different 2010 scenarios	175
5.3.4	Scenarios for 2010 : conclusions	185
5.4	Applications of FRAME : summary	188
6	Conclusions and Perspectives	190
6.1	Perspectives	194
A	Monitoring Networks	208
B	FRAME Versions	217
C	List of Publications	220

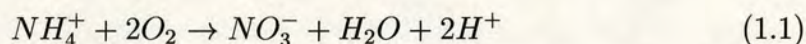
Chapter 1

Introduction

Acidifying and eutrophying pollutants originate from anthropogenic emissions of sulphur dioxide (SO_2), nitrogen oxides (NO_x) and ammonia (NH_3). Most of SO_2 and NO_x is emitted to the atmosphere through the combustion of fossil fuels in electricity generating power stations, industrial plants, residential heating, commercial and service sectors. Road transport, shipping and aircraft are the major sources of NO_x emissions (RGAR, 1997; NEG-TAP, 2001). By contrast, NH_3 emissions are mostly related to agricultural activities such as animal farming, storage of manure, soil fertilisation as well as some non-agricultural sources (Bujisman *et al.*, 1987; Dragosits *et al.*, 1998; Sutton *et al.*, 2000).

When emitted to the atmosphere, acidifying and eutrophying pollutants may remain in air for several days and therefore, be dispersed and carried over long distances by winds. They can be transported across national boundaries and

cause damaging effects far from the source of emission. Acidifying pollutants are removed from the atmosphere by wet deposition ("acid rain") or dry deposition (direct uptake by vegetation and surfaces). Effects of acid deposition are widespread and appear in a number of ways, including e.g. acidification of freshwater systems resulting in the loss of fisheries, impoverishment of soils, damage to forests and vegetation, corrosion of buildings, cultural monuments and materials (Arya, 1999). The gaseous emissions of sulphur and nitrogen are precursors to the formation of small particles (PM_{2.5}) which impact human health (Turpin *et al.*, 2000). Deposition of nitrogen-containing compounds also contributes to the eutrophication ("excess nutrient enrichment") of terrestrial and marine ecosystems (Sutton *et al.*, 1994). The eutrophying effect is associated with changes in the semi-natural ecosystems leading to vegetation changes favouring nitrogen-tolerant species and with increased leaching of nitrogen to ground water, streams and lakes (INDITE, 1994). Although atmospheric ammonia is not an acid, acidification also occurs with biological transformation in the soil or uptake and assimilation by plants (Nihlgard, 1985; Hornung *et al.*, 1995). Indeed, acidification from NH₄⁺ may be important and is caused by the oxidation of NH₄⁺ to NO₃⁻ by micro-organisms :



which can lead to the production of H⁺ and subsequent leaching of the NO₃⁻ by metal cations.

Long-range transport of air pollutants between European countries was recognised as an important ecological and political issue during the late 1960s, and formalised with the 1979 Geneva Convention on Long-range Transboundary Air Pollution (CLRTAP) (Tarrason and Schaug, 1999). The Convention has contributed substantially to the development of international environmental law and has created a framework for reducing the damage to the environment and to human health caused by transboundary air pollution.

The history of the Convention can be traced back to the 1960s, when Oden (1969) demonstrated the interrelationship between sulphur emissions in continental Europe and the acidification of Scandinavian lakes (NPCA, 1999). The 1972 United Nations Conference on the Human Environment in Stockholm was the start for active international cooperation to combat acidification. Between 1972 and 1977 several studies confirmed the hypothesis that air pollutants could travel several thousands of kilometres before deposition and damage occurred (OECD, 1977). This also implied that cooperation at the international level was necessary to solve problems such as acidification. In response to these problems, the CLRTAP was established in 1979 with the signature by 34 Governments and the European Community (EC). The Convention was the first international legally binding instrument to deal with problems of air pollution on a broad regional basis. Apart from laying down the general principles of international cooperation for air pollution abatement, the Convention brings together research and policy. It has been extended by eight protocols, the latest being the 1999 Gothenburg Protocol to

Abate Acidification, Eutrophication and Ground-level Ozone which includes NH_3 in the process of emissions reduction for the first time. As the geographical extent of acidic deposition and the magnitude of its effects became clear, the pressure to introduce control measures increased and led to international agreements to reduce pollutant emissions.

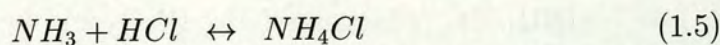
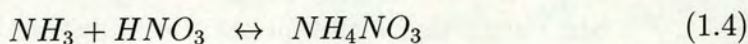
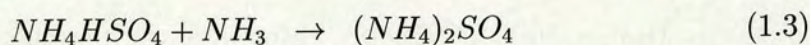
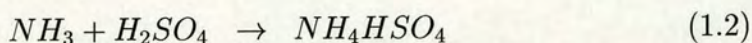
Consistent with the agreed commitments of the CLRTAP protocols, the United Kingdom (UK) emissions of most of the pollutants, including sulphur dioxide (SO_2), the nitrogen oxides (NO_x) and Volatile Organic Compounds (VOC) have declined over the last decade. Annual UK SO_2 emissions decreased from 1900 kt S in 1990 to 800 kt S in 1998. Annual UK NO_x emissions decreased from 850 kt N in 1990 to 530 kt N in 1998. However, among all the pollutants contributing to acidification and eutrophication, ammonia (NH_3) emission has decreased only slightly in the UK between 1990 (300 kt N) and 1998 (290 kt N) (NEG-TAP, 2001).

1.1 Ammonia in the atmosphere

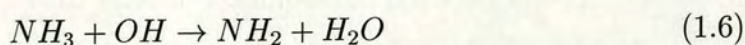
Ammonia is the most prevalent alkaline gas in the atmosphere. It is highly reactive and readily dry deposited. Hence the rate of conversion to form ammonium (NH_4^+) aerosols, which are less easily deposited until taken up into cloud droplets and precipitation, significantly affects the long-range transport of NH_x (Hov and Hjøllø, 1994; Barrett and Seland, 1995). This reaction depends on the presence

of other species derived from SO_2 and NO_x emissions. A significant proportion of NH_3 is likely to be redeposited locally in the area where it is emitted (Sutton *et al.*, 1995b). Asman (1998) and Singles (1996) employed multi-layer models and estimated that typically 60 % of the emissions had been dry deposited, respectively, within 2000 m and 5000 m of an NH_3 source. The remainder contributes to longer-range transport of N with a mean residence time in the atmosphere of 1 to 3 days (Moller and Schieferdecker, 1989).

Ammonia is emitted at ground level and diffuses upwards according to the intensity of turbulent mixing, reacting readily with acidic species, H_2SO_4 , HNO_3 and HCl , to form NH_4^+ salts in the form of hygroscopic aerosols which are effective condensation nuclei :



Ammonia can also react with the hydroxyl radical :



but this reaction is too slow, by comparison with the previous ones (1.5), to be of general significance (Seinfeld, 1986).

As a result of conversion to NH_4^+ compounds, concentrations of NH_3 gas fall off rapidly with height away from the surface within the lowest two or three hundred metres of the boundary layer (Asman and van Jaarsveld, 1992). Thus surface concentrations are not directly indicative of boundary layer contents and fluxes (Allen *et al.*, 1988). By contrast, NH_4^+ aerosol concentrations vary much less spatially (Allen *et al.*, 1988) and change comparatively little over the depth of the boundary layer, although the profiles of aerosol acidity tend to show some increase with height (INDITE, 1994).

Although reactions of NH_3 with acids can be very rapid, modelling studies (ApSimon *et al.*, 1994) show that inhomogeneous mixing of, for example, rural air with urban plumes, may delay conversion of NH_3 to NH_4^+ , typically by up to a few hours. The situation is further complicated by diurnal variations in emissions and meteorological conditions, combined with temporal and spatial changes in the production of acids. Moreover the reactions of NH_3 with HNO_3 and HCl are reversible, with equilibria established between aerosol ammonium nitrate (NH_4NO_3), the gases NH_3 , HNO_3 and between NH_4Cl - NH_3 - HCl which depend on temperature and humidity (Stelson and Seinfeld, 1982).

NH_3 and NH_4^+ aerosol are both easily soluble in clouds and are efficiently removed in precipitation. Dissolution of NH_3 raises the pH of cloud water and can substantially affect the solubility of ozone or its capacity to oxidise SO_2 in solution. Therefore the presence of NH_3 can alter the wet removal efficiency of other species (Kruse-Plass *et al.*, 1993).

Since European emissions of reduced nitrogen as NH_3 are comparable with those of oxidised nitrogen as NO_x (Vestreng, 2001), the conversion to NH_4^+ aerosols and subsequent long-range transport are important in relation to N deposition and exceedance of thresholds for environmental impacts.

A major question in modelling the transport of NH_3 concerns the nature of the emissions, since both emission and deposition fluxes occur over land surfaces such as crops. The relationship of the direction of fluxes to air concentrations may result in mean transport distances and deposition not being linearly related to the magnitude of emissions. As a consequence, local scale inhomogeneities in land-use also affect the budgets of reduced nitrogen (INDITE, 1994).

1.2 Ammonia emissions

1.2.1 Ammonia sources

The major ammonia sources include enzymatic decomposition of urea in animal urine and manures and losses during the production and application of fertilisers (Sutton *et al.*, 1995a). A variety of industrial activities release ammonia, including paper manufacture, wastewater treatment, manufacturing processes, petroleum refining and coal combustion while other sources include emissions by soils, biomass burning, wild animals and people (Sutton *et al.*, 2000). Ammonia is thus primarily a product of biological activity as well as a byproduct of agri-

culture and waste production and processing (both human and animal waste). Atmospheric concentrations of ammonia are greater over the continents than over the oceans (Quinn *et al.*, 1990) and there is little transport of ammonia or ammonium from the ocean to land masses, although the transport from land masses to oceans can be substantial (Quinn *et al.*, 1996).

Ammonia is released via the mineralisation of organic material in animals, soils, and the ocean, and intracellular reactions with plant tissues. Most of the ammonia mineralised is utilised. However, a small pool remains in solution and is subject to volatilisation at sufficiently high pH. Inorganic fertilisers and animal excreta accelerate soil emissions by increasing the NH_3 and NH_4^+ content of the soil, particularly in areas where livestock are concentrated. Ammonia can also be released by plants grown in areas with abundant nitrogen or during senescence when plants are transporting a great deal of N within their tissues (Brasseur *et al.*, 1999).

1.2.2 A detailed inventory of ammonia sources for UK

Ammonia emissions in the UK arise primarily from agriculture, particularly livestock farming and animal wastes. Recent studies (Misselbrook *et al.*, 2000; Goodwin *et al.*, 2000; Sutton *et al.*, 2000) have estimated agricultural and non-agricultural sources, showing that the NH_3 emissions have decreased only slightly since 1990.

Emissions from livestock occur from housed animals, waste storage (farmyard manure and slurries), land-spreading of wastes and from animals grazing in the field. The existence of large numbers of animals housed together results in large point sources of NH_3 in the landscape, while the intermittent nature of slurry and manure spreading results in NH_3 emissions also being very variable with time (Sutton *et al.*, 1995a). This wide diversity of agricultural activities makes estimating emissions a difficult task but increased attention had been focused on the UK inventory of NH_3 emissions.

Table 1.1 shows the inventory of NH_3 agricultural emissions in the UK from Dragosits *et al.* (1998). Ammonia emissions per unit livestock or per hectare crop are dependent on many environmental factors and differences in agricultural practise between farms (Jarvis and Pain, 1990). For instance, annual emissions from grazing livestock such as cattle or sheep vary greatly with the amount of nitrogen applied to pastures. The greater the proportion of the year the animals spend outdoors grazing, the smaller the total annual emissions per animal are expected to be.

The inventory in Table 1.1 indicates that animal production systems provide a very large proportion of the estimated total emissions (87.3%). Cattle constitute the largest agricultural source with an estimated contribution of 57.4%. Other livestock, such as poultry, sheep and pigs, are estimated to contribute smaller though still significant amounts. Much of the remaining agricultural emissions come from the application of nitrogen fertiliser and agricultural crops (12.7%).

Category	Animal numbers x 10 ³ (UK)	Emission/animal (kg N year ⁻¹)	Total NH ₃ -N (kt N year ⁻¹)	Contribution (%)
Cattle	11904	11.23	133.7	57.4
Sheep, goats	41623	0.38	15.9	6.8
Pigs	7506	3.18	23.9	10.3
Poultry	146496	0.19	27.8	12.0
Horses	302	6.56	2.0	0.9
Deer	34	0.95	0.03	0.01
Total livestock			203.2	87.3
Crops, grassland			29.7	12.7
Total emissions			232.9	100.0

Table 1.1: Ammonia agricultural emission estimates in the United Kingdom for 1996 (Dragosits *et al.*, 1998)

They are dependent on the fertiliser type and N fertiliser application rate.

Combined with this current UK estimate of agricultural NH₃ emissions of 233 kt N year⁻¹ (1996), the UK non-agricultural emissions of NH₃ are estimated as 54 kt N year⁻¹ for 1996. Quantifying the magnitude of non-agricultural sources is more uncertain, since there is a wide range of source types, with often little underlying experimental data (Sutton *et al.*, 2000). A detailed estimate of UK contributions of the different non-agricultural sources of NH₃ is given in Table 1.2 for 1996. Direct NH₃ emissions from humans, excepting sewage (works and land-spreading) occur from breath, sweat, infant excrement and cigarette smoking. The estimates consider the horses for pleasure riding and racing, and wild animals (e.g. sea birds, deer). Several UK sources were quantified (Sutton *et al.*, 2000) for the first time, including infant emissions, small deer and other major wild animals (badgers, foxes, feral cats and rabbits), sugar beet processing and other industrial sources, household products

Source	Total NH ₃ -N (kt N year ⁻¹) 1996
Direct human emissions	1.2
Horses	7.3
Pets (cats, dogs)	5.3
Wild animals	5.2
Biomass burning	1.6
Sewage	6.6
Landfill sites	3.3
Fertiliser production	3.3
Sugar beet processing	0.9
Other industrial sources	5.6
Transport (vehicles)	8.9
Coal combustion	2.2
Waste incineration	0.9
Household products	1.0
Non-agricultural fertiliser use	0.3
Total	53.6

Table 1.2: Ammonia emission from non-agricultural sources in the UK for 1996 (Sutton *et al.*, 2000)

(solvents and refrigeration), and garden fertilisers. Mostly these new sources are minor, although combined they amount to 9 kt N year⁻¹ (Sutton *et al.*, 2000).

Thus, the total UK emissions of NH₃ for 1996 represent an amount of 287 kt N year⁻¹ and these are mapped in Figure 1.1. The distribution of NH₃ emissions is modelled in a GIS methodology described by Dragosits *et al.* (1998). For agricultural emissions, parish statistics on livestock numbers and crop areas are combined with satellite-based land-cover data to model emissions at a 1 km resolution, which are subsequently aggregated to the 5 km level. In the UK, the areas of highest emission occur in relation to cattle farming (west and north west

England, Northern Ireland), as well as in pig and poultry farming areas (East Anglia, north east England, central Scotland). The emissions are low in upland areas such as the North Pennines and Lake District of northern England and in the Scottish Highlands.

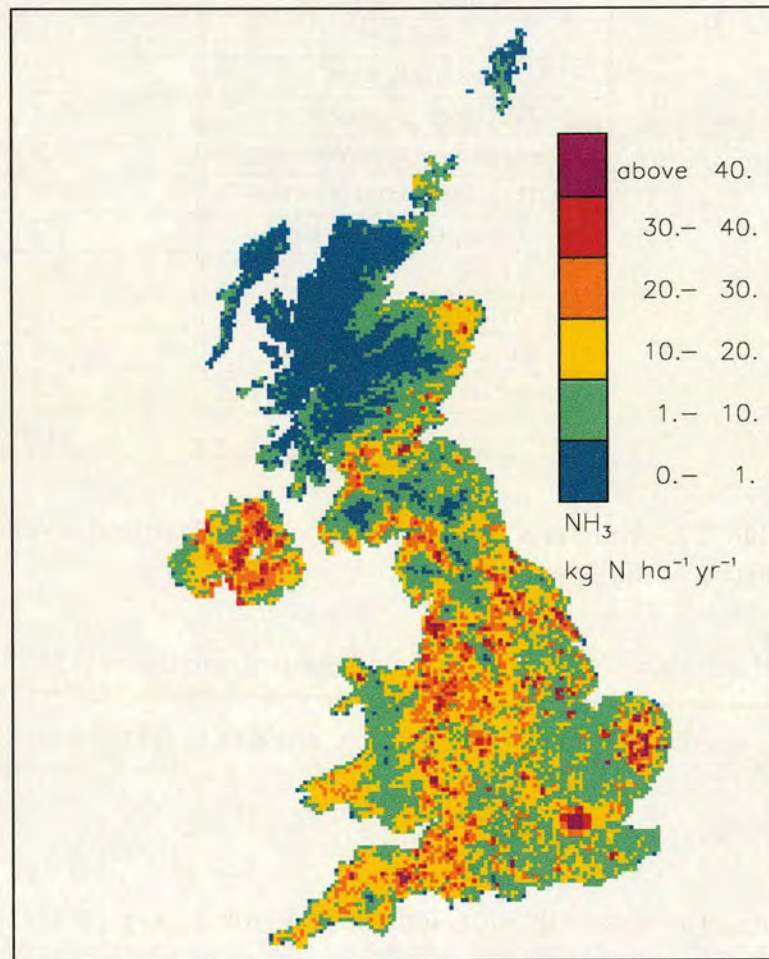


Figure 1.1: 1996 ammonia emissions for the United Kingdom on a 5 km x 5 km grid resolution. Units are kg N ha⁻¹ year⁻¹ (Dragosits *et al.*, 1998).

Total agricultural NH₃ emissions for the UK appear to have declined very slightly between 1988 and 1996, as shown in Table 1.3. Concerning the non-agricultural NH₃ emissions, the estimated magnitude has changed between 1990 and 1996 both because of revised average emissions per source unit (emission factors) compared

Category	Total NH ₃ -N (kt N year ⁻¹) 1988	Total NH ₃ -N (kt N year ⁻¹) 1996
Cattle	133.7	133.7
Sheep, goats	15.6	15.9
Pigs	25.4	23.9
Poultry	25.2	27.8
Horses	2.0	2.0
Deer	0.03	0.03
Total livestock	202.0	203.2
Crops, grassland	32.5	29.7
Total emissions	234.5	232.9

Table 1.3: Ammonia emission from agricultural sources in the UK for 1988 and 1996 (Dragosits *et al.*, 1998)

with earlier estimates (Sutton *et al.*, 1995a) and because of changes in the source activity (Sutton *et al.*, 2000).

However, the robustness and quality of the emission inventory vary between pollutants and depend on the complexity of the emitting processes and the availability of representative data (emission factors). In the case of ammonia, uncertainties are increased by the agricultural emissions dependency on animal feed, housing and waste management techniques (NEG-TAP, 2001). Therefore, there remain very large uncertainties in the emissions of NH₃ in the UK and elsewhere in Europe.

Estimated European Union emissions of NH₃ have decreased slightly (7%) from 1990 to 1996, due to reduced agricultural activity and measures taken by a few Member States (NEG-TAP, 2001). These include Denmark (19 % reduction), Germany (15 %) and the Netherlands (35 %). These reductions are partly the result

of implementing technical abatement measures for ammonia emissions and in the case of Germany is due to economic and social reforms in East Germany following 1989. Until recently no internationally agreed targets existed for ammonia. The proposed NECD (National Emission Ceilings Directive) target represents a 21 % reduction across Europe and the agreed CLRTAP (Convention on Long-Range Transboundary Air Pollution) Protocol is a 12 % reduction below 1990 emissions by 2010 (Tarrason and Schaug, 1999). For the UK, the same target is expected to be set for both agreements (NEGTAP, 2001). However, there are uncertainties about the magnitude of ammonia abatement already achieved, since none of the countries of Europe has published a satisfactory comparison between a measured atmospheric mass balance and national emissions of ammonia (NEGTAP, 2001). Moreover, as European sulphur dioxide (SO₂) emissions have decreased over the last decade, the atmospheric residence time of ammonia and ammonium aerosol has also changed, masking simple relationships between emissions and NH_x monitoring data (Sutton *et al.*, 2001a). Therefore, both abatement measures and atmospheric interactions are involved in the assessment of ammonia changes (NEGTAP, 2001). Within the context of the costs of emission abatement, it is essential to have a sound quantification of the concentrations and fluxes of NH_x in the atmosphere. Since neither the distribution of NH₃ emissions nor the distribution of sensitive habitats is uniform, it is necessary to assess the spatial distribution of NH_x concentrations and deposition. Complementary to this, is the need for monitoring long-term trends, in order to quantify the link to emission changes over periods of several years.

Monitoring the complete distribution of NH_3 concentrations at a national level would require an impracticably large number of stations, due to the spatial variability characteristic of a primary pollutant emitted at or near ground level (Asman *et al.*, 1998). Therefore, atmospheric transport models serve a complementary role since using spatially resolved emission estimates, national maps may be established at the same resolution as emissions (e.g. 5 km). Accurate models of the spatial distribution of ammonia emissions are thus an essential input to models of atmospheric transport and deposition. This is especially important when resulting deposition maps are used to calculate patterns of critical loads (threshold levels of pollutant deposition causing harmful effects to a sensitive receptor) exceedance or to determine suitable abatement measures (Nilsson and Grennfelt, 1988; Bull, 1991; Dragosits *et al.*, 1998). Moreover, by treating the chemical reactions with other pollutants, these models can also be used to assess these interactions and the distribution of aerosols and deposition (Sutton *et al.*, 2001).

1.3 Atmospheric transport models

Models of the long-range transport of acidic sulphur pollutants across Europe were first established through the Long Range Transport of Air Pollution (LR-TAP) programme (Fisher, 1975; OECD, 1977; Eliassen, 1978). The EMEP (Co-operative programme for Monitoring and Evaluation of the Long-range Trans-

mission of air Pollutants in Europe) programme was then established to estimate both present day and future concentrations and deposition, but also to assess the costs and benefits of proposed emissions reductions (Murley, 1995; Warren and ApSimon, 2000). Since 1985, the EMEP atmospheric transport models have been employed to calculate concentrations and depositions of acidifying compounds in Europe (Barrett and Seland, 1995). The UK has, however, recognised that in terms of both the scale of outputs and the representation of processes, the EMEP models (50-km or 150-km resolutions) may not meet the needs of domestic policy. Given the size of both the UK and particular habitats of recognised conservation value, a range of other models, such as the one developed and applied in this study, (Singles *et al.*, 1998; Fournier *et al.*, 2002) are in use in the UK (Fisher, 1978; Metcalfe *et al.*, 1995; Klimova-Murphy and Fisher, 1997).

These models, simulating the transport, chemical interactions and deposition of pollutants, provide the only available instrument to integrate current knowledge of the processes quantitatively and predict the concentrations and deposition of pollutants at future dates at a reasonable spatial scale for the UK. However, it is a great challenge as there are always uncertainties and weaknesses in modelled output values and measurements have to be used where possible. Moreover, atmospheric ammonia, with its short lifetime, exhibits extremely variable emissions, concentration and deposition in space, both on a regional scale as well as on a local scale (NEGTAP, 2001).

1.4 Objectives of this study

In order to model the atmospheric behaviour of ammonia, an existing atmospheric transport model (Singles *et al.*, 1998), FRAME (Fine Resolution AMmonia Exchange), is improved and subsequently used in conjunction with existing measurements. The study is comprised of several parts presented as follows :

- *Chapter 2.* The FRAME Model : general overview of the atmospheric processes parameterised in the model. This gives the state of the model at the beginning of this study.
- *Chapter 3.* Extension of FRAME to the British Isles and Development of Numerical Procedures : extension of the domain of the model from the UK to the British Isles; parallelisation of the model and implementation of an alternative diffusion discretisation.
- *Chapter 4.* Developments of Parameterisations of Atmospheric Processes : these concern the wet deposition process, the dry deposition of oxidised nitrogen and the height of emissions of NO_x and SO_2 .
- *Chapter 5.* Applications of the FRAME Model : evaluation of regional budgets of reduced nitrogen for the British Isles for 1996 and predictions for 2010.
- *Chapter 6.* Conclusions and Perspectives
- *Bibliography*

- *Appendix A. Monitoring Networks* : informations concerning the monitoring sites in the UK.
- *Appendix B. FRAME Versions* : listing and characteristics of the different versions of the FRAME model developed in this study.
- *Appendix C. List of Publications* : gives the details of two papers concerning this work and included at the end of the thesis with the permission of the publishers and of the joint authors.

1.5 Summary

As a result of the research into transport and deposition of acidifying compounds, ammonia has been recognised to play an important role in both problems of acidification and of nitrogen deposition (Sutton *et al.*, 1994). Moreover, in contrast with SO₂ and NO_x emissions, NH₃ emissions in the UK have not changed much since 1990 (RGAR, 1997; NEG-TAP, 2001). Although emissions of NH₃ are difficult to estimate with any accuracy, Dragosits *et al.* (1998) modelled their distribution for the UK at a 5 km level. Combined with the meteorological conditions surrounding the sources, such precise representation of the distribution of ammonia emissions is a fundamental input to models of atmospheric transport and deposition. The ultimate use of such models is to understand the effects of changes in emissions. Indeed, national and international negotiations within the CLRTAP have relied upon the use of these models to predict the future concentra-

tion of a particular pollutant after the implementation of a new pollution control programme. These models are very useful for determining the cost effectiveness of air pollution control strategies, such as the 1999 Gothenburg Protocol, which included for the first time NH_3 in the process of emissions reduction. Therefore, particular attention is focused in this study on the fluxes of reduced nitrogen deposition to the UK simulated by the FRAME model. To quantify them more accurately, the domain of the model is extended to the British Isles and the wet deposition parameterisation reviewed. Numerical and chemical aspects of the FRAME model are also investigated.

Chapter 2

The FRAME model

2.1 Introduction

Air pollution can be transported in the atmosphere far away from its source region. While these pollutants are transported, some chemical, physical and removal processes can occur as pollutants are mixed in the atmosphere. Atmospheric transport models, such as the model used in this study, FRAME (Fine Resolution AMmonia Exchange), are developed to treat the transport, transformation, and removal of species in the atmosphere (Singles, 1996; Singles *et al.*, 1998).

A traditional approach to represent species concentrations and evolution in a model domain has been Eulerian, using grids and differencing schemes that are similar to those for smoothly varying meteorological fields, such as momentum and temperature, calculated in General Circulation Models (GCMs). In these Eulerian models, however, the advection of highly non-homogeneous species can lead to several problems. Many Eulerian advection schemes, such as the second-order centred difference scheme, suffer from the tendency to form negative con-

centrations in the presence of sharp gradients. Solutions to this problem, such as the upstream differencing, filling, and flux-corrected methods (Zalesak, 1979), commonly result in numerical diffusion. Higher-order schemes, while less prone to numerical diffusion, also require shorter time-steps and hence are computationally expensive. Another approach involves use of pseudo-spectral techniques to model the atmospheric dynamics. However, they also produce some negative concentrations and numerical dispersion when applied to atmospheric species transport. Therefore, the accurate representation of the transport of the atmospheric species is not straightforward if negative concentrations, numerical dispersion and short time-steps are to be avoided (Prather, 1986; Chock and Winkler, 1994; Dabdub and Seinfeld, 1994; Leonard *et al.*, 1995).

In the model applied for the present study, a Lagrangian approach is taken by using a constant-volume air column which is advected along prescribed wind fields (Singles, 1996; Singles *et al.*, 1998). The Lagrangian method is particularly well suited to species that are chemically active, such as ammonia, sulphur or nitrogen dioxide, because deviations from chemical equilibrium associated with advection are greatly reduced. Indeed, the chemical reactions of such gases are often quite extended (i.e. their reaction rates cover a wide range) and non-linear, so that small errors in advection can, by disturbing chemical equilibrium, result in the need for significant additional calculations in Eulerian approaches to reestablish the chemical equilibrium which are not necessary in the Lagrangian approach. Furthermore, because the chemistry of the atmosphere involves many species, the traditional Eulerian advection of every species becomes prohibitively expensive in both storage and computation time. By contrast, a disadvantage of the Lagrangian approach is the inability to treat the distortion of the model air column (or air parcel) due to wind shears, by using a constant uniform advection wind speed throughout the air column as done in the FRAME model. This assumption is essential to render the notion of air column meaningful and to allow physical and chemical processes to be represented in this air column.

This chapter describes these processes : boundary conditions at the frontier of the domain (section 2.2.1), emissions from the domain (section 2.2.1), meteorological conditions (section 2.2.2), vertical diffusion (section 2.2.3), dry

and wet deposition (section 2.2.4), chemical interactions between species (section 2.2.5) and some sensitivity experiments with FRAME (section 2.2.6). Finally, the results from the FRAME model (version 1.1) are discussed in section 2.3.

2.2 Components of FRAME

The FRAME model was originally developed to investigate the atmospheric behaviour of ammonia (NH_3) over Great Britain (Singles, 1996; Singles *et al.*, 1998) (version 1.0). However, the pattern of concentration and deposition of pollutants in Great Britain is strongly influenced by the emissions in Northern Ireland. A first step is to include Northern Ireland in the model domain. Hence, the FRAME model considers now the United Kingdom (UK) in its domain (FRAME 1.1; see Appendix B). Using a detailed emissions inventory and specific meteorological conditions for the UK, it simulates vertical dispersion, chemical conversion to ammonium aerosol (NH_4^+) and removal from the atmosphere by dry and wet deposition. The main goal is to describe the average long-term behaviour of NH_3 , on a national scale, and to describe the spatial distribution of annually-averaged NH_3 surface concentrations and annual deposition fluxes of reduced nitrogen.

2.2.1 Sources and emissions

Sources of pollutant are a fundamental component of an Atmospheric Transport Model (ATM). They originate from the studied domain or they have been advected by winds from other regions or countries. A precise inventory of the emissions is required to simulate accurately the evolution of the pollutants in an ATM.

Initial conditions

FRAME produces annually-averaged concentrations and deposition fluxes at a 5 km × 5 km resolution over the United Kingdom (UK). Therefore, spatially disaggregated emissions are used in the model. They include ammonia emissions but also nitrogen oxides ($\text{NO}_x = \text{NO} + \text{NO}_2$) and sulphur dioxide (SO_2) emissions as the model considers coupled chemistry of SO_2 , NO_x and NH_3 (Sandnes and Styve, 1992; ApSimon *et al.*, 1994). As most of the NH_3 emissions occur at ground level, they are introduced into the lowest layer of the model at a height of 1 m, whereas SO_2 and NO_x emissions are evenly distributed throughout the 300 m of the mixing layer to take into account the more variable emission heights of these species. Emissions are assumed to be temporally constant with no diurnal or seasonal variations.

NH_3 emissions A detailed inventory of UK ammonia emissions for 1996 is provided in the previous chapter (section 1.2.2) and is taken from Sutton *et al.* (2000) and Dragosits *et al.* (1998). This advances the inventory (Sutton *et al.*, 1995a) used by (Singles *et al.*, 1998) by the inclusion of Northern Ireland. The current 1996 UK estimates combine 233 kt N year⁻¹ of agricultural NH_3 emissions with 54 kt N year⁻¹ of non-agricultural emissions. It results in a total 1996 NH_3 emissions for the UK of 287 kt N year⁻¹ which are mapped in Figure 1.1.

SO_2 , NO_x emissions In addition to the emissions of NH_3 , emissions of SO_2 and NO_x are required for the UK. These data come from the National Atmospheric Emissions Inventory (Salway *et al.*, 1999). The SO_2 and NO_x emissions are estimates at 10 km × 10 km for the UK for 1996 and their distribution is shown, respectively, in Figure 2.1 and 2.2.

The total 1996 UK SO_2 emissions represents 1005 kt S year⁻¹. A large fraction (85 %) is concentrated in a few areas and originates from refineries, power stations and large industrial plant. These areas of high emissions are

often surrounded by rural areas with low emissions. Figure 2.1 highlights the main conurbations and high coal combustion in Stoke-on-Trent, Manchester, Middlesborough and Wrexham. High emissions in Plymouth and Newport result from a combination of shipping and industry. London and Birmingham exhibit significant SO_2 emissions although the main contributors are road transport and industry. Emissions in Northern Ireland are high, particularly in Belfast, as a result of domestic combustion of coal and smokeless fuels (Salway *et al.*, 1999). The total 1996 UK NO_x emissions represents $590 \text{ kt N year}^{-1}$. About 34 % is estimated to come from the major road links. Vehicles travelling at high speeds contribute most. Therefore, the major route-ways, but also the conurbations and city centres, are highlighted in Figure 2.2. Moreover, high emissions occur from shipping in port areas (Salway *et al.*, 1999).

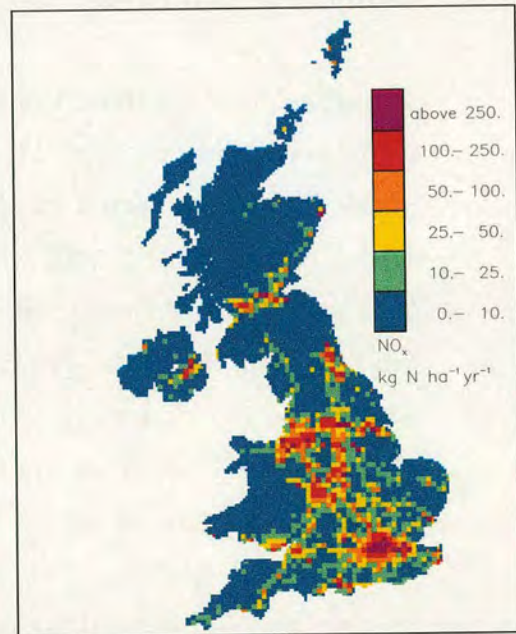
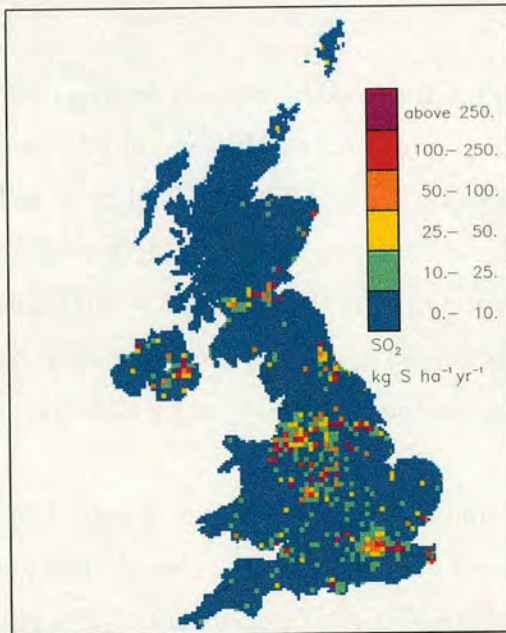


Figure 2.1: 1996 SO_2 emissions for the United Kingdom on a $5 \text{ km} \times 5 \text{ km}$ grid resolution. Units are $\text{kg S ha}^{-1} \text{ year}^{-1}$.

Figure 2.2: 1996 NO_x emissions for the United Kingdom on a $5 \text{ km} \times 5 \text{ km}$ grid resolution. Units are $\text{kg N ha}^{-1} \text{ year}^{-1}$.

Wind origin	NH _x -N import	NO _x -N Import	S Import
north	0.2	2.5	2.1
northeast	2.7	17.2	8.8
east	7.1	46.4	40.7
southeast	6.9	35.5	22.2
south	5.2	12.7	10.3
southwest	1.4	3.0	3.2
west	0.2	0.2	0.8
northwest	0.0	0.0	0.2
Total Import	23.7	117.5	88.3

Table 2.1: Modelled 1996 budgets of import, obtained with the TERN model, for eight wind sectors for the FRAME UK domain (version 1.1). The units are kt N (or S) year⁻¹.

Boundary conditions

The transboundary import of foreign material is assessed by running the TERN model across Europe. The TERN (Transport over Europe of Reduced Nitrogen) model had been created by ApSimon *et al.* (1994). TERN is a Lagrangian model, from which FRAME was developed, which uses EMEP emissions of NH₃, NO_x and SO₂ over Europe on a 150 km grid (Barrett and Seland, 1995). TERN was modified by Singles (1996) to create a set of concentration profiles for the edge of the model domain. These profiles are used to initialise the trajectories of the FRAME model for the UK.

A summarised view of the UK boundary conditions created with TERN for 1996 is shown in Table 2.1. This shows the amount of reduced nitrogen, oxidised nitrogen and sulphur (kilotonnes N or S year⁻¹) imported by the FRAME model along the UK domain from different wind directions.

The import of NH_x, NO_x and S from outside the UK represents respectively 8 %, 20 % and 9 % of the UK NH₃, NO_x and SO₂ 1996 emissions. For reduced nitrogen, it comes mostly from the east, southeast (Belgium, France) in aerosol form (NH₄⁺). The import distribution of oxidised nitrogen and sulphur, with important fluxes from the east and southeast directions, reflects the high NO_x

and SO₂ emissions in continental Europe. Therefore, it is important to include this import component in the FRAME model to describe accurately the spatial distribution of concentration and deposition over the UK.

2.2.2 Meteorological input data

Combined with the emissions and the concentrations at the edge of the domain, other parameters are specified in the FRAME model. To simulate average annual values, the model is run at the spring equinox, when the lengths of the day and night are equal. The height of the cloud base is assigned a value of 250 m (Singles, 1996). In the atmosphere the height would be higher than 250 m, but aqueous chemical reactions may occur at lower levels in mist and fog, so this value takes account of this process (Hertel *et al.*, 1995). The cloud cover is set to 6 oktas and was chosen because it represents a 10-year average over the British Isles (Wallen, 1970; Singles, 1996).

Advection wind speed

The horizontal advection speed used in the model defines the amount of time the air column takes to cross a grid square, and hence how much material is emitted into and deposited from the column. The model uses straight-line trajectories, in relation to specified wind directions. These trajectories start at four different times of the day (00 h; 06 h; 12 h; 18 h). Twenty-four equally-spaced wind directions are considered, and the results are combined statistically, suitably weighted by the frequency of occurrence of the wind from each direction. The wind data are taken from a long-term study of wind trajectories (Jones, 1981) and have been adapted for the FRAME model by Singles (1996). The wind data of Jones (1981) were derived for a height of 400 m and are long-term average data comprising a representative rose for the UK as shown in Table 2.2.

Wind origin (degree)	north 0-45	northeast 45-90	east 90-135	southeast 135-180	south 180-225	southwest 225-270	west 270-315	northwest 315-360
Wind speed	7.50	6.26	5.79	5.95	7.71	7.90	8.61	6.00
Frequency	10.90	7.90	6.60	8.60	11.60	19.30	17.80	17.30

Table 2.2: The wind rose used in the FRAME model (Singles, 1996). The wind data are grouped into eight sectors for which the wind speed (m s^{-1}) and the wind frequency of occurrence (%) are presented.

Land-cover and altitude

To account for ecosystem-dependence of ammonia dry deposition, the model incorporates a land-cover database. Land cover data for Great Britain were taken from the CEH (Centre for Ecology and Hydrology) Land Cover map derived from satellite images, maps and land-use surveys available within the Countryside Information System database (Howard and Brunce, 1996; Smith *et al.*, 2000). This map provides percentages of different land classes at 1 km resolution for Great Britain. This land-cover database was aggregated at the FRAME 5 km resolution over Great Britain and divided into six categories : arable, forest, grassland, moorland, urban areas and sea (RGAR, 1997; Smith *et al.*, 2000). In making the initial extension to the UK (FRAME version 1.1), land-cover data from Northern Ireland were required, and for this purpose the Level 4 'CORINE' data (OSI, 1993) were applied and aggregated into the same land-cover categories by U. Dragosits (CEH, Edinburgh). Therefore, the land-cover database gives for each 5 km grid square of the FRAME domain the contribution (%) of the six different ecosystem classes. Altitude data for the UK were obtained from R. Smith (CEH, Edinburgh) and are derived from CEH Countryside Info System.

Rainfall

The rainfall data for the UK used are 30-year average data (1961-1990) interpolated to $5 \text{ km} \times 5 \text{ km}$ scale from the Meteorological Office database (Thompson

et al., 1982). These data are in the form of an annual rainfall field for the UK on a $5 \text{ km} \times 5 \text{ km}$ grid (Figure 2.3). Rainfall is set at an annual rate of 700 mm over the surrounding ocean and has high rates in mountainous areas and on the west coast of the UK.

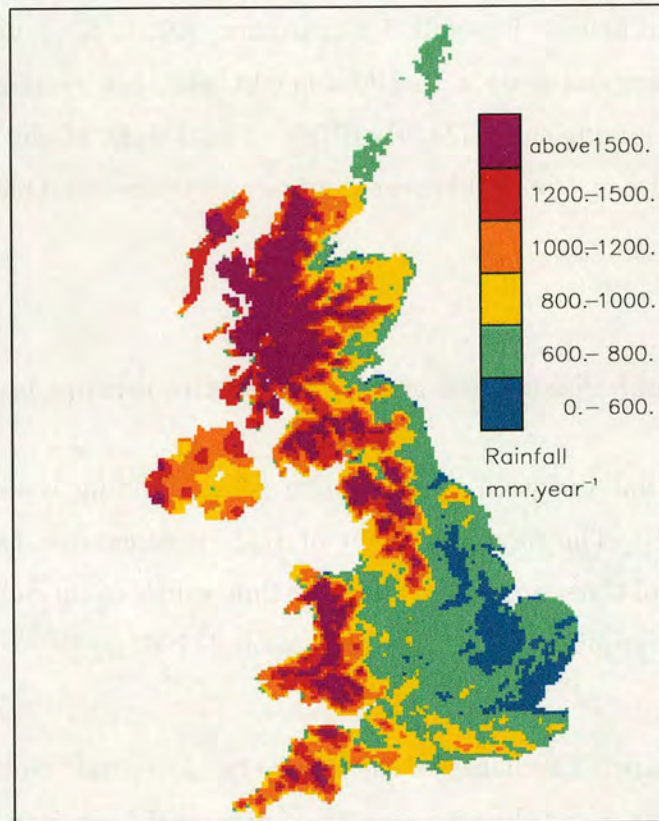


Figure 2.3: 30-year average annual rainfall map for the UK at a $5 \text{ km} \times 5 \text{ km}$ resolution. Units are mm year^{-1} .

2.2.3 Diffusion process

Vertical diffusion in TERN and FRAME is treated explicitly using a multi-layer system with 33 layers of variable depth (ApSimon *et al.*, 1994; Singles, 1996). The highest layer extends to 2500 m, and the layer thicknesses range from 1 m at the bottom to 100 m at the top. Vertical mixing is described using K-theory eddy diffusivity, with the exchange of material between layers being determined by the equation :

$$\frac{\partial c}{\partial t} = \frac{\partial}{\partial z} \left(K_z \frac{\partial c}{\partial z} \right) \quad (2.1)$$

where c is the concentration of the chemical species under consideration and K_z is the vertical diffusivity. K_z depends on atmospheric stability, time of the day and height (Pasquill, 1961; Golder, 1972). K_z is modelled to have a linearly increasing value up a specified height and then remains constant up to the top of the mixing layer (Maul, 1978). This height of the mixing layer and K_z depend also on the cloud cover value, which is fixed at 6 oktas in the FRAME model.

Parameterisation of the height of the mixing layer

A diurnal variation of the height of the mixing layer (H_{mix}) is considered in FRAME. The daytime height of H_{mix} is calculated using an adaptation of the model of Carson (1973). The nighttime values of the height of H_{mix} are calculated using Pasquill stability classes (Pasquill, 1961).

Daytime The depth of the mixing layer depends on the sensible heat flux from the surface and the entrainment of more stable air from above. The sensible heat flux is assessed in the model using the Smith (1979) formulation :

$$H = 0.4 (S_t - 100.0) C_f \quad (2.2)$$

where S_t is the incoming solar irradiance and C_f the cloud reduction factor. Due to the 6 oktas cloud cover used in the FRAME model, C_f has a value of 0.59 following Smith (1975). According to the same author (Smith, 1975), the solar irradiance equation is :

$$S_t = 950.0 \cos(zen) C_f \quad (2.3)$$

where 950.0 is the maximum possible solar irradiance (W m^{-2}) (Smith, 1975), and zen the zenith angle of the sun.

During a time interval Δt , heat energy is added to the boundary layer by surface heating but also by entrainment of warmer air from just above the atmospheric boundary layer. Carson (1973) assumed that the amount of energy absorbed due to entrainment is proportional to the surface heating :

$$\Delta E = \alpha H \Delta t \quad (2.4)$$

where ΔE is the energy absorbed due to entrainment in time Δt and α is the constant of proportionality. In the TERN and FRAME models, a time step of 10 minutes and a value of 0.15 for α are assigned (ApSimon *et al.*, 1994; Singles, 1996).

Consequently, the amount of energy added to the atmospheric boundary layer (ΔE) leads to a change of its potential temperature (θ) and hence, of the corresponding height of this layer (H_{mix}). This calculation is pursued until the end of the day, at which point the model uses a different parameterisation to assess the nighttime values of the height of H_{mix} .

Nighttime The nighttime values of the height of H_{mix} are calculated using the atmospheric stability and the wind speed used to advect the air column. The method of Pasquill (1961) is used to classify atmospheric stability. The different classes depend on the solar irradiance (S_t), described previously, and the 10 metre wind speed ($u(10)$). This latter parameter is approximated, following ApSimon *et al.* (1994), as follows :

$$u(10) = 0.5 G \quad (2.5)$$

over land, and :

$$u(10) = 0.85 G \quad (2.6)$$

u(10) (m s ⁻¹)	Day Time			Night Time
	$S_t > 700$	$350 \leq S_t \leq 700$	$S_t < 350$	
< 2	A	A-B	B	
2 - 3	A-B	B	C	E
3 - 5	B	B-C	C	D
5 - 6	C	C-D	D	D
> 6	C	D	D	D

Table 2.3: Pasquill stability classes for daytime and nighttime depending on the wind speed at 10 metres and the solar irradiance S_t . A: extremely unstable; B: moderately unstable; C: slightly unstable; D: neutral; E: slightly stable.

Stability class	Height of the Mixing Layer (m)
D	$H_{mix} = \max(90 G, 400)$
E	$H_{mix} = \max(50 G, 200)$

Table 2.4: Nighttime values of the height of the atmospheric boundary layer (H_{mix} , m) depending on the Pasquill stability class (D: neutral; E: slightly stable). G is the geostrophic wind speed used to advect the air column (m s⁻¹).

over the sea, where G is the geostrophic wind speed used to advect the air column and described in Table 2.2. This allows the values of $u(10)$ to be easily estimated. Table 2.3 gives an overview of the Pasquill stability classes depending on these parameters and adapted from Seinfeld (1986).

The nighttime values of the height of the mixing layer are then dependent on the appropriate stability class and the advection wind speed as shown in Table 2.4.

Parameterisation of the vertical diffusivity K_z

In the model, the parameterisation of the vertical diffusivity (K_z) is the same as used by ApSimon *et al.* (1994) and follows a similar scheme as Maul (1978). K_z increases to a specified height H_z and then remains constant (K_{max}) up the top of the mixing layer (H_{mix}) as shown in Figure 2.4. However, the values of K_{max} and H_z differ between daytime, nighttime and over the sea.

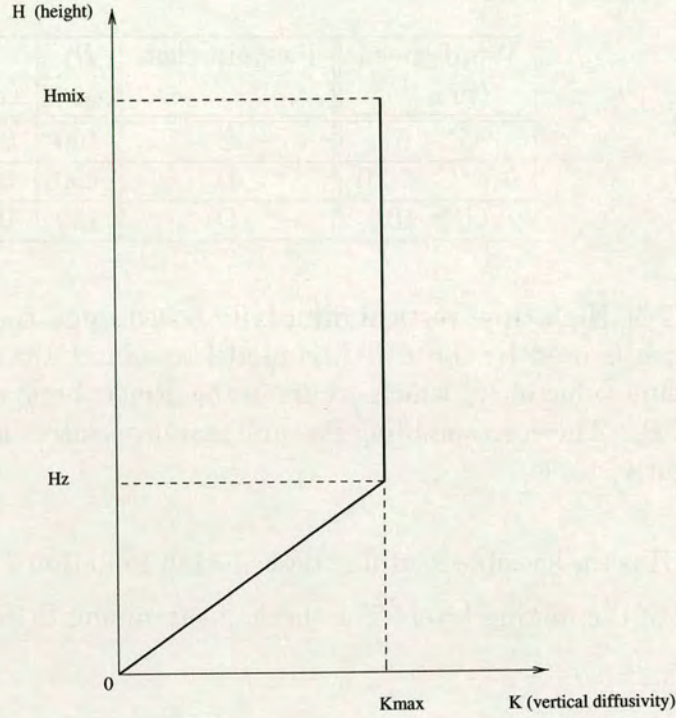


Figure 2.4: Vertical profile of the vertical diffusivity K_z , used in the FRAME model. H_z is the height at which K_z attains its maximum value K_{max} .

Daytime During the day, both convective and mechanical mixing in the air column are assessed in the model. Then, the dominant of these two effects will be considered in the vertical diffusivity parameterisation (subject to a maximum value of $20 \text{ m}^2 \text{ s}^{-1}$) as follows :

$$K_{max} = \max(A, B) \quad (2.7)$$

where A and B are parameters representing convective and mechanical mixing respectively. A is determined with the equation :

$$A = 0.55 \times 10^{-3} \times H^{\frac{1}{3}} \times H_{mix}^{\frac{4}{3}} \quad (2.8)$$

Wind speed (m s ⁻¹)	Pasquill class	H_z (m)	K_{max} (m ² s ⁻¹)
$G \leq 6$	E	100	$0.414 G$
$6 < G < 10$	D	150	$0.16 G^2$
$G \geq 10$	D	150	$0.16 G^2$

Table 2.5: Nighttime vertical diffusivity based upon the geostrophic wind speed G , which is used by the FRAME model to advect the air column. K_{max} is the maximum value of K_z which occurs in the atmospheric boundary layer above the height H_z . The corresponding Pasquill stability classes are presented (D: neutral; E: slightly stable).

where H is the sensible heat flux described in Equation 2.2 and H_{mix} the modelled height of the mixing layer. The mechanical mixing B follows the equation :

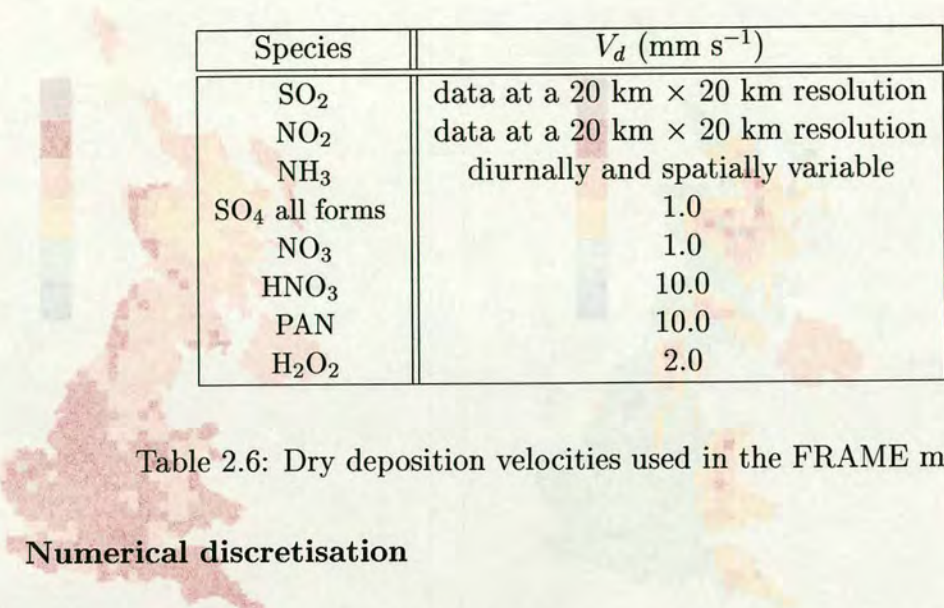
$$B = 0.2 G^2 \quad (2.9)$$

Moreover, during daytime, H_z is assigned a value of 200 m.

Nighttime During the night, only the mechanical mixing is considered. The parameterisation of the diffusivity coefficient depends only on the geostrophic wind speed (G) used to advect the air column. The description of the different cases is shown in Table 2.5.

Over the sea Over the sea, due to a reduction of the surface roughness, another parameterisation is prescribed (ApSimon *et al.*, 1984) for both day and night :

$$\begin{cases} K_{max} = 0.15 G^2 \\ H_z = 75 \end{cases} \quad (2.10)$$



Species	V_d (mm s^{-1})
SO ₂	data at a 20 km × 20 km resolution
NO ₂	data at a 20 km × 20 km resolution
NH ₃	diurnally and spatially variable
SO ₄ all forms	1.0
NO ₃	1.0
HNO ₃	10.0
PAN	10.0
H ₂ O ₂	2.0

Table 2.6: Dry deposition velocities used in the FRAME model.

Numerical discretisation

To integrate the diffusion equation, a fourth-order Runge-Kutta method had been developed by ApSimon *et al.* (1994). Singles (1996) optimised this scheme for FRAME with adaptive time-step to allow different time-steps to be used dependent on the amount of vertical exchange of material in the air column.

2.2.4 Removal processes

Dry deposition

Dry deposition is the direct absorption of the gases and aerosols at the ground (Sutton *et al.*, 1995b). This is treated by assigning a deposition velocity (V_d) to each chemical species. Some species have a specified average value as it is shown in Table 2.6 (ApSimon *et al.*, 1994). However, for SO₂ and NO₂, the values of V_d have been derived from a dry deposition model applied over Great Britain (Figure 2.5 and 2.6) (Smith *et al.*, 2000). For the initial extension to include Northern Ireland in FRAME version 1.1, constant values of V_d were assigned, with respectively, 8.0 and 1.4 mm s^{-1} for SO₂ and NO₂ (M. A. Sutton, 2000. Personal communication).

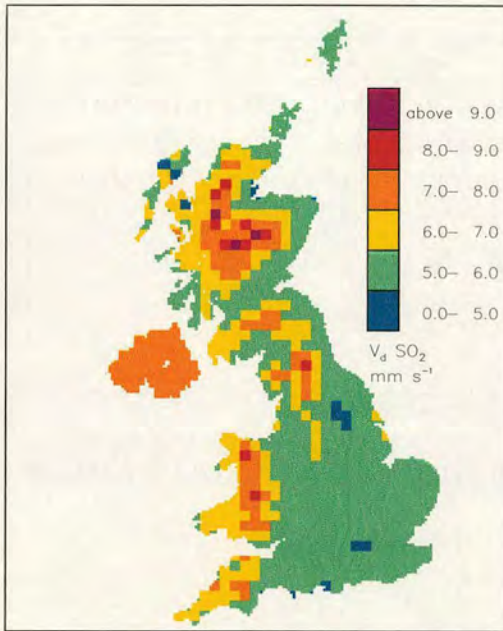


Figure 2.5: Diurnally-averaged values of V_d for SO_2 at a 20 km resolution for the UK. Units are mm s^{-1} .

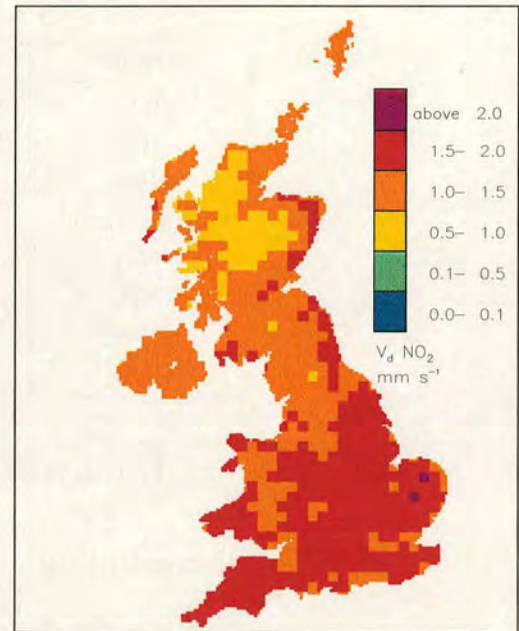


Figure 2.6: Diurnally-averaged values of V_d for NO_2 at a 20 km resolution for the UK. Units are mm s^{-1} .

Dry deposition of ammonia

In the case of NH_3 , a different deposition velocity parameterisation is assigned for arable, forest, grassland, moorland and urban areas. Values of V_d are calculated for each land category using a resistance model. The land-cover database, described previously (section 2.2.2), is used to create a set of land-dependent values of V_d .

This transfer of material through the atmospheric surface layer, molecular sub-layer and to the surface can be viewed as analogous to the electric flow through a series of three resistances. The aerodynamic resistance R_a describes the resistance due to turbulent diffusion of material from the atmosphere to a shallow layer near the surface. The aerodynamic resistance increases with height and is hence given for a land-dependent reference height. The laminar boundary layer resistance R_b describes the resistance due to molecular diffusion (gases) or Brownian diffusion (aerosols) through the very shallow laminar layer near the surface. The surface resistance R_c describes the ability of the surface to receive the airborne material.

Parameter	Arable	Forest	Grass	Moorland	Urban	Sea
R_c (s m ⁻¹)	1000	20	600	20	240	240

Table 2.7: Land-dependent values of the surface resistance (R_c) used in FRAME to calculate values of V_d for NH_3

It depends on the properties of the material and the surface. The three resistances are added together in series to create a total resistance to deposition R_t , which represents the Canopy Resistance Model and is defined as :

$$R_t = R_a + R_b + R_c \quad (2.11)$$

The relation of the resistance (s m⁻¹) to the dry deposition velocity V_d (m s⁻¹) is

$$V_d = (R_a + R_b + R_c)^{-1} \quad (2.12)$$

The dry deposition flux of material to the surface, F (kg m⁻² s⁻¹) is given by

$$F = V_d c \quad (2.13)$$

where c is the concentration of material (kg m⁻³).

To describe land-dependent dry deposition, a specific value of R_c is assigned to each land category (Table 2.7). The values of R_c are chosen to provide a description consistent with the literature on surface-atmosphere exchange of NH_3 with different surface types, e.g. (Sutton *et al.*, 1993, 1994; RGAR, 1997). These values of R_c are then combined with locally calculated values of R_a and R_b which allow V_d to vary diurnally and spatially.

The type of receptor surface is not the only factor that is likely to influence the dry deposition flux of gaseous and particulate materials. The friction velocity, the stability of the atmosphere, the roughness also influence this process and are

Parameter	Arable	Forest	Grass	Moorland	Urban	Sea
z_0 (m)	0.05	1.00	0.03	0.03	1.00	0.01
z_{vd} (m)	1.0	2.0	1.0	1.0	2.0	1.0

Table 2.8: Values of the roughness z_0 and of the reference height z_{vd} for the different land classes used in the model. Units are metre.

taken into account in the parameterisations of R_a and R_b .

Parameterisations of R_a and R_b The aerodynamic resistance R_a is calculated using the formulation of Garland (1977) :

$$R_a(z_{vd}) = \frac{u(z_{vd})}{u_*^2} - \frac{\psi_H - \psi_M}{u_* k} \quad (2.14)$$

where $R_a(z_{vd})$ describes the resistance due to turbulent diffusion of material from the reference height (z_{vd}) to the roughness length (z_0) for each land class. The values of both parameters for the different types of cover used in the model are presented in Table 2.8. u_* is the friction velocity and is calculated using the estimated database wind-speed at 3 m in neutral conditions. The mean wind-speed at a height of 3 m for the UK is shown in Figure 2.7. The wind-speed data used are 30-year average data (1961-1990) interpolated to 20 km \times 20 km scale from the UK Meteorological Office database (Thompson *et al.*, 1982). As no data were available for Northern Ireland, a constant value of 5.1 m s⁻¹ was assigned which represents the average value over Great Britain. $u(z_{vd})$ is the wind-speed at the specified height z_{vd} .

ψ_H and ψ_M are dimensionless stability functions. They have a value of 0 in neutral conditions. In stable conditions, they follow the description of Thom (1975) :

$$\psi_M = \psi_H = -5.2 \frac{z}{L} \quad (2.15)$$

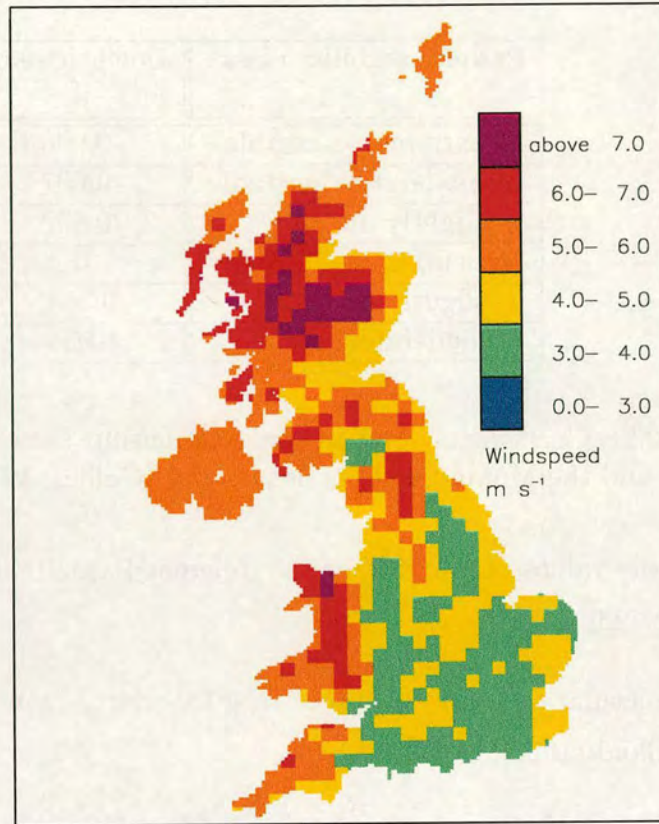


Figure 2.7: Mean wind-speed at a height of 3 m at a $20 \text{ km} \times 20 \text{ km}$ resolution for the UK. Units are m s^{-1} .

and :

$$\begin{cases} \psi_M = 2 \ln \frac{(1+x)}{2} + \ln \frac{(1+x^2)}{2} - 2 \tan^{-1}(x) + \frac{\pi}{2} \\ \psi_H = 2 \ln \frac{(1+x^2)}{2} \\ x = \left(1 - 16 \frac{z}{L}\right)^{0.25} \end{cases} \quad (2.16)$$

for unstable conditions, where x is in radians for the \tan^{-1} term and L is the Monin-Obukhov length scale which assesses the stability of the lowest part of the atmospheric boundary layer (Stull, 1988). Golder (1972) established a relationship between the Pasquill stability classes, described previously (section 2.2.3), the Monin-Obukhov length and the roughness (z_0) :

$$\frac{1}{L} = a + b \log(z_0) \quad (2.17)$$

Pasquill stability class	Coefficients :	
	a	b
A: extremely unstable	-0.096	0.029
B: moderately unstable	-0.037	0.029
C: slightly unstable	-0.002	0.018
D: neutral	0	0
E: slightly stable	0.004	-0.018
F: moderately stable	0.035	-0.036

Table 2.9: Coefficients used in the relationship between the Pasquill stability classes and the Monin-Obukhov length (L) (Golder, 1972).

where the values of a and b for the different Pasquill stability classes are shown in Table 2.9.

The molecular diffusion resistance R_b is calculated by using the formulation given by Garland (1977).

$$R_b = 1.45 Re_*^{0.24} S_c^{0.8} u_*^{-1} \quad (2.18)$$

Re_* is the turbulent Reynolds number with $Re_* = u_* z_0 / \nu$, S_c the Schmidt number given by $S_c = \nu / D$, where ν is the kinematic viscosity of air and D is the diffusion coefficient of the entrained property in air ($D_{NH_3} = 2.1 \times 10^{-5}$). The value of $Sc^{0.8}$ is 0.734 and ν equals 1.4611×10^{-5} .

These descriptions of R_a , R_b and hence, V_d of NH_3 allow us to address a major drawback associated with Lagrangian models such as FRAME. This concerns the lack of vertical wind shear in the modelled air column, which is especially important close to the surface where large vertical gradients can occur. Since all model layers are advected with the same speed (geostrophic wind speed), it causes the lowest layers to spend less time than they should over an emission areas. This is important for ammonia since a significant proportion of it is dry deposited close to the source. However, part of this problem is addressed in the ammonia dry deposition parameterisation. Values of V_d are calculated using the surface wind data at a height of 3 m and hence, a better approximation of the friction velocity u_* is estimated than if the geostrophic wind speed had been used.

Wet deposition

Wet deposition is the removal of chemical species from the atmosphere through precipitation, and is dependent on scavenging, concentration and rainfall rate. The amount of material removed in a time period (Δt) is given by

$$\Delta c_i = c_i (1 - e^{-\lambda_i \Delta t}) \quad (2.19)$$

where Δc_i is the decrease in concentration of species “i” due to removal by precipitation, and λ_i is its scavenging coefficient. The wet deposition flux to the surface is the sum of wet removal from all volume elements aloft, assuming that the scavenged material comes down as precipitation.

The wet deposition process includes the dissolution of pollutants in cloud droplets by the various physical mechanisms during cloud formation, in-cloud scavenging (rain-out), and attachment to the falling hydro-meteors (washout) (Arya, 1999). The main source for washout is impaction and interception, where a rain particle accumulates particles in the layer below the cloud on its way down to the ground. When the rainfall is heavy, this mechanism quickly ceases to be effective, so that this mechanism probably accounts for the enhancement of sulphur and nitrogen concentrations at the beginning of some periods of rain. Snow has a much higher washout scavenging efficiency than rain (Dore *et al.*, 1992b). In the model, as in most atmospheric transport models, no differentiation is made between in-cloud and below-cloud processes and an averaged value of the scavenging ratio Δ_i is used to represent the overall effect. Scavenging ratios reflect the propensity of a species to be removed by precipitation, including all possible below-cloud and in-cloud processes. The scavenging ratios depend on the characteristics of the pollutant (e.g., solubility and reactivity for gases, size distribution for particles) as well as the nature of the precipitation (e.g.,

Species	λ (s ⁻¹)
SO ₂	8.67 x 10 ⁻⁶
Sulphate aerosol	1.14 x 10 ⁻⁴
H ₂ SO ₄	1.14 x 10 ⁻⁴
NH ₃	7.9 x 10 ⁻⁵
HNO ₃	7.9 x 10 ⁻⁵
Nitrate aerosol	1.14 x 10 ⁻⁴

Table 2.10: Scavenging coefficients (λ) used by the model to calculate wet deposition, based on a rainfall rate of 1 mm h⁻¹.

liquid or frozen). Scavenging ratios, consistent with those used in the EMEP model (Tarrason and Schaug, 1999), are combined with the rainfall rates and a 1000 m depth mixing layer to produce appropriate scavenging coefficients (Table 2.10). This depth of the mixing layer represents the height of the cloud top.

Orographic enhancement of wet deposition

Wet deposition in simple long-range transport models of acid deposition is treated as a loss term, based upon observed scavenging rates. However, for the UK conditions, a particular aspect of wet deposition requires careful consideration : the orographic enhancement of deposition from the seeder-feeder effect. Orographic enhancement of precipitation by the seeder-feeder effect is a widely observed and well understood phenomenon whereby precipitation is enhanced over high ground as a result of precipitation from high-level clouds (the seeder cloud) scavenging locally generated cap-clouds (the feeder cloud) on mountain tops (see Figure 2.8).

The process of orographic enhancement of precipitation was first described by Bergeron (1950). The terms seeder and feeder clouds were first used in Bergeron (1965). Bergeron (1965) outlined a mechanism whereby clouds at an upper air level (typically cirrostratus, altostratus or cumulonimbus) seed clouds at a lower level formed above hills (typically nimbostratus, stratus or the base of cumulonimbus) which feed upon the precipitation from above (Lee *et al.*, 2000).

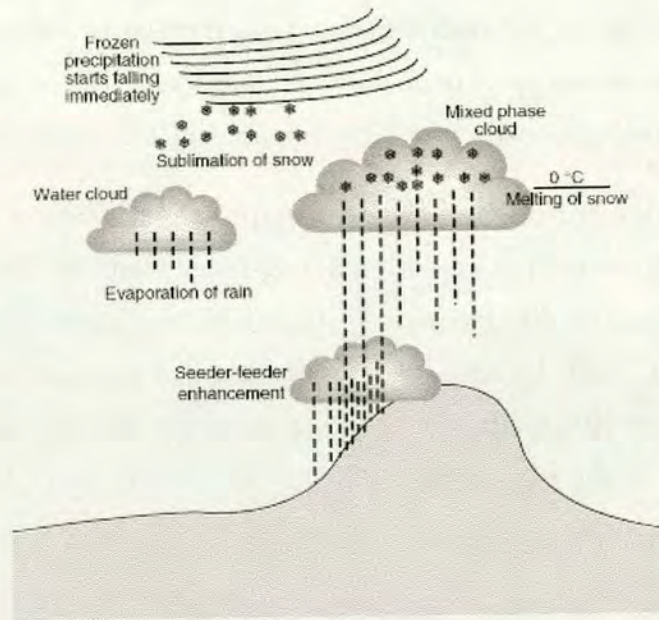


Figure 2.8: The seeder-feeder process of the orographic enhancement of wet deposition.

Since Bergeron (1950, 1965), much effort has been devoted to examining the process of orographic enhancement of precipitation. However, not all orographic precipitation is the result of the seeder-feeder effect. Smith (1979a) classifies the orographic control of precipitation in three ways : broad-scale up-slope rain, small-scale redistribution of rain by hills (the seeder-feeder effect) and orographic convective showers. However, the seeder-feeder mechanism has further effects in the transfer of pollutants to the ground. It has been shown that the concentrations of ions such as sulfate, nitrate and ammonium in cloud-water are much higher than those observed in precipitation such that scavenged cap-cloud results in enhanced wet deposition at altitude (Fowler *et al.*, 1988).

The precipitation composition monitoring network for the UK currently comprises 32 sites, none of which are located at very high elevations for ease of sample collection (NEG-TAP, 2001). Thus, in order to map deposition, precipitation composition is interpolated between these sites and multiplied by a 5 km field of precipitation amount based upon measurements at over 4000 locations within the UK (Lee *et al.*, 2000). Whilst this method for calculating deposition accounts for orographic enhancement of precipitation over high ground, it does not account for variation of its composition with altitude as a result of scavenging of cap-cloud.

Thus, a simple methodology has been devised to account for this process based upon observations of deposition enhancement (Dore *et al.*, 1992). This increases estimates of deposition of inorganic ions at high elevations.

As a full description of the orographic enhancement of wet deposition would be difficult to incorporate within a long-range transport model, a simple parameterisation of the “seeder-feeder” effect had been previously included in the model (Singles, 1996) by application of the method proposed by Dore *et al.* (1992). For locations with rainfall less than an assumed sea-level value of 700 mm yr^{-1} (P_{sl} ; mm h^{-1}), the scavenging coefficient for the species (λ_i) is calculated by :

$$\lambda_i = \frac{\Delta_i P}{H_{mix}} \quad (2.20)$$

where Δ_i is the scavenging ratio for species “i”, P is the precipitation rate (m s^{-1}) and H_{mix} is the mixing height (assumed to be 1000 m). Over areas where rainfall exceeds 700 mm yr^{-1} , it is assumed that this excess rainfall is due to altitudinal effects, and thus a fraction of the chemical species is removed by the seeder-feeder mechanism. In this case, λ_i is calculated by assuming that this excess rainfall will remove twice as much material as normal (enhancement of scavenging coefficients by a factor 2 above the threshold rainfall amount of 700 mm yr^{-1}), and thus :

$$\lambda_i = \frac{\Delta_i P_{sl}}{H_{mix}} + 2 \frac{\Delta_i (P - P_{sl})}{H_{mix}} \quad (2.21)$$

2.2.5 Chemical processes

Although ammonia is the main focus of interest of this study, it is necessary to consider the interactions with other species to simulate accurately its behaviour and more specifically its conversion in ammonium aerosols. Indeed, ammonia neutralises acidic substances such as sulphuric acid (H_2SO_4) and nitric acid (HNO_3) by producing ammonium sulphate ($(\text{NH}_4)_2\text{SO}_4$) and ammonium nitrate (NH_4NO_3). These species exist in either condensed or particulate form and their

Symbol	Definition	Rate of reaction ($\text{cm}^3 \text{s}^{-1} \text{molecule}^{-1}$)
J_{NO_2}	Photolysis : $NO_2 + h \nu \longrightarrow NO + O$	$J_{NO_2} = 7.5 \times 10^{-3} \exp(-0.39 \text{ sec}\theta)$ θ : sun zenith angle
k_{11}	$NO + O_3 \longrightarrow NO_2 + O_2$	$k_{11} = a_{11} \exp(-1450/T)$ $a_{11} = 2.1 \times 10^{-15}$
k_{12}	Rate of the reaction : $2 NO_2 + O_3 + H_2O \longrightarrow$ $2 NO_3^- + 2 H^+ + O_2$ $NO_2 + O_3 \longrightarrow NO_3 + O_2$ $NO_3 + NO_2 \longleftrightarrow N_2O_5$ $N_2O_5 + H_2O \longrightarrow 2 NO_3^- + 2 H^+$	$k_{12} = a_{12} \exp(-2450/T)$ $a_{12} = 2.4 \times 10^{-16}$
k_{21}	$NO_2 + OH \longrightarrow HNO_3$	$k_{21} = 1.1 \times 10^{-11}$
k_{77}	$NO_2 + CH_3COO_2 \longrightarrow PAN$	$k_{77} = 3.2 \times 10^{-12}$
k_P	Thermal decomposition of PAN	$k_P = a_D \exp(-12530/T)$ $a_D = 7.94 \times 10^{14} \text{ s}^{-1}$
q_a	Gas-to-particle conversion : $HNO_3 \longrightarrow NO_3^-$ Rate of reverse conversion is $q_a/2$	$q_a = 10^{-5} \text{ s}^{-1}$

Table 2.11: Chemical conversion rates ($\text{cm}^3 \text{s}^{-1} \text{molecule}^{-1}$) used in FRAME for nitrogen oxides reactions.

respective quantities depend on both concentrations of NH_3 and acids and on the relative humidity in the atmosphere.

Emissions data of NH_3 , NO_x and SO_2 are the main input data to initialise the chemical processes in the model. As the air column is moving along a trajectory, chemical interactions between eleven species take place. These are ammonia (NH_3), ammonium nitrate (NH_4NO_3), ammonium sulphate ($(NH_4)_2SO_4$), nitric oxide (NO), nitrogen dioxide (NO_2), nitric acid (HNO_3), peroxyacetyl nitrate (PAN), particulate nitrate (NO_3^-), sulphur dioxide (SO_2), sulphuric acid (H_2SO_4) and hydrogen peroxide (H_2O_2). The FRAME model combines descriptions of both dry chemistry and aqueous phase chemistry (Kruse-Plass *et al.*, 1993; ApSimon *et al.*, 1994; Barrett and Seland, 1995).

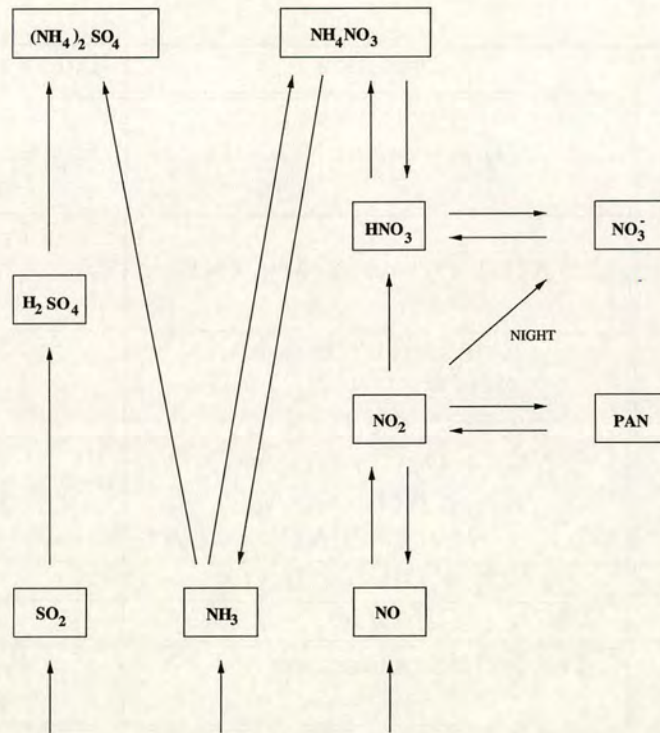


Figure 2.9: Dry chemistry scheme used in the FRAME model.

The dry chemistry in FRAME is represented in Figure 2.9. It shows the main reactions of oxidised nitrogen, sulphur and reduced nitrogen in the lower atmosphere. Table 2.11 gives the main gas phase reactions of oxidised nitrogen with their conversion rates. A detailed description of these reactions, as well as the gas and aqueous phase reactions of oxidised sulphur, can be found in Seinfeld (1986); Barrett and Seland (1995) and Singles (1996).

2.2.6 Sensitivity of FRAME to input parameters

Sensitivity experiments of FRAME to some input parameters have been done by Singles (1996). The first sensitivity study concerned the height of the cloud base which is assigned a value of 250 m in the model. This showed that the main process affected by varying this parameter is the oxidation of SO_2 to H_2SO_4 . Thus, while reduced nitrogen and oxidised nitrogen were hardly affected by a variation of this parameter, the change of the amount of sulphate in the column

with a height of cloud base of 500 m and 800 m led to a decrease of sulphate annual wet deposition by 12 % and 27 %, respectively.

Secondly, Singles (1996) presented a sensitivity analysis of the amount of cloud cover in the model. In FRAME, the cloud cover has been set at 6 oktas. This value was chosen because it represents a long-term average over the British Isles. However, it is interesting to see how sensitive is the model to this parameter. A comparison of annual modelled budgets of reduced nitrogen, oxidised nitrogen and sulphur has been done by Singles (1996) using a range of cloud cover values (i.e. 0, 4, 6 and 8 oktas). For reduced nitrogen, there is no linear relationship between cloud cover and the model results. The largest dry deposition occurs with zero cloud cover, since this state generates large daytime NH_3 dry deposition velocities. As well as large values of V_d , zero cloud cover produces large rates of vertical diffusion. At nighttime, zero cloud cover will have the opposite effect creating a very stable lower atmosphere and will suppress vertical dispersion and NH_3 dry deposition velocities. However, the low rate of vertical diffusion will lead to large modelled NH_3 surface concentration which can give large dry deposition flux.

Using a cloud cover value of 8 oktas means that diurnal variations in both vertical dispersion and deposition velocities will be suppressed and hence day and nighttime deposition fluxes will be similar. The reduced daytime rate of vertical diffusion will lead to larger surface concentration and this may offset the effect of the reduced modelled deposition velocities. Similarly, nighttime deposition velocities will be relatively large, as will the rate of vertical diffusion.

The overall effect on NH_3 dry deposition of varying the cloud cover shows how both the modelled rate of vertical diffusion and V_d are negative correlated with variations in cloud cover during the daytime, and are both positively correlated at night. Using two values which are at the extreme range of cloud coverage (0 and 8 oktas) produced a larger rate of dry deposition than compared with using mid-range values of 4 and 6 oktas. Wet deposition fluxes have an opposite results compared with the dry deposition. Increased dry deposition reduces the amount of reduced nitrogen in the atmosphere, and thus there is less NH_x available to be

wet deposited and exported (Singles, 1996).

The comparison for oxidised nitrogen and sulphur shows a more linear relationship between deposition/export and cloud cover. This is because the model uses an annually-averaged dry deposition map for NO_2 and SO_2 . The magnitude of these values is temporally-invariant and is not affected by any variation in the cloud cover, and thus the main factor is the rate of vertical diffusion. Zero cloud cover means reduced concentrations during the day due to increased vertical mixing. At nighttime, the rate of vertical diffusion will be low, but SO_2 and NO_x emissions are uniformly spread throughout the lowest 300 m, and the increased stability may lead to lower nocturnal concentrations as dry deposition may be greater than the rate of replenishment as material is transported down from higher levels in the air column. Suppression of diurnal variations will occur with complete cloud cover, and it leads to a large annual rate of dry deposition. Wet deposition of oxidised nitrogen and sulphur shows little variation between the results for the different cloud covers. Finally, all along the following chapters, the sensitivity of the model to some specific input parameters such as deposition velocities, scavenging coefficients or height of emissions will be assessed.

2.3 Results of FRAME 1.1

The parameterisations of the processes described in the previous sections are considered in the version 1.1 of the FRAME model. The previous version (FRAME 1.0) developed by Singles *et al.* (1998) considered Great Britain and the inclusion of Northern Ireland in FRAME 1.1 to form the United Kingdom is a first step before extending further the domain with Ireland (next chapter). The motivation of this section is to assess the FRAME model over the UK against measurements (2.3.1). To achieve this, two approaches are used. Firstly, the UK 1996 modelled budgets of reduced nitrogen, oxidised nitrogen and sulphur from FRAME (version 1.1) are analysed (section 2.3.2). Secondly, the performance of FRAME concentrations and deposition predictions against measurements is

investigated (section 2.3.3).

2.3.1 Uncertainties of the measurement based estimates

NEG-TAP (on behalf of the UK Department for Environment, Food and Rural Affairs) provides, through a long-term UK monitoring network, assessments of surface concentrations and UK budgets of the major pollutants. These budgets include the import of material to the UK, the export from the UK and emissions, depositions in the UK.

Our understanding of emissions of sulphur dioxide (SO_2) and oxidised nitrogen (NO_x) is generally sound and it is estimated that NO_x and SO_2 emissions are accurate to $\pm 30\%$ and $\pm 15\%$, respectively (NEG-TAP, 2001). However, ammonia (NH_3) emissions remain poorly characterised. In part this arises from the biological nature of the sources, the wide range of relevant agricultural practices and the influence of soil and climatic conditions. The flux of ammonia to land surfaces is bi-directional with both emission and deposition occurring at different times; this further complicates the estimation of net emissions.

Uncertainties also occur in the the mapping of concentrations and depositions from interpolated measurements, long-range transport models and inferential models. However, the heterogeneous distribution of measurement sites prohibits an overall uncertainty evaluation. Indeed, uncertainties in air concentrations can be expected very close or far from major sources and/or in areas with strongly deviating precipitation climatology. Moreover, the limited accuracy and the non-representativity of measurement sites of some of the precipitation concentration measurements lead to errors on wet deposition maps. Thus, The uncertainty of the wet deposition rate based on interpolated measurements of precipitation concentration and precipitation amount can reach 50 % and larger uncertainties (about 70 %) were found by Van Leeuwen *et al.* (1995) in mountainous areas and complex terrain. Moreover, the same is to be expected if the measurement network is not as dense as in Northwest Europe (Schaug *et al.*, 1993).

The uncertainty in the total UK deposition is determined by the uncertainty in wet, dry and cloud and fog deposition. The latter is not taken into account by most models and rarely measured. The uncertainty of dry deposition is generally much larger than that of wet deposition. Total deposition estimates are more uncertain in areas with complex terrain and with strong horizontal concentration gradients. The uncertainty in total deposition (grid square average) of acidifying compounds (nitrogen and sulphur) can be estimated to be 70-120 % (Draaijers and Erisman, 1993; Erisman and Draaijers, 1995). These large uncertainties illustrate the need of caution when validating the FRAME model results by measurements of airborne concentrations, wet deposition, dry deposition and throughfall.

Finally, it should be noted that the measured-based estimate of the 5 km grid average was used rather than the raw data for the monitoring site, in order to make a valid comparison of the two different 5 km grid-based estimates.

2.3.2 Atmospheric budgets of N and S calculated with FRAME 1.1

Table 2.12 shows the United Kingdom 1996 reduced nitrogen budget obtained with FRAME 1.1. The second column indicates the 1996 NEG-TAP (National Expert Group on Transboundary Air Pollution) estimations derived as far as possible from 1995-97 measurements (NEG-TAP, 2001).

While the dry deposition budget (95 kt N yr^{-1}) is consistent with the NEG-TAP estimations (99 kt N yr^{-1}), FRAME 1.1 strongly underestimates the UK wet deposition budget with an amount of 71 kt N yr^{-1} compared to a NEG-TAP estimate of 110 kt N yr^{-1} . The total deposition over the UK is underestimated and hence, FRAME 1.1 exports too much reduced nitrogen.

Table 2.13 shows similar results from FRAME 1.1 concerning the UK 1996 oxi-

UK reduced nitrogen (kt N yr ⁻¹)	(NEG-TAP, 2001) 1996 estimations	FRAME 1.1 1996
Import	30	24
Emission	282	291
Dry deposition	99	95
Wet deposition	110	71
Total deposition	209	166
Export	103	149

Table 2.12: Budgets of reduced nitrogen for the UK for 1996 compared against the measurement based estimates of NEG-TAP. FRAME 1.1 values are estimated including both Great Britain and Northern Ireland in the domain. Units are ktonnes N yr⁻¹.

dised nitrogen budget. The 1996 UK budget of wet deposition of NO_y is closer to the NEG-TAP estimations than for NH_x but the dry deposition is significantly underestimated. It leads to an underestimation of the total NO_y deposition over the UK. Added to the difference in the import budget with NEG-TAP, FRAME 1.1 overestimates the export of NO_y.

The UK 1996 sulphur budget is presented in Table 2.14. While the FRAME 1.1 and NEG-TAP estimates of total S deposition agree quite well, the partitioning between wet and dry deposition does not match.

UK oxidised nitrogen (kt N yr ⁻¹)	(NEG-TAP, 2001) 1996 estimations	FRAME 1.1 1996
Import	60	117
Emission	615	590
Dry deposition	87	32
Wet deposition	91	107
Total deposition	178	139
Export	497	568

Table 2.13: Budgets of oxidised nitrogen for the UK for 1996 compared against the measurement based estimates of NEG-TAP. FRAME 1.1 values are estimated including both Great Britain and Northern Ireland in the domain. Units are ktonnes N yr⁻¹.

UK sulphur (kt S yr ⁻¹)	(NEGTAP, 2001) 1996 estimations	FRAME 1.1 1996
Import	90	88
Emission	1014	1005
Dry deposition	125	158
Wet deposition	171	142
Total deposition	296	300
Export	808	793

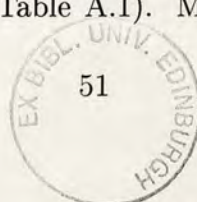
Table 2.14: Budgets of sulphur for the UK for 1996 compared against the measurement based estimates of NEG-TAP. FRAME 1.1 values are estimated including both Great Britain and Northern Ireland in the domain (UK). Units are ktonnes S yr⁻¹.

2.3.3 Comparison with measurements

Although a comparison of budgets allows an overall appraisal of the model, a more precise analysis of the modelled regional distribution of concentration and deposition is necessary to evaluate the performance of the model. To achieve this, both UK maps and comparisons with measurements are shown. As a background, a brief review of the monitoring networks is provided.

Monitoring networks

The UK National Ammonia Monitoring Network (NAMN) was established in 1996 to provide concentration measurements of NH₃ and NH₄⁺ (Sutton *et al.*, 1998). The network involves 70 sites for NH₃ of which 46 measure NH₄⁺ concentration simultaneously. Measuring methods include low cost denuders (DELTA) sampling at 50 sites, diffusion tube sampling at 30 sites and both methods at 10 sites (Sutton *et al.*, 2002, 2001). The DELTA sites were distributed widely across the UK to provide regional patterns of NH₃ and NH₄⁺. Figure 2.10 shows a map of the location of these 70 monitoring sites across the United Kingdom. The measured mean concentrations of NH₃ and NH₄⁺ at the different sites for 1996 are given in Appendix A (Table A.1). Measured mean concentrations of



NO₂ and SO₂ for 1996 from the UK Monitoring Network are also provided in Tables A.2 and A.3, respectively (Appendix A).

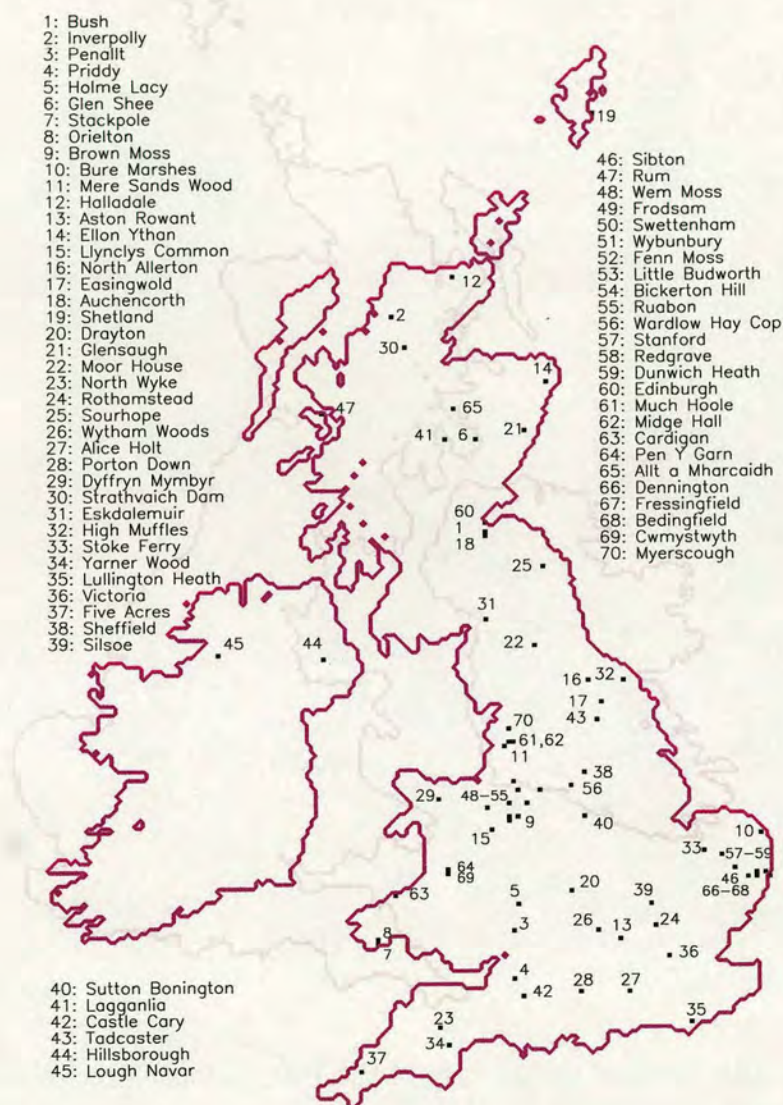


Figure 2.10: Map of sites in the UK National Ammonia Monitoring Network.

Measurements of NH₄⁺, NO₃⁻ and SO₄²⁻ wet deposition are provided through the UK National Precipitation Composition Monitoring Network. These are monitored at a rural network of 32 sites using bulk collectors mounted 1.5 to 2 m above-ground sampled weekly (NEGTAP, 2001). Figure 2.11 shows a map of the location of these 32 monitoring sites across the United Kingdom. The measured mean wet depositions of NH₄⁺, NO₃⁻ and SO₄²⁻ at these sites for 1996 are given in Appendix A (Table A.4).

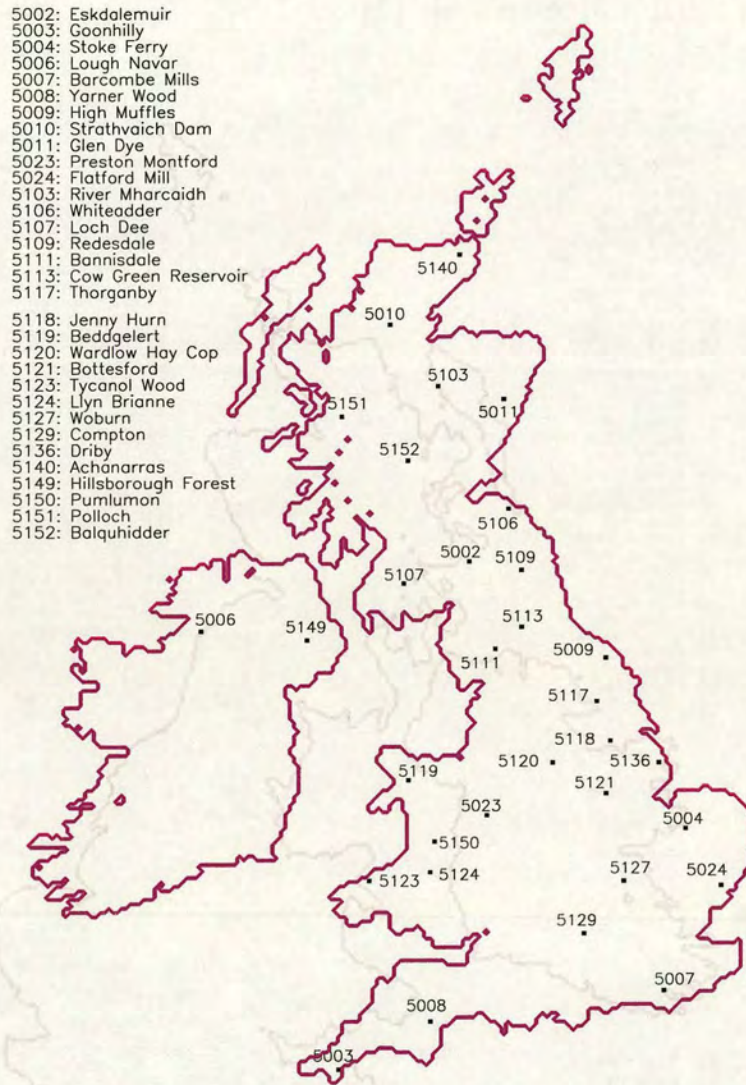


Figure 2.11: Map of the 32 sites of the UK National Precipitation Composition Monitoring Network.

Finally, the performance of FRAME is investigated by comparing the mean measured values for 1996 with the modelled values of the bottom layer (1-2 m) for the corresponding grid square.

Ammonia concentration

Figure 2.12 shows the distribution of NH_3 surface concentration obtained with FRAME 1.1 for 1996 for the UK. The modelled NH_3 surface concentrations are consistent with the distribution of the NH_3 emissions (Figure 1.1), exhibiting a significant spatial variability. The highest air concentrations appear in a broad band along the borders of England and Wales, in Lancashire and in the east of Northern Ireland. This corresponds mainly to livestock, cattle and sheep farming in these areas, as well as more local high emission areas in north-west England. A further high emission area in eastern England (East Anglia and Yorkshire) is associated with large poultry and pig farming. High concentrations are also apparent in large cities such as London. One of the most significant features is the model estimation of extremely small air concentrations over the whole of the Scottish Highlands, reflecting an extremely low emission density in this area.

The performance of the model predictions for NH_3 surface concentrations is illustrated for locations that are included in the UK National Ammonia Monitoring Network. The value for each network site is compared with the FRAME model estimate for the 5 km grid square in which it occurs. Since the measured and modelled NH_3 surface concentrations are log-normally distributed, Figure 2.13 shows the comparison on a logarithmic scale, underlining the large spatial variability of NH_3 which can not be resolved by the 5 km resolution of the model. The central dotted line is a one to one agreement. Each point has a number assigned which corresponds to the location of the monitoring site shown in Figure 2.10. It leads to a low correlation coefficient ($R_{\log}^2 = 0.55$ or $R_{\text{absolute}}^2 = 0.39$) with FRAME providing slightly higher concentrations than the measurements, in some areas, and slightly lower concentrations in remote areas.

Ammonium concentration

The spatial pattern of modelled NH_4^+ aerosol surface concentrations is much less variable than NH_3 . Figure 2.14 shows the highest concentrations occurring

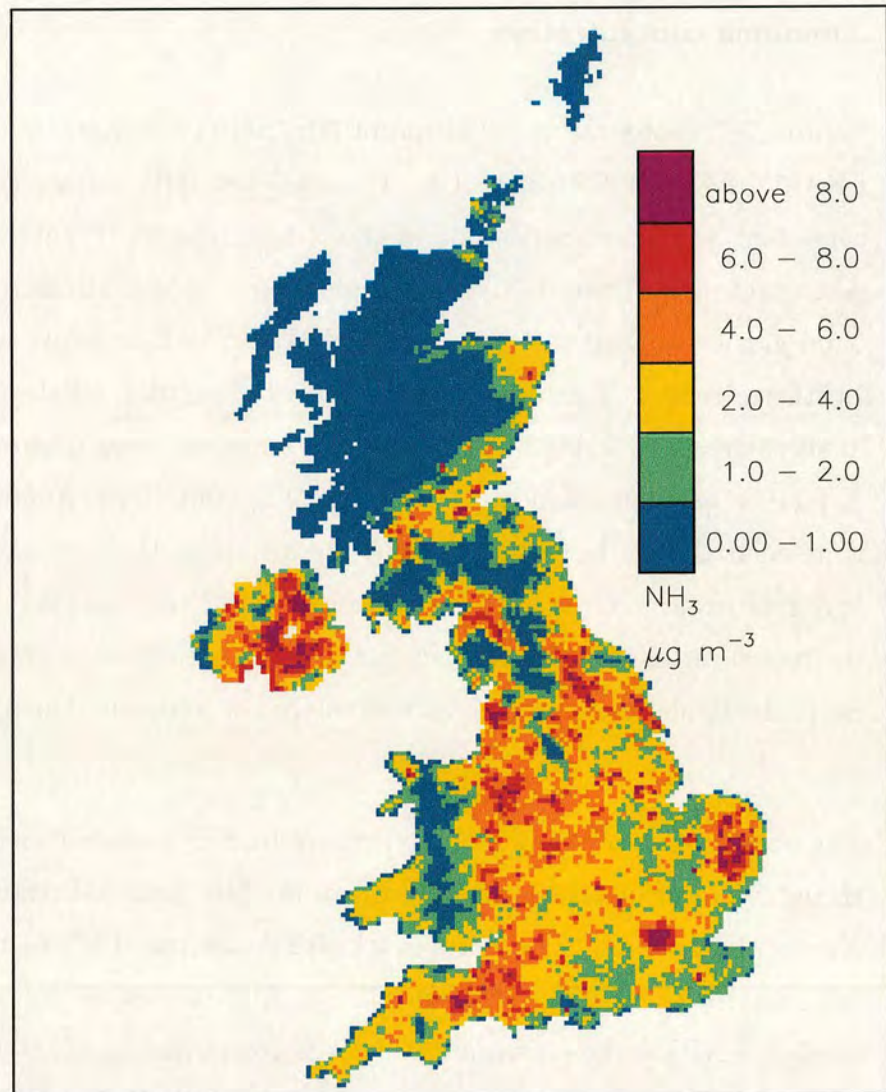


Figure 2.12: Modelled surface concentrations (1-2 m) of NH_3 for the UK for 1996 at a $5 \text{ km} \times 5 \text{ km}$ resolution (FRAME 1.1). Units are $\mu\text{g m}^{-3}$.

in London and in areas of high emissions of SO_2 in northern England (see Figure 2.1). Low concentrations occur in the West of England and in Scotland. Moreover, the longer atmospheric residence time of NH_4^+ allows it to be both transported over larger distances and more vertically mixed than NH_3 . It leads to less spatial variability than NH_3 and hence, a better correlation coefficient ($R^2 = 0.86$) is obtained in the comparison with measurements (Figure 2.16). The solid line is the best fit line produced by a regression analysis. However, the model overestimates the NH_4^+ concentration which may be related to the underestimation of the wet deposition budget of NH_x shown in the previous

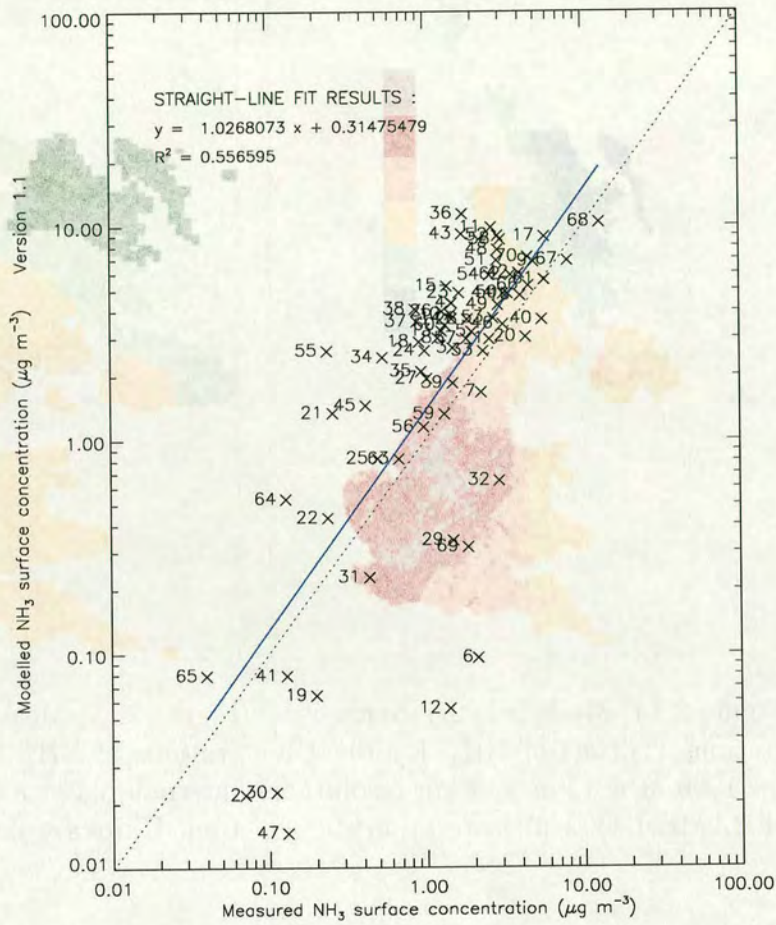


Figure 2.13: Plot of modelled NH_3 surface concentration values (FRAME 1.1) against measured values for 1996. The central dotted line is a one to one agreement. The solid blue line is the best fit line produced by a regression analysis. Each point has a number assigned which corresponds to the location of the monitoring site shown in Figure 2.10.

section (Table 2.12), indicating insufficient scavenging of NH_x . Figure 2.15 shows a map of the measured NH_4^+ surface concentration interpolated at a 5 km resolution over the UK. It underlines the overestimation of this field by the FRAME model, especially in the centre and east of England.

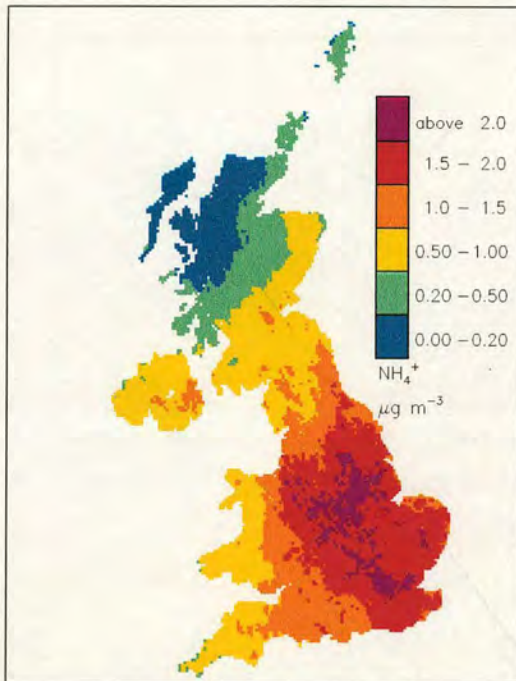


Figure 2.14: Modelled surface concentrations (1-2 m) of NH_4^+ for the UK for 1996 at a $5 \text{ km} \times 5 \text{ km}$ resolution (FRAME 1.1). Units are $\mu\text{g m}^{-3}$.

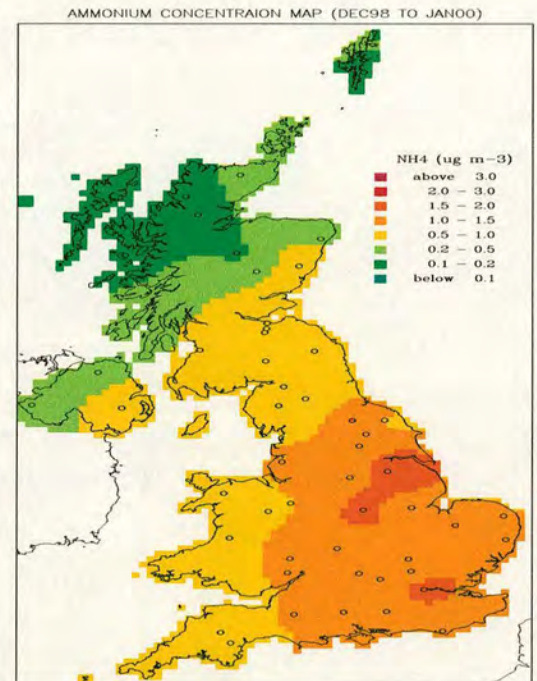


Figure 2.15: Measured surface concentrations of NH_4^+ for the UK for 1996 interpolated at a $5 \text{ km} \times 5 \text{ km}$ resolution. Units are $\mu\text{g m}^{-3}$.

Wet deposition of reduced nitrogen

The modelled distribution of NH_x (NH_4^+ and NH_3) wet deposition for 1996 is presented in Figure 2.17. This shows the highest wet deposition in hill areas of central northern England and Wales. High rates of wet deposition correspond to areas of large precipitation occurring near to regions of intensive agricultural activity.

The performance of FRAME 1.1 predictions for NH_x wet deposition is illustrated for locations from the UK National Precipitation Composition Monitoring Network (Figure 2.19). The model shows a reasonable agreement with the 1996 measurements ($R^2 = 0.67$), but gives smaller values corroborating the underestimation of the budget of NH_x wet deposition obtained previously (Table 2.12). The ratio map (Figure 2.18) with the interpolated measured values of NH_x wet deposition illustrates this underestimation of the modelled values from FRAME 1.1. In this respect, the results of FRAME are similar to those of other

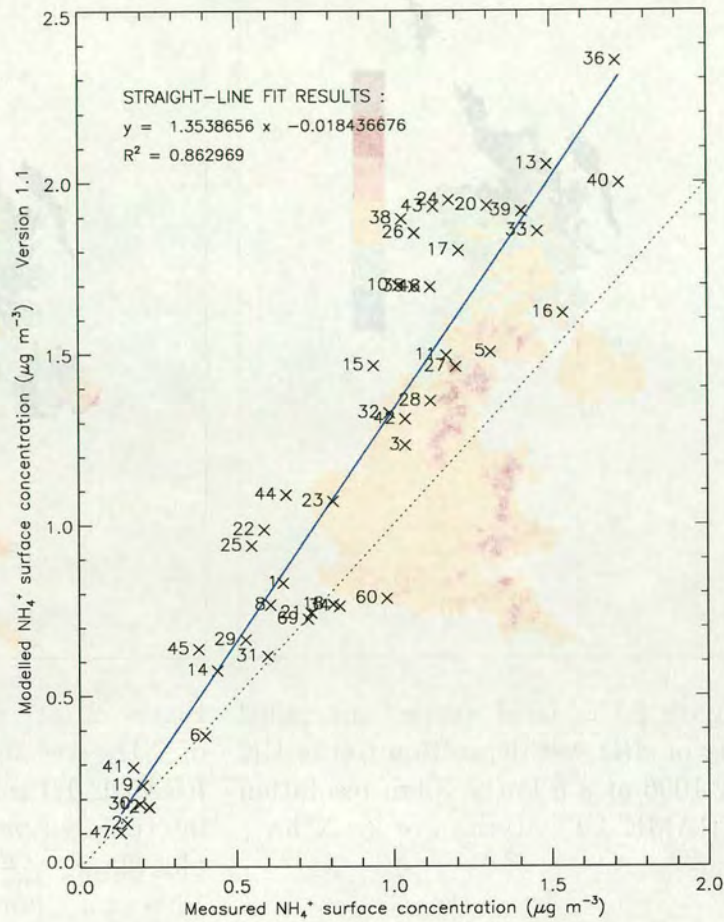


Figure 2.16: Plot of modelled NH_4^+ surface concentration values (FRAME 1.1) against measured values for 1996. The central dotted line is a one to one agreement. The solid blue line is the best fit line produced by a regression analysis. Each point has a number assigned which corresponds to the location of the monitoring site shown in Figure 2.10.

models for the UK, which all underestimate NH_x wet deposition (NEGTA, 2001).

Dry deposition of NH_3

Figure 2.20 shows the 1996 flux of NH_3 dry deposition to the UK modelled with FRAME 1.1. Similar to the map of air concentrations (Figure 2.12), the areas with large deposition rates are generally associated with areas of

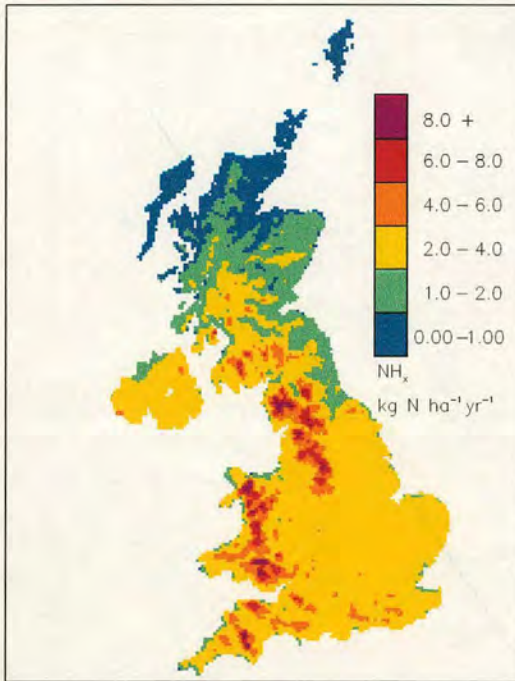


Figure 2.17: Grid average modelled flux of NH_x wet deposition to the UK for 1996 at a $5 \text{ km} \times 5 \text{ km}$ resolution (FRAME 1.1). Units are $\text{kg N ha}^{-1} \text{ year}^{-1}$.

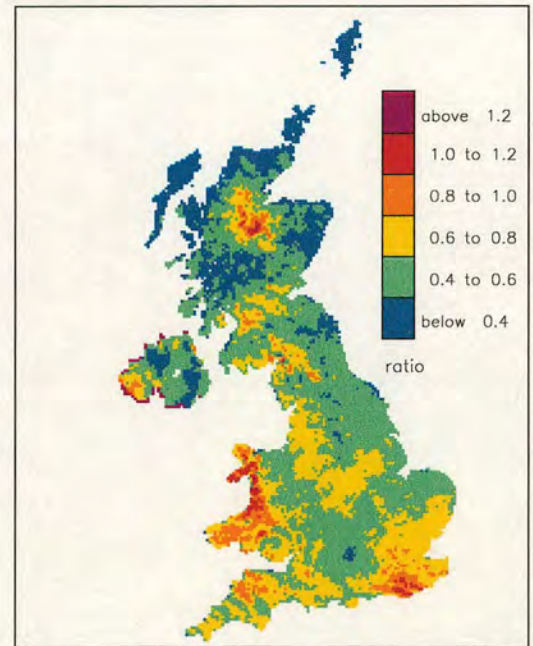


Figure 2.18: Ratio map of the flux of NH_x wet deposition between the FRAME 1.1 modelled values and the interpolated measured values. The plot shows $\frac{\text{FRAME1.1}}{\text{Measurement}}$ to the UK for 1996 at a $5 \text{ km} \times 5 \text{ km}$ resolution.

high emissions. These areas include south-west England, the Wales-England border, north England and parts of Northern Ireland. Otherwise, the largest deposition occurs in areas where there are both high emissions and large areas of semi-natural ecosystems, such as forest and moorland, generally in the west. This is due to large values of V_d calculated for these land cover types by the model. Consequently, in areas where emissions are large, but the modelled deposition velocity is small, such as in East Anglia, regional dry deposition will be smaller but the NH_3 surface air concentration will be greater than in areas with similar emissions in the west. It should be noted that the deposition rates shown in Figure 2.20 are grid-square averages. Since deposition rates are substantially smaller for agricultural land than for forest and semi-natural vegetation, the grid averages shown here are much smaller than received by these ecosystems. Hence, for critical loads comparisons, receptor maps for specific

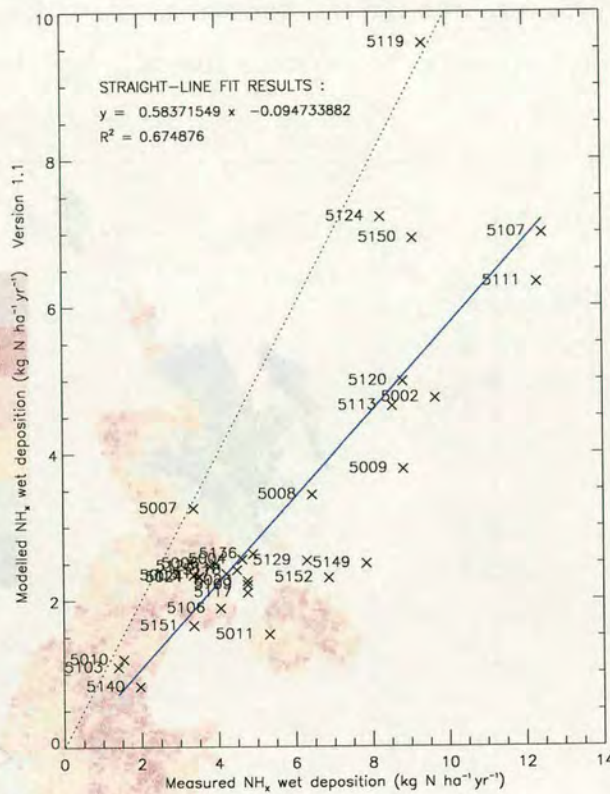


Figure 2.19: Plot of modelled NH_x wet deposition values (FRAME 1.1) against measured values for 1996. The central dotted line is a one to one agreement. The solid blue line is the best fit line produced by a regression analysis. Each point has a number assigned which corresponds to the location of the monitoring site shown in Figure 2.11.

ecosystems should be used (Singles *et al.*, 1998). For example, a plot of the estimated 1996 flux of modelled dry deposition of NH_3 to moorland is given in Figure 2.21. This plot is closely related to the NH_3 surface concentration (Figure 2.12), with the largest estimate of dry deposition occurring in the areas of highest concentration. In these areas, the estimated dry deposition flux is greater than $30 \text{ kg N ha}^{-1} \text{ year}^{-1}$. In most of northern England, Wales and Scotland, the flux to moorland is less than $10 \text{ kg N ha}^{-1} \text{ year}^{-1}$. A similar plot of the annual flux of modelled dry deposition of NH_3 to forest areas is shown in Figure 2.22. The spatial distribution is similar to the previous figure but the values are larger. This is a consequence of the modelled values of the deposition velocity being larger than the value for moorland. The maximum dry deposition fluxes to forest exceed $50 \text{ kg N ha}^{-1} \text{ year}^{-1}$. As with the moorland plot, in areas

of low surface concentrations, such as northern England, Wales and Scotland, the dry deposition flux to forests is generally less than $10 \text{ kg N ha}^{-1} \text{ year}^{-1}$.

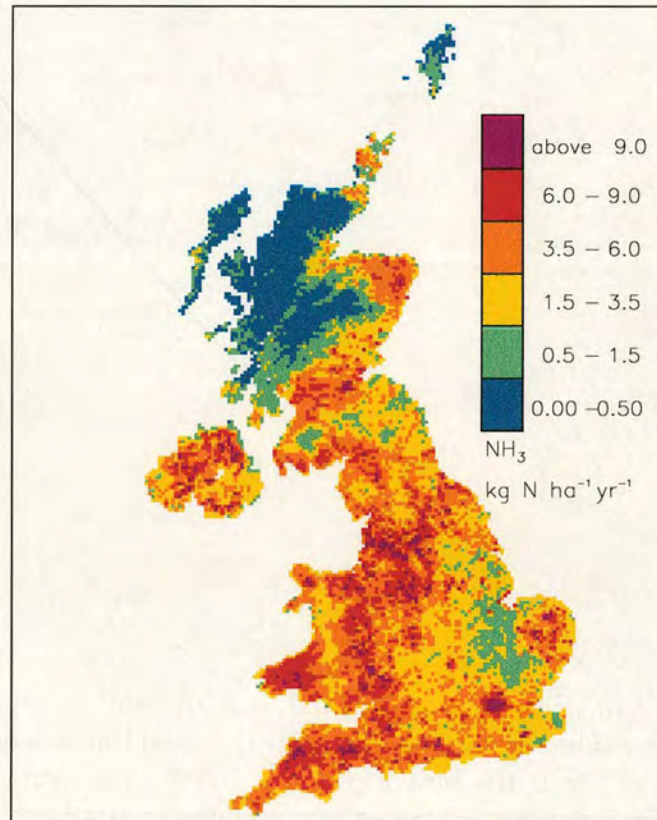


Figure 2.20: Grid average modelled flux of NH_3 dry deposition to the UK for 1996 at a $5 \text{ km} \times 5 \text{ km}$ resolution (FRAME 1.1). Units are $\text{kg N ha}^{-1} \text{ year}^{-1}$.

Sulphur

The modelled SO_2 surface concentrations are shown in Figure 2.23. They reflect the distribution of emissions with the largest concentrations occurring in the north Midlands, south Yorkshire and the south-east of England. These 1996 modelled values are compared with the 1996 measured data, from the UK Rural Sulphur Dioxide Monitoring Network (Appendix A, Table A.3), in Figure 2.25. The central dotted line is a one to one agreement and the solid line is the best fit line produced by a regression analysis. Each point has a number assigned which corresponds to the location of the monitoring site. The model over-predicts the

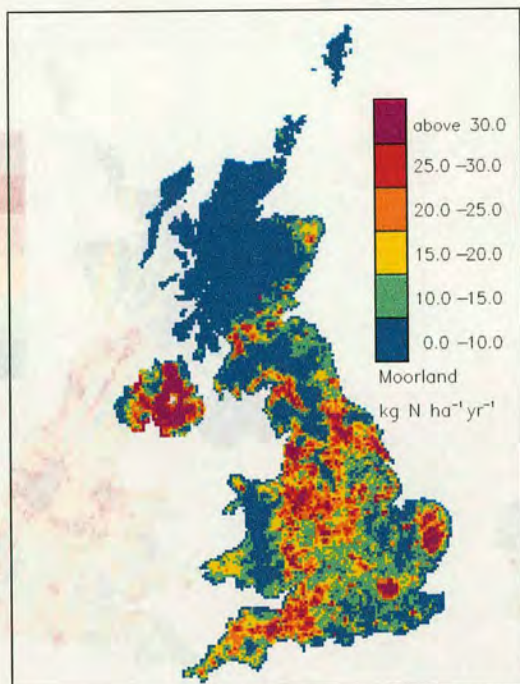


Figure 2.21: Estimated flux of modelled dry deposition of NH_3 to areas of moorland in the UK in 1996 at a $5 \text{ km} \times 5 \text{ km}$ resolution (FRAME 1.1). Units are $\text{kg N ha}^{-1} \text{ year}^{-1}$.

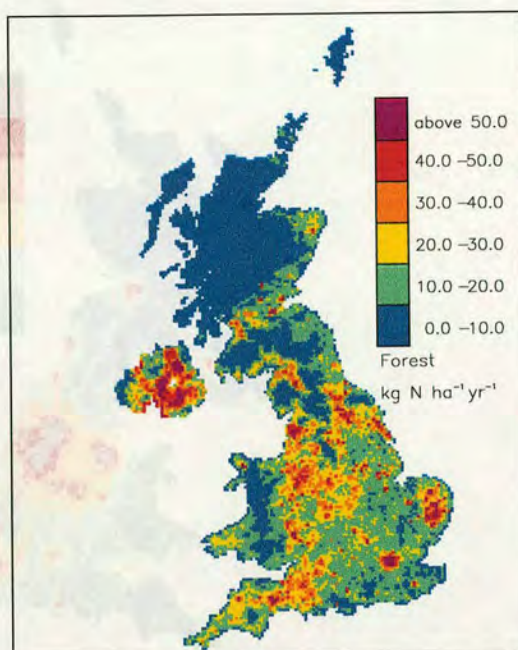


Figure 2.22: Estimated flux of modelled dry deposition of NH_3 to areas of forest in the UK in 1996 at a $5 \text{ km} \times 5 \text{ km}$ resolution (FRAME 1.1). Units are $\text{kg N ha}^{-1} \text{ year}^{-1}$.

measurements in regions of important SO_2 emissions, especially in the Yorkshire (sites 5317, 5315, 5322, 5310, 5303) or in the Thames Estuary (sites 5302, 5333), and under-predicts in the other areas such as Scotland, Wales or Cornwall. This is corroborated in the ratio map (Figure 2.24) with the interpolated measured values (only available for Great Britain).

The SO_4^{2-} wet deposition is underestimated as it can be seen in the comparison with measurements (Figure 2.28) and in the previous study of the UK budgets (Table 2.14). The modelled distribution of SO_4^{2-} wet deposition for 1996 is presented in Figure 2.26. The highest rates of deposition are located in Wales and northern England where there is either high rainfall or high SO_2 emissions. The ratio map between measured and modelled values (Figure 2.27) shows a general underestimation by the FRAME model while local overestimations are associated with high SO_2 emission areas. The uniform distribution of these SO_2 emissions throughout the lowest 300 m of the air

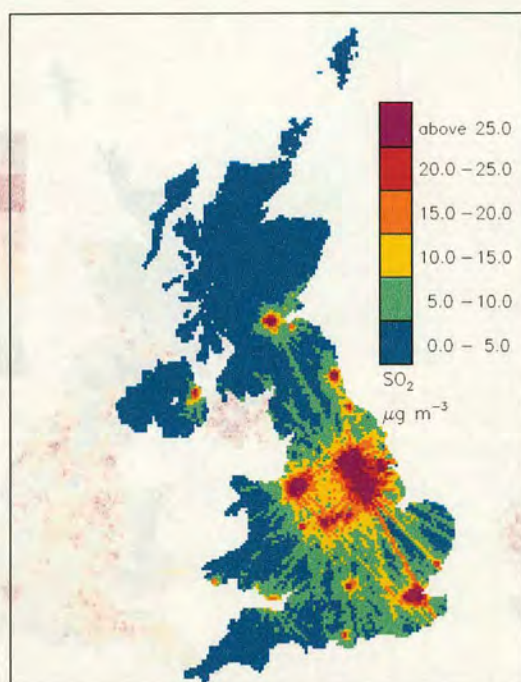


Figure 2.23: Modelled surface concentrations (1-2 m) of SO_2 for the UK for 1996 at a $5 \text{ km} \times 5 \text{ km}$ resolution (FRAME 1.1). Units are $\mu\text{g m}^{-3}$.

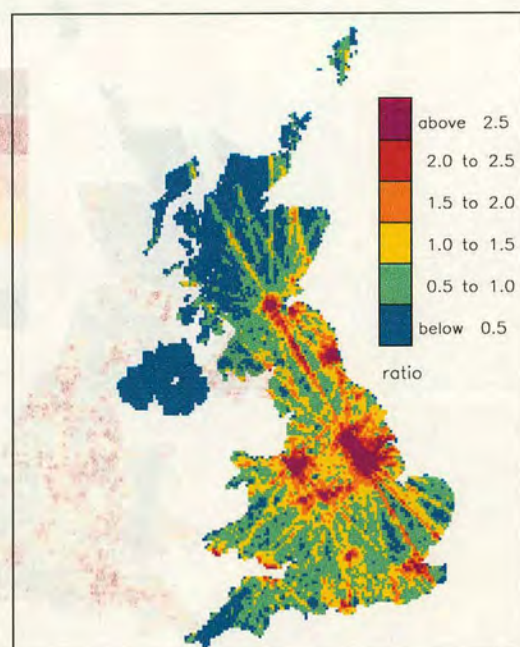


Figure 2.24: Ratio map of SO_2 surface concentration between the FRAME 1.1 modelled values and the interpolated measured values. The plot shows $\frac{\text{FRAME1.1}}{\text{Measurement}}$ to Great Britain for 1996 at a $5 \text{ km} \times 5 \text{ km}$ resolution.

column (instead of using a plume rise parameterisation taking into account the height of the source) could explain this behaviour of SO_4^{2-} wet deposition, the overestimation of the modelled SO_2 surface concentrations in emission areas and thus, leads to the overestimation of the dry deposition. Moreover, the stripes in the sulphur maps reflect the lack of resolution in the wind rose used currently. This species would benefit of considering more wind directions, i.e. using 72 equally-spaced wind directions instead of 24 (5 degree instead of 15).

Oxidised nitrogen

The modelled NO_2 surface concentrations are shown in Figure 2.29. As for SO_2 but less stripy, the pattern follows the distribution of the NO_2 emissions with

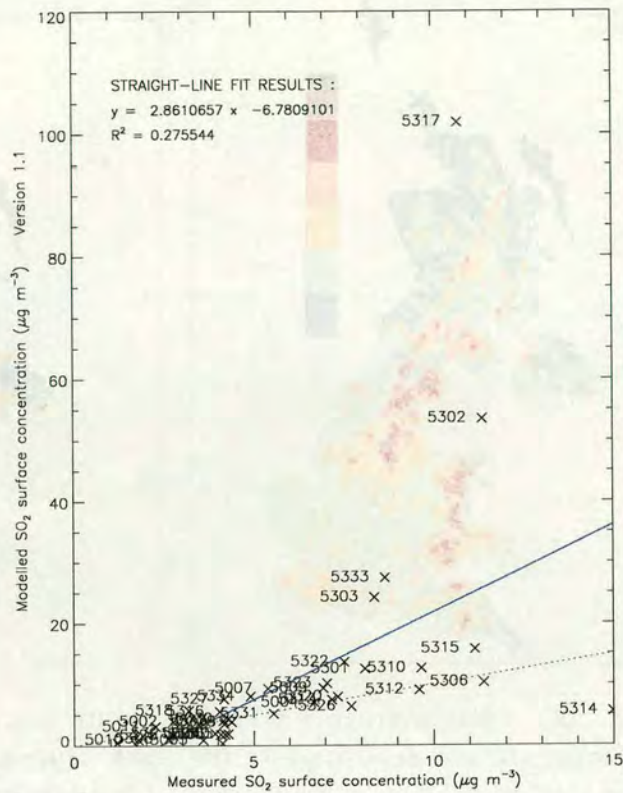


Figure 2.25: Plot of modelled SO₂ surface concentration values (FRAME 1.1) against measured values for 1996. The central dotted line is a one to one agreement. The solid blue line is the best fit line produced by a regression analysis. Each point has a number assigned which corresponds to the monitoring site shown in Table A.3 (Appendix A).

high concentrations between the Midlands and south Yorkshire, and in the area of London. The comparison of the modelled 1996 NO₂ surface concentrations with the measurements, from the UK Nitrogen Dioxide Monitoring Network (Appendix A, Table A.2), is illustrated in Figure 2.31. The model underestimates the measurements by typically 25 %, except in high emission areas. This is corroborated in the ratio map (Figure 2.30) with the interpolated measured values (only available for Great Britain). This will lead partly to the low UK budget of oxidised nitrogen dry deposition (see Table 2.13), although the difference in the budget is much larger which is due to difference in HNO₃. Further studies concerning the role of HNO₃ are carried in Chapter 4. Moreover, it shows again that the uniform distribution of the NO₂ emissions throughout the lowest 300 m of the air column is maybe not appropriate as most of these

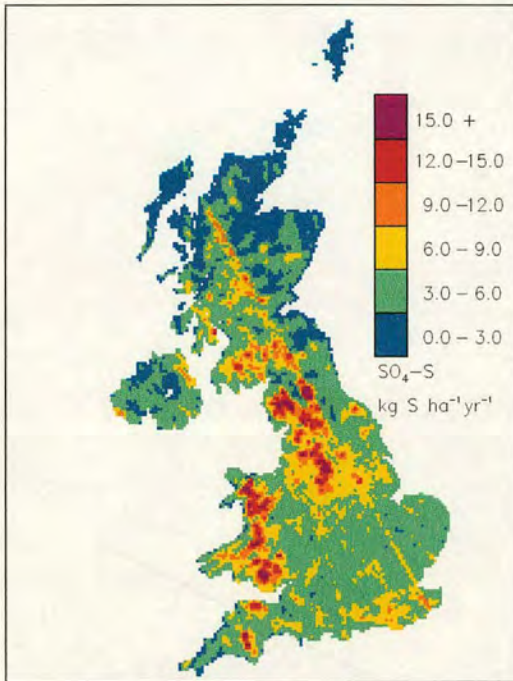


Figure 2.26: Grid average modelled flux of sulphate wet deposition to the UK for 1996 at a $5 \text{ km} \times 5 \text{ km}$ resolution (FRAME 1.1). Units are $\text{kg S ha}^{-1} \text{ year}^{-1}$.

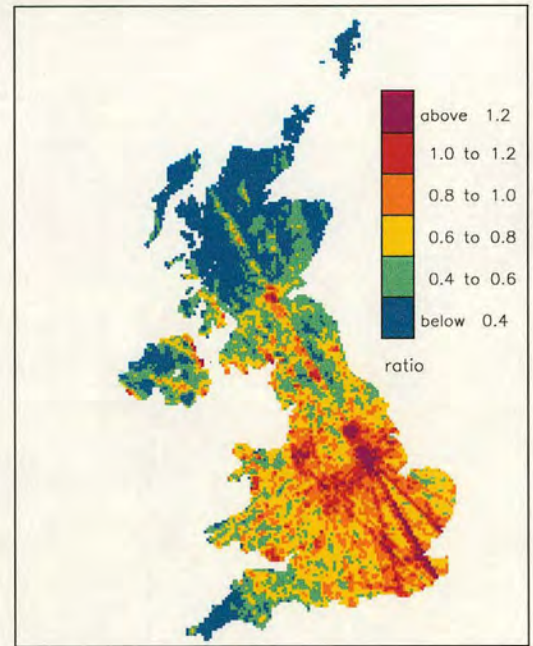


Figure 2.27: Ratio map of sulphate wet deposition between the FRAME 1.1 modelled values and the interpolated measured values. The plot shows $\frac{\text{FRAME1.1}}{\text{Measurement}}$ to the UK for 1996 at a $5 \text{ km} \times 5 \text{ km}$ resolution.

emissions come from road traffic.

The correlation plot between modelled and measured values of NO_3^- wet deposition shows an agreement strongly affected by the predictions of the model in Wales (Figure 2.34; sites 5150, 5124, 5119). The distribution of this NO_3^- wet deposition is presented in Figure 2.32. The highest rates of deposition are located in Wales, around the Pennine hills and in the north west of Scotland where there is either high rainfall or high NO_x emissions. High deposition in Cornwall and Devon is caused by important import from France and Belgium. In these locations, FRAME 1.1 overestimates the interpolated measured values as it is shown in Figure 2.33. This is also the case in Northern Ireland and the south of England.

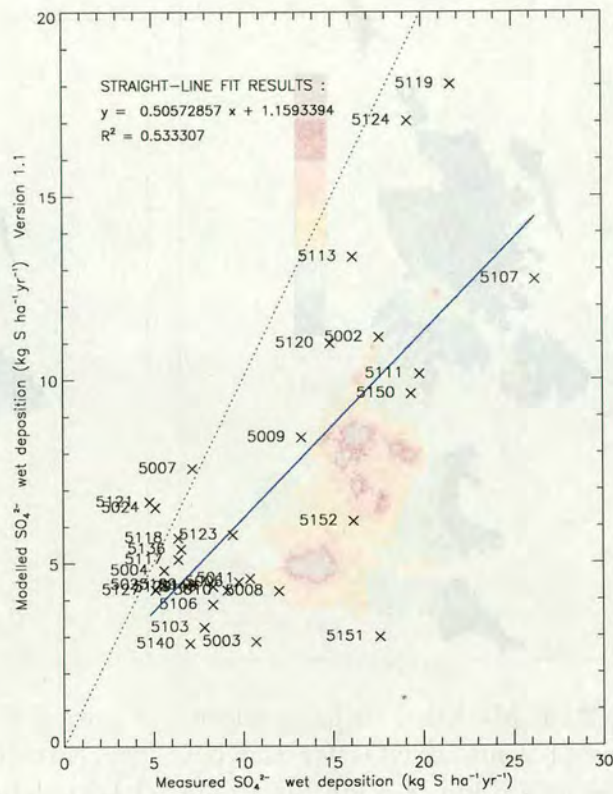


Figure 2.28: Plot of modelled SO_4^{2-} wet deposition values (FRAME 1.1) against measured values for 1996. The central dotted line is a one to one agreement. The solid blue line is the best fit line produced by a regression analysis. Each point has a number assigned which corresponds to the location of the monitoring site shown in Figure 2.11.

2.4 Summary

The FRAME model was developed from the TERN model of ApSimon *et al.* (1994) to simulate the spatial pattern of concentration and deposition of reduced nitrogen over the UK (Singles *et al.*, 1998). FRAME is a long-term statistical trajectory model, at a $5 \text{ km} \times 5 \text{ km}$ resolution, using a detailed NH_3 emission field. FRAME uses a single wind rose with a mean wind speed for each wind direction. Straight-line trajectories are assumed to arrive from 24 wind directions, 15 degrees apart. Each trajectory is run for 4 separate times, 6 hours apart, and combined accordingly to get 24-hour averaged values. FRAME describes the main atmospheric processes taking place in a column of air. The vertical diffusion is treated explicitly using a multi-layer system

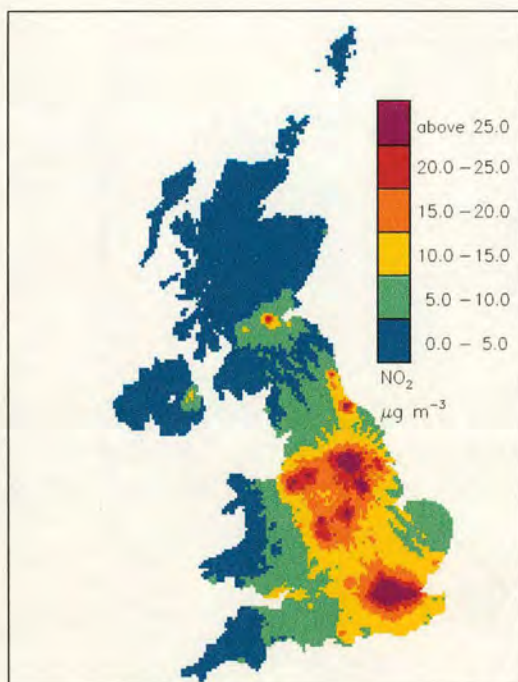


Figure 2.29: Modelled surface concentrations (1-2 m) of NO_2 for the UK for 1996 at a $5 \text{ km} \times 5 \text{ km}$ resolution (FRAME 1.1). Units are $\mu\text{g m}^{-3}$.

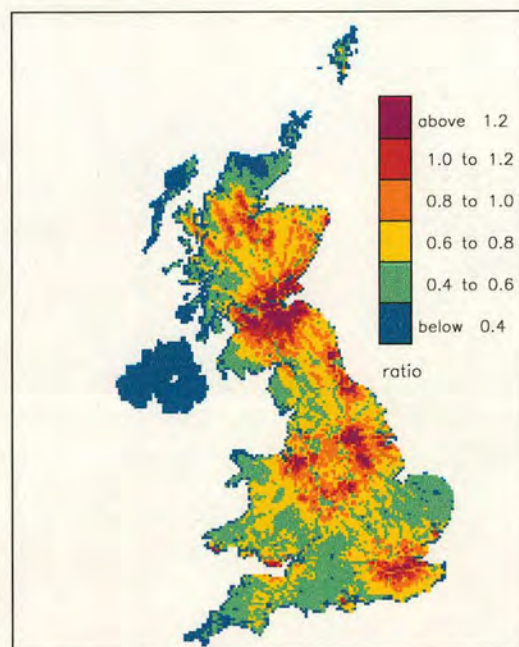


Figure 2.30: Ratio map of NO_2 surface concentration between the FRAME 1.1 modelled values and the interpolated measured values. The plot shows $\frac{\text{FRAME1.1}}{\text{Measurement}}$ to Great Britain for 1996 at a $5 \text{ km} \times 5 \text{ km}$ resolution.

with 33 layers of variable depth. The depth of the mixing layer varies between day and night. As the air column is moving along a straight-line trajectory, chemical interactions between NH_3 , SO_2 and NO_x take place. Emissions of NH_3 are introduced in the lowest layer at a height of 1 m, whereas SO_2 and NO_x emissions are evenly distributed throughout the lowest 300 m of the mixing layer. Concentrations at the edge of the FRAME domain are initialised using output from the European TERN model. Dry deposition of SO_2 and NO_2 is modelled through the use of land-cover dependent deposition velocities (Smith *et al.*, 2000), whereas other species are assigned single specific deposition velocities. In the case of NH_3 , diurnally-varying deposition velocities are calculated using the land-cover, the surface wind speed and the Canopy Resistance Model. Wet deposition is described by scavenging coefficients using constant drizzle. Finally, FRAME produces budgets of reduced nitrogen, oxidised nitrogen, sulphur and

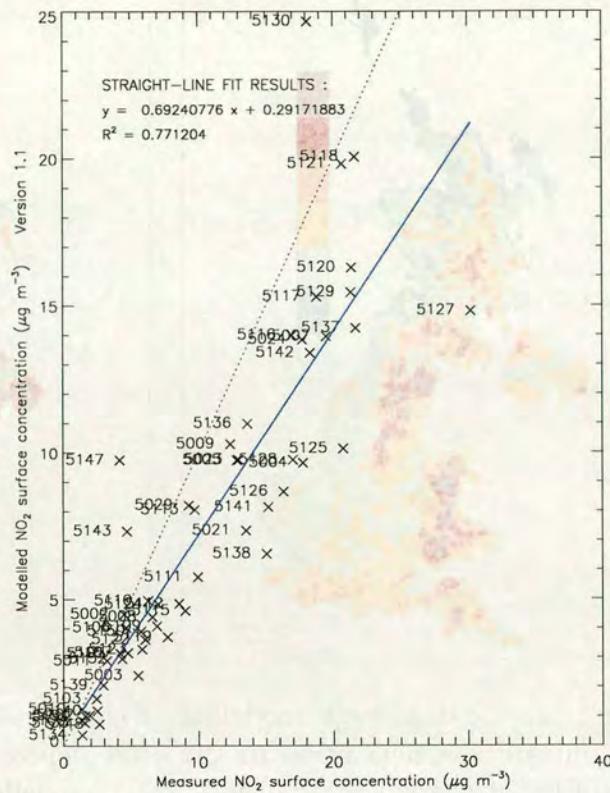


Figure 2.31: Plot of modelled NO₂ surface concentration values (FRAME 1.1) against measured values for 1996. The central dotted line is a one to one agreement. The solid blue line is the best fit line produced by a regression analysis. Each point has a number assigned which corresponds to the monitoring site shown in Table A.2 (Appendix A).

long-term annual mean concentration and deposition for the UK. FRAME is a sequential model (only one trajectory is processed at a time), written in Fortran 77, with a run-time of 6 days on a Sun Ultra 10 workstation (version 1.1).

The availability of a detailed NH₃ emission inventory has allowed FRAME to be run for 1996 providing a realistic pattern of the spatial variability of NH₃ surface concentrations and NH₃ dry deposition to the UK. However, the overestimation of the modelled NH₄⁺ surface concentrations is an important finding for indicating that the model underestimates the wet deposition of reduced nitrogen, since the dry deposition estimate is broadly consistent with estimates derived from measurements (Fowler *et al.*, 1998). In this respect, the

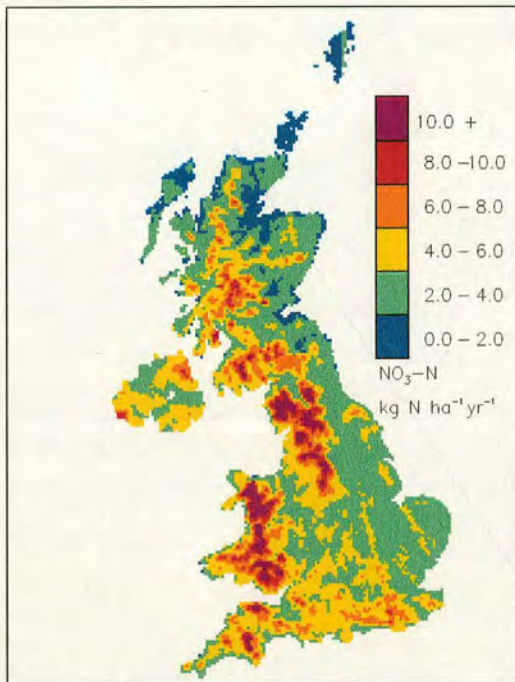


Figure 2.32: Grid average modelled flux of nitrate wet deposition to the UK for 1996 at a 5 km × 5 km resolution (FRAME 1.1). Units are kg N ha⁻¹ year⁻¹.

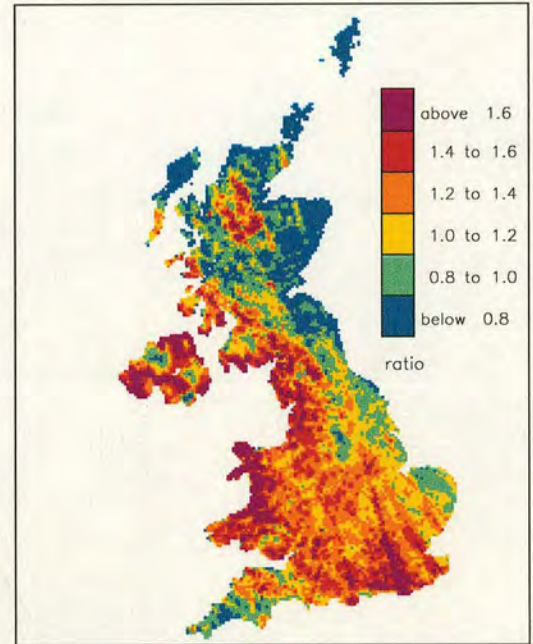


Figure 2.33: Ratio map of nitrate wet deposition between the FRAME 1.1 modelled values and the interpolated measured values. The plot shows $\frac{FRAME1.1}{Measurement}$ to the UK for 1996 at a 5 km × 5 km resolution.

results of FRAME are similar to those of other models for the UK, which all underestimate total deposition (RGAR, 1997; NEG-TAP, 2001). For example, Metcalfe *et al.* (1998) report wet deposition to be only slightly underestimated, but substantially underestimate NH₃ concentrations and dry deposition. In each case, to match the total of wet and dry deposition would require a larger NH₃ emission or less export from the model domain. This points to the need for independent measurement based approaches to assess ammonia emissions and export at the national scale.

However, there is some uncertainty concerning the measurements of NH₄⁺ concentrations in rain. NH₄⁺ is a difficult component to measure and it is the ion that shows least agreement in measurements between bulk and wet-only collectors. Indeed, bulk collectors are not covered with a lid during dry periods, hence

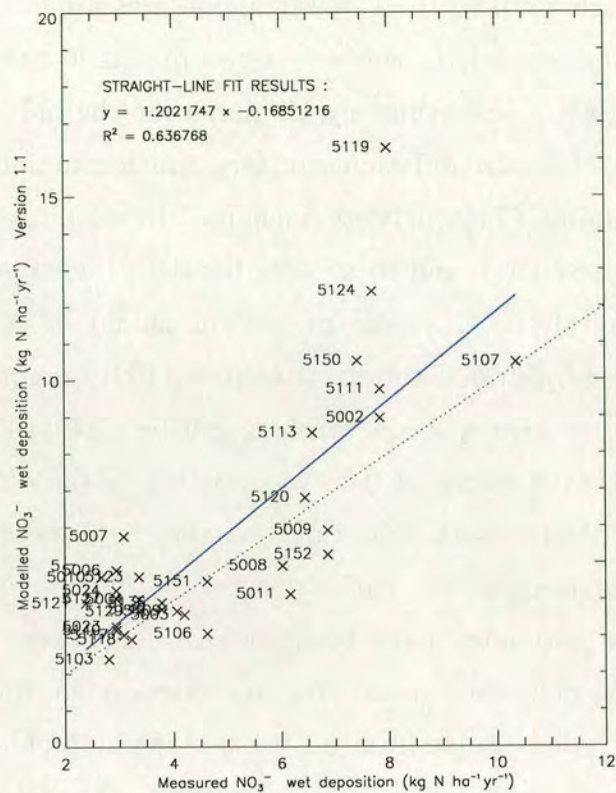


Figure 2.34: Plot of modelled NO_3^- wet deposition values (FRAME 1.1) against measured values for 1996. The central dotted line is a one to one agreement. The solid blue line is the best fit line produced by a regression analysis. Each point has a number assigned which corresponds to the location of the monitoring site shown in Figure 2.11.

some dry deposition is sampled in addition to the wet deposition. Moreover, bird droppings and biological activities may contribute to the measured NH_4^+ concentration although these can normally be removed from the data by screening for Phosphor and Potassium. The magnitude of the dry deposition effect on measured wet deposition is spatially variable and still not fully assessed. Some studies (Buijsman and Erisman, 1988; Asman and van Jaarsveld, 1992) applied a correction factor to take into account this overestimation of the measurements. In our study, we chose to avoid using such factor because of the apparent effect of the age of collectors and the lack of agreed correction factors in the UK at present. However, ongoing work by Cape J.N. (Personal communication), indicates that this correction may be significant.

In an earlier study, the FRAME model was applied to make a first comparison with monitored NH_3 concentrations in Great Britain (Singles, 1996; Singles *et al.*, 1998). Unfortunately, at that time the only data available were from a network of passive diffusion samplers, which contained substantial measurement uncertainties (This network included the monitoring sites operational in the period 1987-1988, and these were the data that were used to compare with the model results). One note of caution should be sounded when using this old network of diffusion tubes. Anderson (1991) reported that the samplers were thought to give a value which is greater than the actual air concentrations, and a scaling factor of 0.45 was applied to the diffusion tube results (Singles *et al.*, 1998). Since that time, reliable NH_3 measurement data have become available from a new national network (Sutton *et al.*, 1998), while the NH_3 emission estimates have been revised. The new monitoring data allow the model performance to be properly assessed for the first time. The modelled concentrations range from $0.1 \mu\text{g.m}^{-3}$ in the highlands of Scotland through to $10 \mu\text{g.m}^{-3}$, as shown in the measurements. The large scatter in the relationship illustrates the spatial variability in NH_3 concentrations. While the broad spatial features are reproduced in the model, the comparison highlights that the actual NH_3 concentration field is even more variable than shown in Figure 2.12.

Finally, FRAME 1.1 underestimates the NO_y dry deposition (32 kt) and overestimates the sulphur dry deposition (158 kt) to the UK. Strong differences with measurements often appeared on the west coast of the UK (Wales, Pennines, west of Scotland), underlining the influence of the import from Northern Ireland and Eire. Thus, while further studies concerning oxidised nitrogen and sulphur will be tackled in Chapter 4, the next step is to consider explicitly the Republic of Ireland in our domain and to analyse the consequences on FRAME results for the different species.

Chapter 3

Extension of FRAME to the British Isles and development of numerical procedures

3.1 Introduction

The FRAME model uses a multi-layer approach to describe vertical concentration profiles in the atmosphere explicitly. Together with the necessary description of atmospheric reactions with sulphur and oxidised nitrogen, this imposes a major computational requirement, with the model having a run-time of 6 days on a mid-range workstation.

While initial developments introduced Northern Ireland (FRAME 1.1), it was apparent that to treat Northern Ireland (NI) properly required the incorporation of Eire in the model domain. This led to further development to produce a British Isles version of FRAME (section 3.2). However, as a consequence of

this extension, the run-time of the model increased (8.5 days). Improvement in the model run-time was sought by developing both a parallel implementation of FRAME (section 3.3) and an alternative diffusion integration technique (section 3.4). The code's portability, its validation with measurements and new maps of its application to the British Isles, are presented in this chapter. With the extension to cover the BI, the model is referred to as FRAME 2.0. The subsequent parallel version of the BI code is FRAME 3.0, while with the improved diffusion scheme the model is referred to as FRAME 4.0 (see Appendix B).

3.2 Domain extension to the British Isles

There are several atmospheric transport models applied to the UK (Fisher, 1978; Metcalfe *et al.*, 1995; Klimova-Murphy and Fisher, 1997), including FRAME 1.1. However, it is important to consider the Republic of Ireland (Eire) as emissions, transport and deposition in this country can have profound effects on the composition of the atmosphere over the UK, especially Northern Ireland. Indeed, the Eire emissions associated with the dominant south-west winds in the BI can induce important export of pollutants towards NI, England and Scotland. Therefore, the emissions (section 3.2.1), the boundary conditions (section 3.2.2) and the meteorological data (section 3.2.3) used previously as input of the FRAME 1.1 for the UK (section 2.2) were updated for the new domain of the British Isles. These developments have also been summarised by Fournier *et al.* (2002).

3.2.1 Emissions

The FRAME model uses a database of NH_3 emissions with a 5 km x 5 km grid-square resolution as input (section 2.2.1 and Figure 1.1). The total United Kingdom NH_3 emissions for 1996 are 287 kt N $year^{-1}$, combining 233 kt of agricultural NH_3 emissions and 54 kt of non-agricultural NH_3 emissions (Dragosits

et al., 1998; Sutton *et al.*, 2000). In addition to the United Kingdom inventory, estimates for Eire were included for the first time (Van den Beuken, 1997). The Eire NH₃ emissions for 1996 are 96 kt N *year*⁻¹ but, at the moment, this inventory does not include non-agricultural sources. However, non-agricultural sources contribute 10 % or less of the Eire NH₃ emissions, hence it should not detract from the validity of the results. Combining these sources leads to a total 1996 NH₃ emissions for the British Isles (BI) of 383 kt N *year*⁻¹ which are mapped in Figure 3.1.

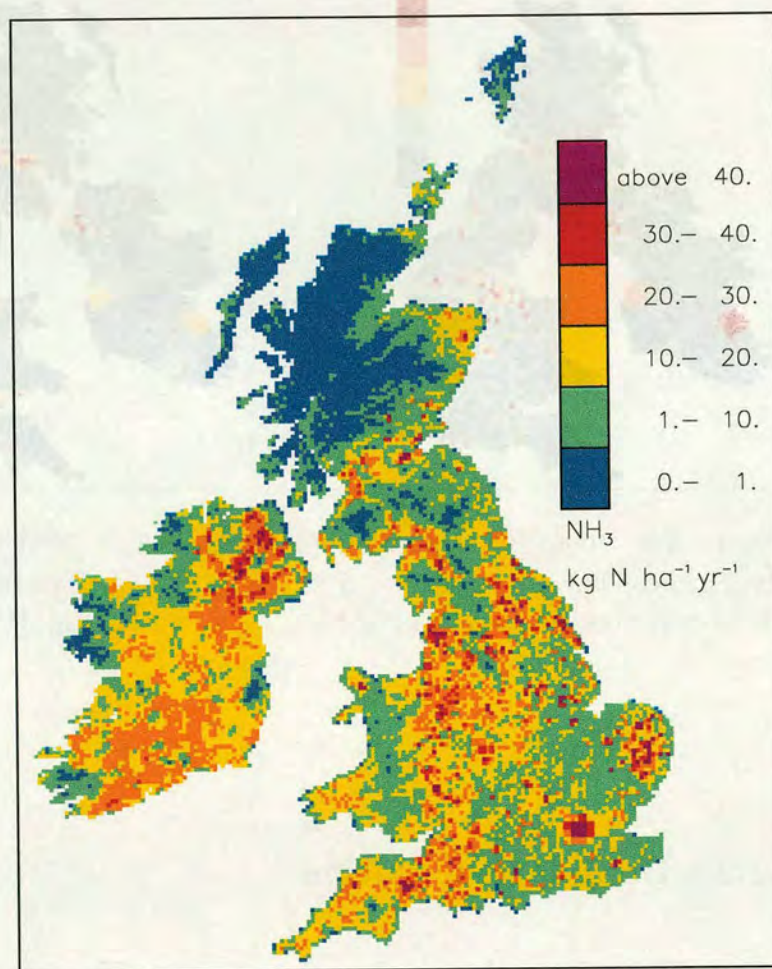


Figure 3.1: 1996 ammonia emissions for the British Isles on a 5 km x 5 km grid resolution. Units are kg N ha⁻¹ year⁻¹ (Van den Beuken, 1997; Dragosits *et al.*, 1998).

In addition to the emissions of NH₃, emissions of SO₂ and NO_x are required for Eire for 1996. These data were provided by EMEP MSC-W (Metoro-

logical Synthesizing Centre - West) on a 50×50 km grid and gives 80 kt S of SO_2 and 37 kt N of NO_x (Støren, 1998; Mylona, 1998). These were combined with the 1996 UK emissions (section 2.2.1) (Salway *et al.*, 1999) and their distribution is shown in Figures 3.2 and 3.3. Thus, the total 1996 BI SO_2 and NO_x emissions represent, respectively, $1085 \text{ kt S year}^{-1}$ and $627 \text{ kt N year}^{-1}$.

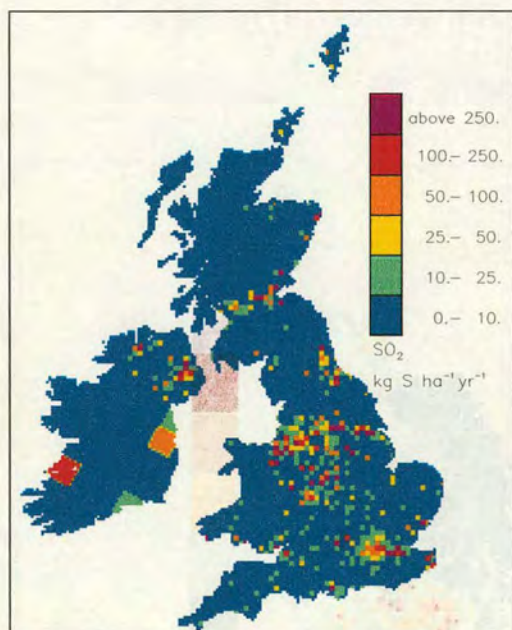


Figure 3.2: 1996 SO_2 emissions for the British Isles on a $5 \text{ km} \times 5 \text{ km}$ grid resolution. Units are $\text{kg S ha}^{-1} \text{ year}^{-1}$.

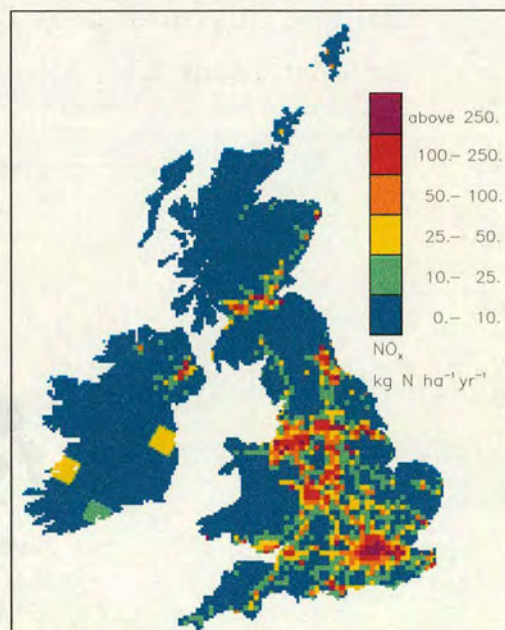


Figure 3.3: 1996 NO_x emissions for the British Isles on a $5 \text{ km} \times 5 \text{ km}$ grid resolution. Units are $\text{kg N ha}^{-1} \text{ year}^{-1}$.

3.2.2 Boundary conditions

As with FRAME 1.1, the transboundary import of foreign material is assessed by running the TERN model across Europe (section 2.2.1) (ApSimon *et al.*, 1994; Singles, 1996). To include Eire, the FRAME model domain was extended 200 km to the west. The revised boundary conditions created with TERN for 1996 for the British Isles are shown in Table 3.1. This shows the amount of reduced nitrogen, oxidised nitrogen and sulphur ($\text{kilotonnes N or S year}^{-1}$) imported by

Wind origin	NH _x -N import	NO _x -N Import	S Import
north	0.7	4.4	4.7
northeast	4.6	27.6	18.9
east	7.2	46.6	40.9
southeast	7.1	36.7	23.0
south	6.0	15.5	13.1
southwest	3.5	7.0	6.9
west	0.2	0.2	0.7
northwest	0.1	0.1	0.3
Total Import	29.4	138.1	108.5

Table 3.1: Modelled 1996 BI budgets of import, obtained with the TERN model, for eight wind sectors, using the FRAME model domain extended 200 km to the west. The units are kt N (or S) year⁻¹.

the FRAME model along the new domain boundary. As a consequence of the extension of the domain from the United Kingdom to the British Isles, there is more import from Europe, especially, from the north and northeast wind directions.

3.2.3 Meteorological and other input data

As the wind rose used previously for the UK (Table 2.2) is representative of the British Isles conditions as well (Jones, 1981; Singles, 1996), it has been retained with the new domain. The land-cover database was extended to cover Eire using the 'CORINE' land-cover map (OSI, 1993) with input from U. Dragosits (Pers. comm.). Long-term annual rainfall data were used for Eire (1951-1980) and interpolated to 5 km × 5 km scale (Aherne and Farrell, 2000). Figure 3.4 shows the combined rainfall field over the British Isles. In Eire, the highest rates of precipitation are located in the mountainous areas of Donegal, Mayo and Galway, Kerry and Cork, and Wicklow.

To calculate the flux of material dry deposited to the British Isles, both deposi-

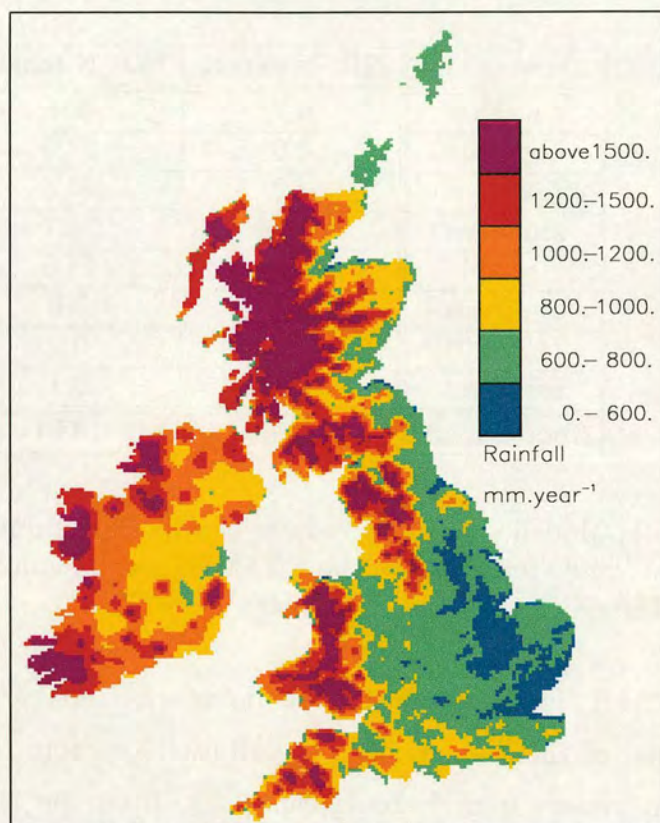


Figure 3.4: Average annual rainfall map for the British Isles at a $5 \text{ km} \times 5 \text{ km}$ resolution. Units are mm year^{-1} .

tion velocities (V_d) of chemical species (section 2.2.4) and the mean wind-speed at a height of 3 m (section 2.2.4) are required for Eire. While the NH_3 deposition velocity is calculated as previously for the UK, no data are available for Eire concerning SO_2 and NO_2 deposition velocities. Therefore, constant values are assigned, equal to those used for Northern Ireland i.e., respectively, 8.0 and 1.4 mm s^{-1} . Secondly, the mean wind-speed at 3 m takes an average value over Eire of 5.1 m s^{-1} as it was prescribed in Northern Ireland (Figure 2.7).

3.2.4 Modifications to allow UK budgets from the BI model

To allow UK budgets to be calculated from the British Isles version of the model (FRAME 2.0), a UK sub-domain was defined. Both the BI and the UK domains are considered by FRAME 2.0, which can assign consequently the budget calculations in the BI or the UK depending on the location of the trajectory. The UK can be seen as a region of the British Isles and hence, the results in the UK are affected by the atmospheric conditions in Eire. Combined with the detailed inventory of the ammonia emissions (Van den Beuken, 1997) and the new set of meteorological data for Eire, this gives the version 2.0 of the FRAME model.

3.2.5 Results of FRAME 2.0

The performances of this new version of the model are investigated in terms of import in the UK, UK budgets and the results for the different species.

UK import

The main change compared with FRAME 1.1 concerns the import of pollutant in the UK in response to the presence of Eire in the FRAME domain (Table 3.2). Indeed, imports of $\text{NH}_x\text{-N}$, $\text{NO}_x\text{-N}$ and S increase from, respectively, 23.7, 117.5, 88.3 kt in FRAME 1.1 (section 2.2.1) to 52.5, 131.5, 116.1 in FRAME 2.0. The main difference is caused by the import from Eire in the southwest and west directions to the UK. The effect is more marked for $\text{NH}_x\text{-N}$ than for the two other species because of the large emissions of NH_3 in Eire.

Wind origin	NH _x -N import	NO _x -N Import	S Import
north	0.3	2.5	2.2
northeast	2.7	17.2	8.8
east	7.1	46.4	40.6
southeast	6.8	35.8	22.2
south	9.7	15.0	13.4
southwest	11.6	8.8	13.5
west	10.5	6.0	12.0
northwest	3.8	1.8	3.4
Total Import	52.5	131.5	116.1

Table 3.2: Modelled 1996 UK budgets of import, from the British Isles version of FRAME (version 2.0), for eight wind sectors. The units are kt N (or S) year⁻¹.

UK budgets

Table 3.3 shows the United Kingdom 1996 reduced nitrogen budget obtained with FRAME 2.0. While the dry deposition budget (97 kt N yr⁻¹) is still consistent with the NEG-TAP estimations, FRAME 2.0 underestimates the UK wet deposition budget with an amount of 82 kt. However, as a consequence of the import of material from Eire to the UK, the UK budget of wet deposition is better than FRAME 1.1 (71 kt; Table 2.12). The import is the main difference between the NEG-TAP estimations and the model. FRAME considers an import of 53 kt of reduced-N to the UK against 30 kt for the NEG-TAP estimations. Firstly, there are uncertainties in the NEG-TAP 2001 estimations (NEG-TAP, 2001). Secondly, the underestimation of the wet deposition in Eire (as in the UK) leads to too much export from this country in FRAME. This is linked with the aerosol NH₄⁺ concentration which is even smaller in Eire than in England as it is shown in Figure 3.7, which is the consequence of lower SO₂ emissions in Eire (see Figure 3.2). Moreover, high NH_x export from Eire is caused by both high emissions of NH₃ and low deposition velocity associated with grassland in this region. The FRAME model ascribes a low deposition velocity to the grassland (Table 2.7) leading to low dry deposition and high NH₃ concentrations over this type of land-cover. This value is quite appropriate in the UK but, in Eire, modelled ammonia concentration and dry deposition would be more

realistic if different sub-types of grassland (with different deposition velocities) were considered.

UK reduced nitrogen (kt N yr ⁻¹)	(NEG-TAP, 2001) 1996 estimations	FRAME 2.0 1996
Import	30	53
Emission	282	291
Dry deposition	99	97
Wet deposition	110	82
Total deposition	209	179
Export	103	165

Table 3.3: Budgets of reduced nitrogen for the UK for 1996 from FRAME 2.0 compared against the measurement based estimates of NEG-TAP. FRAME 2.0 values are estimated including both the UK and Eire in the domain. Units are ktonnes N yr⁻¹.

Table 3.4 shows the results of the UK 1996 oxidised nitrogen budget using FRAME 2.0. The results are similar to those from FRAME 1.1 with the underestimation of the NO_y dry deposition. Combined with the difference in the import budget with NEG-TAP, FRAME 2.0 still overestimates the export of NO_y. The UK 1996 sulphur budget of FRAME 2.0 is presented in Table 3.5 and exhibits slight changes with FRAME 1.0 in response to the difference in import.

Reduced nitrogen

Figure 3.5 shows the distribution of NH₃ surface concentration obtained with FRAME 2.0 for 1996. As with FRAME 1.1 (Figure 2.12), the modelled NH₃ surface concentrations follow the distribution of the NH₃ emissions over the British Isles (Figure 3.1), exhibiting a high spatial variability. Moreover, it shows high air concentrations in the south and north-east of Eire. This is caused by both large NH₃ emissions and low NH₃ deposition velocity associated with grassland. Figure 3.6 shows the comparison with the measurements at monitoring sites

UK oxidised nitrogen (kt N yr ⁻¹)	(NEG-TAP, 2001) 1996 estimations	FRAME 2.0 1996
Import	60	132
Emission	615	590
Dry deposition	87	32
Wet deposition	91	112
Total deposition	178	144
Export	497	578

Table 3.4: Budgets of oxidised nitrogen for the UK for 1996 from FRAME 2.0 compared against the measurement based estimates of NEG-TAP. FRAME 2.0 values are estimated including both the UK and Eire in the domain. Units are ktonnes N yr⁻¹.

UK sulphur (kt S yr ⁻¹)	(NEG-TAP, 2001) 1996 estimations	FRAME 2.0 1996
Import	90	116
Emission	1014	1005
Dry deposition	125	159
Wet deposition	171	154
Total deposition	296	313
Export	808	808

Table 3.5: Budgets of sulphur for the UK for 1996 from FRAME 2.0 compared against the measurement based estimates of NEG-TAP. FRAME 2.0 values are estimated including both Great Britain and Northern Ireland in the domain (UK). Units are ktonnes S yr⁻¹.

in the UK and exhibits similar features to the results of FRAME 1.1 (Figure 2.13).

Figure 3.7 shows the modelled NH₄⁺ aerosol surface concentrations from FRAME 2.0, with the highest values occurring in London and in areas of high emissions of SO₂ in northern England (see Figure 3.2). Low concentrations occur in the west of England and in Scotland, but also in Eire with FRAME 2.0. The ratio map between FRAME 2.0 and FRAME 1.1 (Figure 3.8) shows bigger NH₄⁺ concentration with FRAME 2.0. The inclusion of Eire with its SO₂ emissions increases the formation of NH₄⁺ and, hence its transport from Eire to the UK.

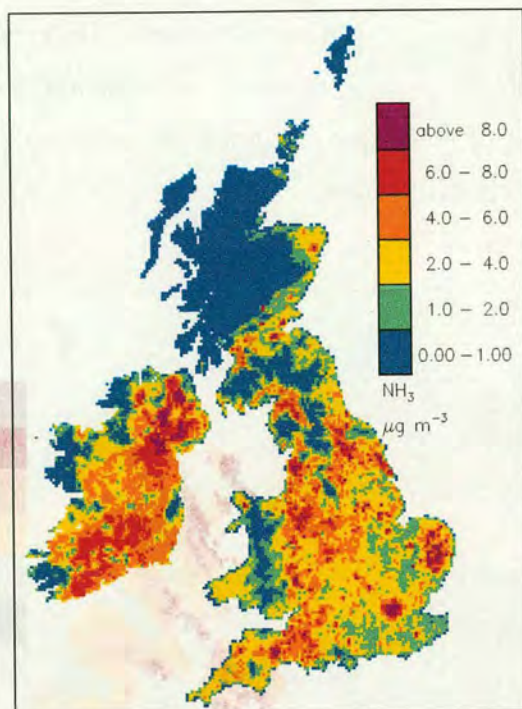


Figure 3.5: Modelled surface concentrations (1-2 m) of NH_3 for the BI for 1996 at a $5 \text{ km} \times 5 \text{ km}$ resolution (FRAME 2.0). Units are $\mu\text{g m}^{-3}$.

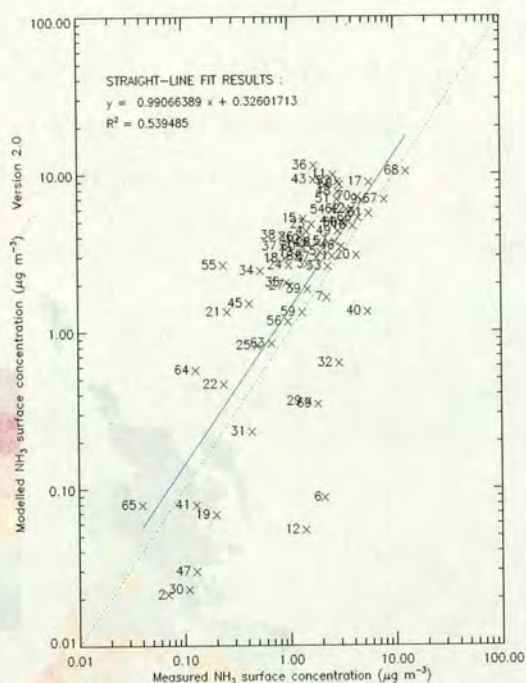


Figure 3.6: Plot of modelled NH_3 surface concentration values (FRAME 2.0) against measured values for 1996. The central dotted line is a one to one agreement. The solid blue line is the best fit line produced by a regression analysis. Each point has a number assigned which corresponds to the location of the monitoring site shown in Figure 2.10.

Therefore, FRAME 2.0 still overestimates the NH_4^+ concentration in comparison with measurements (Figure 3.9), as a consequence of the underestimation of the wet deposition of NH_x (Table 3.3). However, this budget is closer to NEG-TAP than FRAME 1.1 (82 against 71 kt) and hence, improves the performance of the model in the comparison with the NH_x wet deposition measurements (Figure 3.12; slope = 0.73 against 0.58). The modelled distribution of wet deposition for 1996 is presented in Figure 3.10. A similar pattern to FRAME 1.1 is obtained in the UK with the highest rates of wet deposition occurring in Wales and central northern England. Eire exhibits high NH_x wet deposition values in hill areas of Kerry, Cork and Wicklow where there are both large NH_3 emissions and precipitation. The influence of Eire on the wet deposition pattern of the UK

can be seen in Figure 3.11 which shows important differences between FRAME 2.0 and FRAME 1.1 on the west, north-west coasts of the UK and in Northern Ireland. This is the consequence of the export of ammonium aerosol from Eire to the UK in the southwesterly wind direction.

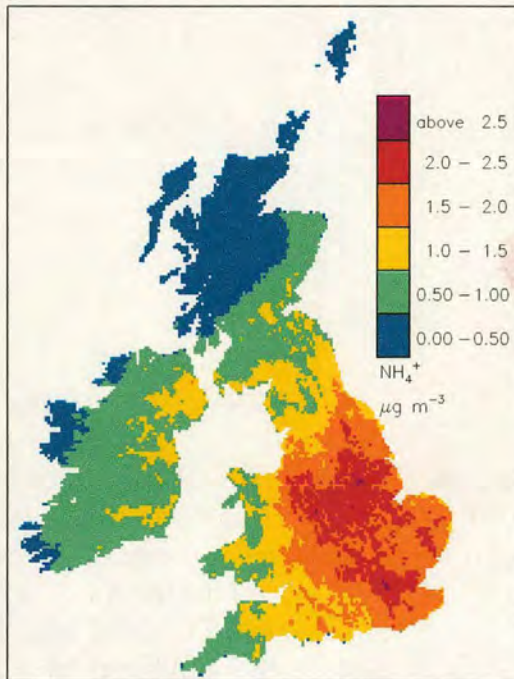


Figure 3.7: Modelled surface concentrations (1-2 m) of NH_4^+ for the BI for 1996 at a $5 \text{ km} \times 5 \text{ km}$ resolution (FRAME 2.0). Units are $\mu\text{g m}^{-3}$.

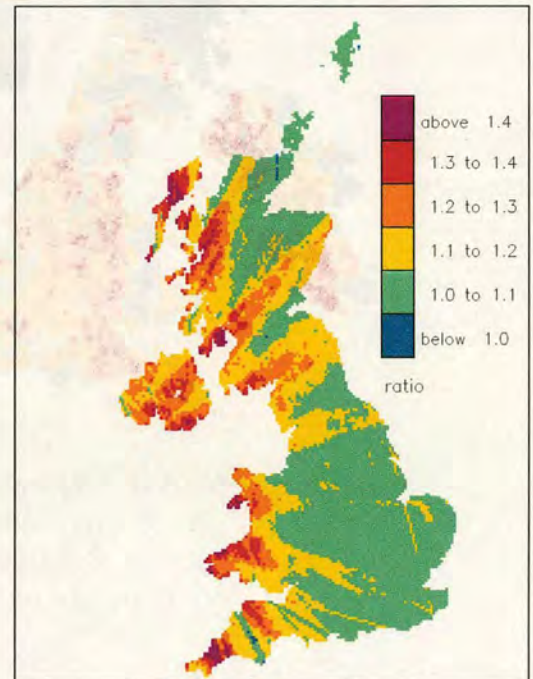


Figure 3.8: Ratio map of NH_4^+ surface concentration modelled values between FRAME 2.0 and FRAME 1.1. The plot shows $\frac{\text{FRAME}2.0}{\text{FRAME}1.1}$ to the UK for 1996 at a $5 \text{ km} \times 5 \text{ km}$ resolution.

Figure 3.13 shows the 1996 flux of modelled NH_3 dry deposition to the BI from FRAME 2.0. Similar to the map of air concentrations (Figure 3.5), the areas with large deposition rates are generally associated with areas of high emissions. These areas include south-west England, the Wales-England border, parts of northern England and the north-east of Northern Ireland. The NH_3 dry deposition in Eire is low, especially in the south despite large emissions and concentrations of NH_3 . This is the consequence of low deposition velocity associated with grassland in FRAME (Table 2.7) leading to low dry deposition and high NH_3 concentrations over this type of land. These high NH_3 concentrations in

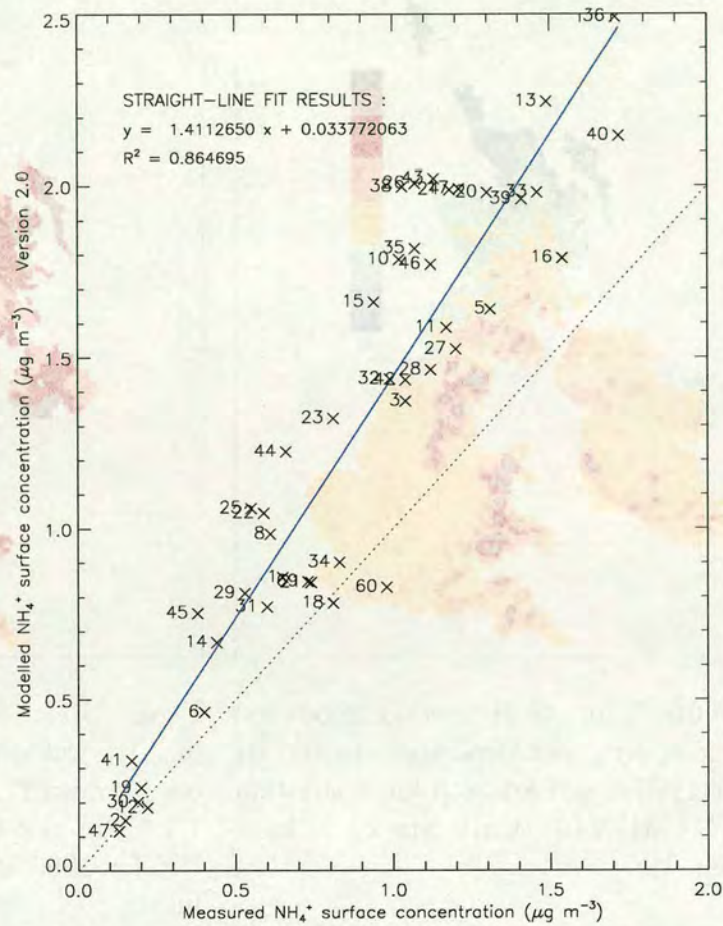


Figure 3.9: Plot of modelled NH_4^+ surface concentration values (FRAME 2.0) against measured values for 1996. The central dotted line is a one to one agreement. The solid blue line is the best fit line produced by a regression analysis. Each point has a number assigned which corresponds to the location of the monitoring site shown in Figure 2.10.

Eire are the main cause of the increased import of reduced nitrogen to the UK between FRAME versions 1.1 and 2.0 (53 kt instead of 24 kt, Tables 3.3 and 2.12).

Concerning oxidised nitrogen and sulphur, the results of FRAME 2.0 are similar to the previous version. The UK budgets (section 3.2.5) exhibit results close to FRAME 1.0 and it is corroborated in the comparisons with measurements. The only slight difference is in the wet deposition component. These amounts are increased with FRAME 2.0 for both species, from 107 kt to 112 kt for oxidised nitrogen and from 142 kt to 154 kt for sulphur. This is the result of including Eire

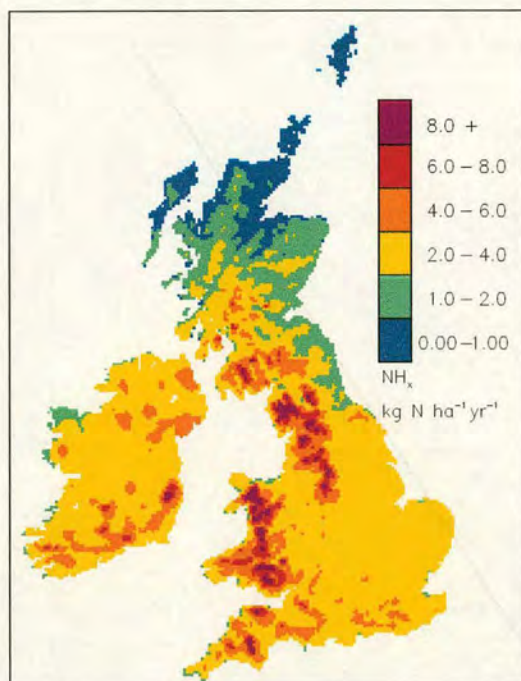


Figure 3.10: Grid average modelled flux of NH_x wet deposition to the BI for 1996 at a $5 \text{ km} \times 5 \text{ km}$ resolution (FRAME 2.0). Units are $\text{kg N ha}^{-1} \text{ year}^{-1}$.

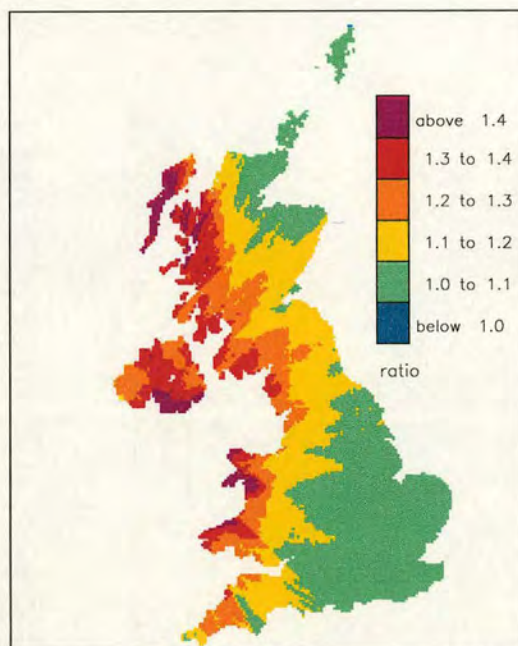


Figure 3.11: Ratio map of the flux of NH_x wet deposition modelled values between FRAME 2.0 and FRAME 1.1. The plot shows $\frac{\text{FRAME2.0}}{\text{FRAME1.1}}$ to the UK for 1996 at a $5 \text{ km} \times 5 \text{ km}$ resolution.

SO_2 and NO_2 emissions, leading to more import to the UK and thus increasing the magnitude of the slopes in the comparison between modelled values and wet deposition measurements. In the case of SO_4^{2-} wet deposition, a slope of 0.58 is obtained against 0.51 with FRAME 1.1 (Figure 2.28). Secondly, for NO_3^- wet deposition, the slope is increased to a value of 1.31 against 1.20 (Figure 2.34).

3.2.6 Conclusions

The extension of the domain of the FRAME model to the British Isles (FRAME 2.0) led to an improvement in 1996 UK concentrations and depositions predictions compared with measurements. However, some input data still need to be

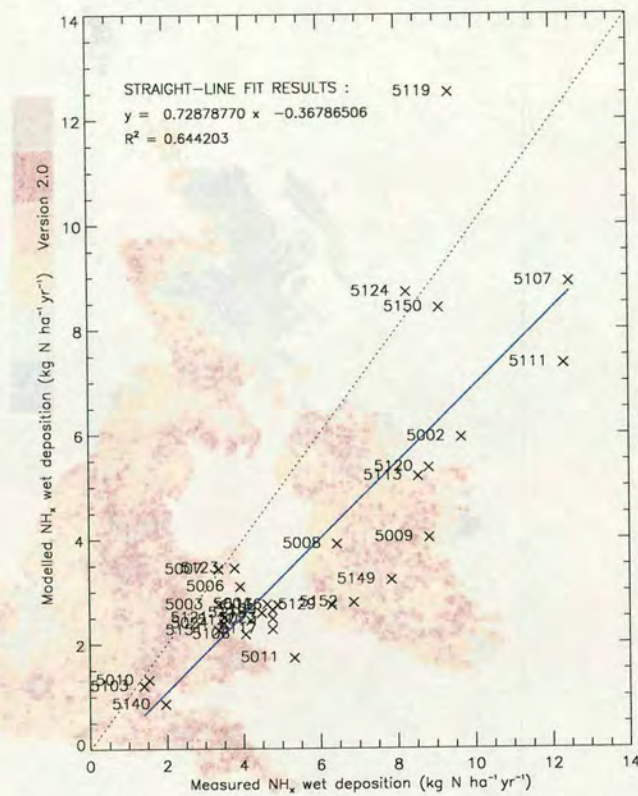


Figure 3.12: Plot of modelled NH_x wet deposition values (FRAME 2.0) against measured values for 1996. The central dotted line is a one to one agreement. The solid blue line is the best fit line produced by a regression analysis. Each point has a number assigned which corresponds to the location of the monitoring site shown in Figure 2.11.

refined to predict accurately these fields over the British Isles. These include SO_2 and NO_2 emissions in Eire (only 50 km resolution); the wind rose (established for the UK); SO_2 , NO_2 deposition velocities and the mean wind-speed at 3 m at a 20 km resolution for Northern Ireland and Eire.

Moreover, FRAME 2.0 still underestimates the reduced nitrogen, sulphur wet depositions and the dry deposition of oxidised nitrogen. This causes an overestimation of the import of material to the UK from Eire. However, before further developing the model to tackle these issues, more needs to be done about the model execution time. By extending the model domain, the execution time of FRAME 2.0 is 8.5 days compared with 6 days for FRAME 1.1. Speeding up the model is the subject of the following sections.

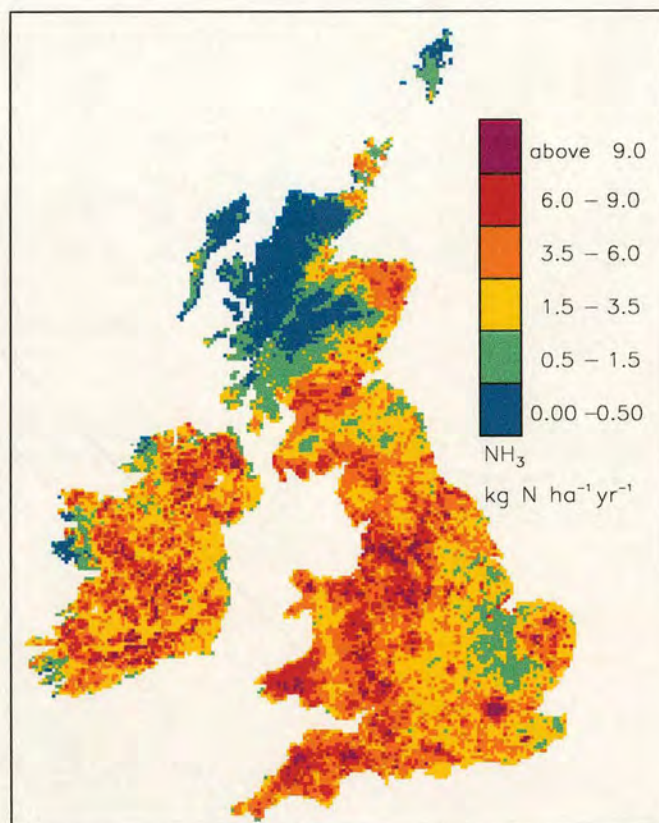


Figure 3.13: Grid average modelled flux of NH_3 dry deposition to the British Isles for 1996 at a $5 \text{ km} \times 5 \text{ km}$ resolution. Units are $\text{kg N ha}^{-1} \text{yr}^{-1}$.

3.3 Parallelisation of the FRAME model

FRAME considers a stratified column of air, traversing the British Isles, in a series of straight line trajectories. The model code is sequential (only one trajectory is processed at a time) and written in Fortran 77. The long execution time of 8.5 days on a Sun Ultra 10 workstation is the main handicap to further development of descriptions of physical processes in the model. Therefore, it becomes necessary to optimise the code and to use more powerful computing facilities before further action could be undertaken. To achieve this, a new parallel version was developed, bearing in mind the need for flexibility in running the code on a range of parallel machines (Fournier *et al.*, 2002). The revised version is referred to as FRAME 3.0.

Previous works have described the parallelisation of atmospheric pollution

transport models. Dabdub and Manohar (1997) parallelised an urban air quality model using a message-passing architecture. On a Cray T3D with 64 processors, the parallel version ran 22 times faster (speedup) than the sequential version on a Sun Sparc 20 workstation. Similarly, Martin *et al.* (1999) parallelised an atmospheric pollution transport model using a message-passing architecture. On a Cray T3D with 128 processors, they obtained a speedup of 20 compared with the sequential version on a Sun Sparc 10 workstation.

3.3.1 Optimisation of the code

The FRAME model uses trajectories along specified wind directions. Twenty four wind directions, at 15° intervals, from 0° to 360° are considered and the results are combined statistically. Trajectories start at four different times of the day (00 h, 06 h, 12 h, 18 h). The first step towards parallelisation was to simplify the structure of the code by gathering these three loops (time, angle, trajectory) in one main loop. Secondly, Fortran 90 features were included to permit dynamic storage allocation, the use of new intrinsic functions and to simplify array operations.

Following these changes, the code of FRAME was re-arranged in three well-defined blocks : *start* (setup and definition of the variables for all the trajectories and reading all the boundary data files); *kernel* (calculations along the trajectories and storing of the results in internal variables); and *exit* (collection of the results, computation of the statistics and outputting to files). A simplified schematic of the structure of the FRAME optimised sequential code is presented in Figure 3.14(A). The purpose of these changes was to simplify the parallelisation by gathering the calculations along each trajectory in one block (*kernel*) and by introducing Fortran 90.

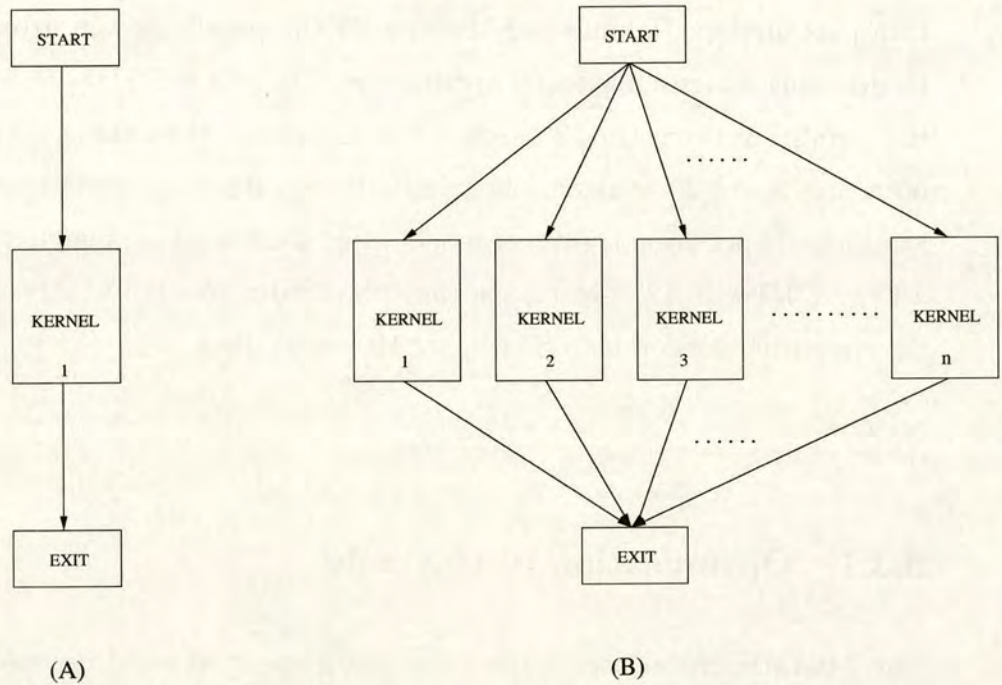


Figure 3.14: Schematic flow chart of the optimised FRAME sequential code (A) and of the FRAME parallel code (B). In the latter, the kernel is replicated onto all the n processors.

3.3.2 Parallelisation of the code

In FRAME, the same computations (emission, diffusion, chemistry and deposition) are executed in all the trajectories. A notable aspect is that the code computes the variables' values for one grid-square from the grid-square executed directly beforehand and, due to the statistical approach of the model, there is no memory in any calculation concerning details of grid-squares generated in a previous trajectory. This has the consequence that each trajectory is independent. Therefore, by taking advantage of the fact that each trajectory is independent, a parallel version of the code was implemented by distributing the different trajectories over multiple processors. The revised code structure (see Figure 3.14(B)) is therefore :

- the *start* block computes variables and parameters as before, the common variables are copied onto all the available processors;
- the *kernel* is replicated onto each processor, which computes only the distributed trajectories without any interaction with the other processors;

- the *exit* block gathers the results from all the processors and performs the last operations as in the sequential code.

3.3.3 High Performance Fortran

The parallelisation of the code was achieved via a data-parallel approach using High Performance Fortran (HPF). HPF is the standard language developed for data-parallel, which assigns parts of the data arrays (in our case, the trajectories) to different processors. A recent review of the HPF history and future can be found in Mehrotra *et al.* (1998). Fortran 90 extensions assist its implementation on parallel computers, as well as directives for specifying how data are to be distributed over the processor memories in a multiprocessor architecture (Merlin and Hey, 1995). The code is run on a single processor, using others when required.

In FRAME, the parallelisation was implemented by distributing the independent trajectories over the available processors. Hence, there is no communication between the processors and the same computation is executed independently by all the processors. Therefore, a data-parallel approach seems adequate to exploit this concurrency that derives from the application of the same calculation to multiple independent trajectories. HPF was chosen because it requires only a few additional parallel constructs and data placement directives to Fortran 90. In contrast, a message-passing architecture (as MPI : Message Passing Interface) would imply more re-coding (Pacheco, 1996). Indeed, message-passing programming is referred to as a multiple-program-multiple-data (MPMD) model to distinguish it from the SPMD (single-program-multiple-data) model, hence providing many specific functions to allow local, global or asynchronous communications between processors. HPF is a very attractive alternative to explicit message passing libraries like the Parallel Virtual Machine (PVM) or MPI. The main advantage is in the ease of programming: complicated packaging of data, sending and receiving procedures are not necessary, and synchronising the processors is also taken care of by the HPF compiler. Recent studies

such as Benkner (2000); Ehold *et al.* (2002) rehabilitate HPF showing that its performances are even competitive with that of well-established numerical libraries based on MPI. On the other hand, it is recognised that the current HPF standard does not provide sufficient support for dealing with unstructured mesh applications (Keppens and Toth, 2000).

To apply the data-parallel approach to the FRAME code, the trajectories data were partitioned and mapped to the processor memories via the *HPF DISTRIBUTE* directive, using a schematic set of statements e.g.

```
!HPF$ PROCESSORS pr(number of processors)
      real X(n)
!HPF$ DISTRIBUTE X(CYCLIC) ONTO pr
```

this indicates that the array X is to be distributed in a cyclic fashion over a given number of processors : processor 0 receives the first element of X (trajectory or any associated parameter in our case), processor 1 the second element, and so on. Therefore, all the variables updated in the computation along a trajectory are distributed (time, grid-square coordinates, concentrations ...). Next, through the statement :

```
EXTRINSIC(HPF_LOCAL) SUBROUTINE sname
```

where "sname" is the name of the subroutine that contains the kernel, which is replicated onto all the processors. This means that each processor has its own copy of the core code and performs all the computations without any interaction with the other processors. Hence, the code is run on a single processor to initialise the model (start procedure) and to gather and output the results (exit procedure), while the total available number of processors are utilised to execute the main computation for each trajectory. The parallel code (FRAME 3.0) is written to be independent of the number of available processors allowing it to be run on different machines.

3.3.4 Computing platforms

Table 3.6 lists the target machines used for running the FRAME model. The Cray T3E-900 of the Edinburgh Parallel Computing Centre (EPCC) was used as the main target machine for FRAME 3.0, due to its high computing capability and the possibility of accessing it through the EC-TRACS Programme at EPCC (European Community-Training and Research on Advanced Computing Systems). This system has 344 Alpha processors (450 MHz), each having a peak performance of 900 MFlops. The majority of the processors are configured with 128 Mbytes, or above, of memory. The processors are divided in two pools : 216 processors and 128 processors. Due to administrative reasons, FRAME was run on the second pool of processors.

Moreover, the parallel version of FRAME was run on the EPCC's Sun HPC 3500. This is an eight-400 MHz UltraSPARC II processor machine with 8 Gbytes of main memory. A four-400 MHz UltraSPARC II processor Sun HPC 450, with 1 Gbyte of main memory, was also available at CEH (Centre for Ecology and Hydrology). Finally, for comparison, the sequential code version of FRAME (version 2.0) was executed on a 1-processor Sun Ultra 10 workstation with 640 Mbytes of main memory.

Machine	Processing node	number of processors	FRAME version	run-time (minutes)
Sun	330 MHz Ultra 10	1	sequential (2.0)	12180
Sun	400 MHz HPC 450	4	parallel (3.1)	5640
Sun	400 MHz HPC 3500	8	parallel (3.1)	2280
Cray T3E	450 MHz Alpha	128	parallel (3.1)	177

Table 3.6: Run-time of the FRAME model on various machines

3.3.5 Load-balance

An important issue when running an application with a parallel machine is to be sure that all processors do roughly the same amount of work (i.e., the “load-balance”), since a parallel run is not finished until every processor has stopped. The parameter used here to measure the load-imbalance (Δ) is :

$$\Delta(\%) = \frac{(CPUt_{max} - CPUt_{min})}{\frac{1}{2}(CPUt_{max} + CPUt_{min})} \quad (3.1)$$

where $CPUt_{max}$ and $CPUt_{min}$ are the maximum and the minimum CPU (Central Processing Unit) time consumed by the processors, respectively.

An initial parallel version of FRAME distributed all the trajectories and the associated parameters cyclically, heedless of any kind of ordering. However, this could cause load-imbalance. As a measure to improve the load-balance, a second version of the parallel model (FRAME 3.1) was developed to take into account the length of the trajectories and sort them before distribution. Along a particular trajectory the execution time is roughly proportional to the number of land squares (over sea, there is less calculation). Thus, to improve the load-balance, the trajectories are assigned over the processors using their length as an ordering parameter. The longer ones are processed first and the shorter last to avoid large gaps in the execution time of the processors' last task.

3.3.6 Results

To test the performance and the portability of the parallel version of FRAME, typical simulations are performed on the different target machines. The results compared well with those from the sequential code (FRAME 2.0). The same UK budgets are obtained for 1996 for reduced nitrogen, oxidised nitrogen and sulphur. A regression analysis of NH_3 surface concentrations showed that the

parallel version estimates the concentrations without scatter and with a near perfect 1 : 1 relationship ($y = 0.9978x - 0.0163$; $R^2 = 0.999$). The cause of this slight difference between the parallel and sequential versions is the variables' type used in the calculations; single precision on the workstation, but double precision on the parallel machines.

Employing the 128-processor pool of the Cray *T3E*, FRAME 3.0 runs in only 189 minutes; 64 times faster than the sequential Sun Ultra 10 workstation version using FRAME 2.0. However, as suspected, the cyclic decomposition of the trajectories over the processors created a load-imbalance. Indeed, the longer and the shorter processors' execution-times were 187 and 138 minutes, respectively. Thus, it caused a load-imbalance of 30%.

The parallel version, with trajectories sorted by length (FRAME 3.1, Table 3.6), decreased the load-imbalance from 30% to 19% and the execution time to 177 minutes. Figure 3.15 represents this load-imbalance via the frequency of the Cray *T3E* processors' execution-times. These vary between 146 and 176 minutes and 36% of the processors' execution-times are between 154 and 160 minutes. Hence, finally, a speedup of 69 was obtained.

To assess its portability, this optimised version was also run on the 8-processor and 4-processor Sun machines (Table 3.6), giving speedup of a factor of 5 and 2, respectively.

3.3.7 Conclusions regarding the development of a parallel version of FRAME

The HPF parallel version of the model (FRAME 3.1) gives a portable code with a significant speedup of 69 when applied on a Cray *T3E*. Its portability allows the code to run on a number of parallel machines without modifications. The speedup obtained with the Cray *T3E* shows that the data-parallel approach with an extrinsic "local" definition for the kernel is well suited to the present

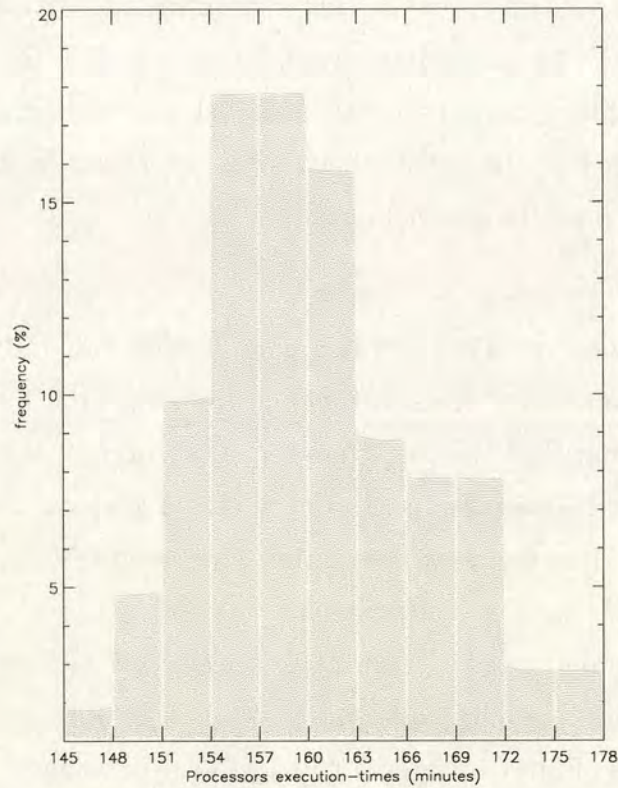


Figure 3.15: Execution-times frequency of the 128 processors in running the parallel code (FRAME 3.1), including improvement in load-balance, on the Cray *T3E*.

model. Indeed, previous studies showed speedups of 20 in Martin *et al.* (1999) and 22 in Dabdub and Manohar (1997). Some parallelisation's performances are limited by the communication between processors (Dabdub and Manohar, 1997). As the number of processors increases, the communications increase and outweigh the advantages of distributing the code on a large number of processors. In the parallel implementation of FRAME 3.1, there is no such limitation as no communication occurs between processors. Therefore, as the number of processors increases, the speedup increases. Hence, it would be of benefit to run the code on a parallel machine where more processors are available.

The load-balance could be improved further by considering a more physical parameter to order the trajectories, for example the number of land squares with significant emission of ammonia. However, this task would significantly increase the execution time of the starting procedure. Therefore, the length of the trajectory is considered to represent a suitable compromise as an ordering parameter.

3.4 Numerical discretisation of the vertical diffusion in FRAME

Although the parallel version of FRAME seems a good remedy to the problem of large run-time of the code, it requires major computing facilities to be really effective. Indeed, for this project, only the 4-processor Sun machine was freely accessed, through CEH (Centre for Ecology and Hydrology), giving a run-time of 4 days (5640 minutes; Table 3.6) against 8.5 days with the previous sequential version. With this practical constraint, more efficient and reliable numerical techniques were necessary before further development of the physics of the model could be undertaken. To achieve this, an alternative more efficient diffusion integration technique, the implicit Finite Volume Method (FVM), was implemented leading to the development of FRAME 4.0. This model version incorporated all the developments of FRAME 2.0 and FRAME 3.1.

The vertical transport of material between adjacent layers in FRAME is described by K-theory diffusion (section 2.2.3). The model solves this equation using a finite difference discretisation referred to as a fourth-order Runge-Kutta scheme (ApSimon *et al.*, 1994; Press *et al.*, 1992). A drawback associated with this method is the need to specify a time-step size, which must be small enough to ensure stability. A more advanced method had been developed by Singles (1996) taking into account the large spatial variability of emissions and deposition occurring in the domain at a 5 km resolution. This involves a scheme with adjusted time-steps to allow the model to use small time-steps in areas where large vertical exchanges of material occur, and keep larger time-steps otherwise (Press *et al.*, 1992). This leads to time-steps varying between 4 and 20 seconds.

The Finite Volume Method is probably the most popular numerical discretisation

method used in CFD (Computational Fluid Dynamics). This method is similar in some ways to the finite difference method, but some implementations of it also draw on features taken from the finite element method (Patankar, 1980).

3.4.1 Finite Difference Method

The Finite Difference Method (FDM) is based upon the Taylor series to build a library of equations that describe the derivatives of a variable as the differences between values of the variable at various points in space or time (Smith, 1985). For example, a typical discretisation of the second derivative of a variable U at the point P is :

$$\left(\frac{\partial^2 U}{\partial x^2}\right)_P = \frac{u_W - 2u_P + u_E}{\delta x^2} \quad (3.2)$$

where the points W and E are respectively the West and East neighbours of P . There is a constant spacing δx between these points (see Figure 3.16).

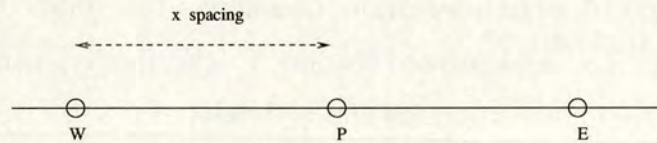


Figure 3.16: An x grid for finite difference method.

3.4.2 Finite Element Method

A powerful method for solving differential equations is the Finite Element Method (FEM). A differential equation can be represented by

$$L(\phi) = 0 \quad (3.3)$$

An approximate solution $\bar{\phi}$ could be

$$\bar{\phi} = a_0 + a_1x + a_2x^2 + \dots + a_mx^m \quad (3.4)$$

the a 's being the parameters. The substitution of $\bar{\phi}$ into the differential equation leaves a residual R , defined as

$$R = L(\bar{\phi}) \quad (3.5)$$

To make this residual small, we define

$$\int WRdx = 0 \quad (3.6)$$

where W is a weighting function and the integration is performed over the domain of interest. By choosing a succession of weighting functions, as many equations as are required can be generated for evaluating the parameters. These algebraic equations containing the parameters as the unknowns are solved to obtain the approximate solution to the differential equation. Different versions of the method result from the choice of different classes of weighting functions. The method was very popular in boundary-layer analysis before the FDM to a large extent replaced it. However, a connection with the FDM can be established if the approximate solution $\bar{\phi}$, instead of being a single algebraic expression over the whole domain, is constructed via piecewise profiles with the grid-point values of ϕ as the unknown parameters. Much of the recent development of the FEM is also based on piecewise profiles used in conjunction with a particular weighted-residual practise known as the Galerkin method.

The simplest weighting function is $W = 1$. From this, a number of weighted-residual equations can be generated by dividing the calculation domain into sub-domains or finite volumes, and setting the weighting function to be unity over one sub-domain at a time and zero everywhere else. This variant of the method of weighted residuals is called the Finite Volume Method. As the weighting function (W) equals 1 over the finite volume at the time considered, the integral of the differential equation over this finite volume must become zero.

3.4.3 Finite Volume Method

The Finite Volume Method is a special version of the FEM (Patankar, 1980; Versteeg and Malalasekera, 1995). The calculation domain is divided into a number of finite volumes such that there is one finite volume surrounding each grid point. The differential equation is integrated over each finite volume. Piecewise profiles expressing the variation of ϕ between the grid points are used to evaluate the required integrals. The result is the discretisation equation containing the values of ϕ for a group of grid points.

The discretisation equation obtained in this manner expresses the conservation principle for ϕ for the finite volume, just as the differential equation expresses it for an infinitesimal finite volume.

The most attractive feature of the finite volume formulation is that the resulting solution would imply that the integral conservation of quantities such as mass, momentum and energy is exactly satisfied over the whole calculation domain.

When the discretisation equations are solved to obtain the grid-point values of the dependent variable, the result can be viewed in two different ways. In the FEM and in most weighted-residual methods, the assumed variation of ϕ consisting of the grid-point values and the interpolation functions (or profiles) between the grid points is taken as the approximate solution. In the FDM, however, only the grid-point values of ϕ are considered to constitute the solution, without any explicit reference as to how ϕ varies between the grid points. In the FVM, this last view is adopted. The solution is sought here in the form of the grid-point values only. The interpolation formula or the profiles are regarded as auxiliary relations needed to evaluate the required integrals in the formulation. Once the

discretisation equations are derived, the profile assumptions can be forgotten. This viewpoint permits complete freedom of choice in employing different profile assumptions for integrating different terms in the differential equation.

To make the discussion more concrete, the FVM is derived for the steady diffusion equation

$$\frac{\partial}{\partial x} \left(k \frac{\partial \phi}{\partial x} \right) = 0 \quad (3.7)$$

where k is the diffusivity, ϕ a variable.

A typical finite volume or cell, is shown in Figure 3.17, where the centre of the volume, point P , is the reference point at which we wish to find a numerical analogue of the partial differential equation.

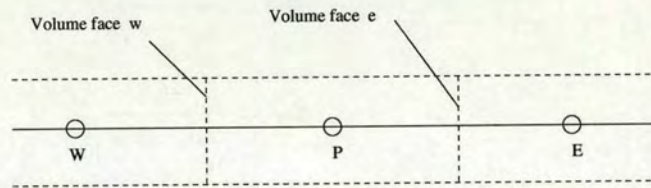


Figure 3.17: A finite volume in one dimension.

The neighbouring volumes are said to have their centres at W and E , i.e. to the West and East of P . As the one-dimensional finite volume is centred on P , it will have one boundary face placed mid-way between W and P at the point labelled w , and another boundary face between P and E at the point e .

For the one-dimensional problem under consideration, a unit thickness is assumed in the y and z directions. Thus, the volume of the finite volume is $\Delta x \times 1 \times 1$. The diffusion equation is integrated over the finite volume

$$\left(k \frac{\partial \phi}{\partial x} \right)_e - \left(k \frac{\partial \phi}{\partial x} \right)_w = 0 \quad (3.8)$$

Then, a profile assumption or an interpolation formula is required. The simplest possibility is to assume that the value of ϕ at a grid point prevails over the finite

volume surrounding it (Patankar, 1980; Versteeg and Malalasekera, 1995). This gives a stepwise profile for which the slope $\partial\phi/\partial x$ is not defined at the finite volume faces (i.e., at w or e). Otherwise, to avoid this discontinuity at the finite volume faces, one can use a piecewise-linear profile. This will allow the evaluation of the derivative at the finite volume faces with interpolation functions. Then, the resulting equation is

$$\frac{k_e(\phi_E - \phi_P)}{x_E - x_P} - \frac{k_w(\phi_P - \phi_W)}{x_P - x_W} = 0 \quad (3.9)$$

or

$$a_P\phi_P = a_E\phi_E + a_W\phi_W \quad (3.10)$$

where

$$a_E = \frac{k_e}{x_E - x_P}, \quad (3.11)$$

$$a_W = \frac{k_w}{x_P - x_W}, \quad (3.12)$$

$$a_P = a_E + a_W \quad (3.13)$$

and

$$k_e = \left(\frac{1 - f_e}{k_P} + \frac{f_e}{k_E} \right)^{-1}, \quad (3.14)$$

$$k_w = \left(\frac{1 - f_w}{k_P} + \frac{f_w}{k_W} \right)^{-1}, \quad (3.15)$$

$$f_e = \frac{x_E - x_e}{x_E - x_P}, \quad (3.16)$$

$$f_w = \frac{x_P - x_w}{x_P - x_W} \quad (3.17)$$

When the interfaces w and e are placed midway, $f_e = 0.5$ and $f_w = 0.5$.

The solution of the discretisation equations for the one-dimensional situation can be obtained by the standard Gaussian-elimination method. Because of the particularly simple form of the equations, the elimination process turns into

a convenient algorithm. This is called the Thomas algorithm or the TDMA (TriDiagonal-Matrix Algorithm) referring to the fact that all the non-zero coefficients align themselves along three diagonals of the matrix (Press *et al.*, 1992).

Turning to the unsteady situation

$$\frac{\partial \phi}{\partial t} = \frac{\partial}{\partial x} \left(k \frac{\partial \phi}{\partial x} \right) \quad (3.18)$$

Many assumptions, about how ϕ_E , ϕ_P and ϕ_W vary with time from t to $t + \Delta t$, can be proposed such as

$$\int_t^{t+\Delta t} \phi_P dt = [f\phi_P^1 + (1-f)\phi_P^0] \Delta t \quad (3.19)$$

where the old (given) values of ϕ at time t are denoted by ϕ_P^0 , ϕ_E^0 and ϕ_W^0 . The new (unknown) values of ϕ at time $t + \Delta t$ are denoted by ϕ_P^1 , ϕ_E^1 and ϕ_W^1 . f is a weighting factor between 0 and 1. Using similar formula for the integrals of ϕ_E and ϕ_W , the result is

$$\begin{aligned} a_P \phi_P^1 = & a_E [f\phi_E^1 + (1-f)\phi_E^0] + a_W [f\phi_W^1 + (1-f)\phi_W^0] \\ & + [a_P^0 - (1-f)a_E - (1-f)a_W] \phi_P^0 \end{aligned} \quad (3.20)$$

where

$$a_E = \frac{k_e}{x_E - x_P}, \quad (3.21)$$

$$a_W = \frac{k_w}{x_P - x_W}, \quad (3.22)$$

$$a_P^0 = \frac{\Delta x}{\Delta t}, \quad (3.23)$$

$$a_P = f a_E + f a_W + a_P^0. \quad (3.24)$$

For certain specific values of f , the discretisation equation reduces to one of the

well-known schemes for parabolic differential equations. In particular, $f = 0$ leads to the explicit scheme, $f = 0.5$ to the Crank-Nicolson scheme and $f = 1$ to the fully implicit scheme. For the explicit and Crank-Nicolson schemes, the coefficient of ϕ_p^0 can become negative (physically unrealistic results could emerge). In the case of the explicit scheme, for this coefficient to be positive, the time-step Δt would have to follow the condition :

$$\Delta t < \frac{(\Delta x)^2}{2k} \quad (3.25)$$

The Crank-Nicolson scheme is usually described as unconditionally stable but the coefficient of ϕ_p^0 can be seen to be $\Delta x/\Delta t - k/\Delta x$. Again, if the time-step is not sufficiently small, this coefficient could become negative. The implicit scheme is chosen because, although it yields equations which are more complex to solve than the other schemes, it is unconditionally stable for all time-step sizes. Thus, the fully implicit scheme satisfies the requirements of simplicity and physically satisfactory behaviour even if for small time-steps it is not as accurate as the Crank-Nicolson scheme (Fletcher, 1991).

Solution of discretised equations TDMA

Thomas (1949) developed a technique for rapidly solving Tri-Diagonal Matrices (TDMA). The TDMA scheme is applicable in cases of regular Cartesian co-ordinates. This is a direct method for one-dimensional situations but can be applied iteratively, in a line-by-line fashion, to solve multi-dimensional problems. It is computationally inexpensive and requires a minimum amount of storage (Versteeg and Malalasekera, 1995). Details of the TDMA, including a Fortran coding, may be found in Press *et al.* (1992); Randerson (1984). However, the methodology of the TDMA is discussed briefly.

Considering the tri-diagonal form of our system of equations :

$$\begin{aligned}
\phi_1 &= C_1 \\
-\beta_2\phi_1 + D_2\phi_2 - \alpha_2\phi_3 &= C_2 \\
-\beta_3\phi_2 + D_3\phi_3 - \alpha_3\phi_4 &= C_3 \\
-\beta_4\phi_3 + D_4\phi_4 - \alpha_4\phi_5 &= C_4 \\
&\dots \dots \dots = \dots \\
-\beta_n\phi_{n-1} + D_n\phi_n - \alpha_n\phi_{n+1} &= C_n \\
\phi_{n+1} &= C_{n+1}
\end{aligned}$$

where the general form of any single equation is

$$-\beta_i\phi_{i-1} + D_i\phi_i - \alpha_i\phi_{i+1} = C_i \quad (3.26)$$

Considering our implicit discretisation of the diffusion equation :

$$a_P\phi_P^1 = a_E\phi_E^1 + a_W\phi_W^1 + a_P^0\phi_P^0 \quad (3.27)$$

and rearrange it to form

$$-a_W\phi_W^1 + a_P\phi_P^1 - a_E\phi_E^1 = a_P^0\phi_P^0 \quad (3.28)$$

gives the same form as Equation 3.26. Thus, as Equation 3.26 can be rewritten

$$\phi_i = \frac{\alpha_i}{D_i}\phi_{i+1} + \frac{\beta_i}{D_i}\phi_{i-1} + \frac{C_i}{D_i} \quad (3.29)$$

Any ϕ can be removed by forward elimination, for example ϕ_2 can be replaced by

$$\phi_3 = A_3\phi_4 + C'_3 \quad (3.30)$$

where

$$A_3 = \alpha_3 / (D_3 - \beta_3 A_2) \quad C'_3 = (\beta_3 C'_2 + C_3) / (D_3 - \beta_3 A_2)$$

$$A_2 = \alpha_2 / D_2 \quad C'_2 = (\beta_2 / D_2) C_1 + C_2 / D_2$$

As ϕ_2 has been removed (3.30), it can be substituted back into Equation 3.29 to remove ϕ_3 , a process that may be repeated until all ϕ are given in terms of the known boundary conditions.

3.4.4 Results of FRAME 4.0 using the FVM

The fully implicit Finite Volume Method is implemented in the FRAME model (version 4.0), to discretise the one-dimensional diffusion equation. The subsequent solution of the resulting system of simultaneous equations is assessed through the TDMA algorithm (Press *et al.*, 1992). This implicit discretisation allows the use of a bigger time step than with the previous Runge-Kutta method. Indeed, instead of using adjusted time steps varying between 4 and 20 seconds, the implicit FVM is found to be stable and accurate with a time step of 120 seconds. This method gave a speedup of 34 in comparison with FRAME 3.1. In implementing this method thanks are due to the collaboration of M. Vieno (Institute for Meteorology, University of Edinburgh) who spotted a mistake in a loop index of this discretisation which otherwise led to errors in the mass budget. Table 3.7 shows the run-time of the different versions. FRAME 4.0 ran in 165 minutes (2 hours 45 minutes), on the 4-processor Sun of CEH, instead of 5640 minutes (4 days) for FRAME 3.1.

Table 3.8 shows the results of the UK 1996 reduced nitrogen budget. The results are not different from those of FRAME 2.0 and FRAME 3.1 (Table 3.3). Similar figures are obtained with oxidised nitrogen and sulphur (Tables 3.9 and 3.10). Slight differences appear between FRAME 4.0 and 3.1 in the NO_x wet deposition with 113 kt N yr^{-1} instead of 112 kt; in the sulphur dry deposition with 161 kt

Machine	Processing node	number of processors	FRAME version	run-time (minutes)
Sun	330 MHz Ultra 10	1	sequential (2.0)	12180
Sun	400 MHz HPC 450	4	parallel (3.1)	5640
Sun	400 MHz HPC 450	4	parallel (4.0)	165

Table 3.7: Run-time of the versions 2.0, 3.1 and 4.0 of the FRAME model

S yr⁻¹ instead of 159 kt and in the sulphur wet deposition with 152 kt S yr⁻¹ instead of 154 kt.

UK reduced nitrogen (kt N yr ⁻¹)	(NEG-TAP, 2001) 1996 estimations	FRAME 3.1 1996	FRAME 4.0 1996
Import	30	53	53
Emission	282	291	291
Dry deposition	99	97	97
Wet deposition	110	82	82
Total deposition	209	179	179
Export	103	165	165

Table 3.8: Budgets of reduced nitrogen for the UK for 1996 from FRAME 3.1 and 4.0 compared against the measurement based estimates of NEG-TAP. FRAME 4.0 considers a new diffusion scheme (FVM). Units are ktonnes N yr⁻¹.

UK oxidised nitrogen (kt N yr ⁻¹)	(NEG-TAP, 2001) 1996 estimations	FRAME 3.1 1996	FRAME 4.0 1996
Import	60	132	132
Emission	615	590	590
Dry deposition	87	32	32
Wet deposition	91	112	113
Total deposition	178	144	145
Export	497	578	577

Table 3.9: Budgets of oxidised nitrogen for the UK for 1996 from FRAME 3.1 and 4.0 compared against the measurement based estimates of NEG-TAP. FRAME 4.0 considers a new diffusion scheme (FVM). Units are ktonnes N yr⁻¹.

The good agreement between the Runge-Kutta version of the model (FRAME

UK sulphur (kt S yr ⁻¹)	(NEGTA, 2001) 1996 estimations	FRAME 3.1 1996	FRAME 4.0 1996
Import	90	116	116
Emission	1014	1005	1005
Dry deposition	125	159	161
Wet deposition	171	154	152
Total deposition	296	313	313
Export	808	808	808

Table 3.10: Budgets of sulphur for the UK for 1996 from FRAME 3.1 and 4.0 compared against the measurement based estimates of NEGTA. FRAME 4.0 considers a new diffusion scheme (FVM). Units are ktonnes S yr⁻¹.

3.1) and the implicit Finite Volume version (FRAME 4.0) is confirmed in the comparison of their results at each grid square of the UK domain. Figures 3.18 and 3.19 illustrate the comparison between versions 4.0 and 3.1 for both modelled NH₃ surface concentration and NH_x wet deposition for 1996.

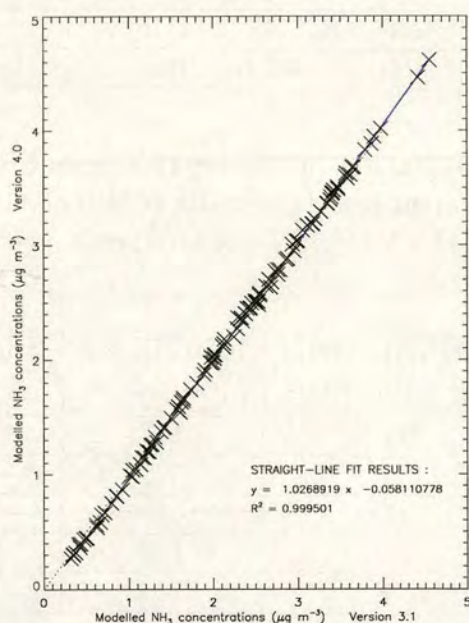


Figure 3.18: Plot of modelled NH₃ surface concentration for 1996 for the UK from FRAME 4.0 against FRAME 3.1. Units are µg m⁻³.

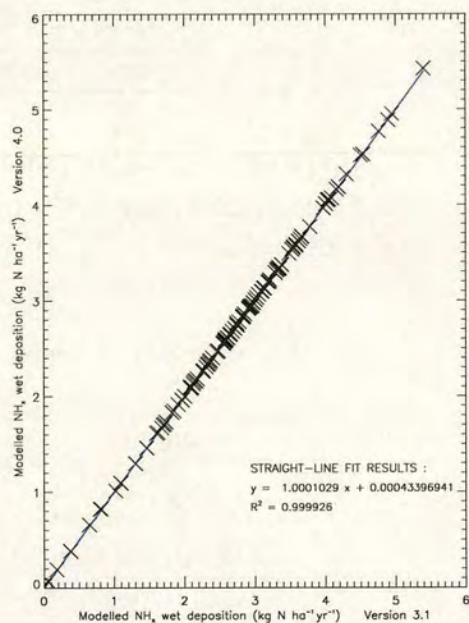


Figure 3.19: Plot of modelled flux of NH_x wet deposition to the UK for 1996 from FRAME 4.0 against FRAME 3.1. Units are kg N ha⁻¹ year⁻¹.

3.4.5 Conclusions regarding the implementation of a FVM in FRAME

A new version (4.0) of the FRAME model has been developed using an implicit Finite Volume Method to discretise the diffusion equation. The main advantage of this implicit scheme in comparison to the previous explicit 4th order Runge-Kutta method is that it allows a bigger time step to be used (120 seconds). It leads to a substantial improvement in the run-time of the FRAME model. Indeed, the implicit FVM (FRAME 4.0) runs 34 times faster than the Runge-Kutta method (FRAME 3.1) and produces similar results in terms of UK budgets, concentrations and depositions for 1996 for the different species.

3.5 Summary of the developments to extend the FRAME domain and improve numerical procedures

The extension of the model from Great Britain to the British Isles was motivated in the first instance by the desire to include Northern Ireland and cover the whole of the United Kingdom. It quickly became apparent, however, that exchange over the Republic of Ireland should also be included as this was partly within the model domain, and results for Northern Ireland would otherwise be inaccurate. Although some input data still need to be refined for Eire, this extension of the domain of the FRAME model to the British Isles (FRAME 2.0) led to improved estimates of UK concentrations and deposition. The reduced nitrogen, sulphur wet depositions and the dry deposition of oxidised nitrogen are still underestimated by FRAME 2.0 and these issues are addressed in the following chapter.

Given the time requirements of the model on a single workstation, particularly for the British Isles version, it was clear that speeding-up the code was an important foundation for further advances to be included in the model (chapter 4). In this regard, an efficient parallel implementation of the FRAME model has been presented (FRAME 3.1). Its portability allows the code to run on a number of parallel machines without modifications. The speedup of 69 obtained with the Cray T3E shows that the data-parallel approach is well suited to the present model.

Moreover, an implicit Finite Volume Method has been implemented in the model (FRAME 4.0) to discretise the diffusion equation. It allows a bigger time step to be used than in the previous explicit Runge-Kutta method implemented in FRAME 1.0-3.1. Thus, it led to a speed-up of 34 between FRAME 3.1 and FRAME 4.0 with similar predictions in concentrations and depositions for 1996. This is a substantial improvement, as by comparison to the parallel version, this development does not require major computing facilities to be effective. Indeed, the FVM could be implemented on a serial version of the FRAME model and be run efficiently on a current powerful 1-processor personal computer.

Finally, it must be recognised that the accuracy of the emissions data is critical to the performance of the model, and for the United Kingdom, this was made possible using the new distribution model of Dragosits *et al.* (1998). By contrast, further work to improve the distribution of NH₃ emissions for the Republic of Ireland must be considered a priority. For example, in the current distribution for the Republic of Ireland, due to data restrictions, pig and poultry NH₃ emissions are modelled at less than 5 km resolution. The effect of this is to provide apparently smoother NH₃ concentrations in the Irish Republic.

Chapter 4

Development of the parameterisation of atmospheric processes in FRAME

4.1 Introduction

The FRAME model has been improved by considering explicitly the Republic of Ireland in its domain and by speeding-up its execution time. This permits further developments of the model without having run-time and domain limitations. Indeed, the Republic of Ireland has important emissions of pollutants and thus, combined with the southwesterly bias in the wind direction, it was fundamental to consider it in order to model accurately the patterns of transport and deposition of pollutants over the United Kingdom. In this chapter, attention is focused particularly on the wet deposition process (section 4.2) as it shows the largest discrepancy in FRAME from the UK reduced nitrogen budgets (Fournier *et al.*,

2002a; NEG-TAP, 2001). Firstly, the influence of orography on rainfall distributions and wet deposition of reduced nitrogen is investigated over the British Isles. Secondly, a new parameterisation of the wet deposition process is developed by considering explicitly the height of the mixing layer calculated in the FRAME model. The second section of this chapter (4.5) deals with the dry deposition of oxidised nitrogen as it is underestimated significantly by the model. Finally, section 4.6 presents results from the model considering point source emissions for SO₂ in the UK.

4.2 Parameterisation of wet deposition

Current pollution models frequently describe the wet deposition of chemical species from the atmosphere using the concentration of the species, its scavenging coefficient and the rainfall rate (RGAR, 1997; NEG-TAP, 2001). However, over the British Isles (BI), the spatial pattern of rainfall intensity often varies on a scale smaller than the spacing between rainfall stations, especially in mountainous areas. Indeed, it is well known that the rainfall rates occurring over mountainous and hilly regions are significantly greater than those over the surrounding low level ground. For the BI conditions, the orographic enhancement of precipitation, and hence wet deposition from the seeder-feeder effect, must be taken into account. In this process, orographically induced or enhanced clouds over high ground (feeder clouds) allow precipitation falling from higher-level clouds (seeder clouds) to grow rapidly, giving greater precipitation amounts than over neighbouring low ground (Bergeron, 1965). The quantitative effects of orographic enhancement over the BI are very dependent on flow direction as has been shown in both experimental studies (Fowler *et al.*, 1988; Dore *et al.*, 1990; Fowler *et al.*, 1998; Dore *et al.*, 2001) and modelling studies (RGAR, 1997; Lee *et al.*, 2000).

A model of directional orographic enhancement of precipitation is developed here (section 4.2.1) which incorporates cloud-water generation by orographic and

synoptic-scale lifting and the conversion of cloud-water to rainwater (Weston and Roy, 1994). The directional orographic precipitation given by this model is incorporated in the FRAME model through the parameterisation of the scavenging coefficients (section 4.2.3). Moreover, a more realistic description of this parameterisation of the scavenging coefficients is implemented. Instead of using a fixed value of the height of the atmospheric boundary layer, a calculated value is considered in the parameterisation (section 4.3). We focus particularly on the UK wet deposition of reduced nitrogen (reduced-N) as all the UK dispersion models underestimate it with respect to available measurements (NEGTAP, 2001; Fournier *et al.*, 2001).

4.2.1 Precipitation model

The parameterisation of the wet deposition process in the FRAME model has been described previously in section 2.2.4. The wet deposition of chemical species from the atmosphere depends on the concentration of the species, the rainfall rate and its scavenging coefficient which is described through the equation :

$$\lambda_i = \frac{\Delta_i P_{sl}}{H_{mix}} + 2 \frac{\Delta_i (P - P_{sl})}{H_{mix}} \quad (4.1)$$

where λ_i is the scavenging coefficient (s^{-1}), Δ_i is the scavenging ratio for species “i”. No differentiation is made between in-cloud and below-cloud processes and hence, an averaged value of the scavenging ratio is used to represent the overall effect. P is the precipitation rate ($m s^{-1}$) and H_{mix} is the mixing height (1000 m). Over areas where rainfall exceeds 700 mm yr^{-1} (P_{sl} ; sea-level rainfall rate), it is assumed that this excess rainfall is due to altitudinal effects, and thus a fraction of the chemical species is removed by the seeder-feeder mechanism. In this case, λ_i is calculated by assuming that this excess rainfall will remove twice as much material as normal (Dore *et al.*, 1992).

The spatial pattern of orographic enhancement of rainfall is highly dependent

on the direction of airflow. To simulate these patterns, a model is developed to represent the change of cloud water content in a column in response to both synoptically and orographically-induced vertical motion (Weston and Roy, 1994). The cloud-water is converted into rainwater by auto-conversion. It can be summarised by the equations :

$$\Delta c = q_z \Delta z + \frac{\Delta x}{u} P_0 - \frac{\Delta x}{u} P \quad (4.2)$$

$$P = k(c - c_0), \text{ for } c \geq c_0$$

$$P = 0, \text{ otherwise}$$

where c is the liquid water content of an air column (kg m^{-2}), Δc its change in moving a horizontal distance Δx . c_0 is a threshold value below which no rain occurs, q_z the rate of increase of c with lifting of the cloud column (kg m^{-3}). Δz is the ground altitude change over a distance Δx (m), u the horizontal wind speed (m s^{-1}), k the inverse of the time constant for conversion of cloud-water to rainwater (s^{-1}). P is the precipitation rate and P_0 the non-orographic component of precipitation ($\text{kg m}^{-2} \text{s}^{-1}$).

The first term, $q_z \Delta z$, represents the change in cloud-water due to orographic lifting of the cloud column. Any increase will lead to an increase in precipitation rate and a subsequent depletion of cloud-water content. Therefore, a range of hills will experience high precipitation on the windward side but, drying out the air stream, so that there is reduced orographic enhancement over succeeding high ground, or a rain shadow. The second term represents the increase in cloud-water due to large-scale vertical motion. Assuming that this term changes relatively slowly both in time and space, large-scale rainfall rate (P_0) is set equal to the rainfall rate upwind of the lift-ground, in practise the rainfall rate at the upwind coast. The final term represents the decrease of cloud-water due to removal as rain. This is assumed to be proportional to the liquid water content of the cloud column above a threshold value, c_0 , which converts to rainwater with a time constant of $1/k$. In the model, if c becomes zero, then any further drying of

Direction	N	N-E	E	S-E	S	S-W	W	N-W
Frequency (%)	6	7	9	6	17	38	12	5

Table 4.1: Annual directional frequency of occurrence of precipitation over the British Isles (%; N: North; S : South; W : West; E : East)

the air column leaves it under-saturated, so that some further ascent is required before condensation of cloud-water will again take place.

The Weston and Roy (1994) model is applied along straight-line trajectories from 24 wind directions in a similar way to those used in FRAME. The model apporitions the observed annual rainfall according to the different wind directions with the same initial conditions. This produces a rainfall rate for each direction and, hence each grid square of the domain. This amount is multiplied by the factor corresponding to its wind direction given in Table 4.1. This factor represents the frequency of occurrence of rainfall in each wind direction in relation to the total mean annual rainfall. For example, 38 % of the precipitation comes from the south-west direction. These weighting factors have been deduced from an analysis of 1985 wind data (K. Weston unpublished data), but are fairly representative of other years. Finally, this rainfall rate is converted into a 'constant drizzle' rate for each direction by taking into account the frequency with which each wind direction occurs (Jones, 1981). It is assumed that the combination of these two different sets of data (frequencies of occurrence) does not lead to significant errors.

To initialise the precipitation model, several parameters need to be assigned a value. The values are those used by Weston and Roy (1994) for q_z (5.0×10^{-3} kg m⁻³), k ($2/3600$ s⁻¹), c_0 (1.0 kg m⁻²) and an uniform rainfall rate of 0.4 mm h⁻¹ is used to initialise the trajectories. These adjustable parameters must allow general agreement with observations. The values were chosen to produce modelled directional orographic rainfall consistent with the observed rainfall distribution prevailing over Scotland during occasions of different flow directions (Weston and Roy, 1994).

4.2.2 Application of the model to estimate the directional orographic precipitation

Figure 4.1 shows the relationship between the directional orographic rainfall obtained with the precipitation model and the orography along a transect in an arbitrary wind direction. The rain-shadow effect of the first range of hills is very pronounced and well reproduced by the model. This can also be seen in the patterns of orographic enhancement of rainfall over the British Isles for the southwest flow direction (Figure 4.2). This map shows significant values of the directional orographic precipitation from the southwesterly direction compared with the values from other sectors as from the east for example (Figure 4.3). This is caused by both the directional frequencies of occurrence of rainfall (Table 4.1) and the orography. Figure 4.2 highlights the effect of the precipitation model over mountainous areas creating alternate regions of high rates of rainfall and rain-shadow areas as occurs in Scotland. This has to be compared with the previous rainfall database used in FRAME (Figure 3.4) which does not exhibit such behaviour.

The modelled directional orographic precipitation is normalised to the observed orographic precipitation to preserve the total amount of the BI observed long-term average precipitation. In the absence of data on orographic and non-orographic components of precipitation across the British Isles, the non-orographic component is determined from the observations (using the 5 km long-term average 1960-1991) and the application of a west to east gradient of 1000 to 400 mm yr⁻¹ (Figure 4.4). The stripy pattern of this map shows that there are large areas (mostly in the west side of the UK and Eire) where there is an orographic component. The observed orographic component is the difference between the total precipitation and this non-orographic component. The non-orographic component and the new normalised orographic component are then used in FRAME in the parameterisation of the scavenging coefficients to quantify the wet reduced-N deposition over the UK.

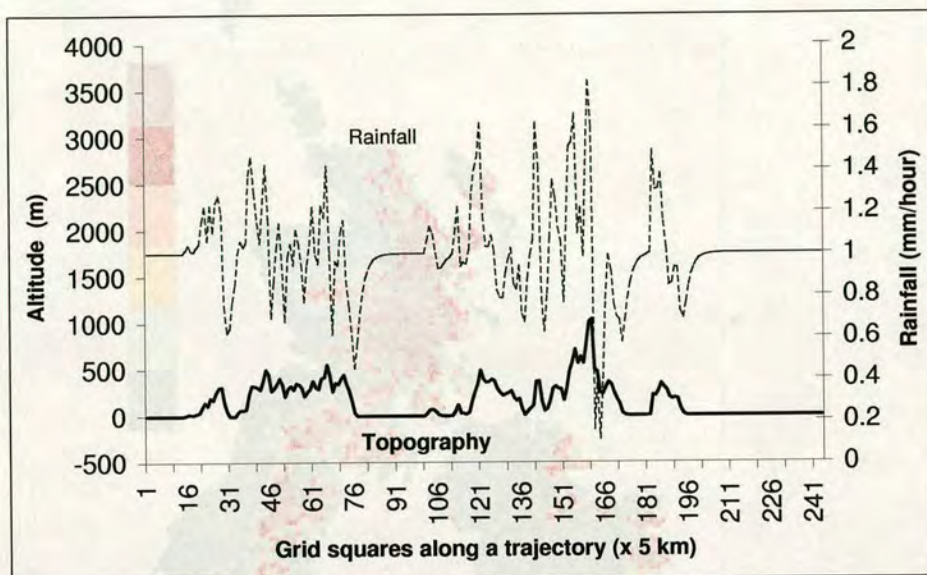


Figure 4.1: Directional orographic rainfall along an arbitrary transect over the British Isles. The wind speed is 7.5 m s^{-1} . The solid line is the ground height (m) in each grid square of the trajectory and the dotted line represents the directional orographic rainfall profile in mm h^{-1} .

4.2.3 Parameterisation of the scavenging coefficients in FRAME

Parameterisation of the scavenging coefficients is central to the description of the wet deposition process. As a result, particular attention is focused on this parameterisation and the seeder-feeder effect previously developed is incorporated in this parameterisation in FRAME (version 4.1).

The seeder-feeder process modifies the local concentrations of ions in precipitation because the feeder cloud water, scavenged by falling precipitation, contains larger average concentrations of the major pollutant ions than seeder rain. The larger concentrations in hill cloud result from the activation of aerosols, which contain the pollutants sulphate, nitrate and ammonium, to create cloud droplets when the air is forced to rise and cool. Thus the seeder-feeder process leads to a

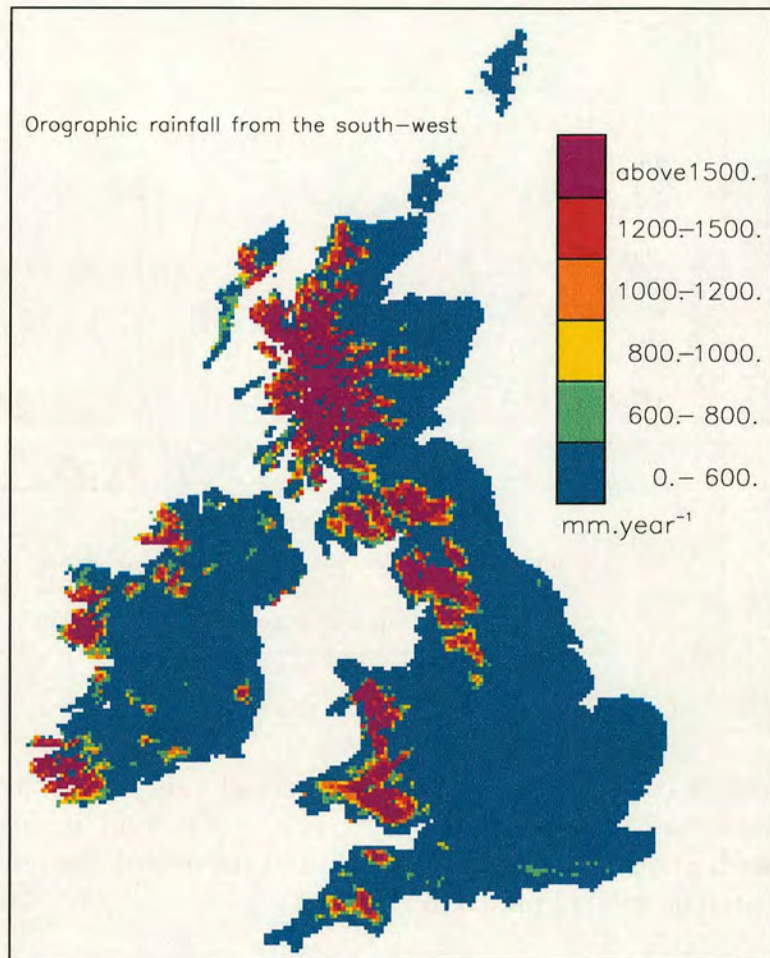


Figure 4.2: Average annual directional orographic rainfall from the South-West obtained with the precipitation model (mm yr^{-1}), at a $5 \text{ km} \times 5 \text{ km}$ resolution.

larger increase in wet deposition of the major ions with altitude than that of precipitation (RGAR, 1997). A “seeder-feeder” enhancement factor must therefore be applied to the scavenging coefficients of these ions on the orographic component of precipitation. The factor of 2 is applied following the studies of Fowler *et al.* (1988); Dore *et al.* (1992); Inglis *et al.* (1995); Fowler *et al.* (1995); Dore *et al.* (2001) on the sulphate, nitrate, ammonium ions. The parameterisation of the scavenging coefficients becomes :

$$\lambda_i = \frac{\Delta_i P_{noc}}{H_{mix}} + E_i \frac{\Delta_i P_{doc}}{H_{mix}} \quad (4.3)$$

where P_{noc} is the non-orographic component of the precipitation, P_{doc} is the di-

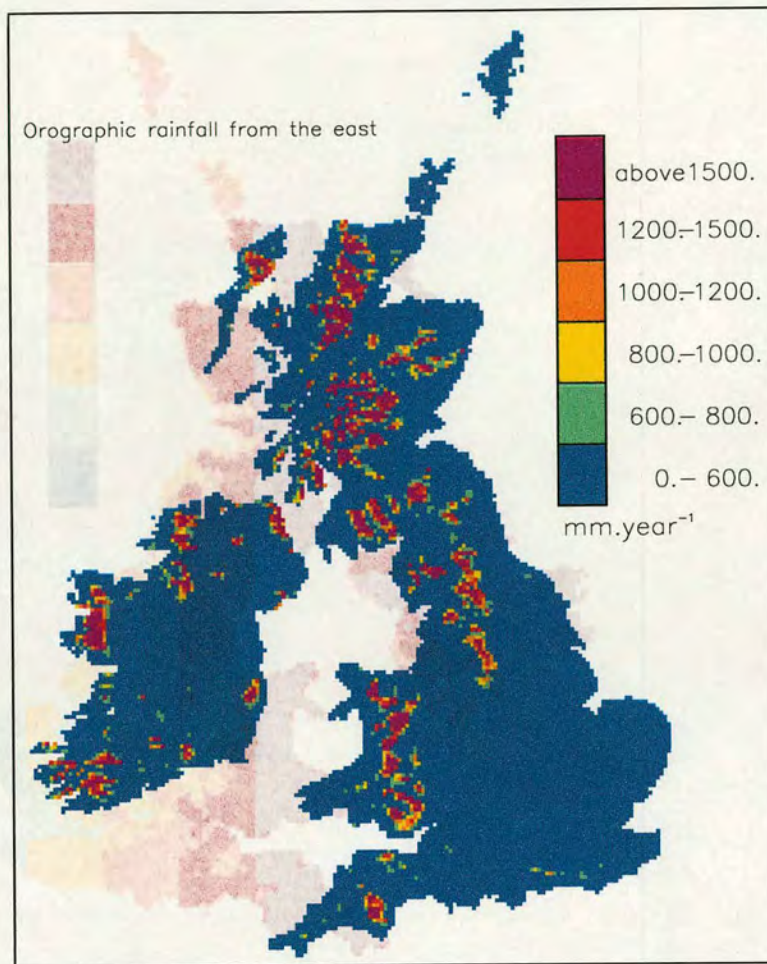


Figure 4.3: Average annual directional orographic rainfall from the East obtained with the precipitation model (mm yr^{-1}), at a $5 \text{ km} \times 5 \text{ km}$ resolution.

rectional orographic component of the precipitation (assessed in the previous section). E_i is the enhancement factor, equal to 2 for sulphate, nitrate, ammonium ions and to 1 for the other species considered in FRAME.

4.2.4 Results of FRAME 4.1 with directional orographic rainfall

Table 4.2 shows the United Kingdom 1996 reduced-N deposition budgets obtained with FRAME 4.0 and FRAME 4.1. The first column indicates the 1996 NEG-TAP (National Expert Group on Transboundary Air Pollution) estimations derived

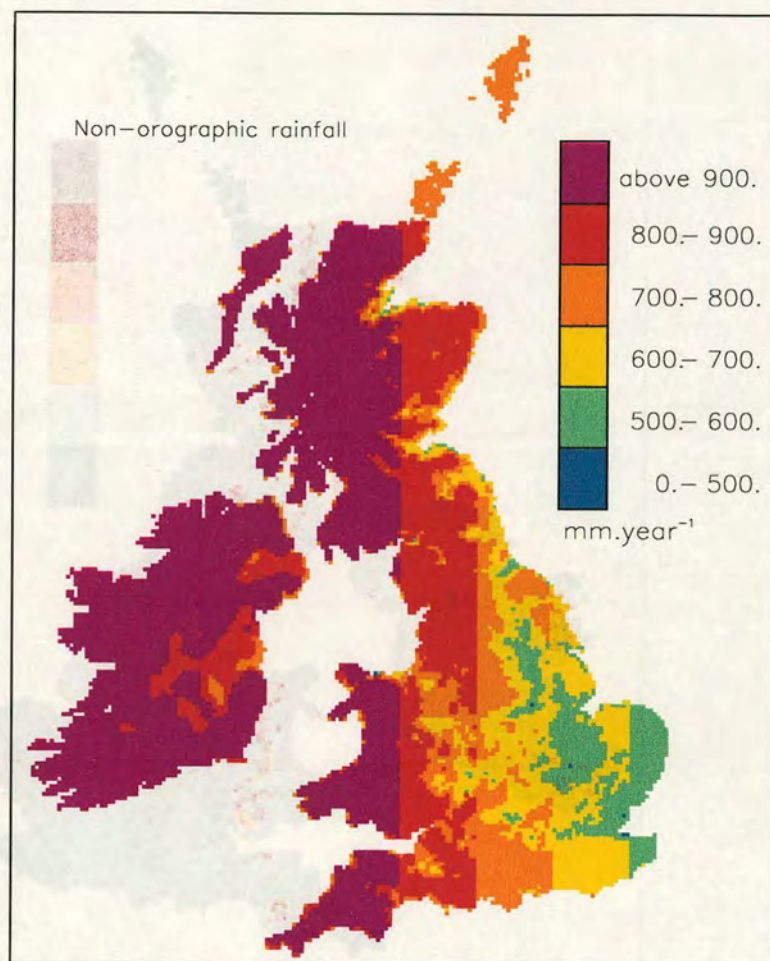


Figure 4.4: Average annual non-orographic rainfall (mm yr⁻¹), at a 5 km × 5 km resolution.

from 1995-97 measurements (NEGTAP, 2001). The basic version of FRAME (4.0) underestimates wet deposition of reduced nitrogen but the dry deposition budget is consistent with measurements (Fowler *et al.*, 1998).

FRAME 4.1, with directional orographic precipitation, underestimates the wet deposition but the general pattern is respected with the highest wet deposition in hill areas of central northern England and Wales. The comparison of the 1996 modelled distributions of reduced-N wet deposition to the BI from FRAME 4.0 and 4.1 (Figure 4.5) shows differences in the upland areas of Scotland, Wales, Pennines, Cornwall, Northern Ireland and south of Eire. Except in Scotland, FRAME 4.1 is not able to predict the expected high rates of wet deposition above 5 kilogramme N ha⁻¹ year⁻¹ (kg) in these regions.

UK reduced-N kt N yr ⁻¹	(NEG-TAP, 2001) 1996 estimations	FRAME 4.0 1996	FRAME 4.1 1996
Dry deposition	99	97 (0)	100 (0)
Wet deposition	110	82 (73)	73 (75)
Total deposition	209	179	173
Slope	-	0.73	0.65
Intercept	-	-0.37	-0.33
R ²	-	0.64	0.75

Table 4.2: Budgets of reduced nitrogen for the UK for 1996 from FRAME 4.0 and 4.1 compared against the measurement based estimates of NEG-TAP. FRAME 4.1 considers directional orographic rainfall. The percentage of dry and wet deposition in the aerosol form NH_4^+ is shown in brackets (%). Units are ktonnes N yr⁻¹. The three last lines give respectively the slope, the intercept and the correlation coefficient (R^2) obtained in the comparison of wet deposition modelled values from FRAME against measured values for 1996.

The performance of the model predictions is illustrated for locations in the UK (Figure 2.11) that are included in the UK National Precipitation Composition Monitoring Network. Comparison of the modelled NH_x wet deposition from FRAME 4.0 with the 1996 measurements (NEG-TAP, 2001) shows a correlation coefficient of $R^2=0.64$, but the model underestimates the measurements (Figure 3.12). The main discrepancies between the measurements and FRAME 4.0 appear in Scotland and are appreciable at Glen Dye (site 5011) and Balqhidder (site 5152); in Wales (Beddgelert, site 5119); in the Pennines (Bannisdale, site 5111); in Yorkshire Moors (High Muffles, site 5009) and in the East of Northern Ireland (Hillsborough Forest, site 5149).

The same scatter plot with the modelled NH_x wet deposition obtained from FRAME 4.1 (Figure 4.6) gives a higher correlation coefficient ($R^2=0.75$) but with a smaller slope (0.65 against 0.73). The lower slope of FRAME 4.1 compared with measurements is mainly due to a decrease of wet deposition at sites in Wales (Beddgelert (site 5119), Pumlumon (site 5150), Llyn Brianne (site 5124)), in the Pennines (Bannisdale (site 5111), Cow Green Reservoir (site 5113)) and in Northern Ireland (Hillsborough Forest, site 5149). The decrease in Wales is the main cause of the improvement of the correlation coefficient.

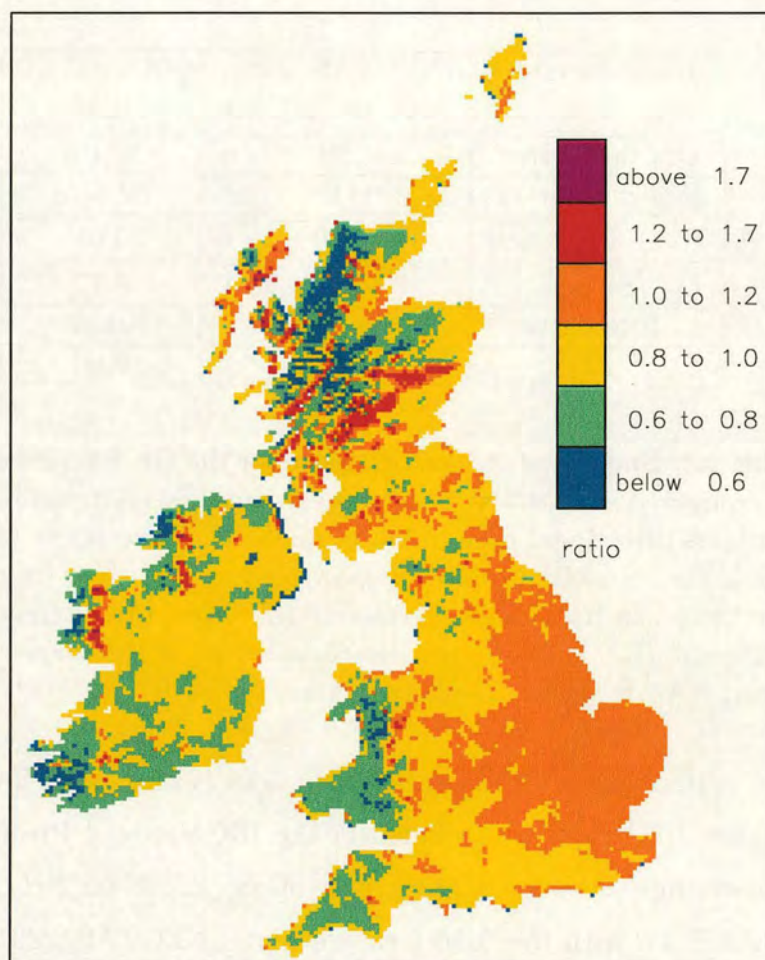


Figure 4.5: Ratio map of the flux of NH_x wet deposition modelled values between FRAME 4.1 and FRAME 4.0. The plot shows $\frac{\text{FRAME4.1}}{\text{FRAME4.0}}$ to the British Isles for 1996 at a $5 \text{ km} \times 5 \text{ km}$ resolution.

The directional orographic rainfall permits to improve the results of FRAME which was overestimating the NH_x wet deposition in Wales. However, in some of the mountainous areas of Scotland (Loch Dee (site 5107), Polloch (site 5151), Balqhidder (site 5152)), where there are significant discrepancies between the measurements and the model, FRAME 4.1 shows a slight increase in the reduced nitrogen wet deposition. Thus, the mountainous areas of the west coast of Great Britain are the most affected, in terms of reduced-N wet deposition, by the use of the directional orographic rainfall in FRAME.

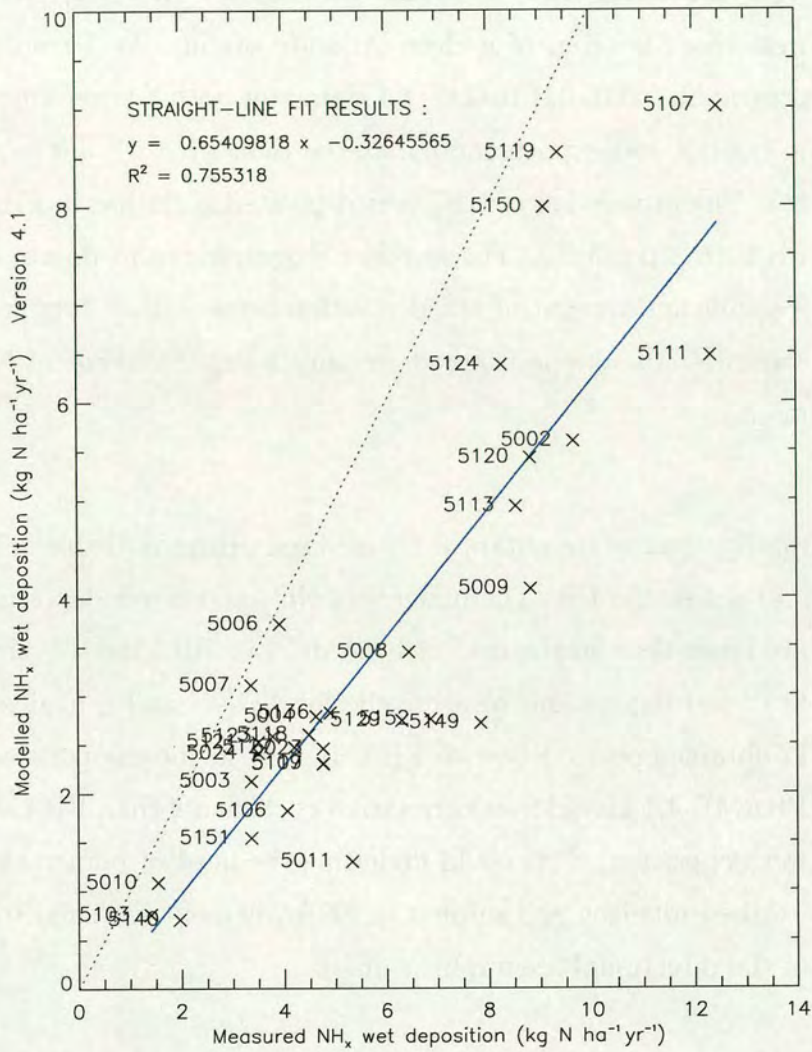


Figure 4.6: Plot of modelled NH_x wet deposition values (FRAME 4.1) against measured values for 1996. The central dotted line is a one to one agreement. The solid blue line is the best fit line produced by a regression analysis. Each point has a number assigned which corresponds to the location of the monitoring site shown in Figure 2.11.

4.2.5 Discussion about the use of directional orographic rainfall in FRAME

The wet deposition patterns are very dependent on meteorological conditions and on whether the air trajectories have crossed major pollution sources. The field of rainfall produced by the precipitation model gives mostly heavy rains

from the south and southwest directions. However, the air arriving on the west coast is often of a clean Atlantic origin. As a result of using directional orographic rainfall, FRAME 4.1 estimates both a lower amount of wet deposition in the UK and exports more material than FRAME 4.0 (with 172 kt against 165 kt). The proportion of NH_4^+ wet deposited is similar in FRAME 4.1 (75 %) and FRAME 4.0 (73 %). The heaviest orographic rains do not succeed in producing a significant amount of wet deposition because they originate from the west and southwest directions from where only a small amount of NH_4^+ is coming in the model.

Similar figures are obtained for oxidised nitrogen (Table 4.3) and sulphur (Table 4.4) across the UK. The budgets of NO_y and S wet deposition from FRAME 4.1 are lower than in the case of FRAME 4.0. FRAME 4.1 produces 96 kt and 130 kt of wet deposition, respectively, for $\text{NO}_y\text{-N}$ and S against the 113 kt and 152 kt obtained previously with FRAME 4.0. In the comparison with measurements, FRAME 4.1 gives lower correlation coefficients than FRAME 4.0 for NO_x and S wet deposition. This could underline the need of refinement of the treatment of oxidised nitrogen and sulphur in FRAME (next sections) to take fully advantage of the directional orographic rainfall.

Several factors may account for the errors in the modelled wet deposition of reduced-N. A “seeder-feeder” enhancement factor of 2 has been applied to the scavenging coefficients of the pollutant ions on the orographic component of precipitation. Field experiments have shown that the highest frequency in which seeder-feeder events occur is in south-westerly flow (Fowler *et al.*, 1998), hence this factor could be applied only in specific wind directions. This is consistent with seeder-feeder events occurring during frontal depressions moving over the UK. Such conditions are the main cause of orographic enhancement of precipitation by the seeder-feeder effects. Experimental and modelling works (Fowler *et al.*, 1988; Dore *et al.*, 1990; RGAR, 1990, 1997; Lee *et al.*, 2000; Dore *et al.*, 2001) emphasised the directional-dependence of this factor (southwesterly bias), but the quantification of this directionality is still uncertain and needs

UK oxidised-N kt N yr ⁻¹	(NEGTAP, 2001) 1996 estimations	FRAME 4.0 1996	FRAME 4.1 1996
Dry deposition	87	32	32
Wet deposition	91	113	96
Total deposition	178	145	128
Slope	-	1.31	1.11
Intercept	-	-0.39	-0.34
R ²	-	0.64	0.57

Table 4.3: Budgets of oxidised nitrogen for the UK for 1996 from FRAME 4.0 and 4.1 compared against the measurement based estimates of NEG-TAP. FRAME 4.1 considers directional orographic rainfall. Units are ktonnes N yr⁻¹. The three last lines give respectively the slope, the intercept and the correlation coefficient (R²) obtained in the comparison of wet deposition modelled values from FRAME against measured values for 1996.

UK sulphur kt S yr ⁻¹	(NEGTAP, 2001) 1996 estimations	FRAME 4.0 1996	FRAME 4.1 1996
Dry deposition	125	161	158
Wet deposition	171	152	130
Total deposition	296	313	288
Slope	-	0.57	0.46
Intercept	-	0.97	1.12
R ²	-	0.55	0.50

Table 4.4: Budgets of sulphur for the UK for 1996 from FRAME 4.0 and 4.1 compared against the measurement based estimates of NEG-TAP. FRAME 4.1 considers directional orographic rainfall. Units are ktonnes S yr⁻¹. The three last lines give respectively the slope, the intercept and the correlation coefficient (R²) obtained in the comparison of wet deposition modelled values from FRAME against measured values for 1996.

further study. Similar uncertainties exist relating to the use of this enhancement factor for the gas phase species. Indeed, gases are dissolved into orographic cloud droplets and are deposited to the ground by the seeder-feeder effect. This mechanism could be important, particularly for NH₃ which is taken up quickly into solution. However, the description of this process is complex as it depends on the lifetime of the cloud and the total surface area and volume of the droplets.

Therefore, these two processes have not been taken into account, currently, in FRAME but are subject of study for further development of the model.

In addition to the seeder-feeder effect, cloud droplets may be deposited directly to the hill surface by turbulent eddies formed by frictional airflow near ground level. However, this process has deposition rates much smaller than in the case of precipitation. Hill *et al.* (1987) made a comparison between models of turbulent deposition and the seeder-feeder effect for sulphate over a hill and found that the seeder-feeder effect was 5 to 10 times more efficient. Nevertheless, Fowler *et al.* (1992) showed that this turbulent deposition can increase the total ion wet deposition by 30 % in Snowdonia, the upland regions of Cumbria and the Scottish Highlands. Similarly, Crossley and Wilson (1992) underlined the importance of this phenomenon at Glentress Forest in Scotland. This effect can be important depending on the local conditions : precipitation, pollutant concentration in the cloud and the type of landcover. Therefore, the cloud water deposition should be explicitly represented in FRAME which considers it, at present, as being incorporated by wet deposition. Moreover, in hilly regions, a significant proportion of annual precipitation falls as snow, hence an orographic enhancement of rainfall can occur over hills due to the scavenging of cloud drops by snowflakes. Dore *et al.* (1992b) used a model of the orographic enhancement of snowfall by the seeder-feeder effect to show that these enhancements of precipitation and pollutant deposition were more important for snowfall than for rainfall.

The main cause of deficiency of wet deposition from FRAME using directional orographic rainfall model is the lack of pollutant from the west and southwest flow directions. The pattern of rainfall used in FRAME 4.1 is more representative of the British Isles meteorological conditions than the one used before (annual average rainfall) but it suffers from a limitation of FRAME and, mainly of TERN (European boundary conditions), which use straight-line trajectories. Indeed, this approach does not allow air from emission sources to be trapped in cyclonic conditions and so to come back to a precipitating part of the depression. A way of improving this will be to create the FRAME boundary conditions using the

EMEP model over Europe as it does not use straight-line trajectories (Tarrason and Schaug, 1999). Another feature which could limit the influence of this directional orographic rainfall is the wind rose used in the FRAME model. It originates from a study of Jones (1981) and thus, it may be out of date. Combined with the different set of frequency for the directional rainfall occurrence (K. Weston, unpublished data, 1985), this creates uncertainties which need to be considered before implementing definitely the directional orographic rainfall in FRAME. Therefore, although FRAME 4.1 led to a substantial improvement in the comparison of reduced nitrogen wet deposition with measurements, FRAME 4.0 will be used in the following sections.

Finally, during recent years, significant efforts have been made to model the long-range transport of ammonia over the UK. To be able to assess the validity of modelled wet deposited ammonium, there is a need for reliable ammonium concentration measurements in precipitation. Indeed, a note of caution must be sounded as there are some uncertainties concerning the measurements we used in our comparisons. NH_4^+ is a difficult component to measure and it is the ion that shows least agreement in measurements between bulk and wet-only collectors (Buijsman and Erisman, 1988).

4.3 Effect of the mixing layer depth on the precipitation scavenging

4.3.1 Introduction

The overestimation of FRAME NH_4^+ surface concentration (Figure 3.9) is an important finding indicating that the model wet scavenging coefficient for NH_4^+ might be too low, resulting in underestimation of the wet deposition. Indeed, a slope of 1.41 ($R^2=0.86$) was obtained in the comparison of NH_4^+ surface concentration with measurements with FRAME 2.0 and FRAME 4.0.

In the previous parameterisation of the scavenging coefficients (Equations 4.1 and 4.3), a fixed depth of the mixing layer was considered. The scavenging ratio in FRAME were consistent with those used in the EMEP model (see section 2.2.4 and Table 2.10) where an air column with a constant depth of 1000 m was assumed. In contrast, in FRAME, the diurnally-varying mixing layer depth is calculated depending on insolation and cloud cover, wind speed and underlying surface (see section 2.2.3). At nighttime, mixing layer depths are assigned according to Pasquill category and wind speed (Pasquill, 1961; ApSimon *et al.*, 1994). The vertical mixing in this mixing layer is then determined by the diffusion equation. As in other atmospheric transport models (Asman and van Jaarsveld, 1992; Baklanov and Sorensen, 2001), a variable depth of the mixing layer is considered to improve the physical description of the scavenging coefficients in the FRAME model (version 4.2). Equation 4.1 can be rewritten :

$$\lambda_i = \frac{\Delta_i P_{sl}}{H_{mixcal}} + 2 \frac{\Delta_i (P - P_{sl})}{H_{mixcal}} \quad (4.4)$$

where H_{mixcal} is the calculated depth of the mixing layer.

4.3.2 Result of considering a variable height of the mixing layer

FRAME 4.2 uses a variable depth of the mixing layer in the parameterisation of the scavenging coefficients. This approach succeeds well in simulating the UK reduced-N wet deposition, giving 106 kilotonnes N yr⁻¹ (Table 4.5).

This close agreement with the estimates derived from measurements (110 kt) is confirmed in the comparison of the modelled NH_x wet deposition with the 1995-97 measurements (Figure 4.7). A slope of 0.85 is obtained with a correlation coefficient of 0.66. There are still some significant differences with measurements in Scotland (sites 5152, 5151, 5011, 5002), in Wales (5119) and in Northern Ireland (5149). The magnitude of this slope (0.85), given the agreement between

UK reduced-N kt N yr ⁻¹	(NEGTAP, 2001) 1996 estimations	FRAME 4.0 1996	FRAME 4.2 1996
Dry deposition	99	97 (0)	98 (0)
Wet deposition	110	82 (73)	106 (72)
Total deposition	209	179	204
Slope	-	0.73	0.85
Intercept	-	-0.37	-0.07
R ²	-	0.64	0.66

Table 4.5: Budgets of reduced nitrogen for the UK for 1996 from FRAME 4.0 and 4.2 compared against the measurement based estimates of NEG-TAP. FRAME 4.2 considers a variable depth of the mixing layer in the parameterisation of the scavenging coefficients. The percentage of dry and wet deposition in the aerosol form NH_4^+ is shown in brackets (%). Units are ktonnes N yr⁻¹. The three last lines give respectively the slope, the intercept and the correlation coefficient (R^2) obtained in the comparison of wet deposition modelled values from FRAME against measured values for 1996.

the results of FRAME and the NEG-TAP estimations (respectively, 106 and 110 kt), reflects some differences between these NEG-TAP estimations and the 1995-97 measurements used in the regression analysis. Indeed, the budget estimations used 1996 rainfall (a dry year), but the 1995-97 measurements used the 1995-97 rainfall, a wetter period, and hence, producing more NH_x wet deposition (125 kt) and a lower value of the slope when compared with FRAME results.

The effect of this new parameterisation is underlined through the comparison of the 1996 modelled distributions of reduced-N wet deposition to the BI between FRAME 4.0 and FRAME 4.2 (Figure 4.8). It shows a strong increase of the wet deposition with FRAME 4.2, especially in places such as England, where important amounts of ammonium aerosol (NH_4^+) are available to be washed out. Thus, the increase of the reduced-N wet deposition budget leads to a decrease of the UK NH_4^+ concentration improving the comparison with measurements. Indeed, a slope of 1.41 ($R^2=0.86$) was obtained for the comparison of FRAME 4.0 versus aerosol NH_4^+ surface concentration measurements (Figure 3.9). Using FRAME 4.2, this is improved to give a slope of 1.28 ($R^2=0.85$) (Figure 4.9). However, the NH_4^+ concentration is still overestimated, especially in the south-

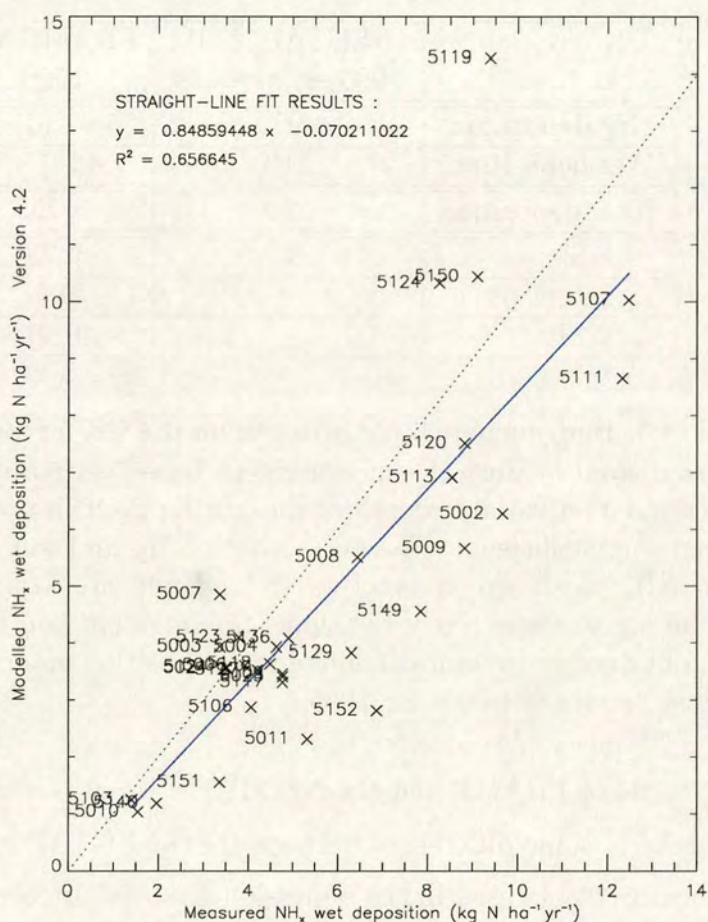


Figure 4.7: Plot of modelled NH_x wet deposition values (FRAME 4.2) against measured values for 1996. The central dotted line is a one to one agreement. The solid blue line is the best fit line produced by a regression analysis. Each point has a number assigned which corresponds to the location of the monitoring site shown in Figure 2.11.

east of England (sites 10, 13, 20, 24, 26, 33, 35, 36, 38, 39 and 46).

The use of a variable mixing layer depth in the parameterisation of the scavenging coefficients therefore improves considerably the results from FRAME for reduced nitrogen. Indeed, the value of this calculated depth of the mixing layer in FRAME ranges between 290 m and 820 m against a fixed value of 1000 m in the previous approach. The use of the variable mixing layer height in the calculation of the scavenging coefficients led to an increase of the value of the scavenging coefficients and hence, of the amount of the wet deposition of reduced-N, causing a closer agreement between FRAME NH_4^+ surface concentration and measurements. On

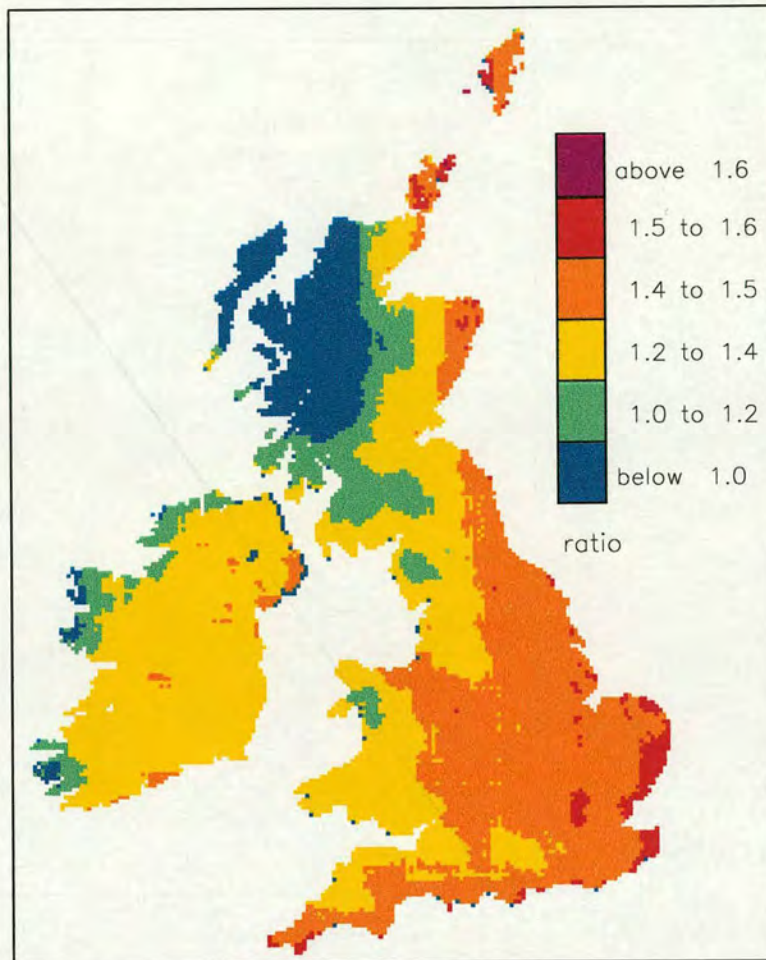


Figure 4.8: Ratio plot of grid average 1996 modelled flux of NH_x wet deposition between version 4.2 and version 4.0. The plot shows $\frac{\text{version 4.2}}{\text{version 4.0}}$ to the British Isles at a $5 \text{ km} \times 5 \text{ km}$ resolution.

the other hand, this change, implemented in FRAME 4.2 caused the increase of both oxidised nitrogen and sulphur wet deposition (see Tables 4.6 and 4.7), leading to overestimation of $\text{NO}_y\text{-N}$ and S wet deposition.

As a consequence of the increased oxidised nitrogen wet deposition in FRAME 4.2, the total deposition agrees better now with the measured 1995-97 estimations (190 kt against 178 kt). This underlines the weaknesses of FRAME to model accurately the NO_y processes. A similar behaviour is exhibited by the sulphur wet deposition which now overestimates the 1996 estimations (212 kt against 171 kt). These two issues are addressed in the next sections.

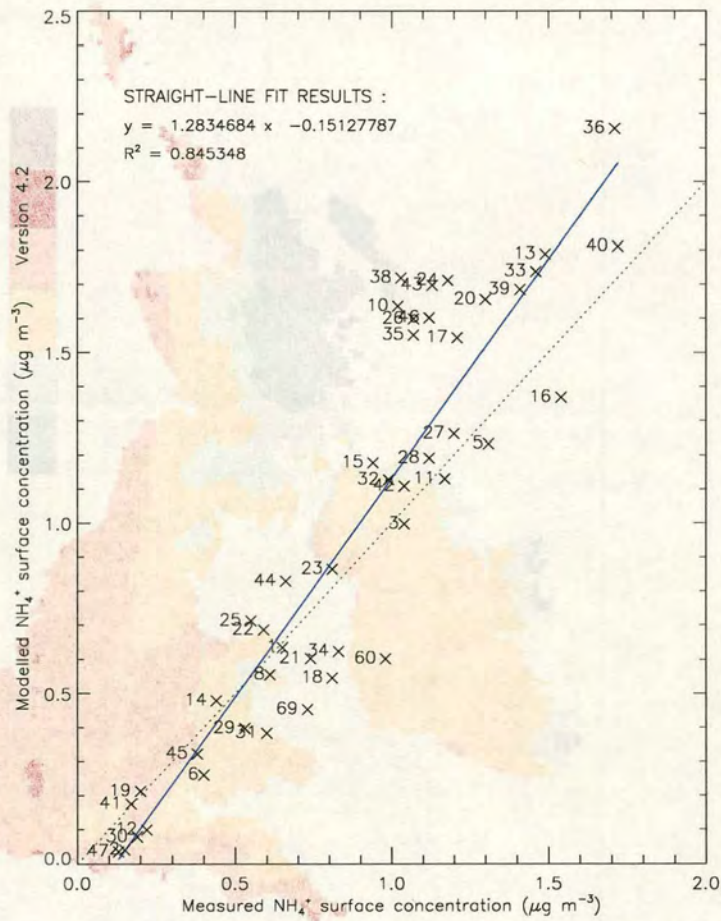


Figure 4.9: Plot of modelled NH_4^+ surface concentration values (FRAME 4.2) against measured values for 1996. The central dotted line is a one to one agreement. The solid blue line is the best fit line produced by a regression analysis. Each point has a number assigned which corresponds to the location of the monitoring site shown in Figure 2.10.

4.4 Conclusions concerning the parameterisation of wet deposition in FRAME

Most precipitation in the BI falls in westerly or southwesterly airflow, as frontal precipitation, in conditions when the seeder-feeder effect occurs. Therefore, a model of orographic enhancement of rainfall over the British Isles was developed. It can reproduce the main features of the seeder-feeder process allowing rain-shadows to occur downwind of mountainous areas. Directional

UK oxidised-N kt N yr ⁻¹	(NEG TAP, 2001) 1996 estimations	FRAME 4.0 1996	FRAME 4.2 1996
Dry deposition	87	32	32
Wet deposition	91	113	158
Total deposition	178	145	190
Slope	-	1.31	1.51
Intercept	-	-0.39	1.00
R ²	-	0.64	0.61

Table 4.6: Budgets of oxidised nitrogen for the UK for 1996 from FRAME 4.0 and 4.2 compared against the measurement based estimates of NEG TAP. FRAME 4.2 considers a variable depth of the mixing layer in the parameterisation of the scavenging coefficients. Units are ktonnes N yr⁻¹. The three last lines give respectively the slope, the intercept and the correlation coefficient (R²) obtained in the comparison of wet deposition modelled values from FRAME against measured values for 1996.

orographic precipitation was obtained from this model on a finer spatial scale than observations. A seeder-feeder enhancement factor of 2 was applied on this directional orographic precipitation which is then combined with the non-orographic component of the precipitation in FRAME.

UK sulphur kt S yr ⁻¹	(NEG TAP, 2001) 1996 estimations	FRAME 4.0 1996	FRAME 4.2 1996
Dry deposition	125	161	154
Wet deposition	171	152	212
Total deposition	296	313	366
Slope	-	0.57	0.68
Intercept	-	0.97	2.86
R ²	-	0.55	0.43

Table 4.7: Budgets of sulphur for the UK for 1996 from FRAME 4.0 and 4.2 compared against the measurement based estimates of NEG TAP. FRAME 4.2 considers a variable depth of the mixing layer in the parameterisation of the scavenging coefficients. Units are ktonnes S yr⁻¹. The three last lines give respectively the slope, the intercept and the correlation coefficient (R²) obtained in the comparison of wet deposition modelled values from FRAME against measured values for 1996.

The results from FRAME 4.1 with the new directional orographic rainfall were compared with 1995-97 measurements. The modelled UK 1996 wet deposition still underestimates the UK reduced-N wet deposition budget and does not reproduce the high rates present in the mountainous regions of Scotland, Wales, Cornwall, the Pennines and Northern Ireland. These regions face heavy orographic rainfalls from the west but the air arriving from this direction is relatively clean, in contrast with the polluted air from the east which is washed out over England. Thus, although this field of directional orographic precipitation is more realistic than the previous average rainfall data, it suffers from the limitations of the FRAME and TERN models which consider straight-line trajectories. Moreover, there are issues such as input data for Eire, the treatment of oxidised nitrogen and sulphur (next sections), frequencies of occurrence of wind and rainfall, which need to be tackled before implementing definitely the directional orographic rainfall in FRAME. Therefore, although FRAME 4.1 allowed a better agreement, in terms of correlation coefficient, between the FRAME modelled reduced-N wet deposition and the measurements, the seeder-feeder parameterisation will not be considered further in this study.

The constant-drizzle approach used for the rainfall in FRAME and commonly used in Lagrangian pollution models is clearly unrealistic. At any particular location, on average in the UK it rains for less than 8 % (range 4-18 %) of the time. However, this does not imply that a Lagrangian statistical model should be run for 92 % of the time dry and 8 % of the time wet. In reality, rain areas process large quantities of air, whereby low-level air flows through the rain area and thus, much of its pollutants is washed out. A Lagrangian model using dry and wet periods is inherently incapable of representing this process. During the wet periods, there is only so much of the pollutants that is available to be removed, while the rest of the time the pollutants are unavailable for wet deposition. Indeed, sensitivity experiments with FRAME, combining wet and dry periods, led to a strong underestimation of the pollutants wet deposition. For example, assuming that the wet periods represent one third of the time of the year, a reduced-N wet deposition budget for the UK of 45 kt is obtained

with a slope of 0.30 in the comparison with measurements ($R^2=0.65$). Therefore, the constant-drizzle description can be considered as a reasonable assumption to compensate the inadequacies of the Lagrangian approach.

The FRAME UK reduced-N wet deposition has been improved by developing a more realistic description of the scavenging coefficients. This parameterisation combines the average rainfall data and a variable mixing layer depth leading to a good agreement with measurements (FRAME 4.2). Therefore, FRAME 4.2 will be now used for future simulations, especially in the case of reduced-N. There are still discrepancies between the FRAME modelled values and the NEG-TAP estimations for oxidised nitrogen and sulphur but, these issues are addressed in the next sections.

4.5 Treatment of oxidised nitrogen in FRAME

4.5.1 Introduction

It has been remarked previously that the FRAME model underestimates the UK budget of oxidised nitrogen dry deposition for 1996. Indeed, an amount of 32 kt N yr^{-1} is obtained in comparison with the 87 kt from the NEG-TAP estimations. Therefore, firstly, we will focus on the contribution of the different species in the budget of NO_y dry deposition (section 4.5.2) to assess the causes of this underestimation. Secondly, as most of the NO_x emissions are at low level, a more representative height of these emissions than the previous 300 m is assessed and used in the FRAME model (section 4.5.3).

4.5.2 Deposition velocities

Oxidised Nitrogen

Table 4.8 gives the contribution of the different oxidised nitrogen components in the 1996 UK budget of dry deposition from FRAME 4.2 (Table 4.6). Only NO_2 exhibited some dry deposition and thus, represented all the 32 kt obtained by FRAME. The other oxidised nitrogen species have a specified deposition velocity which is constant over the BI (Table 2.6). Since the concentrations of these species are larger than zero this implies that a problem occurred during the computations with the values of their deposition velocities. In fact, as FRAME does not calculate deposition over the sea, the deposition velocities of the other NO_y components have been set to zero over the first sea squares and mistakenly not changed over the following land squares. These include all the species (except NH_3 , SO_2 and NO_2) for which the deposition velocity is not calculated in the FRAME model. Table 4.8 shows the results from the reviewed version of the model (FRAME 4.3) with the appropriate deposition velocities from Table 2.6 used over all the landsquares. Dry deposition calculated by FRAME 4.3 is : NO_3^- (6.5 kt), HNO_3 (3.8 kt) and PAN (2.4 kt). Thus, dry deposition increased from 32 kt to 45 kt for the UK. However, this is still far from the NEG-TAP estimations of 87 kt. The main difference with FRAME comes from the contribution of HNO_3 . NEG-TAP (2001) estimates a dry deposition of 62 kt for HNO_3 and 25 kt for NO_2 for the UK for 1996. The contribution of NO_3^- and PAN have not been assessed and hence, are assumed to be zero (R. Smith, personal communication).

The low HNO_3 contribution obtained with the FRAME model could be explained through the deposition velocity used for this species. Indeed, a value of 10 mm s^{-1} is specified in the FRAME model while most of the current studies recommend a value of $30\text{-}40 \text{ mm s}^{-1}$ (Rodgers, 1993; Klimova-Murphy and Fisher, 1997; Metcalfe *et al.*, 1998; NEG-TAP, 2001). Hence, a value of 30 mm s^{-1} is applied to the dry deposition velocity of HNO_3 in FRAME 4.4. The results are shown in Table 4.8. The HNO_3 dry deposition increased from 3.8 to 7.3 kt leading to a total budget of oxidised nitrogen dry deposition of 48 kt. Increasing by a factor

NO _y components kt N yr ⁻¹	(NEG-TAP, 2001) 1996 estimations	FRAME 4.2 1996	FRAME 4.3 1996	FRAME 4.4 1996
NO	0.0	0.0	0.0	0.0
NO ₂	25	31.9	31.9	31.9
HNO ₃	62	0.0	3.8	7.3
NO ₃ ⁻	-	0.0	6.5	6.3
PAN	-	0.0	2.4	2.4
Total deposition	87	31.9	44.6	47.9

Table 4.8: Budgets of oxidised nitrogen dry deposition for the UK for 1996 from FRAME 4.2, 4.3 and 4.4 compared against the measurement based estimates of NEG-TAP (R. Smith, pers. comm.). FRAME 4.2 considers a variable depth of the mixing layer in the parameterisation of the scavenging coefficients. FRAME 4.3 reviewed the version 4.2 with correct deposition velocities. FRAME 4.4 updated FRAME 4.3 with a new deposition velocity for HNO₃. Units are ktonnes N yr⁻¹.

3 the deposition velocity of HNO₃ did not produce 3 times more dry deposition in the UK as it caused also less import (because more deposition in Eire) from Eire to the UK. This illustrates the fact that the difference between the FRAME model and the NEG-TAP estimations is not only caused by the value of the deposition velocity but is also linked with the concentration of HNO₃. Indeed, the FRAME model substantially underpredicts HNO₃ surface concentrations as compared with the measurements made by CEH in the UK Nitric Acid Monitoring Network (Figures 4.10 and 4.11) (Sutton *et al.*, 2001b). The scatter is important as there are only 12 sites in the UK where the measurements are made (Table 4.9). Introducing this new value of HNO₃ dry deposition velocity (FRAME 4.4) causes a decrease in HNO₃ concentration because of the surface depletion due to more HNO₃ dry deposition (see Table 4.9). Conversely, FRAME 4.4 gives a larger correlation coefficient with measurements, in comparison to FRAME 4.3 (Figure 4.11; $R^2=0.67$ against 0.46). This is the consequence of more HNO₃ dry deposition, with FRAME 4.4, in forest areas (site 32 and 69). Indeed, in agricultural areas (sites 1, 24, 33), HNO₃ is consumed by NH₃, hence limiting the effect on the dry deposition of HNO₃. The underestimation of the modelled HNO₃ surface concentration by FRAME is discussed in section 4.5.4.

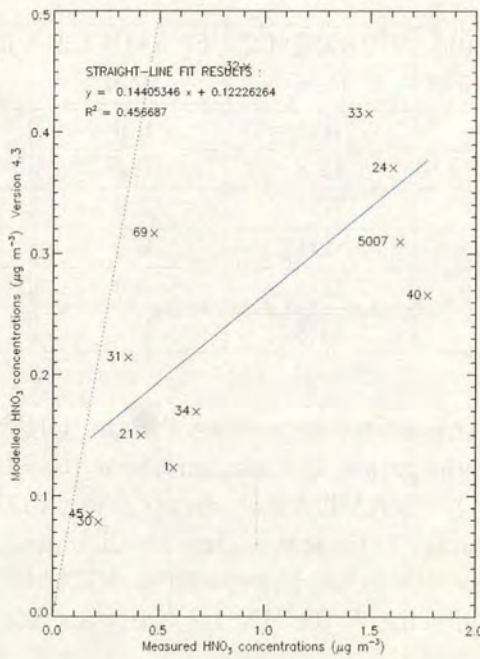


Figure 4.10: Plot of modelled HNO_3 surface concentration against measured values (FRAME 4.3; $V_d=10 \text{ mm s}^{-1}$). The dotted line is a one-to-one agreement and the solid blue line is the best fit line produced by a regression analysis.

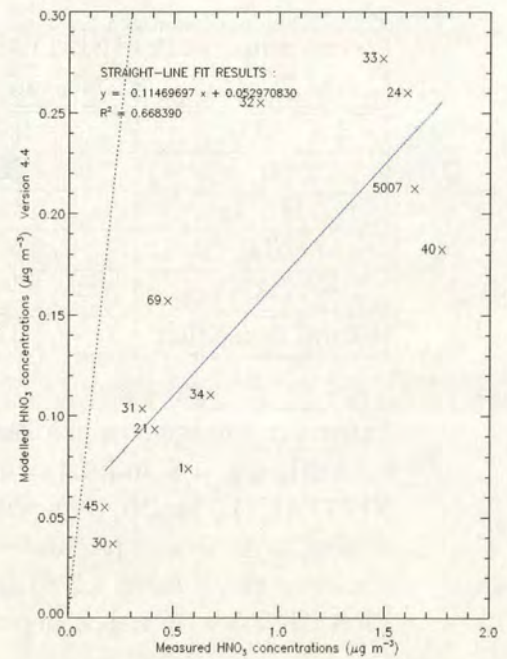


Figure 4.11: Plot of modelled HNO_3 surface concentration against measured values (FRAME 4.4; $V_d=30 \text{ mm s}^{-1}$). The dotted line is a one-to-one agreement and the solid blue line is the best fit line produced by a regression analysis.

Effects of NO_y changes on NH_x and sulphur

The changes in the dry deposition of the NO_y components affected also the dry deposition of sulphur and reduced nitrogen components such as ammonium sulphate ($(\text{NH}_4)_2\text{SO}_4$), sulfuric acid (H_2SO_4) and ammonium nitrate (NH_4NO_3). Therefore, the UK budgets of NH_x and sulphur for 1996 are slightly modified as it is shown in Tables 4.10 and 4.11.

More dry deposition is produced with FRAME 4.4 for both species with 102 kt for NH_x and 163 kt for sulphur instead of, respectively, 98 kt and 154 kt with FRAME 4.2. There is more dry deposition of $(\text{NH}_4)_2\text{SO}_4$ and NH_4NO_3 (as their deposition velocities are now different from 0.0) which are the products of the reactions of NH_3 with, respectively, H_2SO_4 and HNO_3 . These two reactions are competitive processes but NH_3 preferably reacts with H_2SO_4 (Seinfeld, 1986).

Site number	Site Name	measurements	FRAME 4.3	FRAME 4.4
1	Bush	0.57	0.12	0.07
21	Glensaugh	0.41	0.15	0.09
24	Rothamstead	1.60	0.37	0.26
30	Strathvaich Dam	0.21	0.08	0.04
31	Eskdalemuir	0.35	0.21	0.10
32	High Muffles	0.91	0.45	0.25
33	Stoke Ferry	1.49	0.42	0.28
34	Yarner Wood	0.68	0.17	0.11
40	Sutton Bonington	1.77	0.22	0.13
45	Lough Navar	0.17	0.08	0.05
69	Cwmystwyth	0.47	0.32	0.16
83 (5007)	Barcombe Mills	1.64	0.31	0.21

Table 4.9: Mean measured concentrations of HNO_3 from the UK Nitric Acid Monitoring Network (Sutton *et al.*, 2001b). Units are $\mu\text{g m}^{-3}$. The site number corresponds to the location of the monitoring site shown in Figures 2.10 and 2.11.

Moreover, there is less HNO_3 available with its new higher deposition velocity. Therefore, it led to a more important production of $(\text{NH}_4)_2\text{SO}_4$, increasing the sulphur wet deposition and the NH_4^+ wet deposition. However, in the case of NH_x

UK sulphur kt S yr ⁻¹	(NEG-TAP, 2001) 1996 estimations	FRAME 4.2 1996	FRAME 4.3 1996	FRAME 4.4 1996
Dry deposition	125	154	164	163
Wet deposition	171	212	218	220
Total deposition	296	366	382	383
Slope	-	0.68	0.68	0.69
Intercept	-	2.86	2.76	2.75
R ²	-	0.43	0.44	0.45

Table 4.10: Budgets of sulphur for the UK for 1996 from FRAME 4.2, 4.3 and 4.4 compared against the measurement based estimates of NEG-TAP. FRAME 4.2 considers a variable depth of the mixing layer in the parameterisation of the scavenging coefficients. FRAME 4.3 reviewed the version 4.2 with correct deposition velocities. FRAME 4.4 updated FRAME 4.3 with a new deposition velocity for HNO_3 ($V_d=30 \text{ mm s}^{-1}$). Units are ktonnes S yr⁻¹. The three last lines give respectively the slope, the intercept and the correlation coefficient (R^2) obtained in the comparison of wet deposition modelled values from FRAME against measured values for 1996.

UK reduced-N kt N yr ⁻¹	(NEGTAP, 2001) 1996 estimations	FRAME 4.2 1996	FRAME 4.3 1996	FRAME 4.4 1996
Dry deposition	99	98 (0)	103 (5)	102 (5)
Wet deposition	110	106 (72)	105 (76)	105 (77)
Total deposition	209	179	208	207
Slope	-	0.85	0.85	0.85
Intercept	-	-0.07	-0.10	-0.11
R ²	-	0.66	0.64	0.64

Table 4.11: Budgets of reduced nitrogen for the UK for 1996 from FRAME 4.2, 4.3 and 4.4 compared against the measurement based estimates of NEG-TAP. FRAME 4.2 considers a variable depth of the mixing layer in the parameterisation of the scavenging coefficients. FRAME 4.3 reviewed the version 4.2 with correct deposition velocities. FRAME 4.4 updated FRAME 4.3 with a new deposition velocity for HNO₃ ($V_d=30$ mm s⁻¹). The percentage of dry and wet deposition in the aerosol form NH₄⁺ is shown in brackets (%). Units are ktonnes N yr⁻¹. The three last lines give respectively the slope, the intercept and the correlation coefficient (R²) obtained in the comparison of wet deposition modelled values from FRAME against measured values for 1996.

the wet deposition keep a similar value (105 kt instead of 106) because the NH₄⁺ wet deposition increased (81 against 76 kt) but the NH₃ wet deposition decreased (24 against 30 kt). Thus, there is a decrease of NH₄⁺ surface concentrations which can be seen in the comparison with measurements (Figure 4.12) where a slope of 1.10 ($R^2=0.85$) is obtained against 1.28 ($R^2=0.85$) with FRAME 4.2 (Figure 4.9).

4.5.3 NO_x emissions height

Table 4.8 underlined the overestimation of NO₂ dry deposition by the FRAME model compared with NEG-TAP (R. Smith, pers. communication). An amount of 32 kt is simulated while the NEG-TAP estimations predict 25 kt. Moreover, the NO₂ surface concentration is underestimated by FRAME (Figure 2.31). This latter discrepancy could be caused by the way the NO_x emissions are described in the FRAME model. Indeed, as no precise inventory (5 km resolution) of NO_x

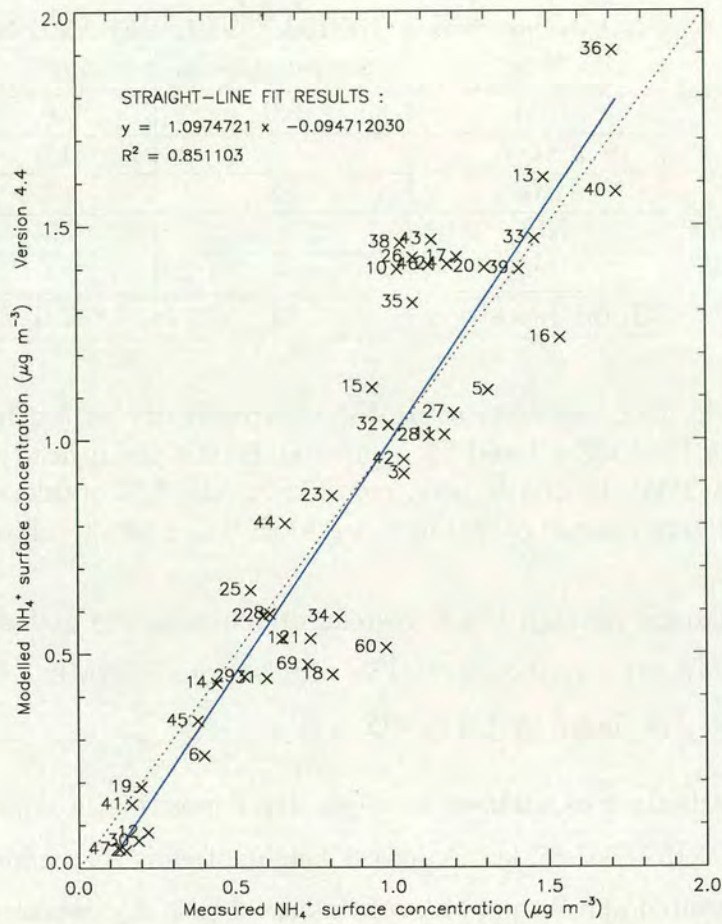


Figure 4.12: Plot of modelled NH_4^+ surface concentration values (FRAME 4.4) against measured values for 1996. The central dotted line is a one to one agreement. The solid blue line is the best fit line produced by a regression analysis. Each point has a number assigned which corresponds to the location of the monitoring site shown in Figure 2.10.

point sources 1996 emissions has been developed yet for FRAME for the UK, FRAME distributes evenly the total NO_x emissions throughout the lowest 300 m of the mixing layer. Whereas this approximation is perfectly valid for SO_2 which incorporates 80 % of high-stack emissions, these high-level emissions account only for 29 % of the NO_x emissions for the UK for 1996 (615 kt). These include 137 kt from public power stations, 33 kt from industrial combustion, 5 kt from refinery combustion and 1 kt from Iron and Steel combustion (NEG-TAP, 2001). Indeed, most of the emissions of NO_x are in the form of low-level sources from road transport (61 %). Thus, it seemed more representative to distribute these

NO _y components kt N yr ⁻¹	(NEGTA _P , 2001) 1996 estimations	FRAME 4.4 1996	FRAME 4.5 1996
NO	0.0	0.0	0.0
NO ₂	25	31.9	43.9
HNO ₃	62	7.3	7.4
NO ₃ ⁻	-	6.3	6.9
PAN	-	2.4	2.5
Total deposition	87	47.9	60.7

Table 4.12: Budgets of oxidised nitrogen dry deposition for the UK for 1996 from FRAME 4.4 and 4.5 compared against the measurement based estimates of NEGTA_P (R. Smith, pers. com.). FRAME 4.5 considers a NO_x emissions height of 100 m instead of 300 m in FRAME 4.4. Units are ktonnes N yr⁻¹.

emissions through 100 m instead of 300 m as the high-stack contribution is less than a third of the total. The results from FRAME 4.5 incorporating this new value are shown in Table 4.12.

The budget of oxidised nitrogen dry deposition is improved to 61 kt closer to the NEGTA_P 87 kt. A lowest height of emissions allows more NO₂ to be dry deposited and, hence 44 kt of this element is dry deposited against 32 previously (FRAME 4.4). It is further than FRAME 4.4 from the 25 kt of the NEGTA_P estimations but, the budget of oxidised nitrogen (Table 4.13) is improved with more dry deposition (61 kt) and less wet deposition (154 kt).

The comparison with measurements of both NO₂ surface concentration and NO₃⁻ wet deposition is improved (Figures 4.13 and 4.14). The former exhibits a good behaviour with a slope close to one. This highlights problems in the NO_y chemistry of the model as the NO₂ surface concentration matches the measurements but not the dry deposition of this component. Moreover, it must be linked with nitric acid as both the concentration and dry deposition of this species are strongly underestimated. The results of FRAME for NH_x and sulphur are not affected by these changes, hence FRAME 4.5 exhibits similar results to FRAME 4.4 for both species.

UK oxidised-N kt N yr ⁻¹	(NEG-TAP, 2001) 1996 estimations	FRAME 4.4 1996	FRAME 4.5 1996
Dry deposition	87	48	61
Wet deposition	91	157	154
Total deposition	178	205	215
Slope	-	1.51	1.47
Intercept	-	0.96	0.96
R ²	-	0.61	0.61

Table 4.13: Budgets of oxidised nitrogen for the UK for 1996 from FRAME 4.4 and 4.5 compared against the measurement based estimates of NEG-TAP. FRAME 4.5 considers a NO_x emissions height of 100 m instead of 300 m in FRAME 4.4. Units are ktonnes N yr⁻¹. The three last lines give respectively the slope, the intercept and the correlation coefficient (R²) obtained in the comparison of wet deposition modelled values from FRAME against measured values for 1996.

4.5.4 Conclusions concerning the NO_y treatment in

FRAME

The concentration of NO₂ has been improved by the consideration of both updated deposition velocities and NO_x emissions height. The modelled surface concentrations of NO₂ compare well with the measurements. However, the modelled dry deposition of NO₂ of 43.9 kt now strongly overestimates the NEG-TAP estimations of 25 kt (NEG-TAP, 2001). The dry deposition terms of other oxidised nitrogen species are also of interest.

As an illustration, R-GAR (1997) evaluated the dry deposition of HNO₃ at 30 kt with a national mean concentration of 0.45 μg HNO₃ m⁻³ and a constant dry deposition velocity of 40 mm s⁻¹. More recently, (NEG-TAP, 2001) evaluated the dry deposition of HNO₃ at 62 kt for the UK for 1996. Using 30 mm s⁻¹ in FRAME, the modelled dry deposition of HNO₃ to the UK is 7.4 kt. Indeed, the average modelled concentration of HNO₃ is 0.12 μg HNO₃ m⁻³, a factor of 8 less than that given by (NEG-TAP, 2001). As an indication, Figure 4.16 shows a map of the measured HNO₃ surface concentration interpolated at a 5 km resolution over the UK for 1999. As there is no large differences in the

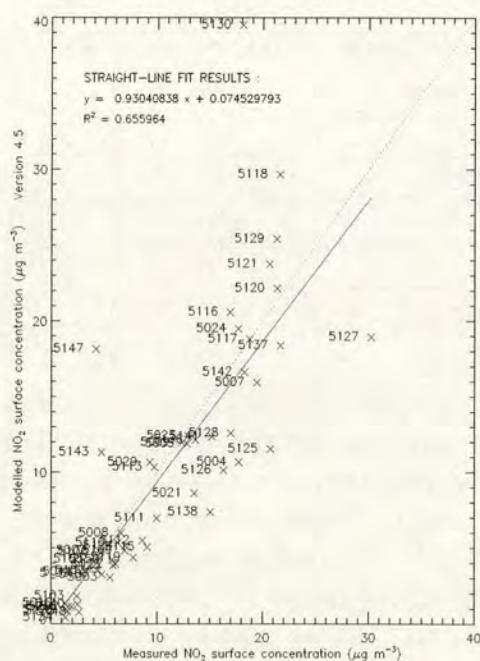


Figure 4.13: Plot of modelled NO_2 surface concentration values (FRAME 4.5) against measured values. The dotted line is a one-to-one agreement and the solid blue line is the best fit line produced by a regression analysis.

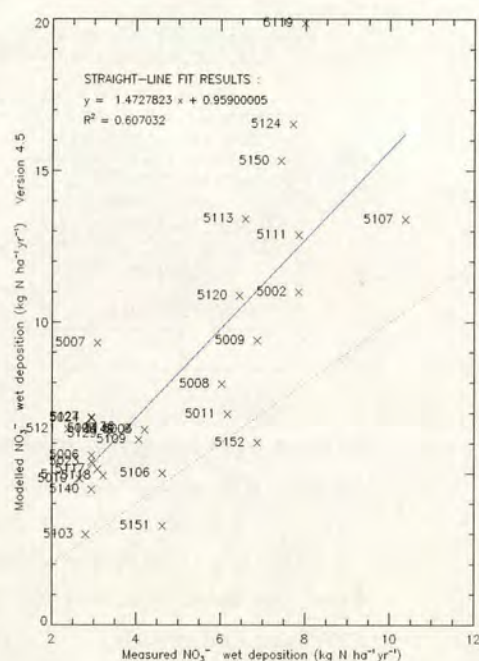


Figure 4.14: Plot of modelled NO_3^- wet deposition values (FRAME 4.5) against measured values. The dotted line is a one-to-one agreement and the solid blue line is the best fit line produced by a regression analysis.

1996 and 1999 scenarios, it is relevant to compare it with the HNO_3 surface concentration modelled by FRAME 4.4 for 1996 (Figure 4.15). This underlines the underestimation of this field by FRAME 4.4, especially in the south-east of England. Moreover, the modelled values would be 4.5 times lower on Figure 4.15 if they were expressed in $\mu\text{g N m}^{-3}$ (instead of $\mu\text{g HNO}_3 \text{ m}^{-3}$) as it is the case for the interpolated measurements. However, this allows to see that the regional patterns observed in the measurements are respected by FRAME 4.4.

In our comparison, at 12 sites, there is a factor of 6 between measurements and modelled values of HNO_3 concentration (Table 4.9). Other modelling studies (Harrison *et al.*, 1996; Lee *et al.*, 2000a) present similar results with factors of 7 and 10, respectively, between measurements and modelled values. Thus, it seems that the model underpredicts surface concentrations of HNO_3 which implies that the dry deposition of $\text{HNO}_3\text{-N}$ could be substantially larger than that calculated

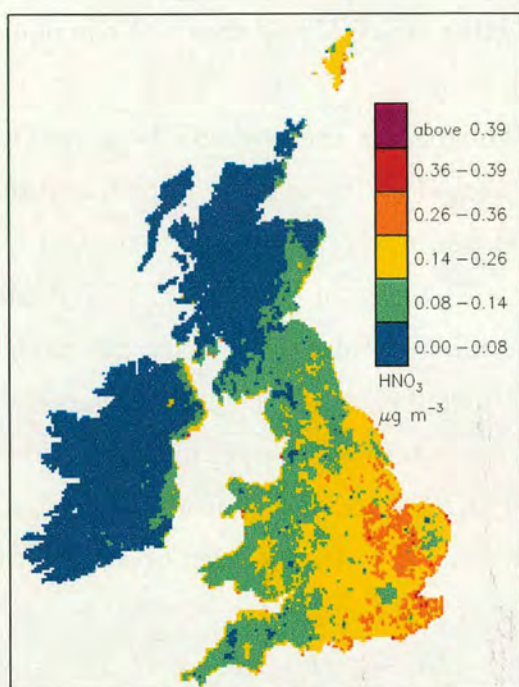


Figure 4.15: Modelled surface concentrations of HNO_3 for the British Isles for 1996 at a $5 \text{ km} \times 5 \text{ km}$ resolution (FRAME 4.4). Units are $\mu\text{g HNO}_3 \text{ m}^{-3}$.

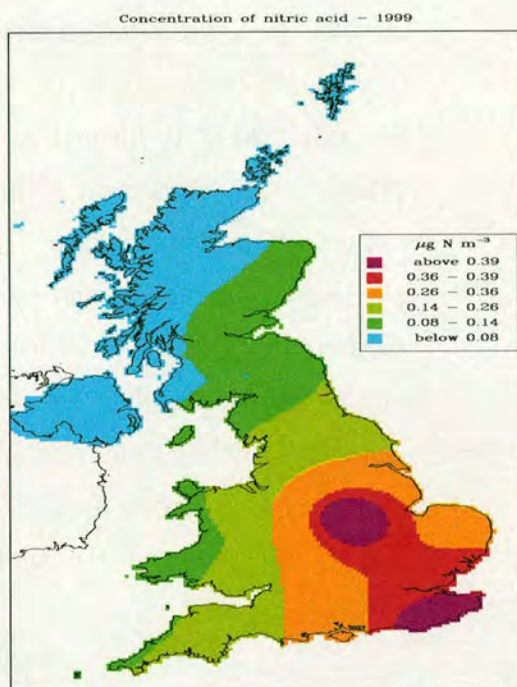


Figure 4.16: Measured surface concentrations of HNO_3 for the UK for 1999 interpolated at a $5 \text{ km} \times 5 \text{ km}$ resolution. Units are $\mu\text{g N m}^{-3}$.

at present of 7.4 kt. This fact could also explain both the overestimation of NO_2 dry deposition and of NO_y wet deposition. This latter is mostly caused by NO_3^- which accounts for 86 % of the NO_y wet deposition. The formation of large nitrate particles is driven by, firstly, the gas-to-particle conversion reaction :



and the reverse reaction :



which is assumed in FRAME to take place at half the rate of the forward reaction. Therefore, this reaction could create too much NO_3^- by converting too much HNO_3 . The rates of conversion and reverse conversion (Table 2.11) are commonly

used in the UK models, hence further study of this chemical reaction is required to evaluate the accuracy of these rates.

Secondly, NO_3^- is formed at nighttime by the reaction between O_3 and NO_2 (Table 2.11). Nitric acid is then formed by the reaction of NO_2 and the hydroxyl radical $\text{OH}\cdot$. Thus, again, if too much NO_3^- is formed there will be less NO_2 available to produce nitric acid. The rate of this reaction (k_{12}) also requires further study as FRAME uses a different value than other UK models (Barrett and Seland, 1995; Metcalfe *et al.*, 1998; Lee *et al.*, 2000a). A detailed study of the chemistry of the model is in process to tackle this issue and seems to corroborate this option. Thirdly, as the fate of NO_2 and HNO_3 from FRAME seems to be linked, the daytime nitric acid formation by the reaction of NO_2 and $\text{OH}\cdot$ has to be investigated



The rate of the model reaction, k_{21} (Table 2.11), is common to the value used in other UK models (Barrett and Seland, 1995; Metcalfe *et al.*, 1998; Lee *et al.*, 2000a) but sensitivity experiments are in process to assess its influence on the NO_y chemistry of the model.

Finally, the effect of the height of the NO_x emissions had been noticeable in the FRAME results. It would be of interest to develop and use a more precise inventory of the low-level sources of NO_x with details concerning their heights and their amplitudes. This would be more realistic and may influence substantially the FRAME modelled NO_y wet deposition and NO_2 dry deposition.

4.6 Treatment of SO_2 sources height in FRAME

4.6.1 Introduction

The previous section emphasised the importance of the vertical distribution of the emissions for NO_x . Whilst injection of low-level sources of NO_x is consistent with

the major source at this height (motor vehicles), a large proportion of the SO₂ sources are emitted from stack heights of up to 260 m. Therefore, the model is modified to allow the injection of SO₂ emissions from point sources at appropriate heights.

4.6.2 Accounting for high-level SO₂ emissions

The emissions of SO₂ have been shown in Figure 3.2. The total 1996 SO₂ emissions represents 1005 kt S year⁻¹ in the UK. 85% of these emissions are concentrated into relatively few 5 km grid squares containing the major sources such as refineries, power stations and large industrial plant. 94% of these major sources originate from 'high stack' emitting sources of up to 260 m. This means that 80% of the total SO₂ emissions, namely 806 kt, are high-level point sources. However, there is a wide range of high-level sources with different heights of emission. These include 689 kt from public power stations, 76 kt from industrial combustions, 37 kt from refinery combustion and 4 kt from iron and steel combustion. Table A.5 in Appendix A, shows the different point sources used in the model for 1996 for the UK (Salway *et al.*, 1999). Details concerning their intensity and stack height are also reported. Figure 4.17 gives an overview of the location and the intensity of these point sources over the BI domain of the FRAME model. This corroborates the general map of SO₂ emissions (Figure 3.2) with point sources located mainly in the conurbation belts around the southern Pennines, in the south of Wales, near London but also around Belfast, Aberdeen and Edinburgh.

FRAME is modified to take into account these point sources of the 1996 SO₂ emissions (FRAME 4.6). In each grid-square of the FRAME domain, a high-level component of the SO₂ emissions is considered. In every grid-square, if this component is larger than zero, its intensity (given in Table A.5, Appendix A) is subtracted from the total SO₂ emissions and injected in the air column at the level corresponding to the height of the stack. The remaining low-level component of

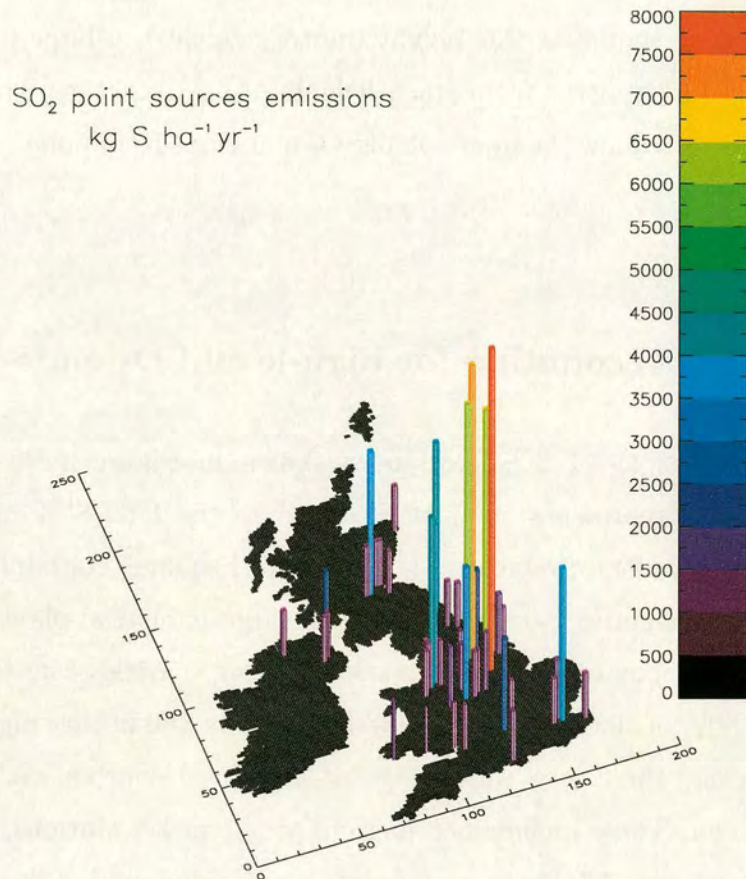


Figure 4.17: Location and intensity of the SO₂ point sources for 1996 over the British Isles domain of the FRAME model at a 5 km × 5 km resolution.

the SO₂ emissions is then evenly distributed in the lowest 300 m of the air column, as previously.

4.6.3 Results of FRAME 4.6 considering high-level sources of SO₂

The performances of FRAME 4.6 are discussed through Table 4.14 showing the UK budget of sulphur for 1996.

The consideration of point sources for the SO₂ emissions brought down both the

UK sulphur kt S yr ⁻¹	(NEGTAPE, 2001) 1996 estimations	FRAME 4.5 1996	FRAME 4.6 1996
Dry deposition	125	163	130
Wet deposition	171	220	199
Total deposition	296	383	329
Slope	-	0.69	0.65
Intercept	-	2.76	2.13
R ²	-	0.45	0.50

Table 4.14: Budgets of sulphur for the UK for 1996 from FRAME 4.5 and 4.6 compared against the measurement based estimates of NEGTAPE. FRAME 4.6 considers point sources for the 1996 SO₂ emissions. Units are ktonnes S yr⁻¹. The three last lines give respectively the slope, the intercept and the correlation coefficient (R²) obtained in the comparison of wet deposition modelled values from FRAME against measured values.

dry and wet deposition budgets of sulphur for the UK. They represent 130 kt and 199 kt, respectively in FRAME 4.6. These are closer than FRAME 4.5 to the 1996 estimations from NEGTAPE (2001) which gives 125 kt and 171 kt, respectively. The total deposition is then in better agreement with these estimations with 329 kt against 296 kt.

Figure 4.18 shows the distribution of sulphate wet deposition to the BI. The main peaks are on the west coast of the Great Britain, in the Pennines hills, in Cumbria, in Wales, in the scottish Highlands and in the north-east of Northern Ireland. It illustrates, as for the wet deposition of NH_x and NO₃⁻ (Figures 3.10 and 2.32), the dominance of the rainfall field (Figure 3.4) in controlling the pattern of wet deposition. The influence of the point sources can be seen in Figure 4.19 which maps the percentage difference between FRAME 4.5 and FRAME 4.6 in the sulphate wet deposition. The main differences appear at the locations of the SO₂ point sources in agreement with Figure 4.17.

FRAME 4.6 gives a slight improvement in the comparison with the measurements of sulphate wet deposition (Figures 4.20 and 4.21). The shape of the plot is similar but the correlation coefficient (0.50 against 0.45) is increased through FRAME 4.6. However, this correlation coefficient is still low and explains, through the

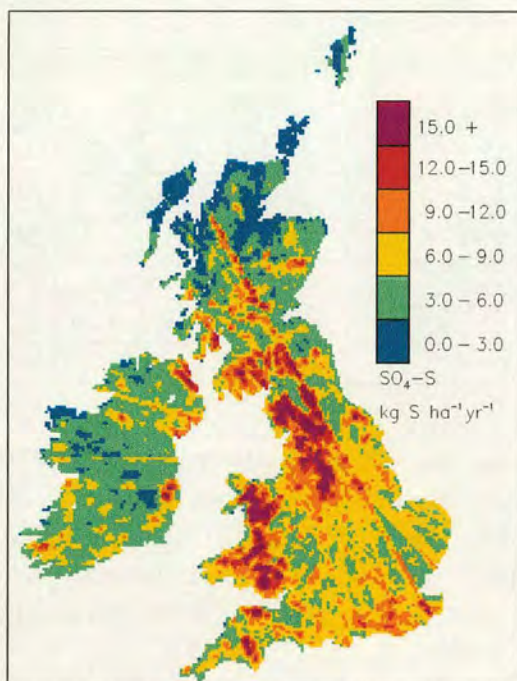


Figure 4.18: Grid average modelled flux of sulphate wet deposition to the British Isles for 1996 at a $5 \text{ km} \times 5 \text{ km}$ resolution (FRAME 4.6). Units are $\text{kg S ha}^{-1} \text{ year}^{-1}$.

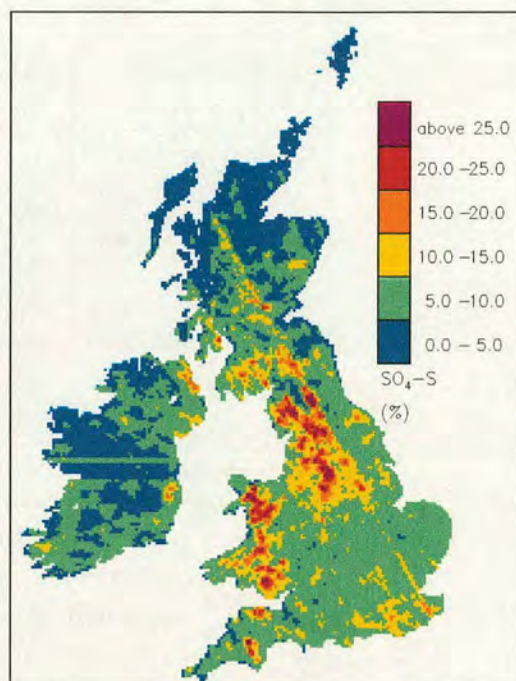


Figure 4.19: Percentage (%) difference between the modelled flux of sulphate wet deposition of FRAME 4.5 and FRAME 4.6. The plot shows $\frac{\text{FRAME4.5} - \text{FRAME4.6}}{\text{FRAME4.5}} \times 100$ to the British Isles at a $5 \text{ km} \times 5 \text{ km}$ resolution.

large scatter of the plot, why the slope of the comparison is inferior to 1.0 while the sulphur wet deposition is overestimated. Indeed, the correlation plot considers a large number of monitoring sites in non-urban areas such as Scotland (sites 5010, 5151, 5152, 5002, 5107 and 5140) or Cornwall (sites 5003 and 5008) where FRAME underestimates the sulphur wet deposition. The modelled values at these sites would be improved by considering a more precise SO_2 emissions inventory over the Republic of Ireland, which exports a lot of SO_4^{2-} towards Scotland. This work is in process in collaboration with the University College of Dublin which produced SO_2 emissions for Eire at a 10 km resolution (De Kluizenaar *et al.*, 2001).

With SO_2 emissions further up in the atmosphere in the areas of high emission, the SO_2 surface concentrations, as well as the sulphur dry deposition are lower

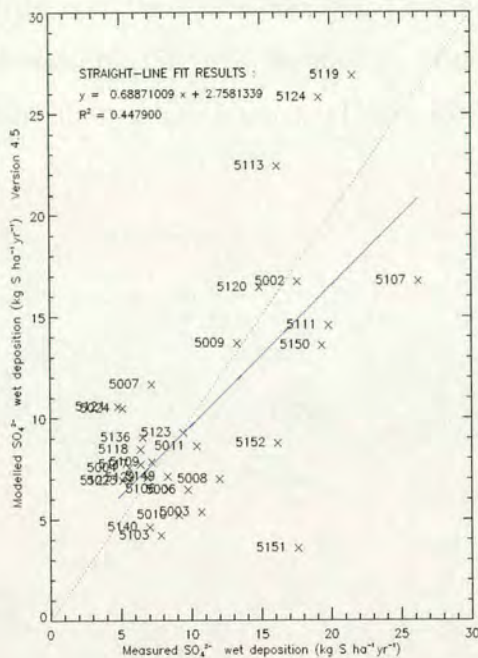


Figure 4.20: Plot of modelled SO_4^{2-} wet deposition values (FRAME 4.5) against measured values. The dotted line is a one-to-one agreement and the solid blue line is the best fit line produced by a regression analysis.

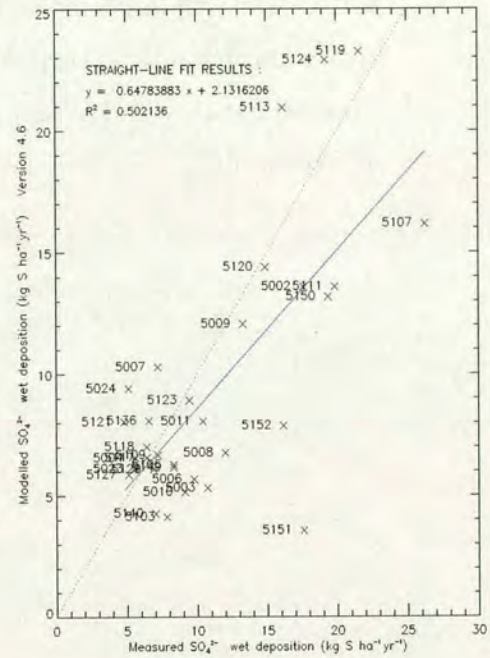


Figure 4.21: Plot of modelled SO_4^{2-} wet deposition values (FRAME 4.6) against measured values. The dotted line is a one-to-one agreement and the solid blue line is the best fit line produced by a regression analysis.

at these locations. This leads to a substantial improvement in the modelled dry deposition (130 kt) and in the comparison between the modelled SO_2 surface concentrations and the measurements (Figures 4.22 and 4.23). Modelled SO_2 concentrations from FRAME 4.6 are now close to the measurements but are still high in Fairseat and Caenby (sites 5333 and 5303, respectively). These two sites are surrounded by places with high-level sources of SO_2 emissions. These correspond to Tilbury, Coryton, Shellhaven, Littlebrook, Gravesend (Table A.5, Appendix A) for Fairseat and Killingholme, Grimsby for Caenby. As there are no high-level sources inventoried at these two monitoring sites (and mostly no low-level emissions), FRAME 4.6 distributes evenly the emissions in the lowest 300 m of the air column. Therefore, driven by the influence of the neighbouring large emissions, FRAME 4.6 overestimates the SO_2 surface concentration at these two locations. The ratio map (Figure 4.24) of SO_2 surface concentration between FRAME 4.6

and the interpolated measured values (only available for Great Britain) corroborates the FRAME overprediction in regions of large SO₂ emissions (Yorkshire, Thames Estuary and Wrexham, Stoke-on-Trent) and underprediction in Scotland or Cornwall.

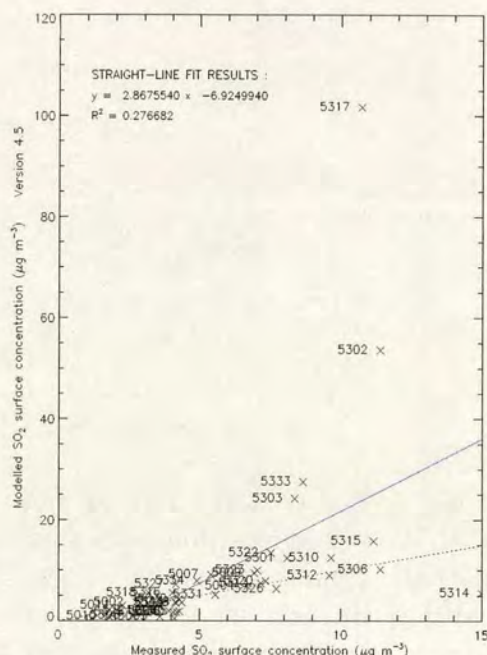


Figure 4.22: Plot of modelled SO₂ surface concentration values (FRAME 4.5) against measured values. The dotted line is a one-to-one agreement and the solid blue line is the best fit line produced by a regression analysis.

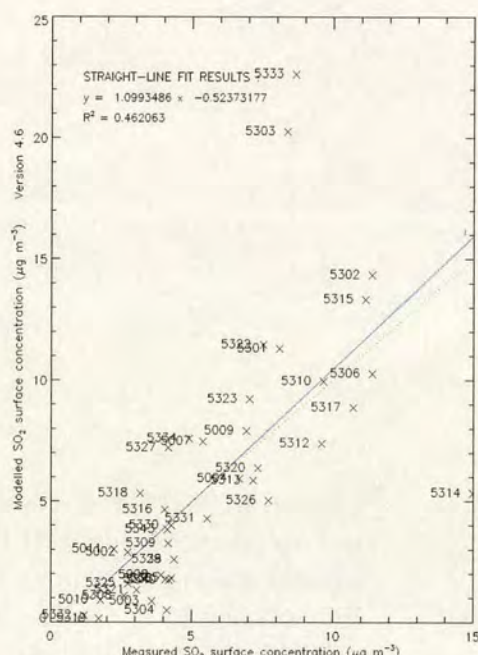


Figure 4.23: Plot of modelled SO₂ surface concentration values (FRAME 4.6) against measured values. The dotted line is a one-to-one agreement and the solid blue line is the best fit line produced by a regression analysis.

The NO_y and NH_x UK budgets are slightly affected by the use of this new vertical distribution of the SO₂ emissions as it can be seen in Tables 4.15 and 4.16. However, the surface concentration of NH₄⁺ is modified in response to the lower amount of SO₂ emissions at low level in FRAME 4.6. This leads to decrease and hence, to improve the NH₄⁺ surface concentration over the UK (see Figures 4.25 and 4.26).

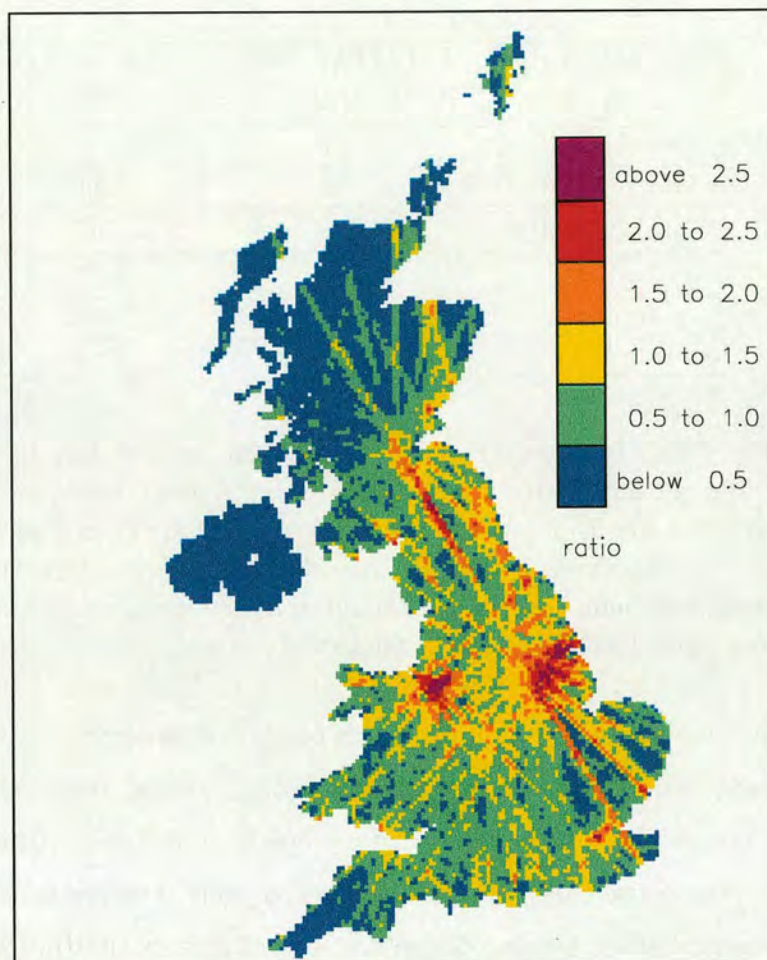


Figure 4.24: Ratio map of SO_2 surface concentration between the FRAME 4.6 modelled values and the interpolated measured values. The plot shows $\frac{\text{FRAME4.6}}{\text{Measurement}}$ to Great Britain for 1996 at a $5 \text{ km} \times 5 \text{ km}$ resolution.

4.6.4 Conclusions on using SO_2 point sources in FRAME

The consideration of high-level point sources in the SO_2 emissions is important because these high stacks represent 80 % of the total emissions. Therefore, including this process in the FRAME model led to substantial improvements in the results of sulphur wet and dry deposition and SO_2 , NH_4^+ surface concentrations. However, this approach is only a step to model correctly the sulphur behavior. Indeed, the sulphur wet deposition is still overestimated by the FRAME model (199 kt) and hence, the SO_2 surface concentration in some areas of high emissions. That is the consequence of the underestimation of the plume rise of the SO_2 emissions, a process which is yet to be included in the FRAME model.

UK oxidised-N kt N yr ⁻¹	(NEG-TAP, 2001) 1996 estimations	FRAME 4.5 1996	FRAME 4.6 1996
Dry deposition	87	61	61
Wet deposition	91	154	155
Total deposition	178	215	216
Slope	-	1.47	1.47
Intercept	-	0.96	0.99
R ²	-	0.61	0.61

Table 4.15: Budgets of oxidised nitrogen for the UK for 1996 from FRAME 4.5 and 4.6 compared against the measurement based estimates of NEG-TAP. FRAME 4.6 considers point sources for the 1996 SO₂ emissions. Units are ktonnes N yr⁻¹. The three last lines give respectively the slope, the intercept and the correlation coefficient (R²) obtained in the comparison of wet deposition modelled values from FRAME against measured values.

The calculation of the plume rise is of crucial importance to model the dispersion of SO₂ emissions from an industrial stack (Arya, 1999). In dispersion models, the plume rise is added to the stack height to estimate the effective stack height. The plume rise can increase the effective source height to several (2 to 10) times the actual stack height. There are several factors that influence plume rise, such

UK reduced-N kt N yr ⁻¹	(NEG-TAP, 2001) 1996 estimations	FRAME 4.5 1996	FRAME 4.6 1996
Dry deposition	99	102 (5)	103 (4)
Wet deposition	110	105 (77)	105 (76)
Total deposition	209	207	208
Slope	-	0.85	0.85
Intercept	-	-0.11	-0.11
R ²	-	0.64	0.64

Table 4.16: Budgets of reduced nitrogen for the UK for 1996 from FRAME 4.5 and 4.6 compared against the measurement based estimates of NEG-TAP. FRAME 4.6 considers point sources for the 1996 SO₂ emissions. The percentage of dry and wet deposition in the aerosol form NH₄⁺ is shown in brackets (%). Units are ktonnes N yr⁻¹. The three last lines give respectively the slope, the intercept and the correlation coefficient (R²) obtained in the comparison of wet deposition modelled values from FRAME against measured values.

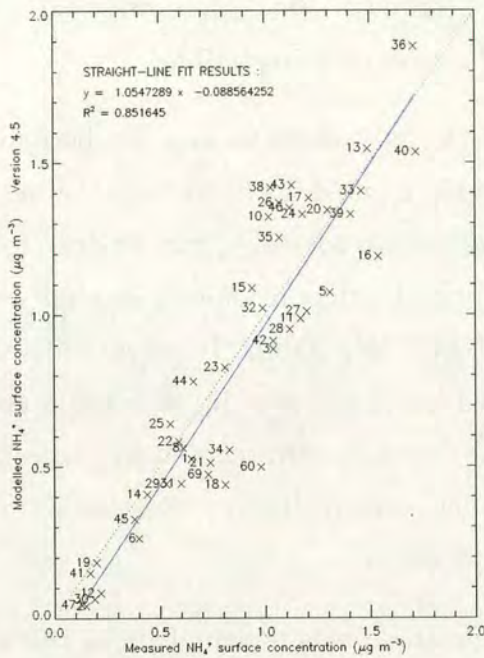


Figure 4.25: Plot of modelled NH_4^+ surface concentration values (FRAME 4.5) against measured values. The dotted line is a one-to-one agreement and the solid blue line is the best fit line produced by a regression analysis.

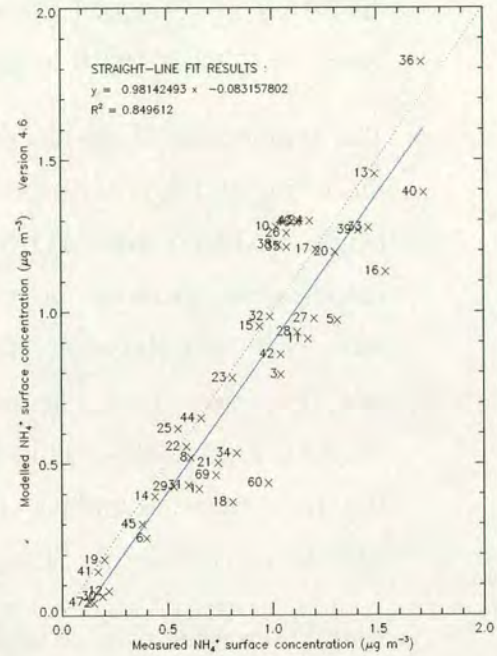


Figure 4.26: Plot of modelled NH_4^+ surface concentration values (FRAME 4.6) against measured values. The dotted line is a one-to-one agreement and the solid blue line is the best fit line produced by a regression analysis.

as the stack height and its diameter, efflux velocity, effluent temperature and density, atmospheric stability, temperature, wind profiles and others (Pasquill and Smith, 1983; Weil and Brower, 1984; Briggs, 1993). The potential effect of plume rise has been investigated in a simple manner with the FRAME model by effectively increasing the stack height of the SO_2 emissions by a factor of 2. This produced a dry deposition budget of sulphur of 124 kt (instead of 130 kt) and a wet deposition budget of 159 kt (instead of 199 kt). The SO_2 and NH_4^+ surface concentrations dropped by roughly an average of 10 % in the main source areas. This underlines the importance of implementing this process in FRAME in the future.

Combined with a more detailed point sources inventory, the plume rise process will allow a better prediction of the sulphur UK budget. Indeed, the current SO_2 point sources inventory could be completed by considering small industrial

operations (with height of emissions around 30 m) and low-level sources, such as houses, explicitly (with height of emissions around 10 m).

The importance of the height of the SO₂ emissions can not be underestimated. Modelling and monitoring studies highlighted the hypothesis that a change in the height of these emissions over the last decade or so, can be one of the causes of the observed faster decline in sulphur dry deposition over sulphur wet deposition rates (Lee and Hayman, 1999; NEG-TAP, 2001). Between 1986 and 1997 the wet deposition of sulphur declined by 42 % while dry deposition declined by 62 % (NEG-TAP, 2001). This phenomenon is corroborated by our study in which the dry deposition budget of sulphur is more affected than the wet deposition of sulphur by considering SO₂ point sources.

Finally, another way of improving these results would be to consider a better resolution of the wind rose used in the model. For instance, using a resolution of 5 degree instead of 15 degree would reduce substantially the stripes obtained in the maps of modelled sulphur wet deposition and SO₂ surface concentration (Figures 4.18 and 2.23).

4.7 Summary of development of the parameterisation of atmospheric processes in FRAME

This chapter tackled the wet deposition process as it was the main area of uncertainty in the FRAME model. A field of directional orographic precipitation had been developed and produced interesting regional patterns of wet deposition through the FRAME model. Considering directional orographic precipitation improved the comparison between the modelled and measured values of NH_x wet deposition, in terms of correlation coefficient. However, the intensity of the NH_x (but also S and NO_y) wet deposition was still underestimated by FRAME. Although the use of directional orographic precipitation is recommended and more realistic than the annual average rainfall used previously, such parameterisation

implies more development of the model before being efficient on a national scale. On another hand, employing a more realistic description of the scavenging coefficients improved the results of the model concerning reduced nitrogen. However, this leads to an overestimation of the wet deposition budgets of both sulphur and oxidised nitrogen. While the former had been mostly sorted out by considering point sources for SO₂ emissions, the latter requires more attention on the NO_y chemistry of the model which exhibits different features from other UK models. On the other hand, surface concentrations and dry deposition of both sulphur and oxidised nitrogen species had been improved by taking into account more realistic deposition velocities and vertical distribution of the emissions. More detailed inventories of the low-level sources of NO_x and SO₂ would be needed to produce more accurate results. Moreover, the effect of plume rise could be very important and should be incorporated to increase the effective stack height of the SO₂ emissions.

Chapter 5

Applications of the FRAME model

5.1 Introduction

The refinement of the FRAME model in terms of both run-time and 1996 UK budget results, especially for reduced nitrogen, allows us to carry out more studies with the model (FRAME 4.6). Firstly, atmospheric budgets of reduced nitrogen for the major political regions of the British Isles (BI) are investigated for 1996 (section 5.2). Secondly, predictions of UK reduced nitrogen, oxidised nitrogen and sulphur budgets for 2010 with different emission scenarios are investigated with the model (section 5.3).

5.2 Assessment of regional budgets of reduced nitrogen for the British Isles

In the past, the derivation of regional budgets to define sources and sinks of S and NO_x has been stimulated because there are large anthropogenic sources (mostly from fossil fuel combustion) and substantial impacts on receiving ecosystems. More recently, NH_x has attracted attention not only because of the distinctiveness of its sources, which are strongly influenced by agricultural practices, but also because of its distinctive impacts.

Assessments of NH_x budgets are fewer in number than those for NO_x and S and regional budgets for the British Isles have not previously been assessed. The FRAME model was developed to provide atmospheric budgets for defined sub-domains of the British Isles. The UK represents one such sub-domain, and the approach is applied to estimate budgets for each of England, Scotland, Wales, Northern Ireland and Eire. This is of particular interest due to the recent regional devolution of environmental policy in the UK, as the atmospheric budgets are an important consideration in developing abatement strategies (Fournier *et al.*, 2002b).

5.2.1 Method of approach

The FRAME model assesses the budgets of NH_x , NO_x and S over the British Isles domain. Import, emission, deposition and export of material are evaluated over this domain. FRAME 4.6 has been modified to allow a sub-domain to be considered similarly. The sub-domain, for example Scotland, is defined with a mask. The mask contains information about the land-cover of the region chosen to be studied but also, differentiates the land-squares from this region to those from the BI. Therefore, two different budgets, for the BI and this specific region, are simulated by the FRAME model. In this study, six regions or countries and hence six masks are considered : the United Kingdom, England, Scotland, Wales,

UK reduced-N kt N yr ⁻¹	(NEG-TAP, 2001) 1996 estimations	FRAME 4.6 1996
Import	30	52
Emission	282	291
Dry deposition	99	103 (4)
Wet deposition	110	105 (76)
Export	103	135

Table 5.1: Budgets of reduced nitrogen for the UK for 1996 from FRAME 4.6 compared against the measurement based estimates of NEG-TAP. The percentage of dry and wet deposition in the aerosol form NH_4^+ is shown in brackets (%). Units are ktonnes N yr⁻¹.

Northern Ireland and Eire. These changes do not affect the results obtained previously for the UK with FRAME 4.6.

5.2.2 Performance of the FRAME model

Table 5.1 shows the UK 1996 reduced nitrogen (reduced-N) budget obtained with FRAME 4.6 (see previous chapter). The second column indicates the 1996 NEG-TAP estimations derived from measurements (NEG-TAP, 2001). The modelled budget of dry deposition is broadly consistent with the NEG-TAP estimations. The main difference is in the import component, which is larger in FRAME causing more reduced nitrogen to be exported with the FRAME model than in the NEG-TAP estimations. The reasons for this difference have been explained in section 3.2.5.

The 1996 modelled distribution of reduced nitrogen wet deposition had been improved in the previous chapter and is shown in Figure 5.1. This shows the highest wet deposition in hill areas of central northern and south-west England, Wales, Northern Ireland and south of Eire. Peak wet deposition values correspond to areas of large precipitation occurring nearby regions of intensive agricultural activity and of significant SO_2 and NO_x emissions.

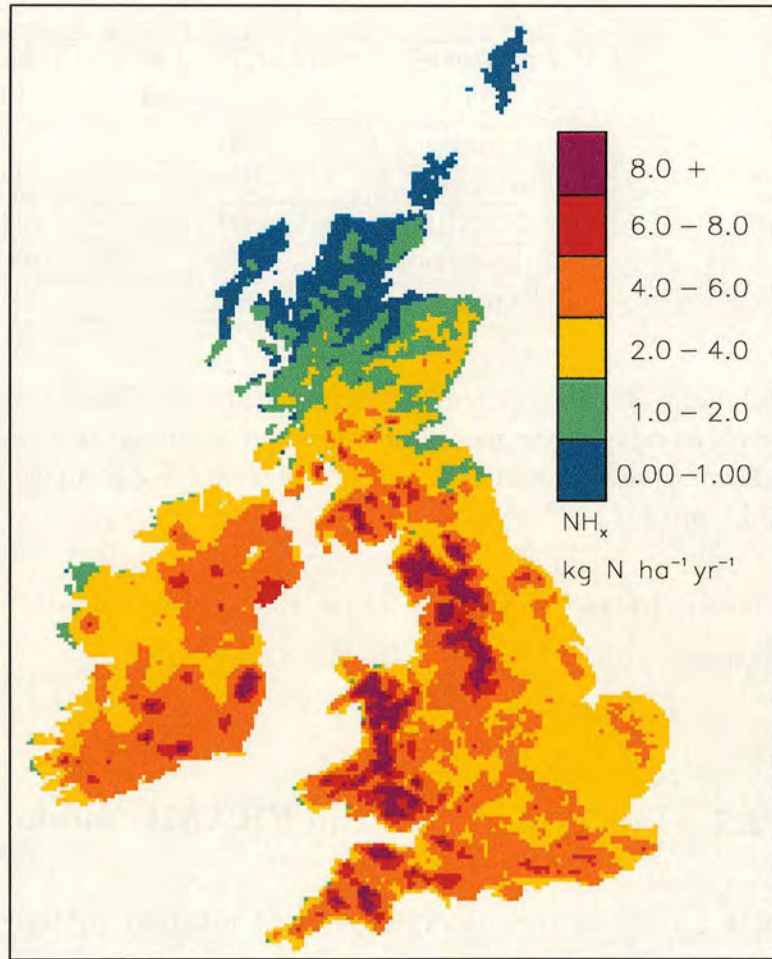


Figure 5.1: Grid average 1996 modelled flux of NH_x wet deposition to the British Isles at a $5 \text{ km} \times 5 \text{ km}$ resolution (FRAME 4.6).

In Figure 5.2, model predictions for NH_x wet deposition is compared to observations for locations included in the National Precipitation Composition Monitoring Network for the UK and in the European Forest Ecosystem Monitoring Network for Eire. For the first time, the results from the FRAME model are compared with 1996 measurements in Eire. The Forest Ecosystem Research Group (FERG) sample precipitation at four sites in Eire using bulk precipitation collectors (Farrell *et al.*, 1996; Boyle *et al.*, 1997). The close agreement with the NEG-TAP estimations (110 kt) is confirmed in the comparison of the modelled NH_x wet deposition with the 1995-97 measurements. The network average for each site is compared with the model estimate for 1996 for the 5 km grid square in which it occurs. The sites are classified by the major countries and regions of the British Isles. A slope of 0.86 is obtained with a coefficient (R^2) of 0.63. Similarly, the

modelled NH_4^+ aerosol surface concentration compares well with measurements giving a slope of 0.98 ($R^2=0.85$; see Figure 4.26).

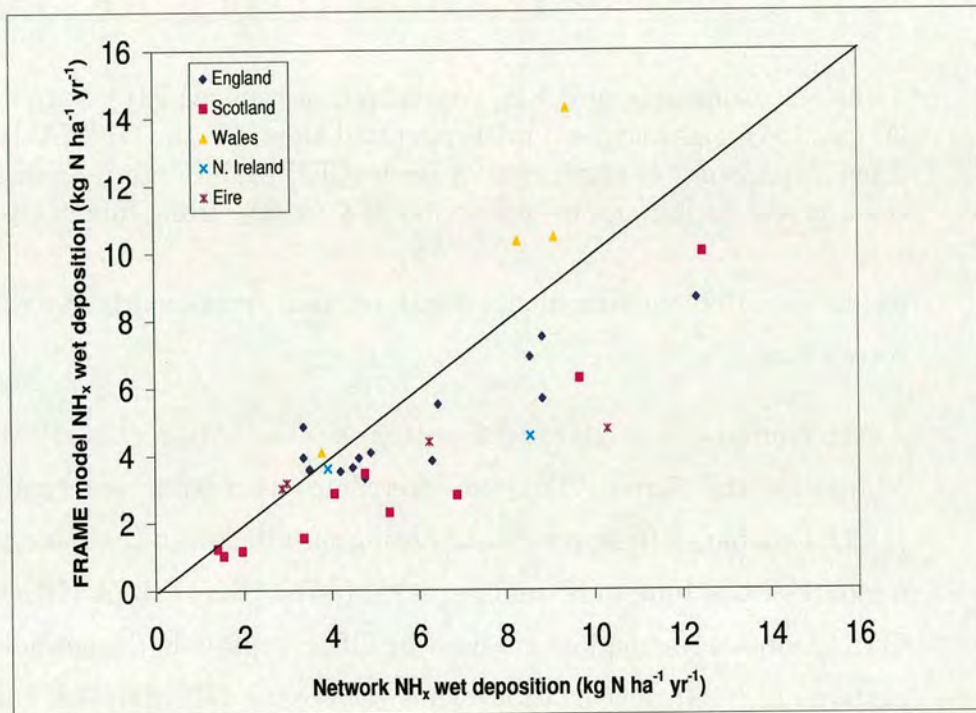


Figure 5.2: Comparison of measured NH_x wet deposition with estimates of FRAME 4.6 classified by regions of the British Isles for 1996. The central solid line is a one-to-one agreement. The regression analysis gives : $\text{FRAME} = 0.8609 \text{ Network} - 0.037$, $R^2=0.6325$

The comparison of FRAME estimates with the network measurements for gaseous NH_3 is shown in Figure 5.3. Measurements for Great Britain and Northern Ireland are from the United Kingdom National Ammonia Monitoring Network (Sutton *et al.*, 1998). For the first time, the results from FRAME are compared with 1996 measurements at four sites in Eire (Farrell *et al.*, 1996; Boyle *et al.*, 1997). Moreover, this monitoring network had been extended by 36 stations since 4 January 1999 (De Kluizenaar and Farrell, 2001). Since there was little trend in NH_3 emissions from 1996 to 1999 (NEG-TAP, 2001) and the FRAME model uses long-term average climatological data, the comparison between the FRAME 1996

Techniques	Mean value $\mu\text{g m}^{-3}$	Slope	Intercept	R ²
DTs	3.05	1.15	0.72	0.64
ALPHA samplers	1.81	0.81	0.23	0.88
Willems badge	1.79	0.65	0.51	0.59

Table 5.2: Comparison of NH₃ concentration from ALPHA samplers, membrane DTs and Willems badge samplers operated alongside the DELTA denuder system. The comparison was conducted at Bush (CEH, Edinburgh Research centre) using the different techniques over a period of 6 months from June to November 1999.

results and 1999 measurements is still relevant, particularly the extent of spatial correlation.

As the sampling methods are different in the UK (Sutton *et al.*, 1998) and Eire (De Kluizenaar and Farrell, 2001), an intercomparison study was conducted at Bush (CEH, Edinburgh Research Centre) using the different techniques over a period of 6 months from June to November 1999. In the UK, DELTA (DENuder for Long-Term Ammonia) denuders are used by CEH to provide the spatial and temporal patterns of NH₃ concentration, while membrane DT (diffusion tubes) (replaced by ALPHA (Adapted Low-cost Passive High Absorption) samplers in 1999) are used to assess regional and local scale variability in NH₃ concentrations in source regions (Tang *et al.*, 2001; Sutton *et al.*, 2002). In Eire, Willems badge samplers are used to measure NH₃ concentration (De Kluizenaar and Farrell, 2001). The performances of the membrane DTs, ALPHA samplers and the Willems badge samplers are assessed for this period against the CEH DELTA denuders. Table 5.2 presents the results. This shows that the ALPHA and the Willems badge samplers give relatively similar values of NH₃ concentrations during this six-months weekly sampling periods. Therefore, both sets will be used in the comparison of NH₃ concentrations from the FRAME model over the British Isles. However, the ALPHA samplers show better agreement with the reference method (DELTA denuders) with a slope of 0.81 (against 0.65 for the Willems badge samplers) and a correlation coefficient of 0.88 (against 0.59 for the Willems badge samplers).

Figure 5.3 presents the comparison between the FRAME 1996 NH₃ surface con-

centrations and the different sets of measurements. These include the measurements from the different regions of the UK for 1996 (England, Scotland, Wales and Northern Ireland), from 4 sites in Eire for 1996 (Eire I (1996)), at the same 4 sites for 1999 (Eire I (1999)) and from the new 36 stations in Eire for 1999 (Eire II (1999)).

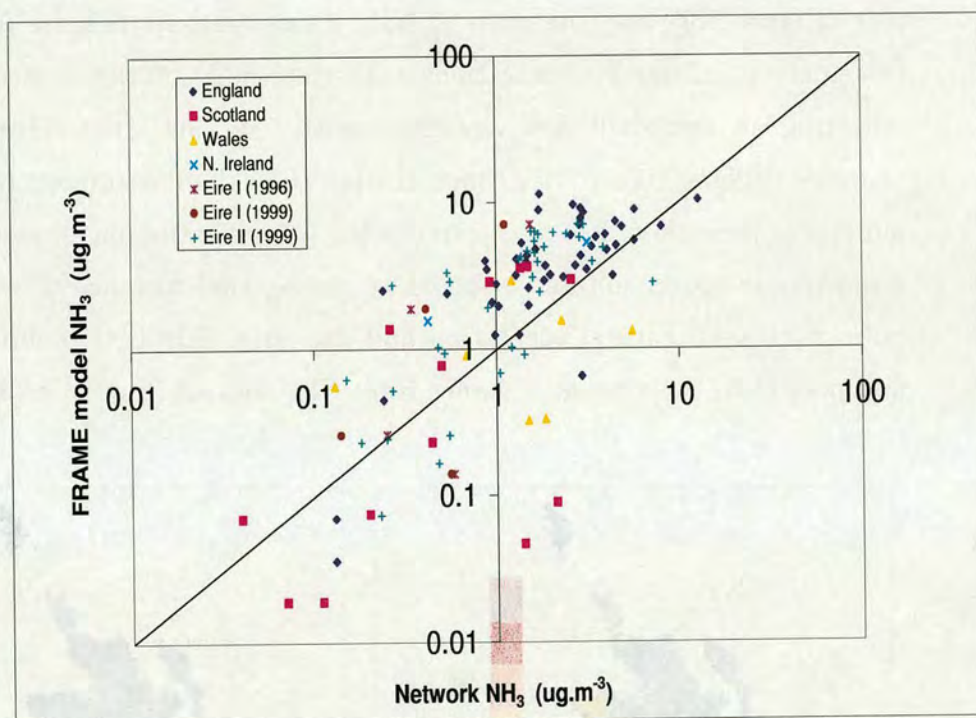


Figure 5.3: Comparison of measured NH_3 concentration with estimates of FRAME 4.6 classified by regions of the British Isles for 1996. The central solid line is a one-to-one agreement. The regression analysis gives : $\log(\text{FRAME}) = 0.9909 \log(\text{Network}) + 0.1865$, $R^2=0.54$

Since the concentrations in the network and FRAME are log-normally distributed, Figure 5.3 shows the comparison on a logarithmic scale. The network Eire I (4 sites) allows the measurements of NH_3 surface concentrations for 1996 and 1999 to be compared. It shows slight differences between the two sets. The large spatial variability of NH_3 (see Figure 5.4) leads to a correlation coefficient ($R_{\log}^2 = 0.54$ or $R_{\text{absolute}}^2 = 0.37$) much lower than for NH_4^+ concentration (see

Figure 5.5 and 4.26) or NH_x wet deposition. The highest NH_3 air concentrations appear mainly in the livestock, cattle and sheep farming areas along the England-Wales border, north-west England and Northern Ireland. Another high concentration area is East Anglia with large poultry and pig farming. High air concentrations in the south and north-east of Eire are caused by both significant emissions and low deposition velocity associated with grassland in the FRAME model. However, the model, as it can be seen on both the scatter plot (Figure 5.3) and the map of NH_3 concentrations (Figure 5.4), simulates extremely small air concentrations over the whole of the Scottish Highlands, reflecting an extremely low emission density in this area. Overall, FRAME provides slightly higher NH_3 concentration than the measurements. There are a number of possible causes of this, including uncertainties in emissions, dispersion, atmospheric conversion and removal processes, the existence of a compensation point with semi-natural vegetation and the possibility that monitoring stations are more than the average distance from NH_3 sources (Sutton *et al.*, 2001).

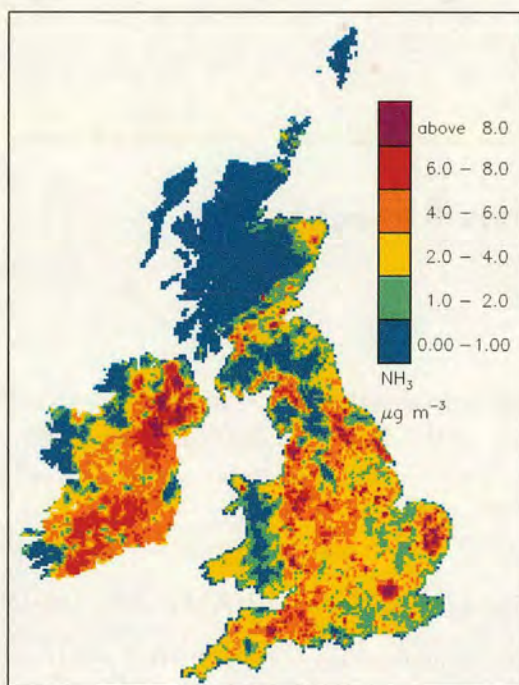


Figure 5.4: Modelled surface concentrations (1-2 m) of NH_3 for the BI for 1996 at a $5 \text{ km} \times 5 \text{ km}$ resolution (FRAME 4.6). Units are $\mu\text{g m}^{-3}$.

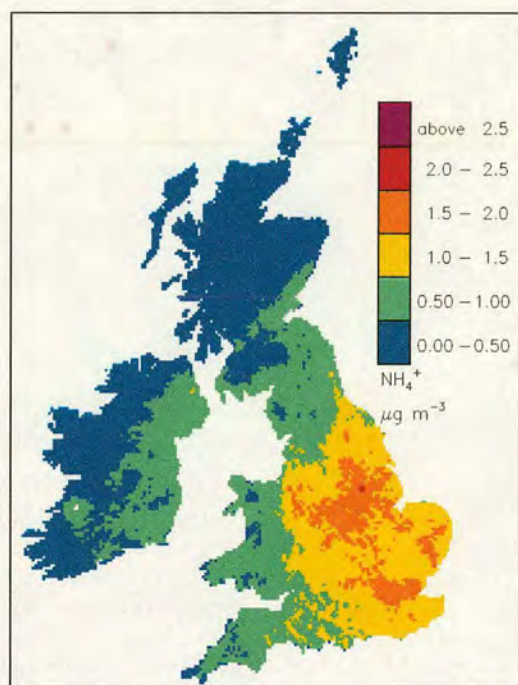


Figure 5.5: Modelled surface concentrations (1-2 m) of NH_4^+ for the BI for 1996 at a $5 \text{ km} \times 5 \text{ km}$ resolution (FRAME 4.6). Units are $\mu\text{g m}^{-3}$.

Regions	Import	Emissions	Dry Deposition	Wet Deposition	Export	E/I	W/T
British Isles	29	387	132	136 (73)	148	5.1	51
UK	52	291	103	105 (76)	135	2.6	50
England	56	199	62	64 (80)	129	2.3	51
Scotland	25	40	19	21 (79)	26	1.0	53
Wales	29	23	13	15 (76)	24	0.8	54
N. Ireland	13	29	9	9 (58)	24	1.8	50
Eire	11	96	29	31 (57)	47	4.3	52

Table 5.3: Regional 1996 budgets of reduced nitrogen from FRAME 4.6 (ktonnes N yr⁻¹). The percentage of wet deposition from scavenging of NH₄⁺ aerosol is shown in brackets (%). The two last columns give, respectively, the ratio of Export to Import (E/I) and the percentage (%) of total deposition as wet deposition (W/T).

5.2.3 Regional budgets of reduced nitrogen

A detailed assessment of the import, emissions, depositions and export of reduced nitrogen in the different countries and regions of the British Isles for 1996 from FRAME 4.6 is provided in Table 5.3. These countries and regions are England, Scotland, Wales, Northern Ireland (United Kingdom) and Republic of Ireland (Eire).

The total BI NH₃ emissions for 1996 as N are 387 kt, combining 96 kt in Eire and 291 kt in the UK. The component regional emissions for the UK are 199 kt for England, 40 kt for Scotland, 23 kt for Wales and 29 kt for Northern Ireland. The import of reduced nitrogen to the UK represents 52 kt. This includes a large component from Eire and explains that this amount is superior to the 29 kt of import to the BI. Therefore, Eire as the BI, with a low import and large emissions, have a high export-import ratio. Given the location of the BI on the western edge of Europe and the predominant south-west flow the British Isles are a net exporter of NH_x with an export-import ratio of 5.1. With a source of reduced nitrogen of 416 kt (import and emissions) and 64% of this amount being deposited, the British Isles is estimated to export 148 kt N. While England is also a substantial exporter, Scotland and Wales are approximately

Regions		N	N-E	E	S-E	S	S-W	W	N-W	Tot
British Isles	Import	0.7	4.6	7.2	7.1	6.0	3.5	0.2	0.1	29.4
	Export	17.6	10.2	3.6	6.3	19.0	35.3	33.0	23.4	148.4
UK	Import	0.3	2.7	7.1	6.5	9.7	11.7	10.6	3.8	52.4
	Export	13.6	8.6	4.3	4.8	17.1	34.5	32.4	20.0	135.3
England	Import	1.4	2.5	6.0	5.3	5.3	10.0	15.7	9.7	55.9
	Export	11.2	7.9	5.8	6.5	15.6	29.8	31.5	20.8	129.1
Scotland	Import	0.0	0.3	2.1	5.1	8.4	7.8	1.0	0.0	24.7
	Export	1.5	0.9	0.6	1.3	3.6	7.5	8.1	2.7	26.2
Wales	Import	2.9	4.1	3.0	2.6	1.9	2.4	7.9	4.7	29.5
	Export	2.3	2.1	1.0	1.1	2.1	4.5	6.2	5.0	24.3
N. Ireland	Import	0.3	0.8	1.2	1.7	4.2	4.0	0.6	0.3	13.1
	Export	1.7	1.2	0.7	1.1	3.4	6.1	6.5	3.6	24.3
Eire	Import	2.0	3.1	3.2	2.1	0.1	0.2	0.2	0.2	11.1
	Export	5.5	3.1	1.8	2.1	4.8	11.2	9.1	9.7	47.3

Table 5.4: Regional 1996 directional budgets of reduced nitrogen (ktonnes N yr^{-1}). The direction indicates where the wind is coming from (N: North; S : South; W : West; E : East). The last column (Total) shows, in brackets, the percentage of export or import of NH_x in the form of NH_4^+ aerosol as compared with NH_3 gas (%).

“ammonia-neutral” with export-import ratios close to one.

Table 5.4 gives a more detailed description of the import and export of reduced nitrogen for different wind directions for the different regions, taking into account their frequency of occurrence. For example, the first column (wind direction N) shows the import from the North and, hence, the export from North to South. The last column gives the total import and export of reduced nitrogen and, in brackets, the percentage of the import or export in the form of NH_4^+ aerosol as compared with NH_3 gas.

The BI import is 29 kt and comes mainly from the east (24%, 7.2 kt N yr^{-1}), south-east (24%, 7.1 kt) and south (20%, 6.0 kt) wind directions. This import originates largely from The Netherlands, Belgium and France. The English budget corroborates this fact by importing 30% of its pollutant from these wind

directions. The main import sources for England are Eire, Wales and Northern Ireland with the most important one being Wales (west, 15.7 kt or 28%). Wales exports most of its pollutant to the east (27%), south-east (20%) and north-east (19%) under west, north-west and south-west winds, respectively. Indeed, Eire exports 63% of its total reduced-nitrogen to the north-east (11.2 kt), east (9.1 kt) and south-east (9.7 kt) under south-west, west and north-west winds, respectively. Similarly, Northern Ireland exports 67% of its total reduced-nitrogen to the north-east (6.1 kt), east (6.5 kt) and south-east (3.6 kt) directions. Eire and Northern Ireland have both a low import budget (11 and 13 kt) originating mainly from Northern Ireland and England for Eire, and from Eire (south and south-west, 8.2 kt, 63 %) for Northern Ireland. This latter important transfer of reduced nitrogen from Eire to Northern Ireland is not surprising in regard to the main south-westerly component of the wind direction in the BI. The same pattern applies to Scotland which imports mainly from the south (8.4 kt) and the south-west (7.8 kt). The southern source corresponds to England which exports mainly to the east (31.5 kt), north-east (29.8 kt) directions but also towards the north (15.6 kt). The south-west source of pollutant entering Scotland comes from Northern Ireland which exports 6.1 kt of its reduced nitrogen in this direction. Scotland exports 26 kt overall, with 8.1 kt to the east and 7.5 kt to the north-east directions preferentially.

The export of material between regions is driven by the amount of pollutant imported, emitted and the deposition occurring in these regions. The dry and wet depositions depend on the amount of pollutant available (import and emissions), the meteorological conditions and the land cover type. The maps of wet and dry depositions reflect these effects (Figures 5.6 and 5.7). In the regional budgets, dry and wet depositions represent roughly 50% each of the total reduced nitrogen deposition. However, the total deposition varies between the regions. For instance, Scotland, Wales and Northern Ireland have a similar export but the amount of material deposited is quite different. In these three regions, the combination of import and emissions gives, respectively, 65 kt, 52 kt and 42 kt. 62% of this amount is deposited in Scotland, 52% in Wales and 43% in Northern

Ireland. It results in differences between their ratios of export to import (Table 5.3). This ratio is near 1.0 for Scotland (1.0) and Wales (0.8) implying that these regions are not net exporters of NH_x . Conversely, this ratio equals 1.8 for Northern Ireland, which acts as a net exporter of NH_x and provides then an important contribution to the British Isles budget of reduced nitrogen. Northern Ireland has larger sources (import and emissions) than Scotland or Wales in relation to its surface area. The import in Wales derives largely from Eire and is caused by both high NH_3 emissions and low deposition in this region. While the cause of the low dry deposition has been described in the previous section, the low wet deposition budget is linked with the aerosol NH_4^+ concentration. The NH_4^+ aerosol concentration is less in Eire and Northern Ireland than in England as is shown in Figure 5.5. This is the consequence of lower SO_2 emissions in these two regions (Figure 3.2). It leads to low contribution of NH_4^+ scavenging to wet deposition in Eire and Northern Ireland with a respective contribution of 57% and 58% (Table 5.3).

5.2.4 Conclusions concerning the assessment of regional NH_x budgets

The FRAME model has been used to investigate the regional reduced nitrogen budgets over the British Isles. Regional atmospheric budgets are useful to build up an overview of reduced nitrogen fluxes and as a basis for quantitative modelling. The study shows that NH_3 emissions, transport and deposition in a specific region can have profound effects on the composition of the atmosphere over other regions. The large NH_3 emissions in Eire and Northern Ireland produce a substantial export to the east and north-east directions towards England and Scotland, contributing to the pollution in these regions. England is also a net exporter of reduced nitrogen. By contrast, Scotland and Wales are approximately “ammonia neutral” as import of reduced nitrogen roughly balances export. Overall, only 7% of reduced nitrogen in the British Isles is derived from non-British Isles sources

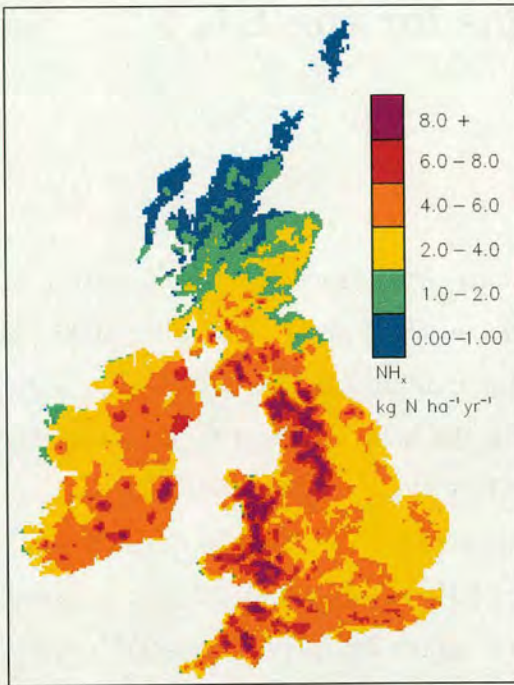


Figure 5.6: Grid average modelled flux of NH_x wet deposition to the BI for 1996 at a $5 \text{ km} \times 5 \text{ km}$ resolution (FRAME 4.6). Units are $\text{kg N ha}^{-1} \text{ year}^{-1}$.

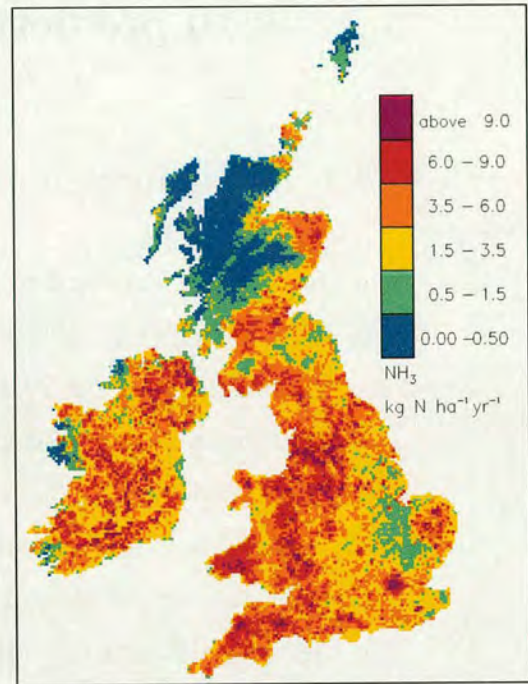


Figure 5.7: Grid average modelled flux of NH_3 dry deposition to the UK for 1996 at a $5 \text{ km} \times 5 \text{ km}$ resolution (FRAME 4.6). Units are $\text{kg N ha}^{-1} \text{ year}^{-1}$.

(29 kt N yr^{-1}), compared with emissions of 387 kt N yr^{-1} . Most of the reduced nitrogen is deposited in the British Isles (64%), while 36% is exported (148 kt N yr^{-1}).

Detailed information on the regional distribution of reduced nitrogen is decisive in investigation of sources, sinks and fluxes of the pollutant in the British Isles. It contributes to increased awareness of regional features which could be used to develop specific efficient regional abatement strategies in the British Isles. For example, Table 5.3 shows that of the NH_x sources for Wales, 29 kt is a result of import compared with 23 kt from emissions. This may be contrasted with Eire, where import and emissions account for 11 and 96 kt , respectively. This illustrates how strategies to reduce NH_x deposition in Wales are highly dependent on NH_x abatement in other regions of the British Isles.

5.3 2010 predictions for the UK

5.3.1 Introduction

The Gothenburg Protocol to Abate Acidification, Eutrophication and Ground-level Ozone (UN/ECE, 1999) was adopted on 30 November 1999. The Protocol sets emission ceilings for 2010 for four pollutants: SO_2 , NO_x , VOC_s and NH_3 . These ceilings were negotiated on the basis of scientific assessments of pollution effects and abatement options. Once the Protocol is fully implemented, Europe's SO_2 emissions should be cut by at least 75 %, its NO_x emissions by 50 %, its VOC emissions by 40 % and its NH_3 emissions by 12 % compared with 1990. The Protocol also sets tight limit values for specific emission sources (e.g. combustion plant, electricity production, dry cleaning, cars and lorries) and requires best available techniques to be used to keep emissions down. VOC emissions from such products as paints or aerosols will also have to be cut. In many countries, farmers will have to take specific measures to control ammonia emissions (UN/ECE, 1999). It has been estimated that once the Protocol is implemented, the area in Europe with excessive levels of acidification will reduce from 93 million hectares in 1990 to 15 million hectares. The area with excessive levels of eutrophication will fall from 165 million hectares in 1990 to 108 million hectares (UN/ECE, 1999).

To consider the effect of these changes on the British Isles, FRAME 4.6 is applied here to model deposition of sulphur and nitrogen considering the implementation of different scenarios of emissions for 2010 throughout the BI and Europe.

Species	SO ₂		NO _x		NH ₃	
	1990	2010 (GP)	1990	2010 (GP)	1990	2010 (GP)
Europe	8202	2050 (-75 %)	4050	2025 (-50 %)	2990	2631 (-12 %)
UK	1877	306 (-84 %)	840	355 (-58 %)	301	245 (-19 %)

Table 5.5: Comparison of 1990 SO₂, NO_x, NH₃ emissions in the European Union with 2010 emission ceilings from the Gothenburg Protocol (GP) in ktonnes N (S) yr⁻¹. The percentage of change related to 1990 is shown in brackets (%).

5.3.2 2010 emissions

European 2010 emissions

Emissions reduction of sulphur dioxide (SO₂), nitrogen oxides (NO_x) and ammonia (NH₃) for the time period 1990 to 2010 have been estimated over Europe by UN/ECE (1999) and Amann *et al.* (1999). These estimates are based on the latest projection of economic activities and energy consumption and include emission control measures that are implied by the proposal for a Directive on National Emission Ceilings (NEC) (CEU, 2000). For the year 2010, these projections were updated by national experts in the process of reviewing the input data to the scenario calculations conducted for the negotiations on the Gothenburg Protocol (UN/ECE, 1999). Table 5.5 presents the 1990 emissions of SO₂, NO_x, NH₃ in the Europe Union (15 countries) and compares them with the obligations of the Gothenburg Protocol for 2010 (NEGTAP, 2001).

For the European Union emissions assessed here, it is assumed, in this study, that the Gothenburg Protocol emission ceilings will be achieved by 2010. Therefore, a reduction of 75 %, 50 % and 12 % in the 1990 emissions of SO₂, NO_x and NH₃, respectively, is applied (Table 5.5).

The transboundary import of foreign material to the FRAME model is assessed by running the TERN model across Europe for 2010 (ApSimon *et al.*, 1994; Singles, 1996). The boundary conditions created with TERN and FRAME 4.6 for 2010 for the UK are shown in Table 5.6. This shows the amount of reduced nitrogen,

Wind origin	NH _x -N import	NO _x -N Import	S Import
north	0.2	0.9	0.4
northeast	1.7	7.6	1.4
east	5.0	20.7	4.9
southeast	4.8	16.0	3.5
south	7.7	7.1	2.7
southwest	10.0	4.8	3.6
west	9.2	3.5	3.4
northwest	3.3	1.1	1.0
Total Import	41.9	61.7	20.9

Table 5.6: Modelled 2010 budgets of import, obtained with the TERN model and FRAME 4.6, for eight wind sectors for the UK. The units are kt N (or S) year⁻¹.

oxidised nitrogen and sulphur (kilotonnes N or S year⁻¹) imported by FRAME 4.6 along the UK. As a consequence of the reduction in European emissions in 2010, there is less import from Europe than in 1996 (see Table 3.2). The imports of NH_x, NO_x and sulphur into the UK decreased, respectively, by 21, 53 and 82 % from 1996 to 2010. It produced 2010 imports of 42, 62 and 21 kt for NH_x, NO_x and sulphur, respectively, against 52, 132 and 116 kt in 1996.

It must be noticed that European meteorological and input data other than emissions has not been altered (1996 values) to produce these 2010 boundary conditions for the UK. Moreover, as there are still some uncertainties concerning the 2010 emissions of European countries, these 2010 European boundary conditions from the Gothenburg Protocol will be used for the different 2010 emission scenarios applied to the BI in the next section (Common Position and H1). Indeed, in many countries such as the UK the emissions achieved in 2010 by the implementation of current standards (i.e., those derived from the projected economic development and the present set of emission and fuel standards) will be lower than the obligations of the Gothenburg Protocol. There are, however, other countries where present legislation would not achieve the Gothenburg target given the projected economic development and where additional measures will be necessary.

UK 2010 emissions

For the 2010 emissions of SO₂, NO_x and NH₃, UK-specific scenarios are considered. The implementation of the current UN/ECE legislation (UN/ECE, 1999) will lead to greater reductions in the emissions of the UK than those required in the Gothenburg Protocol (GP). Therefore, 2010 emissions for the UK follow the estimates from NEG-TAP (2001). Table 5.5 gives an overview of the amplitude and reduction of these emissions. Annual emissions of SO₂ are anticipated to decline from 1877 kt S in 1990 to 306 kt S in 2010. An amount of 1005 kt S was used previously for 1996 by the FRAME model. Annual emissions of NO_x will decline from 840 kt N in 1990 to 355 kt N in 2010. 590 kt N were considered in 1996. Finally, the least certain of these pollutants, NH₃, might decrease from 301 kt N in 1990 to 245 kt N in 2010. The FRAME model considered 291 kt N of NH₃ for the UK in 1996. There are more uncertainties about the 2010 emissions estimates for Ireland which is also part of the FRAME domain. Although the emission reductions in Ireland might not be as important as in the UK (Cofala *et al.*, 2000), an uniform reduction from 1990 to 2010 is considered for the British Isles in our study. This means that a reduction of 84 %, 58 % and 19 % is applied on the 1990 emissions of SO₂, NO_x and NH₃, respectively, in the British Isles (Table 5.5).

The 2010 ammonia emissions for the British Isles are mapped in Figure 5.8. In addition, emissions of SO₂ and NO_x are shown in Figures 5.9 and 5.10. These maps can be compared with the previous 1996 emissions (Figures 3.2 and 3.3).

To model the different 2010 scenarios, only the emissions over the BI are updated in FRAME 4.6. In June 2000, the Council of the Environment Ministers reached a Common Position on the Commission's proposal for the NEC Directive (CEU, 2000). While the Directive was generally supported (scenario H1), the Common Position (scenario CP) specifies for a number of countries less ambitious emission ceilings than those proposed by the Commission for sulphur. Emissions of the Common Position (CP) and of H1 are given Table 5.7. This table contains the GP emissions, which are the levels achieved by implementing only current legislation and/or the Gothenburg Protocol. The scenarios CP and H1 affect

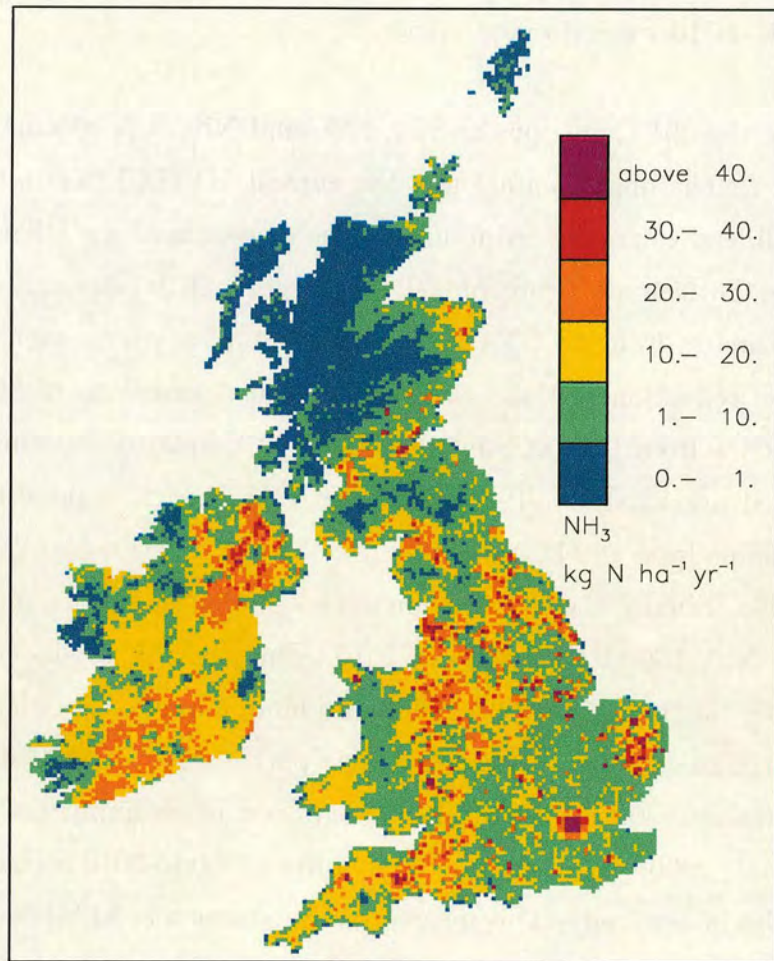


Figure 5.8: 2010 ammonia emissions for the British Isles on a 5 km x 5 km grid resolution (Gothenburg Protocol). Units are $\text{kg N ha}^{-1} \text{yr}^{-1}$.

only the 2010 sulphur emissions by cutting, respectively, 5 % (292 kt) and 19 % (248 kt) of their GP values. In our study, these emissions reductions for CP and H1 are applied to the UK and Eire but European boundary conditions similar to GP are used.

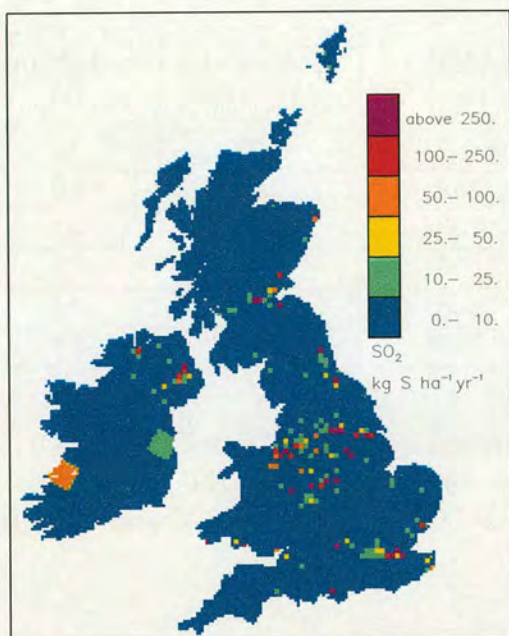


Figure 5.9: 2010 SO_2 emissions for the British Isles on a $5 \text{ km} \times 5 \text{ km}$ grid resolution (Gothenburg Protocol). Units are $\text{kg S ha}^{-1} \text{ yr}^{-1}$.

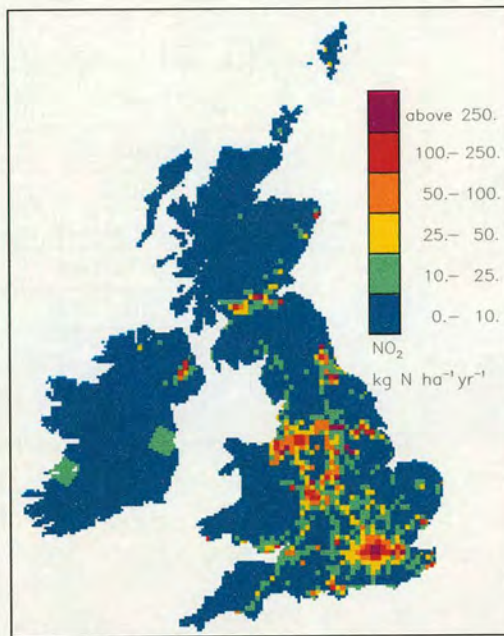


Figure 5.10: 2010 NO_x emissions for the British Isles on a $5 \text{ km} \times 5 \text{ km}$ grid resolution (Gothenburg Protocol). Units are $\text{kg N ha}^{-1} \text{ yr}^{-1}$.

Species 2010	SO_2			NO_x			NH_3		
	GP	CP	H1	GP	CP	H1	GP	CP	H1
UK	306	292	248	355	355	355	245	245	245

Table 5.7: SO_2 , NO_x , NH_3 emissions in the UK for the different 2010 emission scenarios : Gothenburg Protocol (GP), Common Position (CP) and H1. Units are ktonnes N (or S) yr^{-1} .

5.3.3 Results from FRAME 4.6 with different 2010 scenarios

FRAME 4.6 is used to model deposition and concentration of reduced nitrogen, oxidised nitrogen and sulphur over the UK for three different 2010 scenarios : GP, CP and H1. The results are compared with the 1996 modelled values.

UK reduced-N kt N yr ⁻¹	FRAME 4.6 1996	FRAME 4.6 2010 (GP)	Reduction (%)
Import	52	42	-21
Emission	291	245	-16
Dry deposition	103	96	-7
Wet deposition	105	83	-21
Total deposition	208	179	-14
Export	135	108	-21

Table 5.8: Budgets of reduced nitrogen for the UK from FRAME 4.6 for 1996 and 2010 (Gothenburg Protocol). The last column shows the percentage of reduction of the different components of the budget between 1996 and 2010 (GP). Units are ktonnes N yr⁻¹.

Gothenburg Protocol

Table 5.8 shows the UK reduced nitrogen budget obtained with the FRAME model for the 2010 Gothenburg Protocol scenario. This scenario corresponds to 70 %, 40 % and 16 % reduction in the 1996 SO₂, NO_x and NH₃ emissions, respectively, over the BI. The first column indicates the previous results obtained for 1996 with FRAME 4.6 (see section 4.6.3).

The reduction in both import (-21 %) and emissions (-16 %) of reduced nitrogen in 2010 led to less deposition to the UK than in 1996. The total deposition declined by 14 % from 208 kt to 179 kt. The decrease in dry deposition between 1996 to 2010 (GP) represents 7 % from 103 kt to 96 kt. Figure 5.11 presents this modelled flux of NH₃ dry deposition to the British Isles for 2010 (GP) and exhibits similar regional patterns to the 1996 modelled values. However, Figure 5.12 underlines intensity differences. The NH₃ dry deposition dropped up to 13 % between 1996 and 2010 to the major NH₃ source areas but also increased in 2010 in some areas (negative values in blue in Figure 5.12). The reason is that the NH₃ concentrations went up in these areas in 2010 (Figure 5.13). Less SO₂ emissions in 2010 led to less formation of ammonium aerosol (Figure 5.14) and hence, increase the NH₃ concentrations in areas such as the Scottish hills (north, north-west, south), Lake District, the Pennines, Wales, the south-east of England (except East Anglia and London) as it can be seen in Figure 5.13.

Indeed, this map of NH_3 concentrations shows similar features to the map of NH_3 dry deposition (Figure 5.12). The NH_3 concentrations in 2010 decreased more in the high NH_3 emissions areas than in the remote areas due to these interactions with SO_2 .

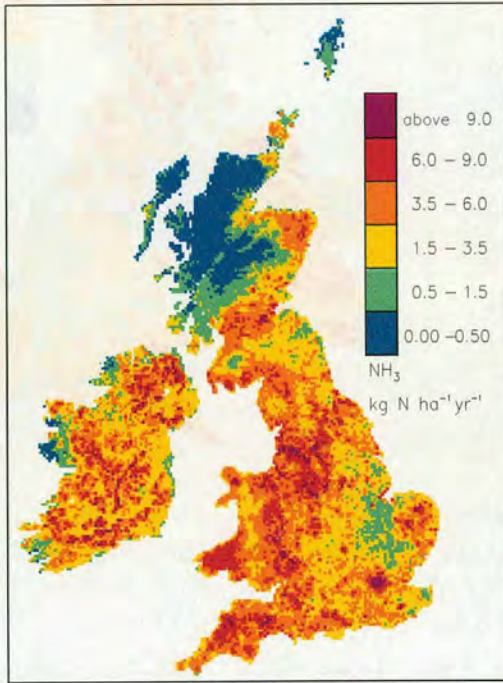


Figure 5.11: Grid average modelled flux of NH_3 dry deposition to the British Isles for 2010 (GP) at a $5 \text{ km} \times 5 \text{ km}$ resolution. Units are $\text{kg N ha}^{-1} \text{ year}^{-1}$.

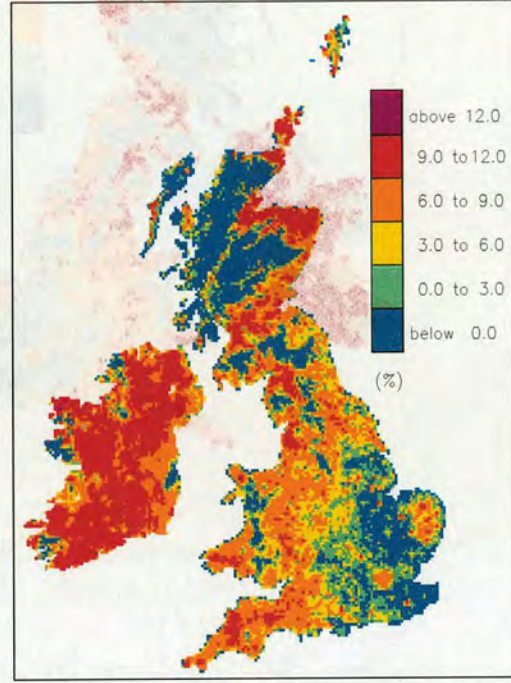


Figure 5.12: Percentage (%) difference between the modelled flux of NH_3 dry deposition in 1996 and 2010 (GP) with FRAME 4.6. The plot shows $\frac{1996-2010(\text{GP})}{1996} \times 100$ to the British Isles at a $5 \text{ km} \times 5 \text{ km}$ resolution.

The wet deposition dropped by 21 % in 2010 reaching 83 kt as illustrated in Figure 5.15. The regional patterns are similar to 1996 with high rates in hill areas but the amplitude is smaller as it can be seen in Figure 5.16, which shows the percentage of difference between 1996 and 2010 (GP) in the modelled NH_x wet deposition. These differences can be explained through the behaviour of ammonium aerosol which is the main contributor to NH_x wet deposition. Figure 5.14 shows a strong decline in the ammonium aerosol concentration from 1996 to 2010. This is caused by the decrease of NH_3 , NO_x and SO_2 emissions in 2010. The latter being the most important as illustrated by the stripes of Figure 5.14.

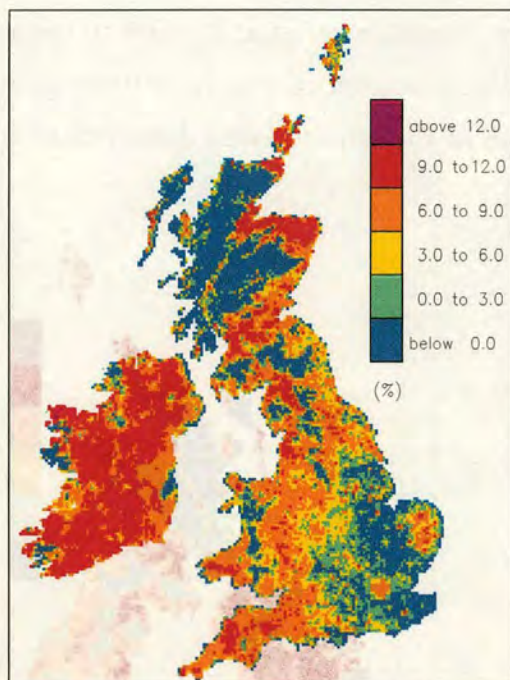


Figure 5.13: Percentage (%) difference between the modelled NH_3 surface concentration in 1996 and 2010 (GP) with FRAME 4.6. The plot shows $\frac{1996-2010(\text{GP})}{1996} \times 100$ over the British Isles at a $5 \text{ km} \times 5 \text{ km}$ resolution.

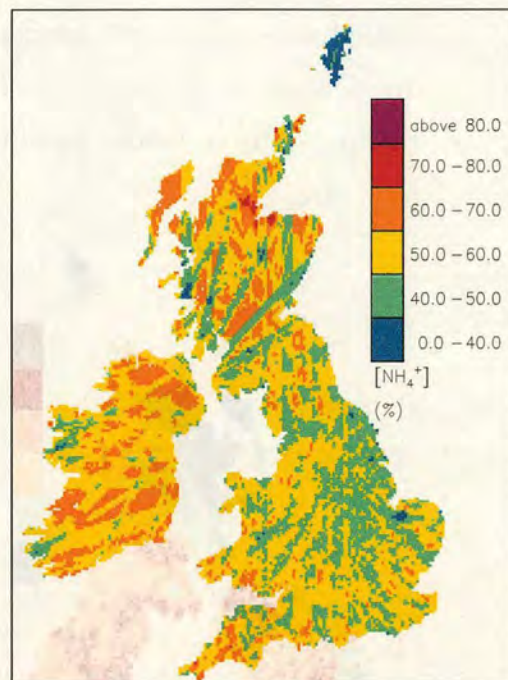


Figure 5.14: Percentage (%) difference between the modelled NH_4^+ surface concentration in 1996 and 2010 (GP) with FRAME 4.6. The plot shows $\frac{1996-2010(\text{GP})}{1996} \times 100$ over the British Isles at a $5 \text{ km} \times 5 \text{ km}$ resolution.

Therefore, there is substantially less ammonium aerosol, ammonium nitrate and ammonium sulphate formed and thus, less of these components available to be transported over the British Isles in the main south-west, west wind directions. This produces the high differences in NH_x wet deposition between 1996 and 2010 on the north-east, east and south-east side of the UK. Moreover, the east and south-east areas are strongly affected by the reduction of import from Europe in 2010. The export of reduced nitrogen outside the UK in 2010 (108 kt) is estimated to fall by 21 % in comparison with 1996. This is more than the decline of both emissions (-16 %) and total deposition (-14 %).

The stripes observed in Figure 5.14 are caused by the treatment of SO_2 emissions in FRAME. As it has been remarked in the previous chapter, firstly, the

SO₂ emissions inventory must be refined over Eire. The low resolution of the description of the Eire emissions causes the main stripes over Eire, Northern Ireland and Scotland in Figure 5.14. Secondly, a plume rise should be considered for the high-level SO₂ sources. Finally, a better resolution of the wind rose used in FRAME (for instance 5 degree instead of 15 degree) would substantially reduce the stripes obtained in this map but also, in the maps of modelled sulphur wet deposition and SO₂ surface concentration. These three aspects require further developments which are in process in collaboration with, respectively, J. Aherne (De Kluzenaar *et al.*, 2001), M. Vieno (Institute for Meteorology, Univ. of Edinburgh) and A. J. Dore (CEH).

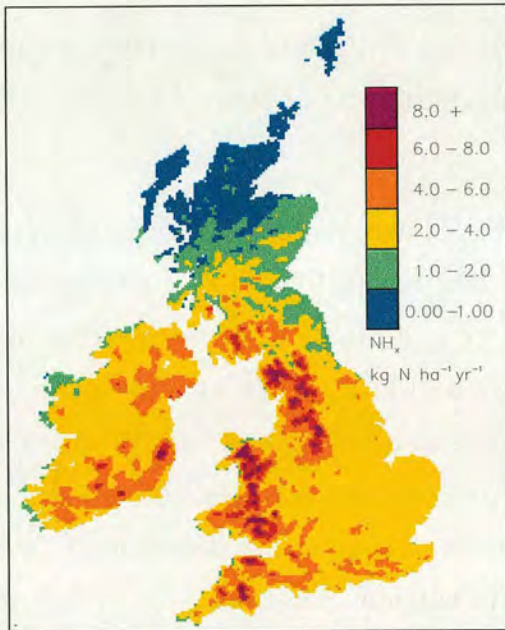


Figure 5.15: Grid average modelled flux of NH_x wet deposition to the British Isles for 2010 (GP) at a 5 km × 5 km resolution. Units are kg N ha⁻¹ year⁻¹.

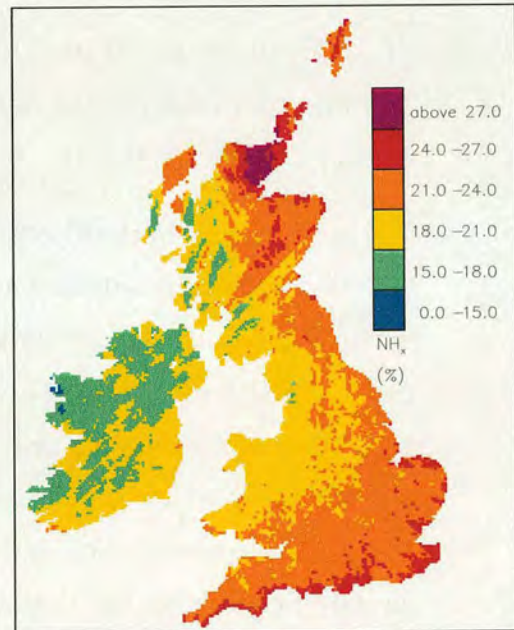


Figure 5.16: Percentage (%) difference between the modelled flux of NH_x wet deposition in 1996 and 2010 (GP) with FRAME 4.6. The plot shows $\frac{1996-2010(GP)}{1996} \times 100$ to the British Isles at a 5 km × 5 km resolution.

The reduction in SO₂ emissions from 1996 to 2010 (GP, -70 %) affects the UK reduced nitrogen budget of FRAME. The UK sulphur budget obtained with

UK sulphur kt S yr ⁻¹	FRAME 4.6 1996	FRAME 4.6 2010 (GP)	Reduction (%)
Import	116	21	-82
Emission	1005	306	-70
Dry deposition	130	34	-74
Wet deposition	199	72	-64
Total deposition	329	106	-68
Export	792	221	-72

Table 5.9: Budgets of sulphur for the UK from FRAME 4.6 for 1996 and 2010 (Gothenburg Protocol). The last column shows the percentage of reduction of the different components of the budget between 1996 and 2010 (GP). Units are ktonnes S yr⁻¹.

FRAME 4.6 for the 2010 Gothenburg Protocol scenario is shown in Table 5.9. The first column indicates the previous results obtained for 1996 with FRAME 4.6 (see section 4.6.3).

The reduction in both import (-82 %) and emissions (-70 %) of sulphur in 2010 (GP) led to less deposition to the UK than in 1996. The total deposition declined by 68 % from 329 kt to 106 kt. The decrease in dry deposition between 1996 to 2010 (GP) represents 74 % from 130 kt to 34 kt and is shown in Figure 5.17. This flux of sulphur dry deposition follows the distribution of SO₂ surface concentration which shows exactly the same features. Indeed, the decrease of SO₂ surface concentration and, hence of sulphur dry deposition (-74 %) is nearly linearly linked with the decline in sulphur emissions (-70 %) and import from surrounding countries (-82 %). However, the sulphur wet deposition shows a lower decline of only 64 % between 1996 and 2010 from 199 kt to 72 kt. The comparison of the distributions of sulphur wet deposition in 1996 and 2010 is presented in Figure 5.18. This shows that the decrease in SO₄²⁻ aerosol and precipitation concentrations is less important than in SO₂ surface concentration. This indicates that there are non-linearities in the relationship between emission and wet deposition patterns. This is caused at least in part by the increased neutralisation of ammonia. Ammonia emissions are not estimated to decrease as much as SO₂ emissions between 1996 and 2010. In 1996, SO₂ was in excess over NH₃ and thus, NH₃ was the limiting factor in aerosol formation. However,

in 2010, SO_2 and NH_3 are equally present in the atmosphere, which means that aerosol formation is limited by either of the gases, depending on the local pattern in their concentrations (Alcamo *et al.*, 1987; Fricke and Beilke, 1992; Erisman and Draaijers, 1995; NEG-TAP, 2001).

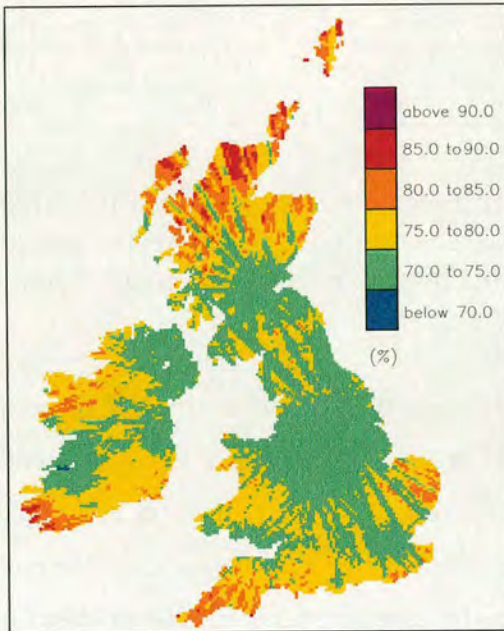


Figure 5.17: Percentage (%) difference between the modelled flux of sulphur dry deposition in 1996 and 2010 (GP) with FRAME 4.6. The plot shows $\frac{1996-2010(GP)}{1996} \times 100$ to the British Isles at a $5 \text{ km} \times 5 \text{ km}$ resolution.

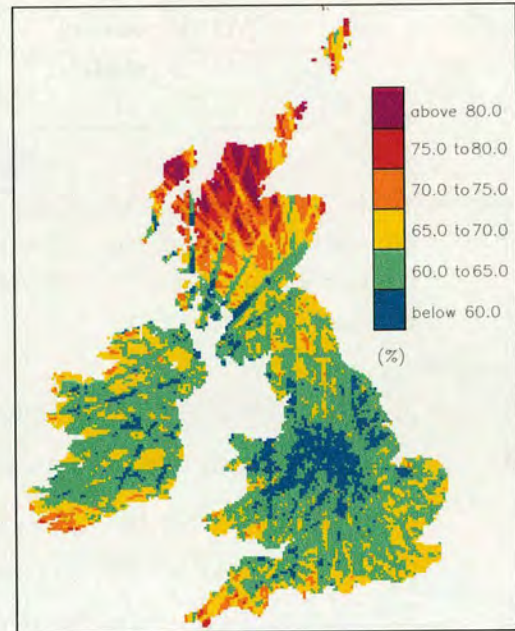


Figure 5.18: Percentage (%) difference between the modelled flux of sulphur wet deposition in 1996 and 2010 (GP) with FRAME 4.6. The plot shows $\frac{1996-2010(GP)}{1996} \times 100$ to the British Isles at a $5 \text{ km} \times 5 \text{ km}$ resolution.

Finally, the export of sulphur outside the UK in 2010 (121 kt) fell by 72 % in comparison with 1996. This is similar in amplitude to the decline in SO_2 emissions (-70 %) and total deposition (-68 %).

Table 5.10 shows the UK oxidised nitrogen budget obtained with the FRAME model for the 2010 Gothenburg Protocol scenario. The first column indicates the previous results obtained for 1996 with the FRAME model (see section 4.6.3).

The reduction in both import (-53 %) and emissions (-40 %) of oxidised nitrogen

UK oxidised nitrogen kt N yr ⁻¹	FRAME 4.6 1996	FRAME 4.6 2010 (GP)	Reduction (%)
Import	132	62	-53
Emission	590	355	-40
Dry deposition	61	36	-41
Wet deposition	155	85	-45
Total deposition	216	121	-44
Export	506	296	-41

Table 5.10: Budgets of oxidised nitrogen for the UK from FRAME 4.6 for 1996 and 2010 (Gothenburg Protocol). The last column shows the percentage of reduction of the different components of the budget between 1996 and 2010 (GP). Units are ktonnes N yr⁻¹.

in 2010 (GP) is estimated to lead to less deposition to the UK than in 1996. The total deposition declines by 44 % from 216 kt to 121 kt. The decrease in dry deposition between 1996 to 2010 (GP) represents 41 % from 61 kt to 36 kt and is mapped in Figure 5.19. The amplitude of the dry deposition decline follows the NO_x emissions reduction as it was the case for sulphur. The oxidised nitrogen wet deposition is estimated to decline by 45 % between 1996 and 2010 from 155 kt to 85 kt. The comparison of the distributions of wet deposition in 1996 and 2010 is presented in Figure 5.20. This does not exhibit significant non-linearities between emission and deposition. The decline of both dry and wet deposition roughly follows the 40 % amplitude in NO_x emissions reduction. Previous studies (Allen *et al.*, 1989; Stelson and Seinfeld, 1982) expected a lower decline in the NO_y wet deposition as the result of the SO₂ and NH₃ interactions. Indeed, because the SO₄²⁻ production is limited by the SO₂ availability, there is more NH₃ available to form nitrates, especially in remote areas (see Figure 5.13). However, in 2010, the level of the NO_x emissions is substantially lower than the amplitude of the NO_x emissions of the future scenarios considered in these studies from the 1980s. Therefore, there is not enough NO₂ and hence, HNO₃ to combine with NH₃ to form substantially higher ammonium nitrate concentrations. Moreover, this effect is amplified in the FRAME model by the fact that, along with other atmospheric transport models in the UK, it underestimates the formation of HNO₃ (see section 4.5.4).

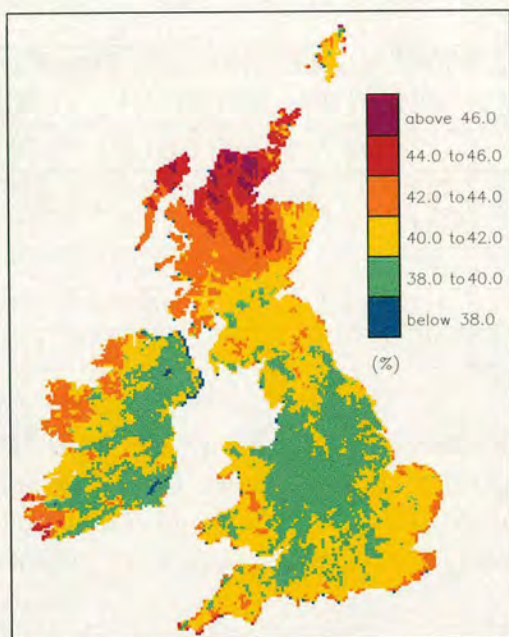


Figure 5.19: Percentage (%) difference between the modelled flux of oxidised nitrogen dry deposition in 1996 and 2010 (GP) with FRAME 4.6. The plot shows $\frac{1996-2010(GP)}{1996} \times 100$ to the British Isles at a 5 km \times 5 km resolution.

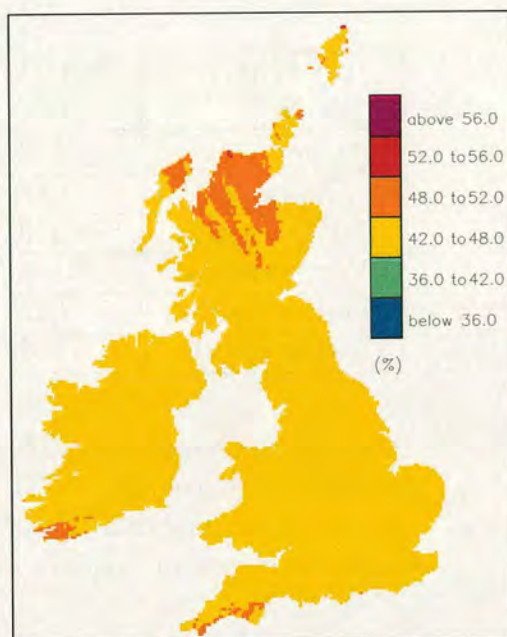


Figure 5.20: Percentage (%) difference between the modelled flux of oxidised nitrogen wet deposition in 1996 and 2010 (GP) with FRAME 4.6. The plot shows $\frac{1996-2010(GP)}{1996} \times 100$ to the British Isles at a 5 km \times 5 km resolution.

Common Position and H1 scenarios

The Common Position and H1 scenarios extend the Gothenburg Protocol by amplifying the reduction in SO₂ emissions for 2010 (see Table 5.7). The Common Position (CP) considers a slight decline of 5 % of the GP SO₂ emissions from 306 kt (GP) to 292 kt. The H1 scenario goes further by cutting 19 % of the GP SO₂ emissions from 306 kt to 248 kt. The ammonia and oxidised nitrogen emissions in the British Isles are unchanged from the Gothenburg Protocol. As it has been described previously, the same SO₂ emissions reduction is applied to Ireland and the UK for the CP and H1 scenarios. Moreover, these two scenarios consider the European boundary conditions (import) and the meteorological input data used for the Gothenburg Protocol. In regard to these assumptions, this study is a first step in the assessment of the effect of the CP and H1 scenarios on deposition to the UK.

UK sulphur kt S yr ⁻¹	FRAME 4.6 1996	FRAME 4.6 2010 (GP)	FRAME 4.6 2010 (CP)	FRAME 4.6 2010 (H1)
Import	116	21 (-82 %)	20 (-83 %)	19 (-83 %)
Emission	1005	306 (-70 %)	292 (-71 %)	248 (-75 %)
Dry deposition	130	34 (-74 %)	32 (-75 %)	27 (-79 %)
Wet deposition	199	72 (-64 %)	69 (-65 %)	62 (-69 %)
Total deposition	329	106 (-68 %)	101 (-69 %)	89 (-73 %)
Export	792	221 (-72 %)	211 (-73 %)	178 (-78 %)

Table 5.11: Budgets of sulphur for the UK from FRAME 4.6 for 1996 and the different 2010 scenarios : GP (Gothenburg Protocol), CP (Common Position) and H1. The reduction (%) of the different components of the budget compared to 1996 is shown in brackets for each 2010 scenario. Units are ktonnes S yr⁻¹.

The UK budget of reduced and oxidised nitrogen are not significantly affected by these two scenarios, being approximatively the same as for the Gothenburg Protocol. The results for sulphur are shown in Table 5.11. Firstly, the import from Eire to the UK is modified by considering the CP and H1 scenarios. Indeed, the SO₂ emissions reductions in Eire led to less export from Eire to the UK from 21 kt (GP) to 20 kt and 19 kt in CP and H1, respectively. The amplitude of the response to the CP and H1 scenarios, in terms of sulphur deposition, is similar to the GP scenario. This means that the sulphur dry deposition follows linearly, in both scenarios, the reduction in SO₂ emissions. However, the results of sulphur wet deposition confirms the non-linearities underlined previously in the case of the Gothenburg Protocol scenario.

The reduction in both import and emissions (-5 %) of sulphur in 2010 (CP) led to less deposition to the UK than in 2010 (GP). The total deposition declined by 5 % from 106 kt to 101 kt. The decrease in dry deposition between 2010 (GP) to 2010 (CP) is 6 % from 34 kt to 32 kt. The sulphur wet deposition shows a lower decline with 4 % between 2010 (GP) and 2010 (CP) from 72 kt to 69 kt. Thus, the export of sulphur outside the UK is 5 % lower than in the 2010 (GP) scenario with 211 kt instead of 221 kt.

The H1 scenario is an interesting modelling study to experiment the sensitivity

of the model to further SO₂ emissions reduction and to investigate if the model reacts in the same way as with the GP and CP 2010 scenarios. By cutting 19 % of the 2010 (GP) SO₂ emissions, the effect on sulphur deposition corroborates the results obtained with the two previous scenarios. Firstly, it reduced the import in the UK by 9 % from 21 kt (GP) to 19 kt. The total deposition declined by 16 % from 106 kt to 89 kt. The decrease in dry deposition between 2010 (GP) to 2010 (H1) is 21 % from 34 kt to 27 kt. The sulphur wet deposition shows again a lower decline than the dry deposition with 14 % between 2010 (GP) and 2010 (H1) from 72 kt to 62 kt. Finally, the export of sulphur is 19 % lower than in the 2010 (GP) scenario with 178 kt instead of 221 kt.

5.3.4 Scenarios for 2010 : conclusions

This modelling study shows that the application of European policies (UN/ECE, 1999; CEU, 2000) to reduce further emissions of SO₂, NO_x and NH₃ by 2010 would be beneficial, in terms of deposition and concentrations of nitrogen and sulphur compounds, for the UK in 2010. The Gothenburg Protocol agreed to cut the 1990 European SO₂, NO_x and NH₃ emissions by 75, 50 and 12 %, respectively in 2010. This Protocol might lead, in the UK, to a reduction in 1996 emissions by 70, 40 and 16 %, respectively in 2010. The success in fully implementing this Protocol in both Europe and the British Isles would lead to reduce substantially the total deposition of nitrogen and sulphur. Considering these targets of emissions reductions in 2010 in FRAME 4.6 led to decreases in the total deposition of sulphur, oxidised and reduced nitrogen to the UK by 68, 44 and 14 %, respectively from 1996 to 2010. This decline is illustrated in the Figures 5.21, 5.22 and 5.23.

Non-linearities in the relationship between the emissions and wet deposition patterns of sulphur have been detected. Ammonia, for which emissions will not decline as much as for SO₂ and NO_x, has an increasing role and the relative contribution of nitrogen compounds to the total deposition has increased from 1996 to 2010. In particular, because of a reduced rate of formation of NH₄⁺ in 2010,

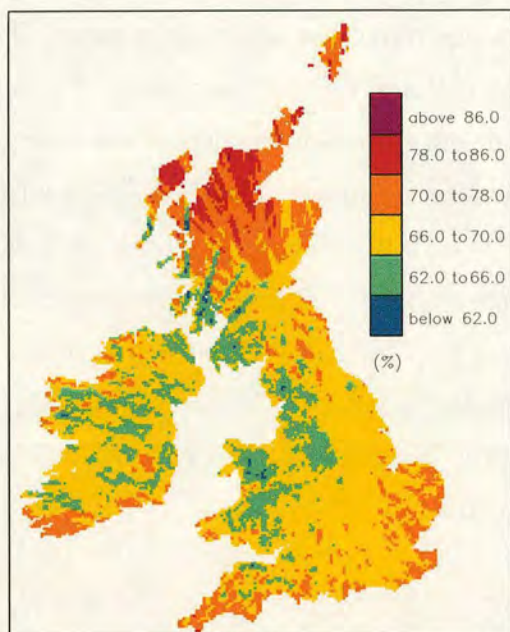


Figure 5.21: Percentage (%) difference between the modelled flux of sulphur total deposition in 1996 and 2010 (GP) with FRAME 4.6. The plot shows $\frac{1996-2010(GP)}{1996} \times 100$ to the British Isles at a 5 km \times 5 km resolution.

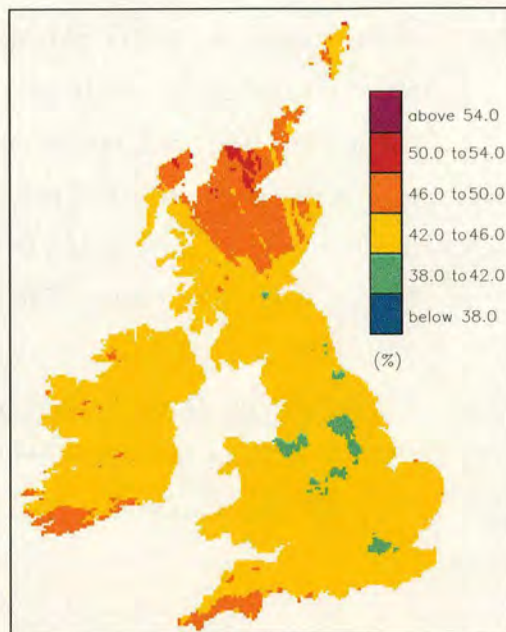


Figure 5.22: Percentage (%) difference between the modelled flux of oxidised nitrogen total deposition in 1996 and 2010 (GP) with FRAME 4.6. The plot shows $\frac{1996-2010(GP)}{1996} \times 100$ to the British Isles at a 5 km \times 5 km resolution.

concentrations of NH_3 will not decrease as much as NH_3 emissions. This has the result that dry deposition of NH_3 is only expected to decrease by 7 % in 2010 compared with 1996. It should be noted that there is also much regional variation in the projected decreases. The two other 2010 scenarios investigated with FRAME 4.6 (CP and H1), via further reduction in SO_2 emissions, corroborates the results obtained in the case of the Gothenburg Protocol scenario.

However, although this modelling study gives an interesting idea of what can be expected by 2010 with these different scenarios, some approximations (the use of 1996 meteorological input data, specific Eire emissions reductions in 2010) and weaknesses of the FRAME model limit the accuracy of the results. These latter include the underestimation of the nitric acid concentration and the overestimation of the oxidised nitrogen wet deposition by the FRAME model in comparison with the 1996 measurements. Moreover, some monitoring studies (Hensen and

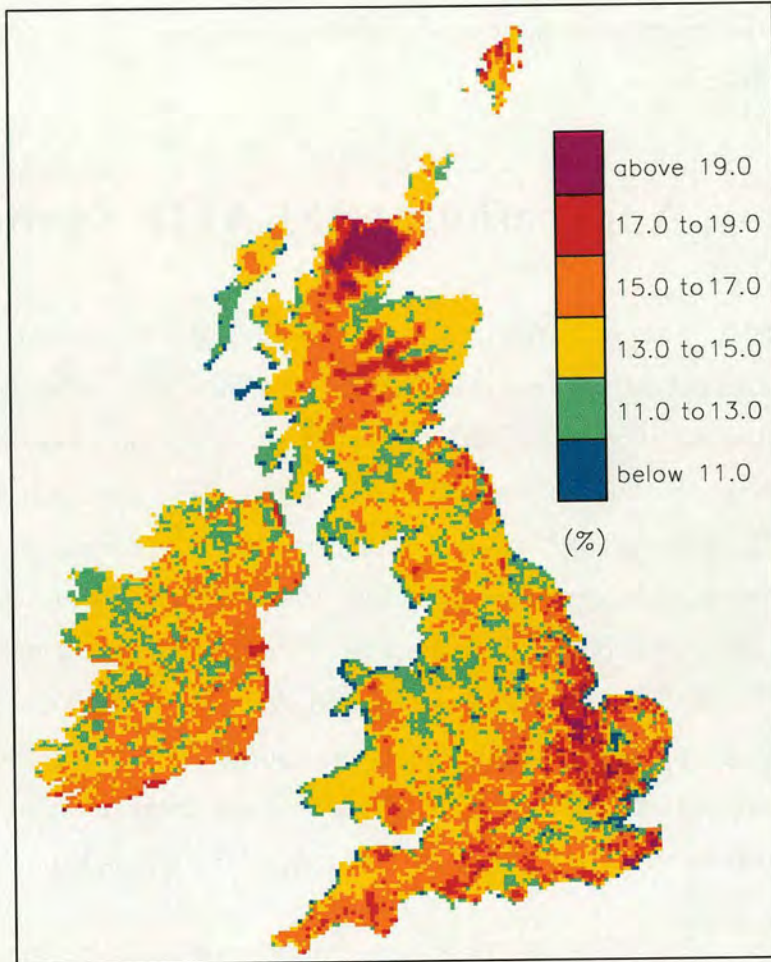


Figure 5.23: Percentage (%) difference between the modelled flux of reduced nitrogen total deposition in 1996 and 2010 (GP) with FRAME 4.6. The plot shows $\frac{1996-2010(GP)}{1996} \times 100$ to the British Isles at a $5 \text{ km} \times 5 \text{ km}$ resolution.

Erismann, 1999; Fowler *et al.*, 2001) show a complicating factor in the dry deposition of SO_2 , which would amplify the response to the 2010 emissions reduction we obtained in the study with the FRAME model. Indeed, the dry deposition of SO_2 might not decrease at the same rate as the decrease in SO_2 concentration in 2010. The dry deposition velocity might increase because the surface is less saturated by SO_2 uptake. Similarly, the NH_3 dry deposition velocity might decrease. Therefore, more SO_2 might be lost at the surface and even less NH_3 lost to the surface. This process is not parameterised in FRAME 4.6 as well as the bi-directional exchange of ammonia, currently in development in the model, which would allow both emissions and deposition to occur from the canopy (Sutton *et al.*, 1995b). These processes could have a significant impact in the assessment

of the effects of emissions abatement strategies.

5.4 Applications of FRAME : summary

Firstly, the FRAME model has been used to investigate regional reduced nitrogen budgets over the British Isles for 1996. The study shows that NH_3 emissions, transport and deposition in a specific region can have profound effects on the composition of the atmosphere over other regions. The large NH_3 emissions in Eire and Northern Ireland produce a substantial export in the east and north-east directions towards England and Scotland, contributing to the pollution in these regions. England is also a net exporter of reduced nitrogen. By contrast, Scotland and Wales are “ammonia neutral” as import of reduced nitrogen roughly balances export. Overall, in 1996, only 7% of reduced nitrogen is derived from non-British Isles sources; most of the NH_x from the BI is deposited in the British Isles (64%), while 36% is exported.

Secondly, predictions of reduced nitrogen, oxidised nitrogen and sulphur budgets for 2010 for the UK are investigated with the FRAME model. The study shows that a reduction in SO_2 , NO_x and NH_3 emissions following the Gothenburg Protocol would significantly decrease the deposition and concentrations of nitrogen and sulphur compounds in the UK in 2010. The Gothenburg Protocol should lead, in the UK, to a reduction in emissions of SO_2 , NO_x and NH_3 by 70, 40 and 16 %, respectively, from 1996 to 2010. Considering a similar success in the surrounding European countries to implement this Protocol, this would lead to reduce substantially the total deposition of nitrogen and sulphur to the UK. Applied to 2010 in the emissions reduction conditions of the Gothenburg Protocol, the FRAME model predicts a decline of the total deposition of sulphur, oxidised and reduced nitrogen to the UK by 68, 44 and 14 %, respectively, compared to 1996. Further reductions in SO_2 emissions in 2010 by 5 % (CP) and 19 % (H1) led to increase the decline of sulphur deposition without significantly affecting NH_x and NO_y deposition patterns. However, the strong decline of the SO_2 emissions

between 1990 and 2010 gives an increasing role to ammonia. Indeed, ammonia emissions did not decrease as much during this period leading to an increase in the amount of NH_3 available compared with SO_2 and NO_x . FRAME estimates that this would provide decreases in NH_4^+ aerosol faster than the decline in NH_3 emissions, while NH_3 concentrations will decrease less than the decline in NH_3 emissions. The consequence of these factors is that wet deposition of NH_x in remote areas will decrease substantially under the Gothenburg Protocol. Conversely, NH_3 dry deposition and here total NH_3 deposition in agricultural areas will not decrease as much as the decline in NH_3 emissions. This highlights the fact that NH_3 deposition, and particularly in agricultural regions, will continue to be a problem in 2010.

Chapter 6

Conclusions and Perspectives

Ammonia is the main alkaline gas present in the atmosphere. It is emitted in gaseous form (NH_3), mainly from livestock and fertilised agricultural land. Once emitted, it reacts with atmospheric acids (e.g. H_2SO_4 , HNO_3) to form aerosols containing ammonium sulphate and nitrate (e.g. $(\text{NH}_4)_2\text{SO}_4$, $(\text{NH}_4)\text{HSO}_4$, NH_4NO_3). The deposition of these species can cause ecological changes through acidification and through increasing the nitrogen content of the soil. Gaseous ammonia is typically deposited close to the sources, whereas the ammonium ion in the aerosols has a smaller deposition velocity, and is hence transported over larger distances. The short atmospheric lifetime of NH_3 and the location of sources at ground level in the rural environment result in NH_3 concentrations that are highly spatially variable. This makes it difficult to produce accurate maps of concentrations from observations alone, since it would be necessary to set up a very dense array of stations. Therefore, to complement measurement-based estimates, models are applied to estimate concentrations and deposition.

An atmospheric transport model, FRAME (Fine Resolution AMmonia Exchange), is further developed and applied here to model the spatial pattern of reduced nitrogen concentrations and deposition over the United Kingdom (UK).

The model is also applied for other species such as oxidised nitrogen and sulphur. The pattern of concentration and deposition of these species in the UK is strongly influenced by the emissions from the Republic of Ireland, hence the domain of the FRAME model was extended, in this study, to the British Isles (BI). On one hand, this change improved the predictions of the model in comparison with the measurements but, on another hand, it increased its run-time. Indeed, the model uses a multi-layer approach with diffusion through 33 layers to describe vertical concentration profiles in the atmosphere explicitly. Together with the necessary description of atmospheric reactions with sulphur and oxidised nitrogen over the BI, this imposed a major computational requirement, with the model having a run-time of 8.5 days on a mid-range workstation.

Improvement in the model run-time was sought, firstly, by developing a parallel implementation coded in a data-parallel approach using High Performance Fortran. Running the code on a Cray *T3E* with 128 processors provided a speed-up by a factor of 69. The portability of this code allows it to run on different parallel machines without modifications. Secondly, an alternative diffusion discretisation to the explicit fourth-order Runge-Kutta scheme was used in FRAME. An implicit Finite Volume method was implemented producing a speed-up by a factor of 34. Combined, these two approaches yielded a speed-up of 2346 and the results for 1996 for the BI of this new version compared well with those of the previously validated sequential code.

Attention was then focused on the wet deposition process, as it is the main weakness in the UK reduced nitrogen budgets of the FRAME and other UK models. Current pollution models frequently describe the wet deposition of chemical species from the atmosphere using the concentration of the species, its scavenging coefficient and the rainfall rate. However, over the BI, the spatial pattern of rainfall intensity often varies on a scale smaller than the spacing between rainfall stations, especially in mountainous areas. Indeed, it is well known that the rainfall rates occurring over mountainous and hilly regions are significantly greater than those over the surrounding low-level ground. For the BI conditions, the orographic enhancement of precipitation and wet deposition

from the seeder-feeder effect, must be taken into account, hence a model of directional orographic enhancement of precipitation was developed. The field of directional orographic precipitation given by this model was incorporated in FRAME and produced interesting regional patterns of wet deposition to the BI. Considering directional orographic precipitation improved the comparison between the modelled and measured values of NH_x wet deposition, in terms of correlation coefficient. However, the intensity of the NH_x (but also of S and NO_y) wet deposition was still underestimated by FRAME. While this method represents a significant advance, a number of limitations refrains. The heavy orographic rains from the west and southwest directions did not succeed in producing a significant amount of wet deposition because only a small amount of NH_4^+ originated from these directions in FRAME. Although the use of directional orographic precipitation is recommended and is more realistic than the annual average rainfall used previously, such parameterisation implies more development of the model before being efficient on a national scale. In addition, the FRAME UK reduced nitrogen wet deposition budget had been improved by developing a more realistic description of the scavenging coefficients. Instead of using a fixed value of the height of the atmospheric boundary layer (1000 m), a calculated value is considered in the parameterisation leading to a really better agreement with the UK reduced nitrogen budget.

Concerning oxidised nitrogen and sulphur, some parameters were adjusted more realistically to improve the results obtained with the FRAME model for the UK for 1996. These included the values of the dry deposition velocities and the height of emissions of NO_x and SO_2 . Indeed, FRAME distributed evenly these emissions throughout the lowest 300 m of the mixing layer. However, it seemed more representative to distribute the NO_x emissions through 100 m instead of 300 m as the high-stack contribution is less than a third of the total. For SO_2 , a database was available of source heights, and therefore FRAME was modified to allow emissions from point sources at different heights. Significant improvements were obtained by considering these aspects in the model.

Finally, the refinements of the FRAME model in terms of both run-time and 1996 UK budget results (FRAME 4.6), especially for reduced nitrogen, were applied to consider different analyses with the model. Firstly, atmospheric budgets of reduced nitrogen for the major political regions of the British Isles were investigated for 1996. Indeed, assessments of NH_x budgets are fewer in number than those for NO_x and S and regional budgets for the British Isles had never been evaluated. The study showed that NH_3 emissions, transport and deposition in a specific region can have profound effects on the composition of the atmosphere over other regions. An important feature was the high export of reduced nitrogen from Eire and Northern Ireland to England and Scotland. England was also a net exporter of reduced nitrogen. By contrast, Scotland and Wales were “ammonia neutral” as import of reduced nitrogen roughly balanced export. Overall, only 7% of reduced nitrogen in the British Isles was derived from non-British Isles sources. Most of the reduced nitrogen was deposited in the British Isles (64%), while 36% was exported.

Secondly, predictions of reduced nitrogen, oxidised nitrogen and sulphur budgets for 2010 for the UK were investigated with the FRAME model. The study showed that a reduction in SO_2 , NO_x and NH_3 emissions following the Gothenburg Protocol would significantly decrease the deposition and concentrations of nitrogen and sulphur compounds in the UK in 2010. The Gothenburg Protocol should lead, in the UK, to a reduction in emissions of SO_2 , NO_x and NH_3 by 70, 40 and 16 %, respectively, from 1996 to 2010. Considering a similar success in the surrounding European countries to implement this Protocol, this would lead to a substantial reduction in the total deposition of nitrogen and sulphur to the UK. Applied to 2010 in the emissions reduction conditions of the Gothenburg Protocol, the FRAME model predicted a decline of the total deposition of sulphur, oxidised and reduced nitrogen to the UK by 68, 44 and 14 %, respectively, compared to 1996. Further reductions in SO_2 emissions in 2010 by 5 % (CP) and 19 % (H1) led to additional decline of sulphur deposition without substantially affecting NH_x and NO_y deposition patterns. However, the strong decline of the SO_2 emissions between 1990 and 2010 gives an increasing role to ammonia which,

mainly through its dry deposition, will continue to be a serious problem in 2010.

6.1 Perspectives

One of the main uncertainties of the FRAME model is the parameterisation of the NO_y chemistry. Indeed, the FRAME model under-predicts the surface concentrations of HNO_3 and hence, the dry deposition of $\text{HNO}_3\text{-N}$. Moreover, the NO_y wet deposition is over-estimated. These aspects could be explained by the over-formation of NO_3^- at night-time in the model which considers a different reaction rate (k_{12}) than most of the other UK models. Moreover, it would be of interest to have a more precise inventory of the low-level sources of NO_x with details concerning their heights and their amplitudes. This would be more realistic and could improve significantly the NO_y wet deposition budget. Indeed, the consideration of high-level point sources for the SO_2 emissions led to substantially improve the results of sulphur wet and dry depositions, SO_2 and NH_4^+ surface concentrations.

For sulphur, there is still overestimation of the sulphur wet deposition and of the SO_2 surface concentration as the FRAME model does not include yet the plume rise of the SO_2 emissions. The combination of a more detailed point sources inventory and a better wind rose resolution for both the UK and Eire, would improve the sulphur wet deposition budget and the SO_2 surface concentration (less stripes in the BI maps).

The wind rose used in FRAME 4.6 is another limitation as it is derived from a 1981 study for the UK (Jones, 1981). This needs to be updated and a study is in process with A. J. Dore (CEH). Combined with the straight-line trajectories of both the FRAME and TERN models, it limited the benefit of considering the directional orographic rainfall developed in Chapter 4.

Throughout the application of the FRAME model, for 1996 simulations or 2010 predictions, it has been assumed that there was no relationship between the magnitude of emissions, deposition velocities and canopy resistances. However, this modelling study and some monitoring studies (Sutton *et al.*, 1995b; Hensen and Erisman, 1999; Fowler *et al.*, 2001) showed non-linearities of both SO₂ and NH₃ dry depositions in response to important change in emissions. Therefore, the processes involve, namely the dry deposition of SO₂ and bi-directional exchange of NH₃, need to be parameterised in the FRAME model to assess accurately the effects of emissions abatement strategies. These are both areas which are already the subject of further development.

Some sensitivity experiments have been done with the FRAME model. Singles (1996) assessed how sensitive the model was to a variation in the height of the cloud base and in the cloud cover. The present study also illustrated the sensitivity of FRAME to input parameters such as the dry deposition velocities, the scavenging coefficients and the height of emissions. There would need further sensitivity analysis with FRAME concerning the reaction rates in the NO_y chemistry and the wind rose pattern and resolution. That could help to explain the discrepancies between the modelled NO_y, S deposition and the NEG-TAP estimations for the UK for 1996.

However, there are also large uncertainties in the measurement based estimates from NEG-TAP for 1996. This illustrates the need of caution when trying to validate the FRAME model results by measurements of concentrations and wet deposition. For example, concerning the measurements of NH₄⁺ concentrations in rain, the magnitude of the dry deposition sampled in addition to the wet deposition is spatially variable and still not fully assessed. However, ongoing work by Cape J.N. (Personal communication) indicates that this contribution could reach 30 % in some areas. Therefore, as several similar monitoring studies are in process at CEH, it would be of significant interest to evaluate precisely the uncertainties of the measurements used in the comparison with FRAME. Indeed, measurement based estimates suffer from the non-representativeness or the paucity of the monitoring sites (NH_x wet deposition and HNO₃ surface concentration, respectively), or from the measurement techniques used (Tang *et al.*, 2001; Sutton *et al.*, 2002).

Bibliography

- Aherne, J. and Farrell, E. P.: 2000. Determination and mapping of critical loads for sulphur and nitrogen and critical levels for ozone in Ireland. *Tech. rep.*, Environmental Protection Agency, Dublin, 212pp.
- Alcamo, J., ApSimon, H., and Builtjes, P.: 1987. *Interregional Air Pollutant Transport: The Linearity Question*. IIASA, RR-87-20, Laxenburg, Austria.
- Allen, A. G., Harrison, M. R., and Walker, M. T.: 1988. A meso-scale study of the behaviour of atmospheric ammonia and ammonium. *Atmospheric Environment* **22**, 1347–1353.
- Allen, A. G., Harrison, R. M., and Erisman, J. W.: 1989. Field measurements of the dissociation of ammonium nitrate and ammonium chloride aerosols. *Atmospheric Environment* **23**, 1591–1599.
- Amann, M., Bertok, I., Cofala, J., Gyarmas, F., Heyes, C., Klimont, Z., and Schoepp, W.: 1999. *Integrated Assessment Modelling for the Protocol to Abate Acidification, Eutrophication and Tropospheric Ozone in Europe*. Ministry of Housing, Spatial Planning and the Environment, The Hague, Netherlands, November 1999.
- Anderson, H.: 1991. Ammonia monitoring - passive diffusion tube sampling. In Nitrogen and Phosphorus in Soil and Air project abstracts of the Danish NPO Research Programme. *Tech. rep.*, Ministry of the Environment Protection, Kobenhavn, Denmark.
- ApSimon, H. M., Barker, B. M., and Kayin, S.: 1994. Modelling studies of the atmospheric release and transport of ammonia - applications of the TERN model to an EMEP site in eastern England in anticyclonic episodes. *Atmospheric Environment* **28**, 665–678.
- ApSimon, H. M., Goddard, A. J. H., Wrigley, J., and Crompton, S.: 1984. Atmospheric transport of radioisotopes and the assessment of population doses on a European scale. *EN*, CEC report EUR 9128.
- Arya, S. P.: 1999. *Air Pollution Meteorology and Dispersion*. Oxford University Press.

- Asman, W. A. H.: 1998. Factors influencing local dry deposition of gases with special reference to ammonia. *Atmospheric Environment* **32**, 415–421.
- Asman, W. A. H. and van Jaarsveld, H. A.: 1992. A variable-resolution transport model applied for NH_x in Europe. *Atmospheric Environment* **26A**, 445–464.
- Asman, W. A. H., Sutton, M. A., and Schjoerring, J. K.: 1998. Ammonia : emission, atmospheric transport and deposition. *New Phytologist* **139**, 27–48.
- Baklanov, A. and Sorensen, J. H.: 2001. Parameterisation of Radionuclide Deposition in Atmospheric Long-Range Transport Modelling. *Phys. Chem. Earth (B)* **26**(10), 787–799.
- Barrett, K. and Seland, Ø.: 1995. European Transboundary Acidifying Air Pollution - Ten years calculated field and budgets to the end of the first Sulphur Protocol. *EMEP*, 1/95, Norwegian Meteor. Inst. Oslo, Norway.
- Benkner, S.: 2000. Optimizing irregular HPF applications using halos. *Concurrency: Practice and Experience* **12** (4), 137–155.
- Bergeron, T.: 1950. Uber der mechanismus der ausgiebigen Niederschlage. *Ber. Deutsch. Wetter.* **12**, 225–232.
- Bergeron, T.: 1965. On the low-level redistribution of atmospheric water caused by orography. *Proceedings of the Int. Conf. Cloud Phys.* Tokyo, May 1965.
- Boyle, G. M., Farrell, E. P., Cummins, T., and Nunan, N.: 1997. Monitoring of forest ecosystems in Ireland. *FOREM3 Project, Final Report. Forest Ecosystem Research Group Report Number 21*, Department of Environmental Resource Management, University College, Dublin, 186 pp.
- Brasseur, G. P., Orlando, J. J., and Tyndall, G. S.: 1999. *Atmospheric Chemistry and Global Change*. Oxford University Press.
- Briggs, G. A.: 1993. Plume dispersion in the convective boundary layer. *J. Appl. Meteorol.* **32**, 1388–1425.
- Buijsman, E. and Erisman, J. W.: 1988. Wet Deposition of Ammonium in Europe. *Journal of Atmospheric Chemistry* **6**, 265–280.
- Buijsman, E., Maas, H. F. M., and Asman, W. A. H.: 1987. Anthropogenic ammonia emissions in Europe. *Atmospheric Environment* **21**, 1009–1022.
- Bull, K. R.: 1991. The critical loads/levels approach to gaseous pollution emission control. *Environmental Pollution* **69**, 105–123.
- Carson, D. J.: 1973. The development of a dry inversion-capped convectively unstable boundary layer. *Quarterly Journal of the Royal Meteorological Society* **99**, 450–467.

- CEU: 2000. *Proposal for a Directive of the European Parliament and of the Council on national emission ceilings for certain atmospheric pollutants*. Council of The European Union, Brussels, Belgium.
- Chock, D. P. and Winkler, S. L.: 1994. A comparison of advection algorithms coupled with chemistry. *Atmospheric Environment* **28**, 2659–2675.
- Cofala, J., Heyes, C., and Klimont, Z.: 2000. *Integrated Assessment of Acidification, Eutrophication and Tropospheric Ozone Impacts in Europe*. IIASA, Laxenburg, Austria. Document available in Internet (<http://iiasa.ac.at/rains/>).
- Crossley, A. and Wilson, D. B.: 1992. Pollution in the upland environment. *Environmental Pollution* **7**, 81–87.
- Dabdub, D. and Manohar, R.: 1997. Performance and portability of an air quality model. *Parallel Computing* **23**, 2187–2200.
- Dabdub, D. and Seinfeld, J. H.: 1994. Numerical advective schemes used in air quality models - sequential and parallel implementation. *Atmospheric Environment* **28**, 3369–3385.
- De Kluzenaar, Y., Aherne, J., and Farrell, E. P.: 2001. Modelling the spatial distribution of SO₂ and NO_x emissions in Ireland. *Environmental Pollution* **112**, 171–182.
- De Kluzenaar, Y. and Farrell, E. P.: 2001. Ammonia monitoring in Ireland. A full year of ammonia monitoring; set-up and results. *Final Report. Series No. 8*, Environmental Protection Agency, Dublin, Ireland.
- Dore, A. J., Choularton, T. W., and Fowler, D.: 1992. An improved wet deposition map of the United Kingdom incorporating the seeder-feeder effect over mountainous terrain. *Atmospheric Environment* **26A**, 1375–1381.
- Dore, A. J., Choularton, T. W., Fowler, D., and Crossley, A.: 1992b. Orographic enhancement of snowfall. *Environmental Pollution* **75**, 175–179.
- Dore, A. J., Choularton, T. W., Fowler, D., and Storton-West, R.: 1990. Field measurements of wet deposition in an extended region of complex topography. *Quarterly Journal of the Royal Meteorological Society* **116**, 1193–1212.
- Dore, A. J., Choularton, T. W., and Inglis, D. W. F.: 2001. Monitoring studies of precipitation and cap cloud chemistry at Holme Moss in the southern Pennines. *Water, Air and Soil Pollution* **1**, 381–390.
- Draaijers, G. and Erisman, J. W.: 1993. Atmospheric deposition onto forest stands: throughfall estimates compared to estimates from inference. *Atmospheric Environment* **27A**, 43–55.

- Dragosits, U., Sutton, M. A., Place, C. J., and Bayley, A.: 1998. Modelling the spatial distribution of ammonia emissions in the United Kingdom. *Environmental Pollution* **102(S1)**, 195–203.
- Ehold, H. J., Gansterer, W. N., Kvasnicka, D. F., and Ueberhuber, C. W.: 2002. Optimizing local performance in HPF. *Parallel Computing* **28**, 415–432.
- Eliassen, A.: 1978. The OECD study of long-range transport of air pollutants: long range transport modelling. *Atmospheric Environment* **12**, 479–487.
- Erismann, J. W. and Draaijers, G. P. J.: 1995. *Atmospheric deposition in relation to acidification and eutrophication*. Studies in Environmental Research 63, Elsevier, The Netherlands.
- Farrell, E. P., Boyle, G. M., Cummins, T., Aherne, J., and van den Beuken, R.: 1996. Continued monitoring of a forest ecosystem in Ireland, Ballyhooly. *Final Report. Forest Ecosystem Research Group Report Number 17*, Department of Environmental Resource Management, University College, Dublin, 122 pp.
- Fisher, B. E. A.: 1975. The long-range transport of sulphur dioxide. *Atmospheric Environment* **9**, 1063–1070.
- Fisher, B. E. A.: 1978. The calculation of long-term sulphur deposition in Europe. *Atmospheric Environment* **12**, 489–501.
- Fletcher, C. A. J.: 1991. *Computational techniques for fluid dynamics*. Springer-Verlag, Berlin.
- Fournier, N., Pais, V. A., Sutton, M. A., Weston, K. J., Dragosits, U., Tang, Y. S., and Aherne, J.: 2002. Parallelisation and application of an atmospheric transport model simulating dispersion and deposition of ammonia over the British Isles. *Environmental Pollution* **116(1)**, 95–107.
- Fournier, N., Tang, Y. S., Dragosits, U., De Kluizenaar, Y., and Sutton, M. A.: 2002b. Regional atmospheric budgets of reduced nitrogen over the British Isles assessed using a multi-layer atmospheric transport model. *Atmospheric Environment*, (under review).
- Fournier, N., Weston, K. J., Dore, A. J., and Sutton, M. A.: 2002a. Modelling the wet deposition of reduced nitrogen over the British Isles using a multi-layer atmospheric transport model. *Quarterly Journal of the Royal Meteorological Society*, (under review).
- Fournier, N., Weston, K. J., Sutton, M. A., and Dore, A. J.: 2001. Inclusion of an improved parameterisation of the wet deposition process in an atmospheric transport model. *Proceedings of the 25th NATO/CCMS International Technical Meeting on Air Pollution Modelling and its Application*, pp. 181–188. Louvain-la-Neuve, Belgium, 15–19 October 2001.

- Fowler, D., Cape, J. N., Leith, I. D., Choularton, T. W., Gay, M. J., and Jones, A.: 1988. The influence of altitude on rainfall composition at Great Dun Fell. *Atmospheric Environment* **22**, 1355–1362.
- Fowler, D., Duyzer, J. H., and Baldocchi, D. D.: 1992. Inputs of trace gases, particles and cloud droplets to terrestrial surfaces. *Proc. of the Royal Society of Edinburgh, section biological sciences* **97**, 35–39.
- Fowler, D., Leith, I. D., Binnie, J., Crossley, A., Inglis, D. W. F., Choularton, T. W., Gay, M., Longhurst, J. W. S., and Conland, D. E.: 1995. Orographic enhancement of wet deposition in the United Kingdom: continuous monitoring. *Water, Air and Soil Pollution* **85**, 2107–2112.
- Fowler, D., Sutton, M. A., Flechard, C., Cape, J. N., Storeton-West, R., Coyle, M., and Smith, R. I.: 2001. The control of SO₂ dry deposition onto natural surfaces by NH₃ and its effects on regional deposition. *Water, Air and Soil Pollution* .
- Fowler, D., Sutton, M. A., Smith, R. I., Pitcairn, C. E. R., and Coyle, M.: 1998. Regional mass budgets of oxidized and reduced nitrogen and their relative contribution to the N inputs of sensitive ecosystems. *Environmental Pollution* **102(S1)**, 337–342.
- Fricke, W. and Beilke, S.: 1992. Indications for changing deposition patterns in Central Europe. *Environmental Pollution* **75**, 121–127.
- Garland, J. A.: 1977. The dry deposition of sulphur dioxide to land and water surfaces. *Proc. Roy. Soc. London A* **345**, 245–268.
- Golder, D.: 1972. Relation amongst Stability Parameters in the Surface Layer. *Boundary Layer Meteorology* **3**, 47–58.
- Goodwin, J. W. L., Salway, A. G., Murrels, T. P., Dore, C. J., Passant, N. R., and Eggleston, H. S.: 2000. UK Emissions of Air Pollutants 1970-1998. *AEA Technology*, AEAT/R/EN/0270.
- Harrison, R. M., Peak, J. D., and Collins, G. M.: 1996. The tropospheric cycle of nitrous acid. *J. Geophys. Res.* **101**, 14,429–14,439.
- Hensen, A. and Erisman, J. W.: 1999. Towards development of a deposition monitoring network for air pollution in Europe. *ECN-C-99-075*, ECN, Petten, The Netherlands.
- Hertel, O., Christensen, J., Runge, H., Asman, W. A. H., Berkowicz, R., and Hovmand, M. F.: 1995. Development and testing of a new variable scale air pollution model - ACDEP. *Atmospheric Environment* **29**, 1267–1290.
- Hill, T. A., Jones, A., and Choularton, T. W.: 1987. Modelling sulphate deposition onto hills by washout and turbulence. *Quarterly Journal of the Royal Meteorological Society* **113**, 1217–1236.

- Hornung, M., Sutton, M. A., and Wilson, R. B.: 1995. Mapping and modelling of critical loads for nitrogen - a workshop report. (*Report of an UN-ECE workshop, Grange over Sands, 23-26 october 1994*), Institute of Terrestrial Ecology, Edinburgh.
- Hov, Ø. and Hjøllø, B. A.: 1994. Transport distance of ammonia and ammonium in Northern Europe. Its relation to emissions of SO₂ and NO_x. *J. Geophys. Res.* **99**, 18,749–18,755.
- Howard, D. C. and Brunce, R. G. H.: 1996. The countryside information system: a strategic-level decision support system. *Environmental Monitoring and Assessment* **39**, 373–384.
- INDITE: 1994. *Impacts of Nitrogen Deposition in Terrestrial Ecosystems*. Department of the Environment, London, UK.
- Inglis, D. W. F., Choularton, T. W., and Wicks, A. J.: 1995. The effect of orography on wet deposition in an industrial area. *Quarterly Journal of the Royal Meteorological Society* **121**, 1575–1588.
- Jarvis, S. C. and Pain, B. F.: 1990. Ammonia volatilisation from agricultural land. *Proceedings of the Fertiliser Society No. 298*. The Fertiliser Society, Thorpe Wood, Peterborough.
- Jones, J. A.: 1981. The estimation of long-range dispersion and deposition of continuous releases of radionuclides to atmosphere. *National Radiological Protection Board*, NRPB-R123, Oxfordshire.
- Keppens, R. and Toth, G.: 2000. Using High Performance Fortran for magnetohydrodynamic simulations. *Parallel Computing* **26**, 705–722.
- Klimova-Murphy, E. and Fisher, B. E.: 1997. Application of a long-range transport model for the assessment of air quality on a local scale. *Int. J. Environment and Pollution* **8**, 408–419.
- Kruse-Plass, M., Apsimon, H. M., and Barker, B. M.: 1993. A modelling study of the effect of ammonia on in-cloud oxidation and deposition of sulphur. *Atmospheric Environment* **27A**, 223–234.
- Lee, D. S. and Hayman, G. D.: 1999. Modelling long-term trends in sulphur deposition. *Report 2. DTI JN 5/5/2*, Department of Trade and Industry, ETSU, Harwell, UK.
- Lee, D. S., Kingdon, R. D., Garland, J. A., and Jones, M. R.: 2000. Parameterisation of the orographic enhancement of precipitation and deposition in a long-term, long range transport model. *Annales Geophysicae* **18**, 1447–1466.

- Lee, D. S., Kingdon, R. D., Jenkin, M. E., and Garland, J. A.: 2000a. Modelling the atmospheric oxidised and reduced nitrogen budgets for the UK with a Lagrangian multi-layer long-range transport model. *Environmental Modeling and Assessment* **5**, 83–104.
- Leonard, B. P., Lock, A. P., and McVean, M. K.: 1995. The NIRVANA scheme applied to one dimensional advection. *Int. J. Heat Fluid* **5**, 341–377.
- Martin, M., Oberson, O., Chopard, B., Mueller, F., and Clappier, A.: 1999. Atmospheric pollution transport: the parallelization of a transport and chemistry code. *Atmospheric Environment* **33**, 1853–1860.
- Maul, P. R.: 1978. A prototype time-dependent model for the long-range transport of sulphur dioxide and associated pollutants. *CEGB report SSD/MID/R17/78*.
- Mehrotra, P., van Rosendale, J., and Zima, H.: 1998. High Performance Fortran: history, status and future. *Parallel Computing* **24**, 325–354.
- Merlin, J. and Hey, A.: 1995. An introduction to High Performance Fortran. *Scientific Programming* **4**, 88–113.
- Metcalf, S. E., Whyatt, J. D., and Derwent, R. G.: 1995. A comparison of model and observed network estimates of sulphur deposition across Great Britain for 1990 and its likely source attribution. *Quarterly Journal of the Royal Meteorological Society* **121**, 1387–1411.
- Metcalf, S. E., Whyatt, J. D., and Derwent, R. G.: 1998. Multi-pollutant modelling and the critical loads approach for nitrogen. *Atmospheric Environment* **32** (3), 401–408.
- Misselbrook, T. H., der Weerden, T. J. V., Pain, B. F., Jarvis, S. C., Chambers, B. J., Smith, K. A., Phillips, V. R., and Demmers, T. G. M.: 2000. 2000 ammonia emission factors for UK agriculture. *Atmospheric Environment* **34**, 871–880.
- Moller, D. and Schieferdecker, H.: 1989. Ammonia emission and deposition of NH_x in the G.D.R. *Atmospheric Environment* **23**, 1187–1193.
- Murley, L.: 1995. Clean air around the world: national approaches to air pollution control. *IUAPP*, EPA.
- Mylona, S.: 1998. Estimated dispersion of acidifying and eutrophying compounds and comparison with observations. *EMEP/MS-CW Report 1/98*, Norwegian Methodological Institute. Oslo, Norway.
- NEG-TAP: 2001. Transboundary Air Pollution : Acidification, Eutrophication and Ground-level Ozone in the UK. *First report of the National Expert Group on Transboundary Air Pollution* Department of the Environment, Transport and the Regions (DETR), London.

- Nihlgard, B.: 1985. The ammonium hypothesis - An additional explanation to the forest dieback in Europe. *Ambio* .
- Nilsson, B. and Grennfelt, P.: 1988. Critical Loads for Sulphur and Nitrogen. (*Report from a workshop at Skokloster, Sweden, 19-24 March 1988*), Nordic Council of Ministers, Copenhagen, Denmark.
- NPCA: 1999. Rivers and lakes are dying. *In Green Issues*. Available at URL: <http://odin.dep.no/html/nofovalt/depter/md/publ/acid/Rivers.html>, Norwegian Pollution Control Authority.
- Oden, E.: 1969. Studies on acidification of Scandinavian lakes by long-range air pollution. Unpublished.
- OECD: 1977. The OECD programme on long range transport of air pollutants. Measurements and findings. *Organisation for Economic Cooperation and Development*. Paris, France.
- OSI: 1993. 1:100,000 CORINE Land Cover Project (Ireland). *Ordnance Survey of Ireland*. Phoenix Park, Dublin.
- Pacheco, P.: 1996. Parallel Programming with MPI. *Morgan Kaufmann* .
- Pasquill, F.: 1961. The estimation of the dispersion of windborne material. *Meteorological Magazine* **90**, 33-49.
- Pasquill, F. and Smith, F. B.: 1983. *Atmospheric Diffusion*. 3rd ed. Ellis Horwood Ltd., Chichester, England.
- Patankar, S. V.: 1980. *Numerical Heat Transfer and Fluid Flow*. Hemisphere (McGraw-Hill), New York.
- Prather, J. M.: 1986. Numerical advection by conservation of second-order moments. *J. Geophys. Res.* **91**, 6671-6681.
- Press, W., Teukolsky, S., Vetterling, W., and Flannery, B.: 1992. *Numerical Recipes in FORTRAN*. Cambridge University Press.
- Quinn, P. K., Barrett, K. J., Dentener, F. J., Lipschultz, F., and Kurz, K. D.: 1996. Estimation of the air/sea exchange of ammonia for the North Atlantic basin. *Biogeochemistry* **35**, 275-304.
- Quinn, P. K., Bates, T. S., Johnson, J. E., Covert, D. S., and Charlson, R. J.: 1990. Interactions between the sulfur and reduced nitrogen cycles over the central Pacific Ocean. *J. Geophys. Res.* **95**, 16,405-16,416.
- Randerson, D.: 1984. Atmospheric boundary layer. In : Atmospheric science and power production. *Tech. rep.*, US DoE / TIC-27601.

- RGAR: 1990. Acid deposition in the United Kingdom 1986-1988. (*Third report of the United Kingdom Review Group on Acid Rain*) Department of the Environment, London.
- RGAR: 1997. Acid deposition in the United Kingdom 1992-1994. (*Fourth report of the United Kingdom Review Group on Acid Rain*) Department of the Environment, London.
- Rodgers, I. R.: 1993. Transport and deposition model needs for power generation. *Tech. rep.*, Conclusions of the National forum, ICON.
- Salway, A. G., Eggleston, H. S., Goodwin, J. W. L., Berry, J. E., and Murrells, T. P.: 1999. Uk Emissions of Air Pollutants 1970-1996. *Report AEAT-3092*, National Atmospheric Emissions Inventory, AEA Technology, National Environmental Technology Centre.
- Sandnes, H. and Styve, H.: 1992. Calculated budgets for airborne acidifying components in Europe, 1985, 1988, 1989, 1990 and 1991. *EMEP 1/92*, Norwegian Methodological Institute. Oslo, Norway.
- Schaug, J., Iversen, T., and Pedersen, U.: 1993. Comparison of measurements and model results for airborne sulphur and nitrogen components with kriging. *Atmospheric Environment* **27A**, 831-844.
- Seinfeld, J. H.: 1986. *Atmospheric Chemistry and Physics of Air Pollution*. Wiley Interscience, New York.
- Singles, R. J.: 1996. *Fine Resolution Modelling of Ammonia Dry Deposition over Great Britain*. Ph.D. thesis, The University of Edinburgh.
- Singles, R. J., Sutton, M. A., and Weston, K. J.: 1998. A multi-layer model to describe the atmospheric transport and deposition of ammonia in Great Britain. *Atmospheric Environment* **32 (3)**, 393-399.
- Smith, F. B.: 1975. Turbulence in the atmospheric boundary layer. *Sci. Prog. Oxford* **62**, 127-151.
- Smith, F. B.: 1979. The relationship between Pasquill stability P and Kazanski-Monin stability u (in neutral and unstable conditions). *Atmospheric Environment* **13**, 879-881.
- Smith, F. B.: 1979a. The influence of mountains on the atmosphere. *Adv. Geophys.* **21**, 87-230.
- Smith, G. D.: 1985. *Numerical Solution of Partial Differential Equations : Finite difference methods*. Oxford University Press.
- Smith, R. I., Fowler, D., Sutton, M. A., Flechard, C., and Coyle, M.: 2000. Regional estimation of pollutant gas dry deposition in the UK: model description, sensitivity analyses and outputs. *Atmospheric Environment* **34**, 3757-3777.

- Stelson, A. W. and Seinfeld, J. H.: 1982. Relative humidity and temperature dependence of the ammonium nitrate dissociation constant. *Atmospheric Environment* **16**, 983–993.
- Støren, E.: 1998. The EMEP/MSC-W Emission Database System. *EMEP/MSC-W Report 1/98*, Norwegian Methodological Institute. Oslo, Norway.
- Stull, R. B.: 1988. *An introduction to boundary layer meteorology*. Kluwer Academic Publishers.
- Sutton, M., Schjoerring, J. K., and Wyers, G. P.: 1995b. Plant-atmosphere exchange of ammonia. *Phil. Trans. Roy. Soc., London* **351**, 261–278.
- Sutton, M. A., Asman, W. A. H., Ellerman, T., van Jaarsveld, J. A., Acker, K., Aneja, V., Duyzer, J. H., Horvath, L., Paramonov, S., Mitosinkova, M., Tang, Y. S., Achermann, B., Gauger, T., Bartniki, J., Neftel, A., and Erisman, J. W.: 2001a. Establishing the link between ammonia emission control and measurements of reduced nitrogen concentrations and deposition. *Background document*, edited by H. Menzi and B. Achermann. UNECE Ammonia Expert Group Meeting, pp. 57-84, Berne, Switzerland.
- Sutton, M. A., Asman, W. A. H., and Schjoerring, J. K.: 1994. Dry deposition of reduced nitrogen. *Tellus* **46B**, 255–273.
- Sutton, M. A., Dragosits, U., Tang, Y. S., and Fowler, D.: 2000. Ammonia emissions from non-agricultural sources in the UK. *Atmospheric Environment* **34**, 855–869.
- Sutton, M. A., Fowler, D., Smith, R. I., Eager, M., Place, C. J., and Asman, W. A. H.: 1993. Modelling the net exchange of reduced nitrogen. *Proceeding of the joint CEC/BIATEX workshop, Aveiro (May 1993)*, edited by J. Slanina, G. Angeletti, and S. Beilke. Air Pollut. Res. Report 47, pp. 117-131, CEC, Brussels.
- Sutton, M. A., Miners, B., Tang, Y. S., Milford, C., Wyers, G. P., Duyzer, J. H., and Fowler, D.: 2002. Comparison of low cost measurement techniques for long-term monitoring of atmospheric ammonia. *J. Environ. Monit.* **3**, 446–453.
- Sutton, M. A., Place, C. J., Eager, M., Fowler, D., and Smith, R. I.: 1995a. Assessment of the magnitude of ammonia emissions in the United Kingdom. *Atmospheric Environment* **29**, 1393–1413.
- Sutton, M. A., Tang, Y. S., Dragosits, U., Fournier, N., Dore, T., Smith, R. I., Weston, K. J., and Fowler, D.: 2001. A spatial analysis of atmospheric ammonia and ammonium in the UK. In *Optimizing Nitrogen Management in Food and Energy Production and Environmental Production : Proceedings of the 2nd International Nitrogen Conference on Science and Policy*. *TheScientificWorld* **1 (S2)**, 275–286.

- Sutton, M. A., Tang, Y. S., Dragosits, U., Love, L., Fowler, D., Hasler, S., Sansom, L., and Hayman, G.: 2001b. Monitoring of nitric acid, particulate nitrate and other species in the UK. *Final report under the UK Acid Deposition Monitoring. CEH Report to NETCEN/DEFRA*, CEH, Edinburgh, Scotland.
- Sutton, M. A., Tang, Y. S., Miners, B. P., Coyle, M., Smith, R. I., and Fowler, D.: 1998. Spatial and temporal patterns of ammonia concentration in the UK. Results of the National Ammonia Monitoring Network. *Final report to the DETR. 79 pp*, Institute of Terrestrial Ecology, Edinburgh.
- Tang, Y. S., Cape, J. N., and Sutton, M. A.: 2001. Development and types of passive samplers for monitoring atmospheric NO₂ and NH₃ concentrations. *TheScientificWorld* **1**, 513–529.
- Tarrason, L. and Schaug, J.: 1999. Transboundary acid deposition in Europe. *EMEP report 1/99 (July 1999)*. EMEP- CCC/MS-CW, Norwegian Meteorological Institute, Blindern.
- Thom, A. S.: 1975. *Momentum, mass and heat exchange of plant communities*, vol. 1. Ed. J. L. Montieth, Academic Press, London.
- Thomas, L. H.: 1949. Elliptic problems in linear difference equations over a network. *Report*, Watson Sci. Comput. Lab., Columbia University, New York.
- Thompson, N., Barrie, I. A., and Ayles, M.: 1982. The Meteorological Office rainfall and evaporation system: MORECS (July 1981). *Hydrological Memorandum No. 45* The Meteorological Office, Bracknell.
- Turpin, B. J., Saxena, P., and Andrews, E.: 2000. Measuring and simulating particulate organics in the atmosphere: problems and prospects. *Atmospheric Environment* **34**, 2983–3013.
- UN/ECE: 1999. *Protocol to the 1979 Convention on Long-range Transboundary Air Pollution to Abate Acidification, Eutrophication, and Ground-level Ozone*. United Nations Economic Commission for Europe, Geneva, Switzerland.
- Van den Beuken, R.: 1997. Mapping emission and dry deposition of ammonia for Ireland. *Forest Ecosystem Research Group Report 24*, Department of Environmental Resource Management, University College Dublin, Ireland.
- Van Leeuwen, E. P., Erisman, J. W., Draaijers, G. P. J., Potma, C. J. M., and Van Pul, W. A. J.: 1995. European wet deposition maps based on measurements. *Report No. 722108006*, National Institute of Public Health and Environmental Protection, Bilthoven, The Netherlands.
- Versteeg, H. K. and Malalasekera, W.: 1995. *An introduction to computational fluid dynamics. The finite volume method*. Longman Group, England.

- Vestreng, V.: 2001. Emission data reported to UNECE/EMEP: Evaluation of the spatial distributions of emissions. *EMEP/MS-CW Note 1/01*, Norwegian Methodological Institute. Oslo, Norway.
- Wallen, C. C.: 1970. *Climates in Northern and Western Europe*. Elsevier Publishing Company.
- Warren, R. and ApSimon, H. M.: 2000. Selection of target loads for acidification in emission abatement policy: the use of gap closure approaches. *Water, Air and Soil Pollution* **121**, 229–258.
- Weil, J. C. and Brower, R. P.: 1984. An updated Gaussian plume model for tall stacks. *J. Air Pollut. Cont. Assoc.* **34**, 818–827.
- Weston, K. J. and Roy, M. G.: 1994. The directional-dependence of the enhancement of rainfall over complex orography. *Meteorol. Appl.* **1**, 267–275.
- Zalesak, S. T.: 1979. Fully multidimensional flux-corrected transport algorithms for fluids. *J. Comput. Phys.* **31**, 335–362.

Appendix A

Monitoring Networks

Site number	Site Name	[NH ₃] μg m ⁻³	[NH ₄ ⁺] μg m ⁻³
1	Bush	2.56	0.65
2	Inverpolly	0.07	0.15
3	Penallt	1.50	1.04
4	Priddy	1.48	
5	Holme Lacy	1.98	1.31
6	Glen Shee	2.11	0.40
7	Stackpole	2.26	
8	Orielton	1.21	0.61
9	Brown Moss	4.90	
10	Bure Marshes	1.46	1.02
11	Mere Sands Wood	2.65	1.17
12	Halladale	1.40	0.22
13	Aston Rowant	1.28	1.49
14	Ellon Ythan	1.48	0.44
15	Llyncllys Common	1.38	0.94
16	North Allerton	4.04	1.54
17	Easingwold	5.76	1.21
18	Auchencorth	0.92	0.81
19	Shetland	0.20	0.20
20	Drayton	4.36	1.30
21	Glensaugh	0.26	0.74
22	Moor House	0.24	0.59
23	North Wyke	1.65	0.81
24	Rothamstead	1.00	1.18
25	Sourhope	0.50	0.55
26	Wytham Woods	1.29	1.07
27	Alice Holt	1.03	1.20
28	Porton Down	1.86	1.12

29	Dyffryn Mymbyr	1.49	0.53
30	Strathvaich Dam	0.11	0.19
31	Eskdalemuir	0.44	0.60
32	High Muffles	2.93	0.99
33	Stoke Ferry	2.33	1.46
34	Yarner Wood	0.54	0.83
35	Lullington Heath	0.95	1.07
36	London Victoria	1.74	1.71
37	Five Acres	0.89	
38	Sheffield	0.87	1.03
39	Silsoe	1.50	1.41
40	Sutton Bonington	5.53	1.72
41	Lagganlia	0.13	0.17
42	Castle Cary	3.96	1.04
43	Tadcaster	1.72	1.13
44	Hillsborough	3.15	0.66
45	Lough Navar	0.42	0.38
46	Sibton	3.13	1.12
47	Rum	0.13	0.13
48	Wem Moss	2.91	
49	Frodsam	2.91	
50	Swettenham	3.35	
51	Wybunbury	2.86	
52	Fenn Moss	2.91	
53	Little Budworth	2.72	
54	Bickerton Hill	2.57	
55	Ruabon	0.24	
56	Wardlow Hay Cop	0.98	
57	Stanford	1.83	
58	Redgrave	3.02	
59	Dunwich Heath	1.33	
60	Edinburgh	1.35	0.98
61	Much Hoole	5.74	
62	Midge Hall	3.52	
63	Cardigan	0.68	
64	Pen Y Garn	0.13	
65	Allt a Mharcaidh	0.04	
66	Dennington	4.55	
67	Fressingfield	8.07	
68	Bedingfield	12.9	
69	Cwmystwyth	1.85	0.73
70	Myerscough	4.51	

Table A.1: 1996 mean measured concentrations of NH_3 and NH_4^+ from the UK National Ammonia Monitoring Network. Units are $\mu\text{g m}^{-3}$.

Site number	Site Name	[NO ₂] μg m ⁻³
5002	Eskdalemuir	4.49
5003	Goonhilly	5.53
5004	Stoke Ferry	17.76
5005	Ludlow	12.85
5007	Barcombe Mills	19.47
5008	Yarner Wood	6.57
5009	High Muffles	12.37
5010	Strathvaich Dam	1.32
5011	Glen Dye	3.21
5021	Malham Tarn	13.53
5023	Preston Montford	12.97
5024	Flatford Mill	17.71
5029	Birds Hill	9.29
5100	Beinn Eighe	1.33
5102	Fort Augustus	1.92
5103	River Mharcaidh	2.42
5105	Loch Ard	4.22
5106	Whiteadder	4.64
5107	Loch Dee	4.77
5109	Redesdale	6.92
5110	Kershope Forest	6.25
5111	Bannisdale	9.95
5112	Glassonby	8.57
5113	Cow Green Reservoir	9.72
5115	Devoke Water	9.03
5116	Hebden Bridge	16.92
5117	Thorganby	18.78
5118	Jenny Hurn	21.61
5119	Beddgelert	7.71
5120	Wardlow Hay Cop	21.35
5121	Bottesford	20.65
5122	Plynlimon	6.05
5123	Tycanol Wood	5.82
5124	Llyn Brianne	6.99
5125	Broom's Barn	20.73
5126	Ridgehill	16.31
5127	Woburn	30.22
5128	Bowood House	17.00
5129	Compton	21.32
5130	Plaxtol	18.10
5134	Gisla	1.37
5135	Broadford	1.57

5136	Driby	13.64
5137	Pitsford	21.67
5138	East Ruston	15.04
5139	Hill of Shurton	2.94
5140	Achanarras	2.49
5141	Hartland Moor	15.17
5142	Liphook	18.28
5143	Loch Leven	4.72
5147	Myres Hill	4.19
5148	Baltasound	2.64
5150	Pumlumon	5.73
5151	Polloch	1.60
5152	Balquhidder	4.35

Table A.2: 1996 mean measured concentrations of NO₂ from the UK Nitrogen Dioxide Monitoring Network. Units are $\mu\text{g m}^{-3}$.

Site number	Site Name	[SO ₂] $\mu\text{g m}^{-3}$
5002	Eskdalemuir	2.74
5003	Goonhilly	3.59
5004	Stoke Ferry	6.69
5007	Barcombe Mills	5.40
5008	Yarner Wood	3.92
5009	High Muffles	6.94
5010	Strathvaich Dam	1.78
5011	Glen Dye	2.26
5301	Brockhill	8.10
5302	Burham	11.38
5303	Caenby	8.37
5304	Camborne	4.13
5305	Camphill	4.29
5306	Cardington	11.39
5308	Corpach	2.62
5309	Cresselly	4.17
5310	Etton	9.66
5312	Husborne Crawley	9.60
5313	Little Horkesley	7.18
5314	Marshfield	14.98
5315	Ratcliffe	11.15
5316	Rockbourne	4.05
5317	Wakefield	10.72
5318	Waunfawr	3.18
5319	Fort Augustus	1.71

5320	Loch Leven	7.35
5321	Redesdale	3.06
5322	Hebden Bridge	7.53
5323	Preston Montford	7.05
5325	Pitlochry	2.75
5326	Bush	7.72
5327	Great Dun Fell	4.17
5328	Wharleycroft	4.38
5330	Cwmystwyth	4.28
5331	Rosemaund	5.56
5332	Forsinard	1.18
5333	Fairseat	8.67
5334	Bylchau	4.91
5335	Crai	4.07
5339	Appleacre	4.38
5340	Garranty	4.20
5343	Benniguinea	4.15

Table A.3: 1996 mean measured concentrations of SO₂ from the UK Rural Sulphur Dioxide Monitoring Network. Units are $\mu\text{g m}^{-3}$.

Site number	Site Name	NH ₄ ⁺ kg N ha ⁻¹ yr ⁻¹	NO ₃ ⁻ kg N ha ⁻¹ yr ⁻¹	SO ₄ ²⁻ kg S ha ⁻¹ yr ⁻¹
5002	Eskdalemuir	9.67	7.85	17.60
5003	Goonhilly	3.36	4.20	10.72
5004	Stoke Ferry	4.62	3.36	5.60
5006	Lough Navar	3.92	2.94	9.76
5007	Barcombe Mills	3.36	3.08	7.20
5008	Yarner Wood	6.44	6.02	12.00
5009	High Muffles	8.82	6.86	13.28
5010	Strathvaich Dam	1.54	2.66	9.12
5011	Glen Dye	5.32	6.16	10.40
5023	Preston Montford	4.76	2.94	5.60
5024	Flatford Mill	3.50	2.94	5.12
5103	River Mharcaidh	1.40	2.80	7.84
5106	Whiteadder	4.06	4.62	8.32
5107	Loch Dee	12.47	10.37	26.24
5109	Redesdale	4.76	4.06	7.20
5111	Bannisdale	12.33	7.85	19.84
5113	Cow Green Reservoir	8.54	6.58	16.16
5117	Thorganby	4.76	3.08	6.40
5118	Jenny Hurn	4.48	3.22	6.40
5119	Beddgelert	9.39	7.99	21.60
5120	Wardlow Hay Cop	8.82	6.44	14.88
5121	Bottesford	3.50	2.38	4.80
5123	Tycanol Wood	3.78	3.36	9.44
5124	Llyn Brianne	8.26	7.71	19.20
5127	Woburn	4.20	2.94	5.12
5129	Compton	6.30	3.36	6.88
5136	Driby	4.90	3.78	6.56
5140	Achanarras	1.96	2.94	7.04
5149	Hillsborough Forest	8.54	4.06	8.80
5150	Pumlumon	9.10	7.43	19.36
5151	Polloch	3.36	4.62	17.60
5152	Balquhidder	6.86	6.86	16.17

Table A.4: 1996 mean measured wet deposition of NH₄⁺, NO₃⁻ and SO₄²⁻ from the UK National Precipitation Composition Monitoring Network. Units are kg N (or S) ha⁻¹ year⁻¹.

Site Name	SO ₂ emission kt S (1996)	Stack height meter
Eggborough	70.7	198
Ferrybridge	61.7	198
Blythe	26.1	168
Drax	21.0	260
Ashington	15.2	114
Wilton	4.0	100
North Tees	3.0	50
Redcar	1.8	60
Seal Sands	1.1	49
Ferryhill	0.8	76
Teeside	0.7	100
Fiddlesferry	38.3	199
Ince	27.4	152
Stanlow	13.7	50
Eastham	4.7	50
Lostock	2.3	66
Ellesmere Port	1.9	88
Winnington	1.9	63
Whitehaven	0.7	140
Cottam	67.2	183
West Burton	62.4	183
Rugley	31.8	183
Ironbridge	14.8	204
Ratcliff-on-Soar	13.9	198
High Marnham	10.3	137
Willington	10.3	130
Drakelow	8.1	168
Sheffield	1.8	168
Stoke-on-Trent	1.1	50
Tilbury	18.6	79
Coryton	12.0	50
Killingholme	14.6	50
Scunthorpe	3.9	56
Shellhaven	2.5	50
Grimsby	2.3	41
Barton-upon-Humber	1.3	41
Didcot	22.2	198
Oxford	1.4	53
Kingsnorth	34.0	198
Fawley	12.0	198
Grain	2.8	240
Littlebrook	2.5	165

Richborough	1.5	127
Gravesend	1.5	122
Bristol	1.2	50
Aberthaw	27.1	152
Port Talbot	6.8	68
Milford Haven elf	5.6	50
Pembroke	5.3	183
Baglan Bay	4.3	117
Milford Haven gulf	3.3	117
Mold	1.2	41
Llanwern	1.7	41
Llandarcy	1.2	117
Longannet	34.5	152
Grangemouth	12.2	100
Cockenzie	10.3	171
Methil	2.9	96
Peterhead	1.8	100
Markinch	0.8	32
Ballylumford	20.1	122
Kilroot	7.1	200
Belfast West	4.6	73
Coolkeeragh	1.7	77
Maydown	0.6	32
Total	806.1	-

Table A.5: Location, intensity and height of the SO₂ point sources over the United Kingdom for 1996.

Appendix B

FRAME Versions

FRAME 1.0 : Great Britain

This version of the FRAME model is issued from (Singles *et al.*, 1998). That was the state of the model when this study started.

FRAME 1.1 : United Kingdom

This version corresponds to the extension of the domain of the model from Great Britain to the United Kingdom by including Northern Ireland.

FRAME 2.0 : British Isles

This version corresponds to the extension of the domain of the model from the United Kingdom to the British Isles by including the Republic of Ireland (Eire).

FRAME 3.0 : Parallelisation

FRAME 3.0 had been obtained by parallelising the serial code of FRAME 2.0 with High Performance Fortran.

FRAME 3.1 : Parallelisation and load-balance

The load-balance of FRAME 3.0 is improved by considering the length of the trajectories before distributing them to the processors.

FRAME 4.0 : Finite Volume method

FRAME 4.0 included a new diffusion scheme, the implicit Finite Volume method, in FRAME 3.1. This discretisation replaced the 4th order Runge-Kutta method.

FRAME 4.1 : Directional orographic rainfall

FRAME 4.1 was developed to incorporate directional orographic rainfall. However, this parameterisation was not kept in the following versions of the model.

FRAME 4.2 : Variable depth of the mixing layer

FRAME 4.2 considered a new parametrisation of the scavenging coefficients in version 4.0. A variable height of the mixing layer was used to calculate these scavenging coefficients.

FRAME 4.3 : Dry deposition velocities correction

FRAME 4.3 was similar to FRAME 4.2 with corrections of specified deposition velocities of the model.

FRAME 4.4 : HNO₃ dry deposition

This version assigned a dry deposition velocity of 30 mm s⁻¹ to HNO₃ instead of the value of 10 mm s⁻¹ used in FRAME 4.3.

FRAME 4.5 : NO_x emissions height

This version upgraded FRAME 4.4 by distributing the NO_x emissions throughout the lowest 100 m instead of 300 m.

FRAME 4.6 : SO₂ point sources

FRAME 4.6 modified FRAME 4.5 to inject SO₂ emissions from high-level point sources. This is the final version of the FRAME model used in Chapter 5.

Appendix C

List of Publications

Fournier N., Pais V. A., Sutton M. A., Weston K. J., Dragosits U., Tang S. Y. and Aherne J. (2002). Parallelisation and application of a multi-layer atmospheric transport model to quantify dispersion and deposition of ammonia over the British Isles. *Environmental Pollution*, **116(1)**, 95-107.

Sutton M. A., Tang S. Y., Dragosits U., Fournier N., Dore A. J., Smith R. I., Weston K. J. and Fowler D. (2001). A spatial analysis of atmospheric ammonia and ammonium in the UK. In *Optimizing Nitrogen Management in Food and Energy Production and Environmental Production : Proceedings of the 2nd International Nitrogen Conference on Science and Policy. TheScientificWorld 1 (S2)*, 275-286.

Parallelisation and application of a multi-layer atmospheric transport model to quantify dispersion and deposition of ammonia over the British Isles

N. Fournier^{a,b,*}, V.A. Pais^c, M.A. Sutton^b, K.J. Weston^a, U. Dragosits^{d,b}, S.Y. Tang^b, J. Aherne^e

^aDepartment of Meteorology, University of Edinburgh, Edinburgh EH9 3JZ, UK

^bCentre for Ecology and Hydrology, Edinburgh Research Station, EH26 0QB, UK

^cENEA — C. R. Frascati, PO Box 65, 00044 Frascati (Rome), Italy

^dDepartment of Geography, University of Edinburgh, Edinburgh EH8 9XP, UK

^eDepartment of Environmental Resource Management, University College Dublin, Ireland

Received 15 September 2000; accepted 8 April 2001

“Capsule”: *A parallel version of an atmospheric transport model (FRAME) is developed and applied to the British Isles for the first time.*

Abstract

An atmospheric transport model, FRAME (Fine Resolution AMmonia Exchange), has been used to model the spatial pattern of ammonia concentrations and deposition over the British Isles for the first time. The model uses a multi-layer approach with diffusion through 33 layers to describe vertical concentration profiles in the atmosphere explicitly. Together with the necessary description of atmospheric reactions with sulphur and oxidised nitrogen, this imposes a major computational requirement, with the model having a run-time of 8.5 days on a mid-range workstation. Improvement in the model run-time was sought by developing a parallel implementation coded in a data-parallel approach using High Performance Fortran. Running the code on a Cray T3E with 128 processors provided a speedup by a factor of 69. The code's portability, its validation with measurements and new maps of its application to the British Isles, are presented. Good agreement is found with measured NH₃ concentrations, while wet de-position is underestimated. In addition to model uncertainties, this may be due to an underestimation of the NH₃ emissions input data. © 2001 Elsevier Science Ltd. All rights reserved.

Keywords: Pollution dispersion model; Ammonia; Dry deposition; Parallelisation; HPF

1. Introduction

Ammonia is the main alkaline gas present in the atmosphere. It is emitted in gaseous form (NH₃), mainly from livestock and fertilised agricultural land. Once emitted, it reacts with atmospheric acids (e.g. H₂SO₄, HNO₃) to form aerosols containing ammonium sulphate and nitrate [e.g. (NH₄)₂SO₄, (NH₄)HSO₄, NH₄NO₃].

The deposition of these species can cause ecological changes through acidification and through increasing the nitrogen content of the soil (Sutton et al., 1994).

Gaseous ammonia is typically deposited close to the sources, whereas the ammonium ion has a smaller deposition velocity, and is hence transported over larger distances. The short atmospheric lifetime of NH₃ and the location of sources at ground level in the rural environment result in NH₃ concentrations with high spatial variability (RGAR, 1997). This makes it difficult to produce accurate maps of concentrations from observations alone, since it would be necessary to set up a very dense array of stations. To complement measurement based estimates, an atmospheric transport model is applied here to estimate concentrations and deposition. The model is called FRAME: Fine Resolution AMmonia Exchange (Singles, 1996; Singles et al., 1998).

* Corresponding author. Tel.: +44-131-650-8744; fax: +44-131-662-4269.

E-mail address: nicolas@met.ed.ac.uk (N. Fournier).

FRAME is a statistical Lagrangian model which considers a stratified column of air, traversing a grid over Great Britain, in a series of straight line trajectories. The first version was sequential (only one trajectory was processed at a time) and written in Fortran 77, with a run-time of 6 days on a Sun Ultra 10 workstation (Singles, 1996). Further development of the model led to an increase in the model's domain to also include Northern Ireland and Eire. However, as a consequence of this extension (British Isles), the run-time of the model increased (8.5 days). This long execution time was the main handicap to further development of descriptions of physical processes in the model. Therefore, it became necessary to optimise the code and to use more powerful computing facilities before further action could be undertaken. To achieve this, a new parallel version was developed, bearing in mind the need for flexibility in running the code on a range of parallel machines. This paper describes the development of the parallel model and its application to extending the model from Great Britain to cover the British Isles. The assessment includes the application of revised NH₃ emissions estimates for Great Britain and Northern Ireland (Dragosits et al., 1998), together with new figures for the Republic of Ireland (Van den Beuken, 1997). The model results are then compared with the first reliable NH₃ monitoring data for the United Kingdom (Sutton et al., 1998) and with NH₄⁺ wet deposition.

Previous works have described the parallelisation of atmospheric pollution transport models. Dabdub and Manohar (1997) parallelised an urban air quality model using a message-passing architecture. On a Cray T3D with 64 processors, the parallel version ran 22 times faster (speedup) than the sequential version on a Sun Sparc 20 workstation. Similarly, Martin et al. (1999) parallelised an atmospheric pollution transport model using a message-passing architecture. On a Cray T3D with 128 processors, they obtained a speedup of 20 compared with the sequential version on a Sun Sparc 10 workstation.

2. FRAME model

2.1. Model description

The main goal of FRAME is to assess the long-term annual mean NH₃ surface concentration and NH_x deposition over the British Isles. FRAME describes the main atmospheric processes (emission, diffusion, chemistry and deposition) taking place in a column of air moving along straight-line trajectories following specified wind directions. Vertical diffusion is treated explicitly using a multi-layer system with 33 layers of variable depth (ApSimon et al., 1994). The highest layer extends to 2500 m, and the layer thicknesses range from 1 m at

the bottom to 100 m at the top. Vertical mixing is described using K-theory eddy diffusivity, with the exchange of material between layers being determined by the equation:

$$\frac{\partial c}{\partial t} = \frac{\partial}{\partial z} \left(K_z \frac{\partial c}{\partial z} \right) \quad (1)$$

where c is the concentration of the chemical species under consideration and K_z is the vertical diffusivity. K_z depends on atmospheric stability (Pasquill, 1961; Golder, 1972) and height.

As each air column moves along its trajectory, chemical interactions between ammonia, sulphur dioxide and nitrogen oxides take place, and deposition to the ground occurs. Dry deposition is the direct absorption of the gases and aerosols at the ground (Sutton et al., 1995a). This is treated by assigning a deposition velocity (V_d) to each chemical species derived from a dry deposition model (Smith et al., 2000). In the case of NH₃, a different deposition velocity is assigned for arable, forest, grassland, moorland and urban areas. Values of V_d are calculated for each land category using a resistance model. This resistance model assumes that the transport of material between the atmosphere and the surface is described by three resistances in series, the aerodynamic resistance (R_a), the laminar boundary layer resistance (R_b) and a canopy resistance (R_c ; Singles et al., 1998).

$$V_d = (R_a + R_b + R_c)^{-1} \quad (2)$$

To describe land-dependent dry deposition, a specific value of R_c is assigned to each land category (Table 1), and these are combined with calculated values of R_a and R_b (Garland, 1977). The values of R_c are chosen to provide a description consistent with the literature on surface-atmosphere exchange of NH₃ with different surface types (Sutton et al. 1993, 1994; RGAR, 1997).

Wet deposition is the removal of chemical species from the atmosphere through precipitation, and is dependent on scavenging coefficients, concentration and rainfall rate. The two major mechanisms are in-cloud and below-cloud scavenging. These processes can be modelled using scavenging coefficients (Table 2), which describe the fraction of the airborne concentration removed per unit time. The amount of material removed in a time period (Δt) is given by

Table 1
Land-dependent values of the canopy resistance R_c used in the resistance model to calculate values of V_d for NH₃

Land category	Arable	Forest	Grassland	Moorland	Urban areas
R_c (s m ⁻¹)	1000	20	600	20	240

Table 2
Scavenging coefficients (λ) used by FRAME to calculate wet deposition, based on an annual rainfall of 1000 mm

Species	λ (s^{-1})
SO ₂	1.1×10^{-5}
SO ₄ ²⁻ all forms	4.0×10^{-5}
NH ₃	5.7×10^{-5}
NH ₄ ⁺ aerosol	4.0×10^{-5}
PAN	0.0
NO	0.0
NO ₂	0.0
NO ₃ ⁻ aerosol	4.0×10^{-5}
HNO ₃	5.7×10^{-5}

After ApSimon et al. (1994).

$$\Delta c = c(1 - e^{-\lambda \Delta t}) \quad (3)$$

where Δc is the decrease in concentration due to removal by precipitation, and λ is the scavenging coefficient. These coefficients (Table 2) are consistent with the scavenging ratios used in the EMEP model (Tarrason and Schaug, 1999).

High altitude areas can have greater ion concentration in precipitation than low altitude sites, due to orographic clouds forming as the air mass flows over the hills. Hence, a “seeder-feeder” process is included in the model to represent this altitude enhancement effect (Singles et al., 1998).

When each trajectory has been completed, the total amounts of material imported, exported, emitted and deposited per unit area are calculated. Annual mean concentration and deposition maps are determined by combining the results from all wind directions, suitably weighted by the frequency with which each wind direction occurs.

3. Modifications to FRAME

3.1. Model's domain and input data

The FRAME model uses a database of NH₃ emissions with a 5×5 km grid-square resolution as input. In the work of Singles et al. (1998), the inventory of Sutton et al. (1995b) for Great Britain was applied. Further work by Dragosits et al. (1998) has updated this inventory and also included Northern Ireland. The inventory of Dragosits et al. (1998) includes a more realistic spatial description of the NH₃ sources at a 5 km level, as well as changes to the emission estimates per source unit, giving for example, less emissions from cattle and more from pigs. The total United Kingdom NH₃ emissions for 1996 are 283 kilotonnes N year⁻¹, combining 229 kilotonnes N year⁻¹ of agricultural NH₃ emissions and 54 kilotonnes N year⁻¹ of non-agricultural NH₃ emissions (although this includes 11 kilotonnes N

year⁻¹ from agriculture related sources; Sutton et al., 2000). In addition to the United Kingdom inventory, estimates for Eire (Van den Beuken, 1997) have been included for the first time. The total Eire NH₃ emissions for 1996 are 96 kilotonnes N year⁻¹ but, at the moment, this inventory does not include non-agricultural sources. However, non-agricultural sources contribute to 10% or less of the Eire NH₃ emissions, hence it should not detract from the validity of the results.

The initial chemical composition of the air columns is provided by import from other areas of Europe. The transboundary import of foreign material has been modelled by using a set of concentration profiles for the edge of the British Isles domain, which are used to initialise trajectories. These profiles have been created by running the TERN model (Transport over Europe of Reduced Nitrogen) along a series of trajectories across Europe, which terminate at the edge of the model domain (ApSimon et al., 1994). Ammonia emission is introduced into the air columns at 1 m above the surface since emissions occur near ground level. Sulphur dioxide and nitrogen oxides are introduced over a height range of 0–300 m to simulate both ground level and elevated sources following the approach of ApSimon et al. (1994). The chemical composition then changes as air columns are advected across the domain.

The horizontal advection speed of the model determines the length of time the air column takes to cross an emission area, and thus how much NH₃ is emitted into the air column. The wind data contain wind frequency estimates for each wind direction, adapted from Jones (1981) following Singles (1996). These wind data are long-term average data comprising a representative rose for the United Kingdom.

Calculations of dry deposition are land-cover specific defined using a British Isles land-cover database (OSI, 1993; Smith et al., 2000). This divides the land into five categories: arable, forest, grassland, moorland and urban areas (RGAR, 1997).

Finally, long-term annual mean rainfall data are used to calculate the flux of material wet deposited over the British Isles (R.I. Smith personal communication; Aherne and Farrel, 2000).

3.2. Parallelisation of FRAME

3.2.1. Optimisation

The model uses trajectories in relation to specified wind directions. Twenty four wind directions, at 15° intervals, from 0 to 360° are considered and the results are combined statistically. Trajectories start at four different times of the day (00:00 h, 06:00 h, 12:00 h, 18:00 h). The first step towards parallelisation was to simplify the structure of the code by gathering these three loops (time, angle, trajectory) in one main loop. Secondly, Fortran 90 features were included to permit dynamic

storage allocation, the use of new intrinsic functions and to simplify array operations.

Following these changes, the code of FRAME was rearranged in three well-defined blocks: *start* (setup and definition of the variables for all the trajectories and reading all the boundary data files); *kernel* (calculations along the trajectories and storing of the results in internal variables); and *exit* (collection of the results, computation of the statistics and outputting to files). A simplified schematic of the structure of the FRAME optimised sequential code is presented in Fig. 1(A). The purpose of these changes was to simplify the parallelisation by gathering the calculations along each trajectory in one block (*kernel*) and by introducing Fortran 90.

3.2.2. Parallelisation

In FRAME, the same computations (emission, diffusion, chemistry and deposition) are executed in all the trajectories. A notable aspect is that the code computes the variables' values for one grid-square from the grid-square executed directly beforehand and, due to the statistical approach of the model, there is no memory in any calculation concerning details of grid-squares generated in a previous trajectory. This has the consequence that each trajectory is independent. Therefore, by taking advantage of the fact that each trajectory is independent, a parallel version of the code is implemented by distributing the different trajectories over multiple processors. The revised code structure [Fig. 1(B)] is therefore:

- the *start* block computes variables and parameters as before, the common variables are copied onto all the available processors;

- the *kernel* is replicated onto each processor, which computes only the owned trajectories without any interaction with the other processors;
- the *exit* block gathers the results from all the processors and performs the last operations as in the sequential code.

3.2.3. High Performance Fortran

The parallelisation of the code has been achieved via a data-parallel approach using High Performance Fortran (HPF). HPF is the standard language developed for data-parallel, which assigns parts of the data arrays (in our case, the trajectories) to different processors. Fortran 90 extensions assist its implementation on parallel computers, as well as directives for specifying how data are to be distributed over the processor memories in a multiprocessor architecture (Merlin and Hey, 1995). The code is run on a single processor, using others when required.

In FRAME, the parallelisation was implemented by distributing the independent trajectories over the available processors. Hence, there is no communication between the processors and the same computation is executed independently by all the processors. Therefore, a data-parallel approach seemed adequate to exploit this concurrency that derives from the application of the same calculation to multiple independent trajectories. HPF was chosen because it required only a few additional parallel constructs and data placement directives to Fortran 90. In contrast, a message-passing architecture (as MPI: Message Passing Interface; Pacheco, 1996) would have implied more re-coding. Indeed, message-passing programming is referred to as multiple program multiple data (MPMD) model to distinguish it

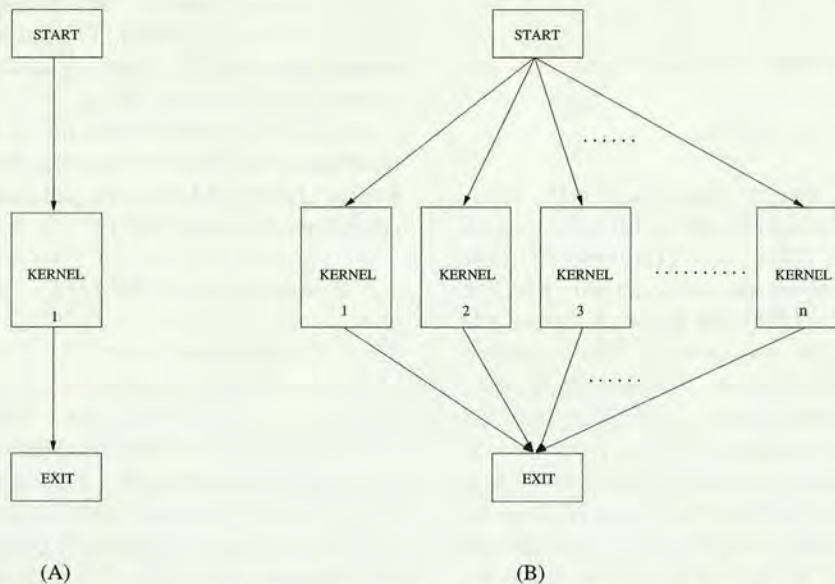


Fig. 1. Schematic flow chart of the optimised FRAME sequential code (A) and of the FRAME parallel code (B). In the latter, the kernel is replicated onto all the n processors.

from the SPMD (single program multiple data) model, hence providing many specific functions to allow local, global or asynchronous communications between processors. The parallel code was written to be independent of the number of available processors allowing it be run on different machines.

3.2.4. Computing platforms

Table 3 shows the target machines for simulation of the FRAME model. The Cray T3E-900 of the Edinburgh Parallel Computing Centre (EPCC) was used as the main target machine for the parallel version of FRAME, due to its high computing capability and the possibility of accessing it through the EC-TRACS Programme at EPCC (European Community-Training and Research on Advanced Computing Systems). This system has 344 Alpha processors (450 MHz), each having a peak performance of 900 MFlops. The majority of the processors are configured with 128 MB, or above, of memory. The processors are divided in two pools: 216 processors and 128 processors. Due to administrative reasons, FRAME was run on the second pool of processors.

Moreover, the parallel version of FRAME was run on the EPCC's Sun HPC 3500. This is an 8–400 MHz UltraSPARC II processor machine with 8 GB of main memory. A 4–400 MHz UltraSPARC II processor Sun HPC 450, with 1 GB of main memory, was also available at CEH (Centre for Ecology and Hydrology). Finally, the sequential code version of FRAME was executed on a 1-processor Sun Ultra 10 workstation with 640 MB of main memory.

3.2.5. Load-balance

An important issue when running an application with a parallel machine is to be sure that all processors do roughly the same amount of work (i.e. the “load-balance”), since a parallel run is not finished until every processor has stopped. The parameter used here to measure the load-imbalance (Δ) is:

$$\Delta(\%) = \frac{(\text{CPU}t_{\max} - \text{CPU}t_{\min})}{\frac{1}{2}(\text{CPU}t_{\max} + \text{CPU}t_{\min})} \quad (4)$$

where $\text{CPU}t_{\max}$ and $\text{CPU}t_{\min}$ are the maximum and the minimum CPU (Central Processing Unit) time consumed by the processors, respectively.

An initial parallel version of FRAME distributed all the trajectories and the associated parameters cyclically, heedless of any kind of ordering. However, this could cause load-imbalance. As a measure to improve the load-balance, a second version of the parallel FRAME was developed to take into account the length of the trajectories and sort them before distribution. Along a particular trajectory the execution time is roughly proportional to the number of land squares (over sea, there is no calculation). Thus, to improve the load-balance, the trajectories were assigned over the processors using their length as an ordering parameter. The longer ones are processed first and the shorter last to avoid large gaps in the execution time of the processors' last task.

4. Results

4.1. Performance of the parallel model

To test the performance and the portability of the parallel version of FRAME, typical simulations were performed on the different target machines. The results compared well with those from the sequential code. A regression analysis of NH_3 surface concentrations showed that the parallel version estimates the concentrations without scatter and with a near perfect 1:1 relationship ($y = 0.9978x - 0.0163$; $r^2 = 0.999$). The cause of this slight difference between the parallel and sequential versions is the variables' type used in the calculations; single precision on the workstation, but double precision on the parallel machines.

The execution times of the FRAME model, for a typical simulation over the British Isles, are presented in Table 3. The parallel version of FRAME British Isles, simulating on employing the 128-processor pool of the Cray T3E, ran in only 189 min; 64 times faster than a sequential Sun Ultra 10 workstation version. However, as suspected, the cyclic decomposition of the trajectories over the processors created a load-imbalance. Indeed, the longer and the shorter processors' execution-times were 187 and 138 min, respectively. Thus, it caused a load-imbalance of 30%.

The parallel version of FRAME, with trajectories sorted by length (Table 3), decreased the load-imbalance from 30 to 19% and the execution time to 177 min. Fig. 2 represents this load-imbalance via the

Table 3
Performance of FRAME on various machines

Machine	Processing node	Number of processors	Version	Run-time (min)
Sun	330 MHz Ultra 10	1	Sequential	12 180
Sun	400 MHz HPC 450	4	Parallel	5640
Sun	400 MHz HPC 3500	8	Parallel	2280
Cray T3E	450 MHz Alpha	128	Parallel	177

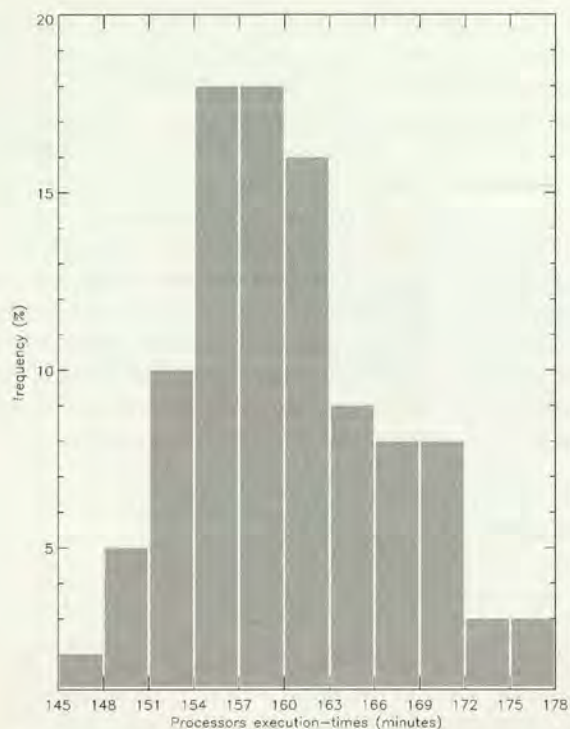


Fig. 2. Execution-times frequency of the 128 processors in running the FRAME parallel code on the Cray T3E.

frequency of the Cray T3E processors' execution-times. These varied between 146 and 176 min and 36% of the processors' execution-times were between 154 and 160 min. Hence, finally, a speedup of 69 was obtained.

To assess its portability, this optimised version was also run on the 8-processor and 4-processor Sun machines, giving speedup of a factor of five and two, respectively.

4.2. Application of the parallel model to the British Isles and comparison with measurements

Example maps of the application of the model to the British Isles are presented. Firstly, Fig. 3 represents the total annual 1996 NH_3 emissions on a 5×5 km grid resolution used as input to the model (Van den Beuken, 1997; Dragosits et al., 1998). A lower spatial variability in NH_3 emissions for Eire may partly be attributed to approximations in the inventory leading to artificial smoothing of emissions from pig and poultry farms.

Fig. 4 shows the distribution of NH_3 surface air concentrations. The highest air concentrations appear in a broad band along the borders of England and Wales and in the north-east of Northern Ireland. This corresponds mainly to livestock, cattle and sheep farming in these areas, as well as more local high emission areas in north-west England. A further high emission area in eastern England (East Anglia) is associated with large poultry and pig farming. Moreover, high air concentrations in

the south and north-east of Eire are caused by both significant emissions and low deposition velocity associated with grassland. One of the most significant features is the model estimation of extremely small air concentrations over the whole of the Scottish Highlands, reflecting an extremely low emission density in this area.

The performance of the model predictions for ground level concentrations is illustrated for locations in Great Britain and Northern Ireland that are included in the United Kingdom National Ammonia Monitoring Network (Sutton et al., 1998). Fig. 5 shows a map of the location of the monitoring sites across United Kingdom used in the comparison with model calculations. Overall, the model shows a good agreement with the 1995–1997 measurements (Fig. 6) reproducing the broad difference between the high and low concentration sites. The substantial amount of scatter illustrates the importance of having a large number of sites for comparison, and is almost certainly due to the local variability in NH_3 concentrations that cannot be resolved by the 5 km resolution model (Dragosits et al., 2001, submitted for publication).

Fig. 7 shows the annual flux of modelled NH_3 dry deposition to British Isles. Similar to the map of air concentrations, the areas with large deposition rates are generally associated with areas of high emission. These areas include south-west England, the Wales-England border, north England and north-east of Northern Ireland. Otherwise, the largest deposition occurs in areas where there are both high emissions and large areas of semi-natural ecosystems, such as forest and moorland, generally in the west. This is due to large values of V_d calculated for these land cover types by the model. Consequently, in areas where emission is large, but the modelled deposition velocity is small, such as in East Anglia, regional dry deposition will be smaller than in areas with similar emissions in the west, but the air concentrations will be greater. It should be noted that the deposition values shown in Fig. 7 are grid-square averages. Since deposition rates are substantially smaller for agricultural land than for forest and semi-natural vegetation, the grid averages shown here are much smaller than received by these ecosystems. Hence, for critical loads comparisons, receptor maps for specific ecosystems should be used (Singles et al., 1998).

The modelled distribution of NH_4^+ in wet deposition is shown in Fig. 8. This shows the highest wet deposition in hill areas of central northern England and Wales. Peak wet deposition values correspond to areas of large precipitation occurring nearby regions of intensive agricultural activity. Comparison of the 1996 modelled wet deposition with measurements (RGAR, 1997) shows a reasonable correlation, but with the model giving smaller values (see Fig. 9).

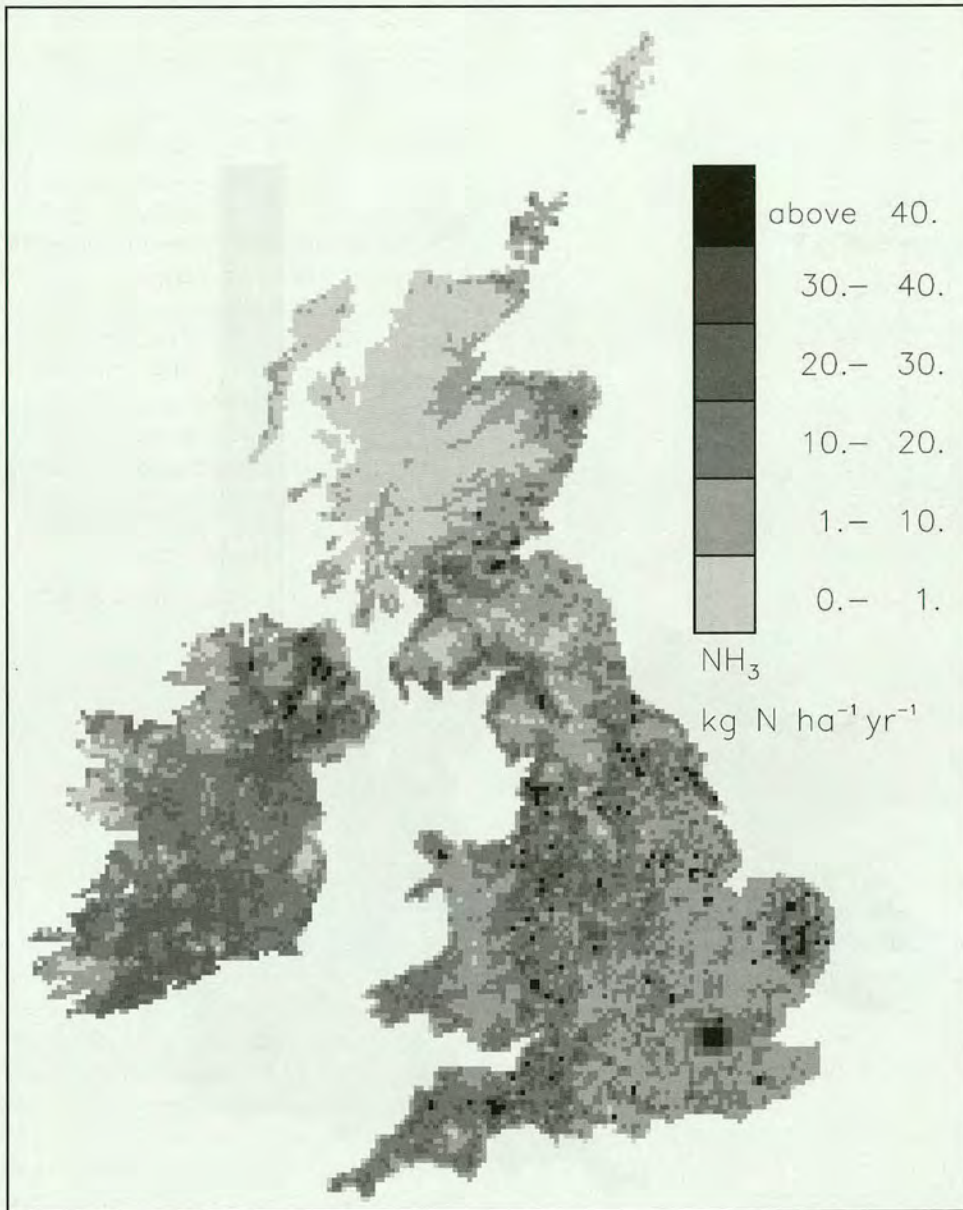


Fig. 3. 1996 ammonia emissions for British Isles mapped on a 5×5 km grid resolution. Units are $\text{kg N ha}^{-1} \text{year}^{-1}$ (Van den Beuken, 1997; Dragosits et al., 1998).

5. Discussion

The HPF parallel version of the FRAME model gave a portable code with a significant speedup of 69 when applied on a Cray T3E. Indeed, previous studies showed speedups of 20 in Martin et al. (1999) and 22 in Dabdub and Manohar (1997). Some parallelisation's performances are limited by the communication between processors (Dabdub and Manohar, 1997). As the number of processors increases, the communications increase and outweigh the advantages of distributing the code on a large number of processors. In the parallel implementation of FRAME, there is no such limitation as no

communication occurs between processors. Therefore, as the number of processors increases, the speedup increases. Hence, it would be of benefit to run the code on a parallel machine where more processors are available.

The load-balance could be improved further by considering a more physical parameter to order the trajectories, for example, the number of land squares with significant emission of ammonia. However, this task would significantly increase the execution time of the starting procedure. Therefore, at the moment, the length of the trajectory represents a good compromise for an ordering parameter.

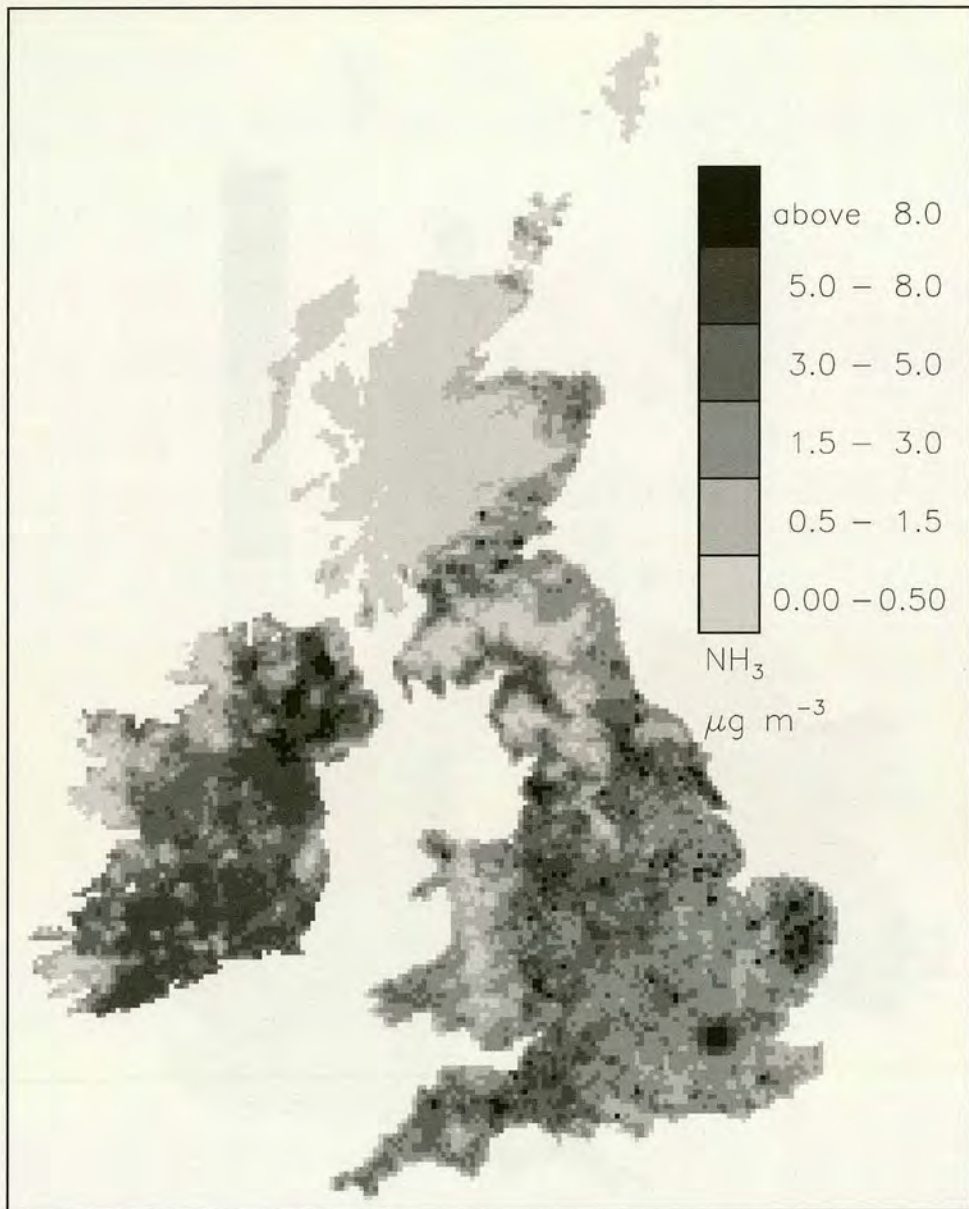


Fig. 4. Modelled surface concentrations (1–2 m) of NH_3 for the British Isles on a 5×5 km grid. Data represent an annual average.

The extension of the model from Great Britain to the British Isles was motivated in the first instance by the desire to include Northern Ireland and cover the whole of the United Kingdom. It quickly became apparent, however, that exchange over the Republic of Ireland should also be included as this was wholly within the model domain, and results for Northern Ireland would otherwise be inaccurate. Given the time requirements of the model on a single workstation, particularly for the British Isles version, it is clear that the speed-up achieved with the parallel code is an important foundation for further advances to be included in the model. These include, for example, consideration of seasonal temporal dynamics in NH_3 bi-directional exchange and wet

deposition, which would be impractical to address with the original version of the model.

In an earlier study, the FRAME model was applied to make a first comparison with monitored NH_3 concentrations in Great Britain (Singles et al., 1998). Unfortunately, at that time the only data available were from a network of passive diffusion samplers, which contained substantial measurements uncertainties [this network included the monitoring sites operational in the period 1987–1988, and these were the data that were used to compare with the model results. One note of caution should be sounded when using results from diffusion tubes. Anderson (1991) reported that the samplers were thought to give a value which is greater than

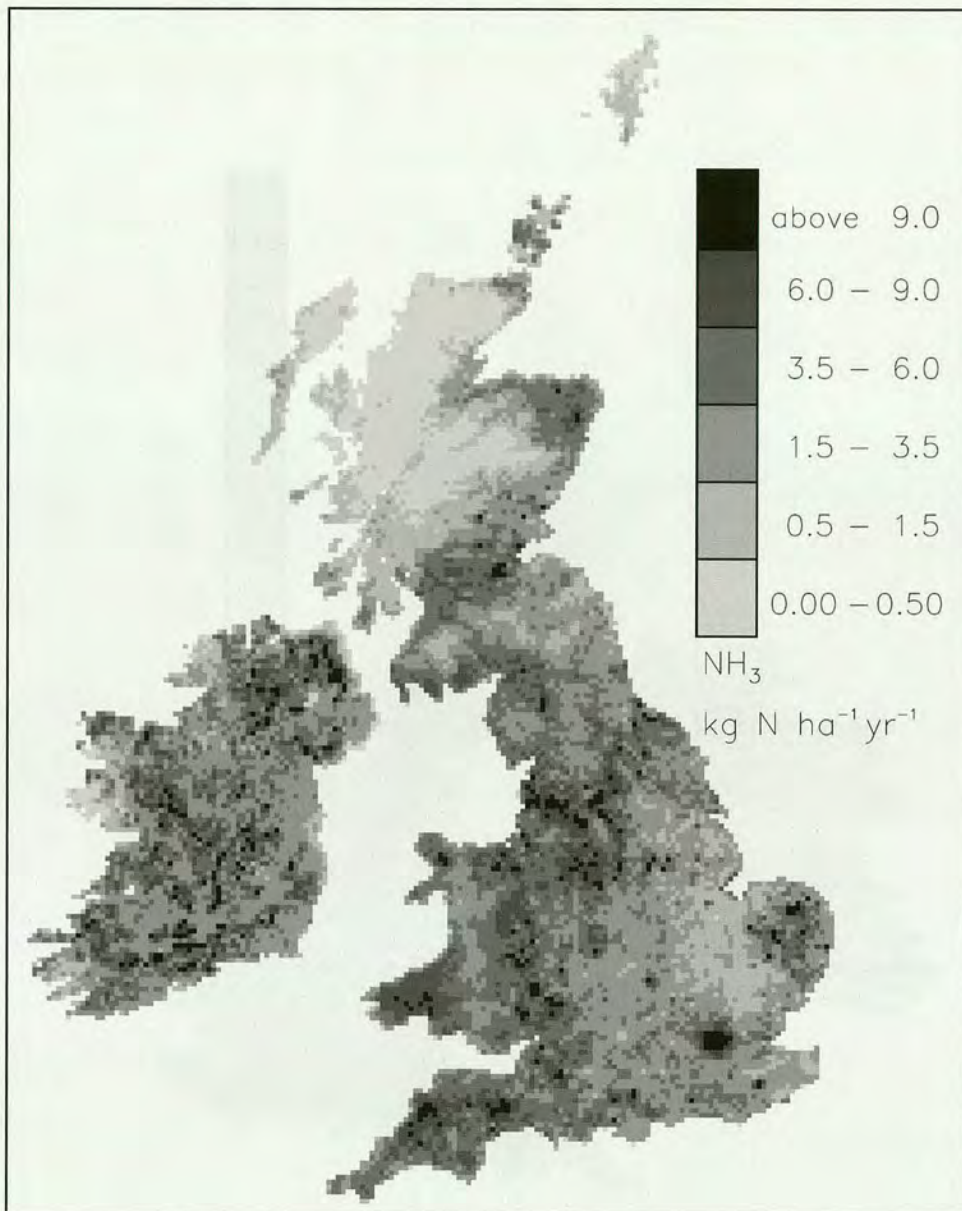


Fig. 5. Grid average modelled annual flux of NH_3 dry deposition to the British Isles at a 5×5 km resolution.

the actual air concentrations, and a scaling factor of 0.45 has been applied to the diffusion tube results (Singles et al., 1998)]. Since that time, reliable NH_3 measurement data have become available from a new national network (Sutton et al., 1998), while the NH_3 emission estimates have been revised. The new data allow the model performance to be properly assessed for the first time. The modelled concentrations range from $0.1 \mu\text{g m}^{-3}$ in the highlands of Scotland through to $10 \mu\text{g m}^{-3}$, as shown in the measurements. The large scatter in the relationship illustrates the spatial variability in NH_3 concentrations. While the broad spatial features are reproduced in the model, the comparison highlights that the actual NH_3 concentration field is even more variable than shown in Fig. 4.

It must be recognised that the accuracy of the emissions data are critical to the performance of the model, and for the United Kingdom, this was made possible using the new distribution model of Dragosits et al. (1998). By contrast, further work to improve the distribution of NH_3 emissions for the Republic of Ireland must be considered a priority. For example, in the current distribution for the Republic of Ireland, due to data restrictions, pig and poultry NH_3 emissions are modelled at less than 5 km resolution. The effect of this is to provide apparently smoother NH_3 concentrations in the Irish Republic.

The FRAME model was primarily developed to address the spatial distribution of NH_3 air concentrations and dry deposition. Notwithstanding this, it is still

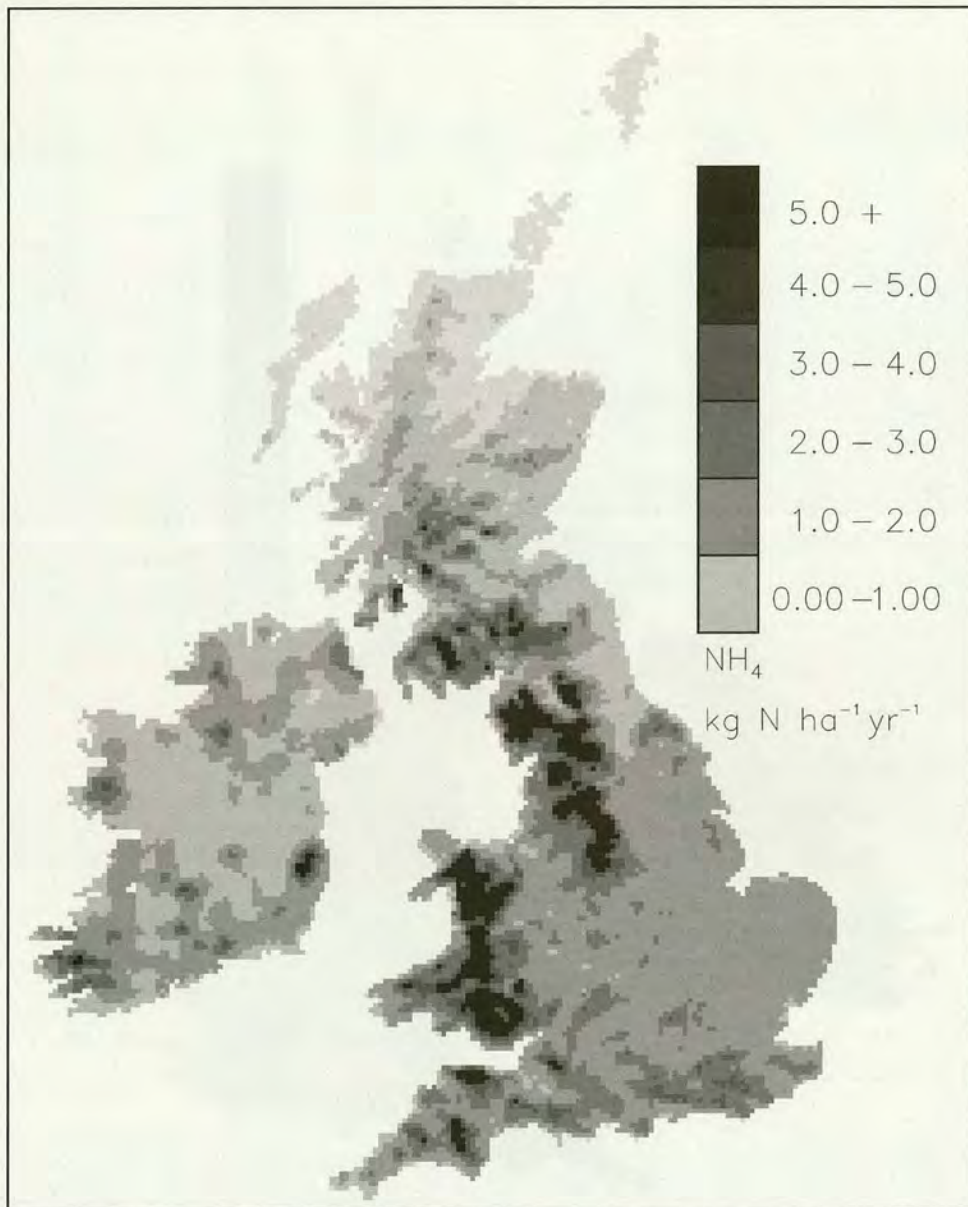


Fig. 6. Grid average modelled annual flux of NH_4^+ wet deposition to the British Isles at a 5×5 km resolution.

relevant to address the model performance for wet deposition of NH_4^+ . The current underestimation for NH_4^+ indicates that the model underestimates total reduced nitrogen deposition, since the dry deposition estimate is broadly consistent with estimates derived from measurements (Fowler et al., 1998). In this respect, the results of FRAME are similar to those of other models for the United Kingdom, which all underestimate total deposition (RGAR, 1997). For example, Metcalfe et al. (1998) report wet deposition to be only slightly underestimated, but substantially underestimate NH_3 concentrations and dry deposition. In each case, to match the total of wet and dry deposition would require a larger NH_3 emission or less export from the model domain. This points to the need for independent

measurement based approaches to assess ammonia emissions and export at the national scale. However, there is some uncertainty concerning the measurements of NH_4^+ concentrations in rain. NH_4^+ is a difficult component to measure and it is the ion that shows least agreement in measurements between bulk and wet-only collectors. Indeed, bulk collectors are not covered with a lid during dry periods, hence, some dry deposition is sampled in addition to the wet deposition.

Moreover, bird droppings and biological activities contribute to the measured NH_4^+ concentration. The magnitude of this change is spatially variable and still not fully assessed. Some studies (Buijsman and Erisman, 1988; Asman and van Jaarsveld, 1990) applied a correction factor to take into account this overestimation

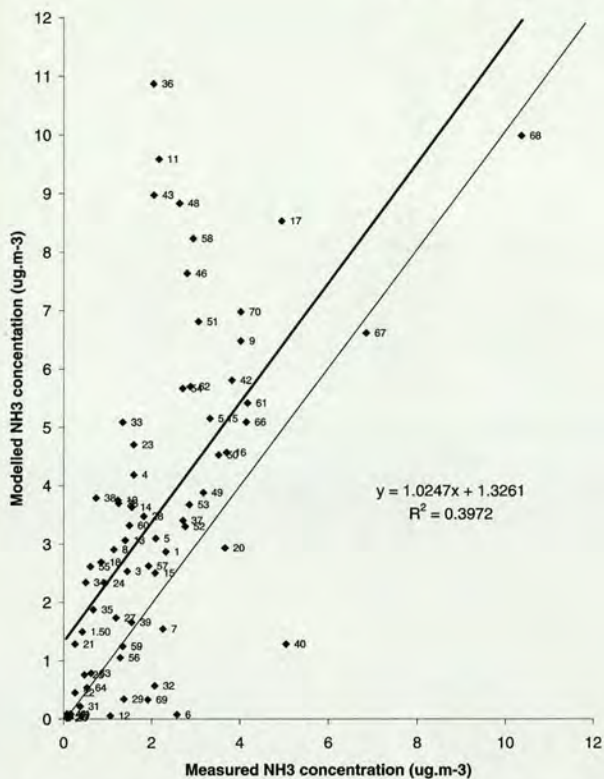


Fig. 7. Correlation plot of modelled NH_3 surface concentration values against measured values for 1996. The central dotted line is a one to one agreement and the solid line is the best fit line produced by a regression analysis.

of the measurements. In our study, we chose to avoid using such a factor because it looks as though new plastic funnels (in contrast with bulk rain gauges) has very small NH_3 dry deposition, thus the correction is probably negligible (J.N. Cape, personal communication).

6. Conclusions

An efficient parallel implementation of the FRAME model has been presented. Its portability allows the code to run on a number of parallel machines without modifications. The speedup of 69 obtained with the Cray T3E shows that the data-parallel approach with an extrinsic “local” definition for the kernel is well suited to the present model. A speedup of this magnitude will allow a more realistic description of physical processes, such as the incorporation of a bi-directional exchange of ammonia or a spatial variation in cloud-base height, to be included in the model. This will reduce modelling errors (errors resulting from inappropriate assumptions or approximations) and will lead to a deeper understanding of the effects of ammonia deposition. Moreover, the large memory of multiprocessor architectures will allow the use of more grid points, thus reducing the

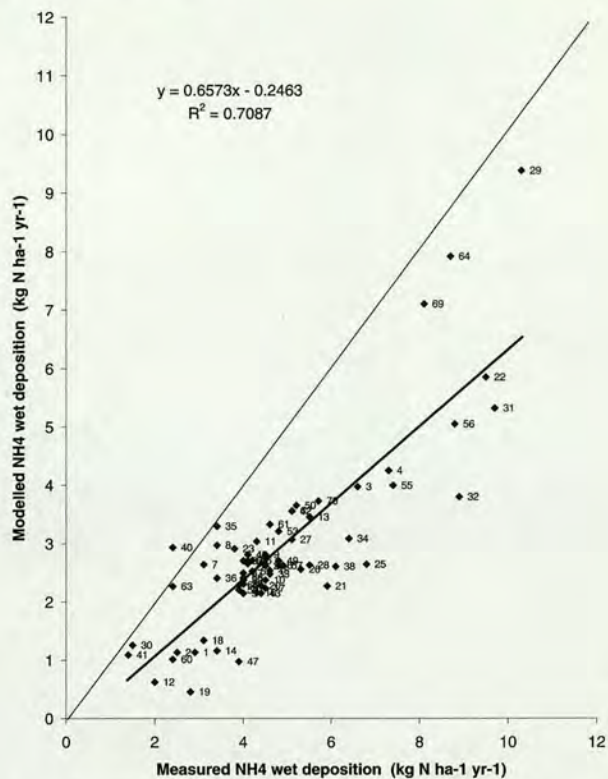


Fig. 8. Correlation plot of modelled NH_4^+ wet deposition values against measured values for 1996. The central dotted line is a one to one agreement and the solid line is the best fit line produced by a regression analysis.

errors related to grid size or resulting from numerical methods, or the move to greater domains.

The parallel model has been applied here to describe the 5 km distribution of NH_3 concentrations, net dry deposition and wet deposition over the British Isles for the first time. Using new data on the NH_3 emission distribution, the model provides a good comparison with NH_3 concentrations measured in the United Kingdom, but underestimates wet deposition. Progress in improving the estimates would benefit from independent measurement based estimates of regional NH_3 emission and export.

Acknowledgements

Financial support for this work is gratefully acknowledged from the UK Natural Environmental Research Council (NERC) and the Department of the Environment, Transport and the Regions, and the Ministry for Agriculture Fisheries and Food. The authors would like to acknowledge the support of the European Commission through TMR grant number ERBFMGECT950051 (the TRACS programme at EPCC), contract ENV4-CT98-0722 (GRAMI-NAE) and the EPCC staff for advice about HPF and the Cray T3E.



Fig. 9. The location of the monitoring sites across United Kingdom.

References

- Aherne, J., Farrell, E.P. (Eds.), 2000. Determination and Mapping of Critical Loads for Sulphur and Nitrogen and Critical Levels for Ozone in Ireland: Final Report. Environmental Protection Agency, Dublin.
- Anderson, H., 1991. Ammonia monitoring — passive diffusion tube sampling. In: Nitrogen and Phosphorus in Soil and Air Project Abstracts of the Danish NPo Research Programme. Ministry of the Environment Protection, Kobenhavn, Denmark.
- ApSimon, H.M., Barker, B.M., Kayin, S., 1994. Modelling studies of the atmospheric release and transport of ammonia — applications of the TERN model to an EMEP site in eastern England in anticyclonic episodes. *Atmospheric Environment* 28, 665–678.
- Asman, W.A.H., van Jaarsveld, J.A., 1990. A Variable Resolution Statistical Transport Model Applied for Ammonia and ammonium (Report 228471007). National Institute of Public Health and Environmental Protection, Bilthoven, The Netherlands.
- Buijsman, E., Erismann, J.-W., 1988. Wet deposition of ammonium in Europe. *Journal of Atmospheric Chemistry* 6, 265–280.
- Dabdub, D., Manohar, R., 1997. Performance and portability of an air quality model. *Parallel Computing* 23, 2187–2200.

- Dragosits, U., Sutton, M.A., Place, C.J., Bayley, A., 1998. Modelling the spatial distribution of ammonia emissions in the United Kingdom. *Environmental Pollution* 102 (S1), 195–203.
- Dragosits, U., Theobald, M.R., Place, C.J., Lord, E., Webb, J., Hill, J., Apsimon, H.M., Sutton, M.A., 2001. Ammonia emission, deposition and impact assessment of the field scale: a case study of sub-grid spatial variability. *Environmental Pollution* (accepted for publication).
- Fowler, D., Sutton, M.A., Smith, R.I., Pitcairn, C.E.R., Coyle, M., Campbell, G., Stedman, J., 1998. Regional mass budgets of oxidized and reduced nitrogen and their relative contribution to the N inputs of sensitive ecosystems (Nitrogen Conference special issue). *Environmental Pollution* 102 (S1), 337–342.
- Garland, J.A., 1977. The dry deposition of sulphur dioxide to land and water surfaces. *Proc. Roy. Soc. London A* 345, 245–268.
- Golder, D., 1972. Relation amongst stability parameters in the surface layer. *Boundary Layer Meteorology* 3, 47–58.
- Jones, J.A., 1981. The Estimation of Long-Range Dispersion and Deposition of Continuous Releases of Radionuclides to Atmosphere. National Radiological Protection Board NRPB-R123, Oxfordshire.
- Martin, M., Oberson, O., Chopard, B., Mueller, F., Clappier, A., 1999. Atmospheric pollution transport: the parallelization of a transport and chemistry code. *Atmospheric Environment* 33, 1853–1860.
- Merlin, J., Hey, A., 1995. An introduction to high performance fortran. *Scientific Programming* 4, 88–113.
- Metcalfe, S.E., Whyatt, J.D., Derwent, R.G., 1998. Multi-pollutant modelling and the critical loads approach for nitrogen (Ammonia special issue). *Atmospheric Environment* 32 (3), 401–408.
- OSI, 1993. 1:100,000 CORINE Land Cover Project (Ireland). Ordnance Survey of Ireland, Phoenix Park, Dublin.
- Pacheco, P., 1996. *Parallel Programming with MPI*. Morgan Kaufmann Publishers Inc., San Francisco.
- Pasquill, F., 1961. The estimation of the dispersion of windborne material. *Meteorological Magazine* 90, 33–49.
- RGAR, 1997. Acid Deposition in the United Kingdom 1992–1994 (Fourth Report of the United Kingdom Review Group on Acid Rain). Department of the Environment, London.
- Singles, R.J., 1996. Fine resolution modelling of ammonia dry deposition over Great Britain. PhD thesis, University of Edinburgh.
- Singles, R.J., Sutton, M.A., Weston, K.J., 1998. A multi-layer model to describe the atmospheric transport and deposition of ammonia in Great Britain (Ammonia special issue). *Atmospheric Environment* 32 (3), 393–399.
- Smith, R.I., Fowler, D., Sutton, M.A., Flechard, C., Coyle, M., 2000. Regional estimation of pollutant gas dry deposition in the UK: model description, sensitivity analyses and outputs. *Atmospheric Environment* 34, 3757–3777.
- Sutton, M.A., Asman, W.A.H., Schjoerring, J.K., 1994. Dry deposition of reduced nitrogen. *Tellus* 46B, 255–273.
- Sutton, M.A., Schjoerring, J.K., Wyers, G.P., 1995a. Plant-atmosphere exchange of ammonia. *Phil. Trans. Roy. Soc., London, Series* 351, 261–278.
- Sutton, M.A., Dragosits, U., Tang, Y.S., Fowler, D., 2000. Ammonia emissions from non-agricultural sources in the UK. *Atmospheric Environment* 34 (6), 855–869.
- Sutton, M.A., Place, C.J., Eager, M., Fowler, D., Smith, R.I., 1995b. Assessment of the magnitude of ammonia emissions in the United Kingdom. *Atmospheric Environment* 29 (3), 1393–1413.
- Sutton, M.A., Fowler, D., Smith, R.I., Eager, M., Place, C.J., Asman, W.A.H., 1993. Modelling the net exchange of reduced nitrogen. In: Slanina, J., Angeletti, G., Beilke, S. (Eds.), *General Assessment of Biogenic Emissions and Deposition of Nitrogen Compounds, Sulphur Compounds and Oxidants In Europe*. Proceeding of the Joint CEC/BIATEX Workshop, Aveiro (May 1993) (Air Pollut. Res. Report 47). CEC, Brussels, pp. 117–131.
- Sutton, M.A., Tang, Y.S., Miners, B.P., Coyle, M., Smith, R.I., Fowler, D., 1998. Spatial and Temporal Patterns of Ammonia Concentration in the UK. Results of the National Ammonia Monitoring Network (Report). ITE Edinburgh.
- Tarrason, L., Schaugh, J., 1999. Transboundary Acid Deposition in Europe. [EMEP Report 1/99 (July 1999)]. EMEP-CCC/MS-C-W. Norwegian Meteorological Institute, Blindern.
- Van den Beuken, R., 1997. Mapping Emission and Dry Deposition of Ammonia for Ireland (Forest Ecosystem Research Group Report 24). Department of Environmental Resource Management, University College Dublin, Dublin.

A Spatial Analysis of Atmospheric Ammonia and Ammonium in the U.K.

M.A. Sutton^{1,*}, Y.S. Tang¹, U. Dragosits^{1,2}, N. Fournier^{1,3}, A.J. Dore¹, R.I. Smith¹, K.J. Weston³, and D. Fowler¹

¹Centre for Ecology and Hydrology, Edinburgh Research Station, Bush Estate, Penicuik, EH26 0QB, U.K.; ²University of Edinburgh, Department of Geography; ³University of Edinburgh, Department of Meteorology

As measures are implemented internationally to reduce SO₂ and NO_x emissions, attention is falling on the contribution of NH₃ emissions to acidification, nitrogen eutrophication, and aerosol formation. In the U.K., a monitoring network has been established to measure the spatial distribution and long-term trends in atmospheric gaseous NH₃ and aerosol NH₄⁺. At the same time, an atmospheric chemistry and transport model, FRAME, has been developed with a focus on reduced nitrogen (NH_x). The monitoring data are important to evaluate the model, while the model is essential for a more detailed spatial assessment.

The national network is established with over 80 sampling locations. Measurements of NH₃ and NH₄⁺ (at up to 50 sites) have been made using a new low-cost denuder-filterpack system. Additionally, improved passive sampling methods for NH₃ have been applied to explore local variability. The measurements confirm the high spatial variability of NH₃ (annual means 0.06 to 11 μg NH₃ m⁻³), consistent with its nature as a primary pollutant emitted from ground-level sources, while NH₄⁺, being a slowly formed secondary product, shows much less spatial variability (0.14 to 2.4 μg NH₄⁺ m⁻³). These features are reproduced in the FRAME model, which provides estimates at a 5-km level. Analysis of the underlying NH₃ emission inventory shows that sheep emissions may have been underestimated and nonagricultural sources over-

estimated relative to emissions from cattle. The combination of model and measurements is applied to estimate spatial patterns of dry deposition to different vegetation types. The combined approach provides the basis to assess NH_x responses across the U.K. to international emission controls.

KEY WORDS: acidification, eutrophication, aerosol, monitoring, atmospheric transport model, deposition

DOMAIN: environmental modeling, environmental monitoring

INTRODUCTION

Atmospheric ammonia (NH₃) is of interest because of its effects on atmospheric chemistry and on seminatural ecosystems. In the atmosphere, NH₃ reacts to form ammonium (NH₄⁺) aerosol, which has a negative effect on radiative forcing, reduces visibility, and may have negative effects on human health. In addition, the formation of NH₄⁺ affects the atmospheric transport distance of SO₂ and NO_x emissions, while NH₄⁺ salts are the vector for most of the transboundary transport and deposition of atmospheric acidity[1,2]. Once deposited, NH₄⁺ releases acidity, since the nitrogen is either accumulated in organic R-NH₂ forms (1 H⁺ produced, originating from SO₂ or NO_x) or nitrified and leached as NO₃⁻ (producing 2 H⁺, including one H⁺ from NH₃ itself)[2]. In addition to the acidifying effect, the input of nitrogen from either

NH_3 or NH_4^+ (collectively NH_x) leads to eutrophication of seminatural habitats, which may result in species composition changes[3].

As with other atmospheric pollutants, NH_3 emissions have increased substantially in the 20th century[4,5], and there is currently international momentum to set policy measures to reduce these emissions. For example, under the UNECE Convention on Long-Range Transboundary Air Pollution, international ceilings of NH_3 emissions have been set for the first time with the 1999 Gothenburg Protocol. Within the context of expected ecological effects and investigation of the costs of emission abatement, it is essential to have a sound quantification of the concentrations and fluxes of NH_x in the atmosphere. Since neither the distribution of NH_3 emissions nor the distribution of sensitive habitats is uniform, it is necessary to assess the spatial distribution of NH_x concentrations and deposition. Complementary to this is the need to be able to monitor long-term trends in order to quantify the link to emission changes over periods of several years.

Monitoring the complete distribution of NH_3 concentrations at a national level would require an impracticably large (>1000) number of stations, due to the spatial variability characteristic of a primary pollutant emitted at or near ground level[6,7]. Atmospheric transport models therefore serve a complementary role, since, using spatially resolved emission estimates, national maps of predicted NH_3 concentrations may be established at, e.g., 5-km resolution[8,9]. By treating the chemical reactions with other pollutants in such models, they may also be used to assess the interactions with and distribution of NH_4^+ aerosol and wet deposition. A finding of models of this kind is that the distribution of NH_4^+ aerosol is expected to be less spatially variable, since it is formed over the course of minutes to hours as a secondary atmospheric product[10].

Most monitoring data for NH_x in the atmosphere are available for NH_4^+ in precipitation, but there is much less monitoring information available for speciated measurements of gaseous NH_3 and NH_4^+ aerosol[5]. One of the reasons for this is the need for active sampling to distinguish the gas and aerosol, which is either cumbersome or expensive. Similarly, although methods have been reported for passive sampling of NH_3 (see review[11]), these have experienced mixed success, with, in some cases, substantial and uncertain correction factors needing to be applied to data.

To address these problems in the U.K., a new low-cost denuder-filterpack system was developed tuned for long-term sampling. The method, referred to as the DELTA (DENuder for Long-Term Ammonia)[12], allows sampling with 2-weekly or monthly duration and operates robustly for concentrations in the range 0.01 to >40 $\mu\text{g m}^{-3}$. In this approach, NH_3 is collected in two acid-coated glass denuders in series, while NH_4^+ aerosol is captured on a subsequent acid-coated paper filter. In parallel, improvements in NH_3 passive sampling have been made to allow reliable implementation. First, the performance of 35-mm path-length diffusion tubes has been improved to permit monthly measurements down to a level of c.1 $\mu\text{g m}^{-3}$ [11,13]. Second, the ALPHA (Adapted Low-cost Passive High Absorption) sampler with 6-mm path length was developed[14], which is able to sample down to <0.05 $\mu\text{g m}^{-3}$ with a monthly sampling period.

In this article, we report the application of these new sampling methods in the U.K. National Ammonia Monitoring Network (NAMN)[15] and show how these compare with estimates

from the Fine Resolution AMmonia Exchange (FRAME) atmospheric dispersion model[9]. Combined with a disaggregation of NH_3 emissions data, the results are used to compare areas of the U.K. dominated by different major source sector types. Finally, the combination of the measurements and modeling is used to estimate the spatial patterns of NH_3 dry deposition across the U.K. and to consider the implications of the results for environmental policy.

METHODS

Monitoring Network Strategy

The NAMN was established to provide the best-measured NH_3 concentration field for the U.K. and at the same time to provide data for the assessment of models. Given the expense of high time-resolution monitoring[16,17], the strategy for the network was to sample at a large number of sites to assess spatial variability, using low-frequency sampling to allow long-term trends to be assessed at low cost. This strategy of high network density and low sampling frequency contrasts with the alternatives of hourly or daily monitoring[16], which would permit sampling at only a very few (2 to 4) sites with similar resources. A total of 120 potential sites were identified for consideration, and the following criteria for selection were identified[15]:

- Representative spatial coverage of the U.K.
- Representative coverage in relation to predicted FRAME NH_3 concentrations at a 5-km grid level, including key emission peak and trough areas
- Relationship of the sites to local NH_3 sources (avoiding being <150 m from point sources)
- Availability and access to a willing and helpful local contact
- Availability of mains electricity at a site (for DELTA sampling)
- Co-location of the sites in relation to other air-quality and ecosystem-monitoring activities
- Nature conservation interest of the site, particularly in relation to plant community sensitivity to nitrogen deposition and nature reserve status.

On the basis of these criteria, and following establishment of the sampling methods[11], the network was established with 70 sites in 1996, with DELTA sampling at 50 sites, diffusion tube sampling at 30 sites, and both methods implemented at 10 sites. Following a review of the network in 1998, changes were made, resulting in a total of 80 sites and introduction of NH_4^+ sampling. DELTA sites were distributed widely across the U.K. to provide regional patterns of NH_3 and NH_4^+ , while passive sampling concentrated on the assessment of mesoscale variability in source areas as a test of the NH_3 emission-dispersion modeling (Fig. 1). Three mesoscale study areas were identified: Welsh Borders/Shropshire, the Norfolk/Suffolk border, and the Yorkshire Vale. An absence of mains electricity at three active sampling sites led to the development of three solar-wind-powered DELTA systems[12]. Data are reported here up to November 2000, starting in September 1996 for NH_3 and April 1999 for NH_4^+ .



FIGURE 1. Map of sites in the U.K. National Ammonia Monitoring Network using either denuders, triplicate diffusion tubes, or both. (Site numbers are explained in the Appendix.)

Chemical analysis of aqueous extracts from each of the DELTA and passive sampling methods was performed using flow injection analysis with selective membrane diffusion of NH_3 at high pH and detection of NH_4^+ by conductivity[18].

Emission and Atmospheric Transport Modeling

The distribution of NH_3 emissions for the U.K. is modeled in a GIS methodology described by Dragosits et al.[19] For agricultural emissions, parish statistics on livestock numbers and crop areas are combined with satellite-based land-cover data to model emissions at a 1-km resolution, which are subsequently aggregated to the 5-km level. Spatial inventories have been established with this approach for 1988 and 1996.

The FRAME atmospheric chemistry and dispersion model[9,20] is run using the disaggregated NH_3 emissions together with SO_2 and NO_x emissions. FRAME is a statistical Lagrangian dispersion model, which employs straight trajectories and a multilayer dispersion scheme[21] to simulate the vertical profiles of trace gases. In addition, a land-cover-dependent dry deposition scheme is applied for NH_3 . In the model version applied here, dry deposition is limited by characteristic canopy resistances (R_c) set for different vegetation types[9]. It should be noted that the domain of FRAME covers both Britain and Ireland, although results are presented here only for the U.K., which includes Great Britain and Northern Ireland.

The spatial distribution of NH_3 emission source sectors is not uniform across the country. Hence, one of the advantages of a network with many sites is that areas with emissions dominated by different source sectors can be compared. To do this, the spa-

tial NH_3 inventory was analyzed to show areas where >45% of the emission was due to a given source. Areas of background emission ($<1 \text{ kg N ha}^{-1} \text{ year}^{-1}$) were distinguished, while pig and poultry farms were combined to allow improved visualization and comparison between nonland-based and land-based farming. The resulting map of dominant NH_3 source sectors is shown in Fig. 2. Due to disclosivity issues regarding the data for 1996, Fig. 2 shows the results for 1988, although the patterns for the 2 years are similar.

Deposition Modeling

While the FRAME model provides estimates of the dry deposition field for different vegetation types and with a resolution of 5 km, deposition estimates derived directly from the measurements would be considered more reliable. In the first instance, dry deposition fields may be estimated using the interpolated measured NH_3 concentrations and an inferential resistance model. However, this implies large assumptions in the interpolation of con-

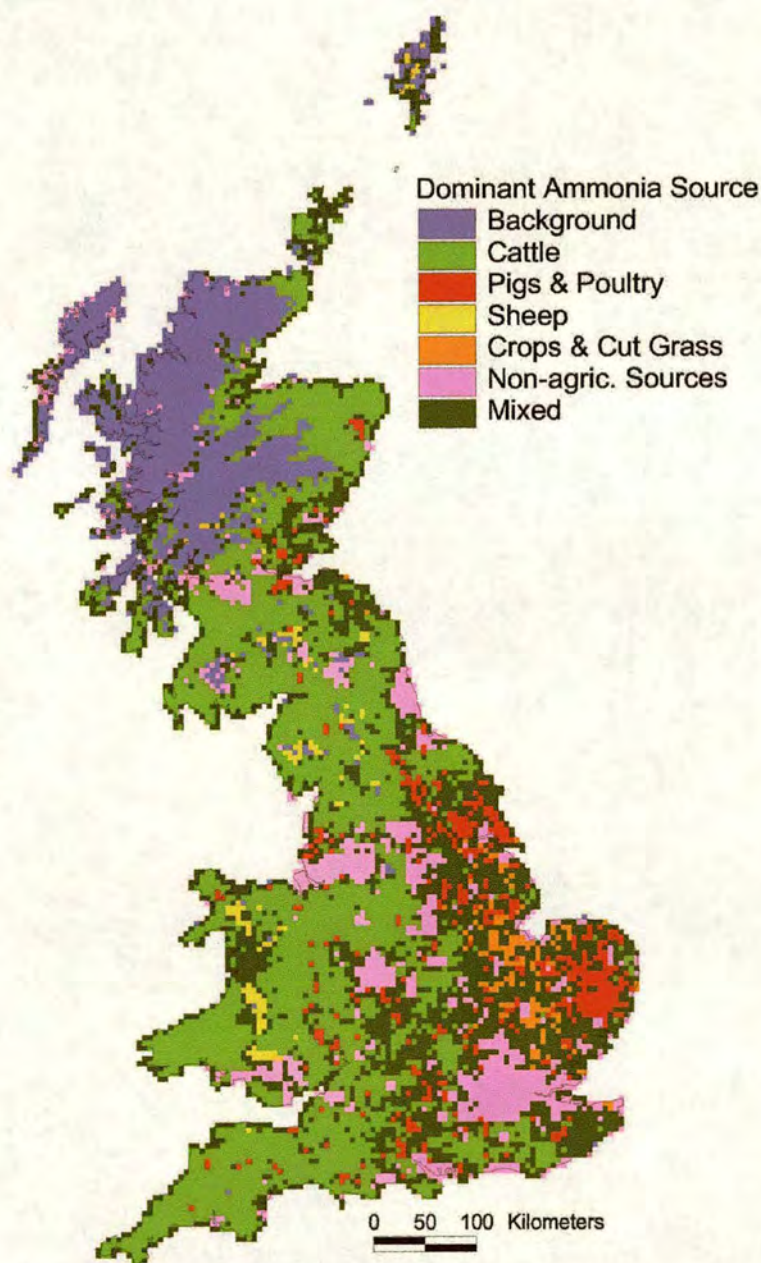


FIGURE 2. Classification of 5-km grid resolution NH_3 emissions for Great Britain (Northern Ireland not included) according to estimated dominant (>45% contribution) source sector. Background is set here at $<1 \text{ kg N ha}^{-1} \text{ year}^{-1}$.

centrations. Unless the dispersion model provides a perfect fit to the measurements, an alternative approach is therefore to calibrate the dispersion model output concentration estimates, and this method has been applied here. The regression between the mean NAMN concentrations and the FRAME-predicted NH_3 concentrations at the same sites (see Figure 5a) is applied to the FRAME estimates for each grid square in the U.K. to provide a revised NH_3 concentration field. It should be noted that this is merely a calibration of model output, rather than an internal change to the model. The revised NH_3 concentration field is then applied as input in the inferential model of Smith et al.[22]

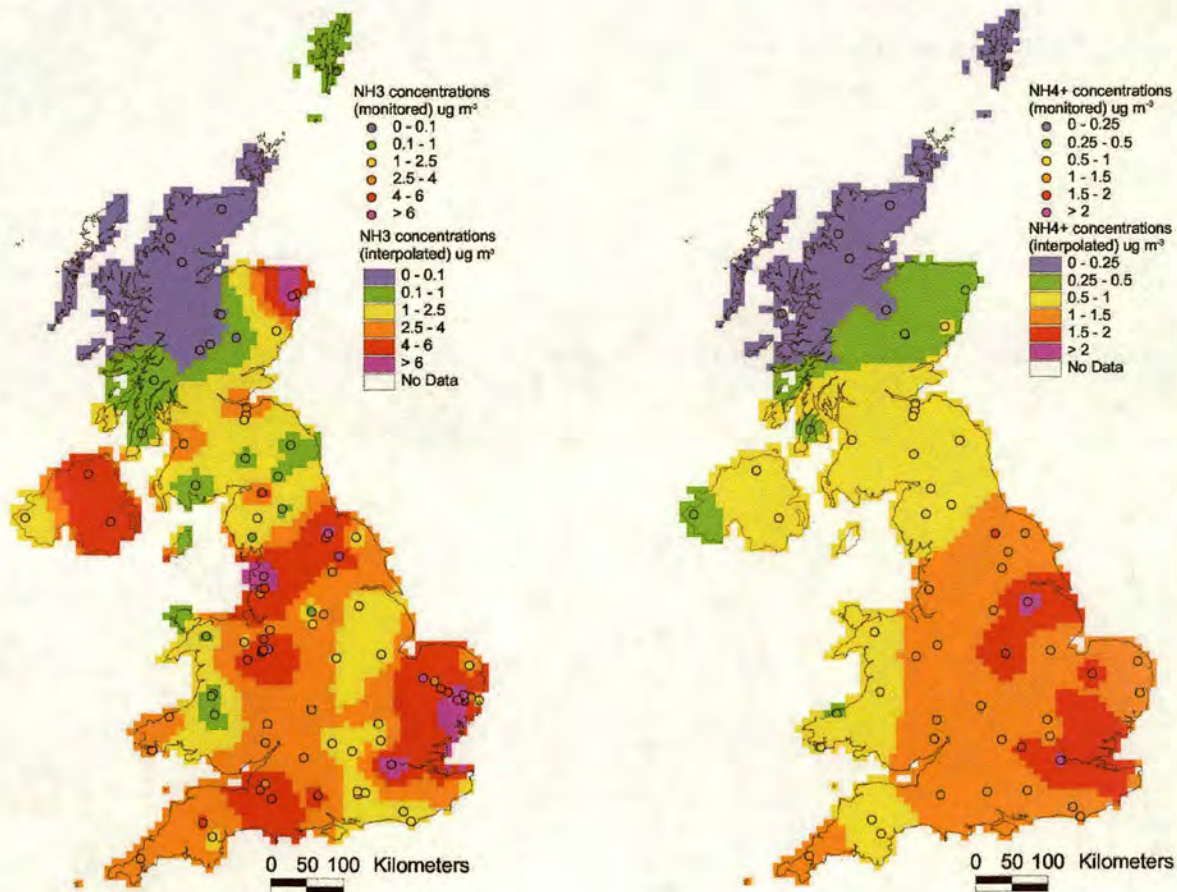
RESULTS AND DISCUSSION

Measured NH_3 and NH_4^+ Concentrations

Overall, the mean concentrations in the network for the sampling periods reported above were in the range 0.06 to $11 \mu\text{g NH}_3 \text{ m}^{-3}$ and 0.14 to $2.4 \mu\text{g NH}_4^+ \text{ m}^{-3}$ (Fig. 3). A summary of the data is given in the Appendix. In the case of NH_3 , much larger concentrations were seen in source areas, particularly in areas with intensive cattle, pig, and poultry farming, while, within only a few tens of kilometers, much smaller concentrations were found in areas with few NH_3 sources. For example, at North Wyke in De-

von (site 23), the mean concentration was $1.71 \mu\text{g m}^{-3}$, while 25 km southeast the concentration at Yarnar Wood (site 34) was $0.52 \mu\text{g m}^{-3}$. This high level of spatial variability is seen even more in the mesoscale variability sampling results. The measurements in Norfolk/Suffolk cover both intensive farming and sink areas and show mean concentrations in the range 1.23 (Dunwich Heath, site 59) to $10.7 \mu\text{g m}^{-3}$ (Bedlingfield, site 68) with gradients of up to $0.4 \mu\text{g NH}_3 \text{ m}^{-3} \text{ km}^{-1}$ over distances of 10 to 20 km. This illustrates the substantial local spatial variability of NH_3 concentrations, even when sampling in the vicinity of point sources is avoided. Even larger gradients occur adjacent to point sources[7,23], making it difficult to assess regional-level variability of NH_3 concentrations, and it was for this reason that sampling near known point sources was avoided.

By contrast, NH_4^+ aerosol showed much less local spatial variability, with a smooth interpolated field decreasing from $2.4 \mu\text{g m}^{-3}$ in central London (site 36c) and $2.2 \mu\text{g m}^{-3}$ in a high SO_2 emission area of northern England (Jenny Hurn, site 73) to $0.14 \mu\text{g m}^{-3}$ at Rum on the northwest coast of Scotland (site 47). This reflects the nature of NH_4^+ aerosol as a secondary product that is produced throughout the boundary layer. By sampling with a large number of sites, it was hypothesized that it should be possible to demonstrate this expected smooth pattern, since adjacent sites should have similar concentrations. This is shown in Fig. 3, with the local effects that occur for NH_3 , generally not being seen. For



example, the NH_4^+ concentrations at North Wyke and Yarnar Wood are 0.93 and $0.90 \mu\text{g m}^{-3}$, respectively. Such small differences between adjacent sites are typical. As a consequence of this, following November 2000, the number of aerosol sampling sites has been reduced to 30, which is sufficient to resolve the main spatial features of the U.K. NH_4^+ aerosol field.

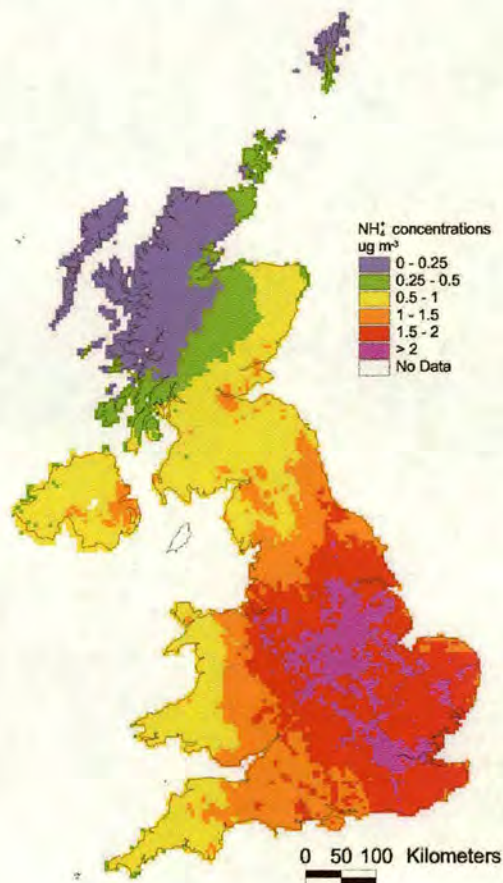
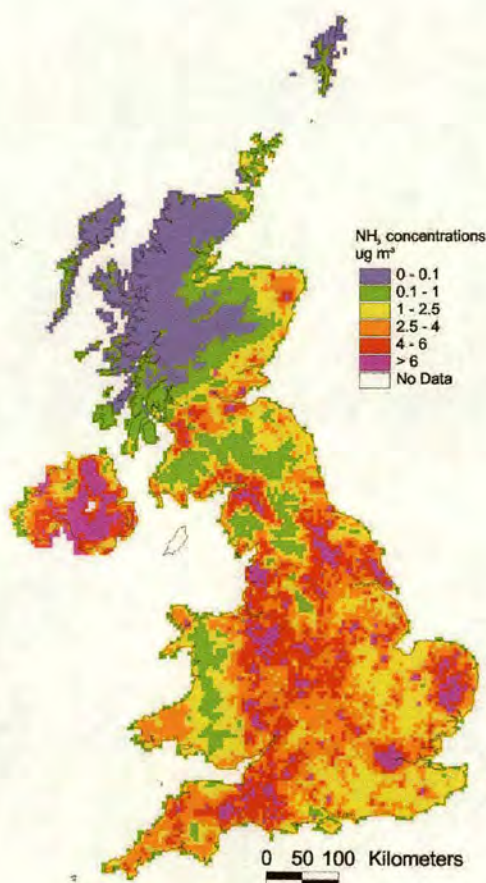
Modeled NH_3 Concentrations and Comparison with Measurements

The performance of the FRAME model in predicting average NH_3 and NH_4^+ concentrations is shown in Fig. 4. As FRAME is a multilayer model, concentrations can be reported for different heights, and the values in Fig. 4 are the average of the layer at 1 to 2 m. Consistent with NH_3 emissions arising from ground level, the modeled NH_3 concentration field shows substantial spatial variability, and this matches closely to the distribution of NH_3 emissions. The other major factors affecting NH_3 concentration are the removal rates by wet and dry deposition. Hence for a given emission rate, modeled concentrations of NH_3 are higher in eastern rather than western Britain, due to less precipitation scavenging and increased occurrence of agricultural croplands, which experience less dry deposition. The highest modeled concentrations of NH_3 occur in areas with intensive pig and poultry farming (East Anglia, Yorkshire), cattle farming (Shropshire,

Lancashire, Northern Ireland), and nonagricultural emissions (London) (cf. Fig. 2).

As with the measurements, the spatial pattern of modeled NH_4^+ aerosol is much less spatially variable than NH_3 . The highest concentrations again occur in London and in high SO_2 emission areas of northern England, while the lowest concentrations occur in northern and western parts of the U.K.

A comparison of the FRAME predictions with the network measurements for gaseous NH_3 and NH_4^+ aerosol is shown in Fig. 5. The network average for each site is compared against the model estimate for the 5-km grid square in which it occurs, and the point is classified according to the estimated dominant source sector of the square. Since the concentrations in the network and FRAME are log-normally distributed, Fig. 5 shows the comparison on a logarithmic scale. The first point to note is that the correlation for NH_4^+ aerosol ($R^2_{[\log \text{ values}]} = 0.91$; $R^2_{[\text{absolute values}]} = 0.82$) is much higher than that for NH_3 ($R^2_{[\log \text{ values}]} = 0.70$; $R^2_{[\text{absolute values}]} = 0.57$). This may be explained by the large spatial variability of NH_3 , with the result that it is difficult to monitor at the most representative location in a 5-km grid square. Many of the sites where the model overestimates the measurements are, in fact, nature reserve or forest sites. The reason for the overestimation may therefore be due to subgrid variability not addressed by the model, as the monitoring sites in these sink areas would be more than the average distance from sources in the same 5-km grid square. Conversely, some of the outliers, where the



measurements are larger than the model, show some indication of being affected by nearby sources. For example, at Glenshee (site 7, emissions dominated by cattle) in the Scottish highlands, the measurement estimate was $2.66 \mu\text{g m}^{-3}$, while FRAME estimated $0.28 \mu\text{g m}^{-3}$. The 5-km grid square in question consists of a narrow agricultural valley surrounded by seminatural hill moorland. It was initially hypothesized that the higher value at this site was due to site 7 being located at the valley bottom. To investigate such issues of site representativity requires a detailed assessment of local spatial variability. In this case, the 1-km NH_3 emission inventory was analyzed with a local dispersion model, combined with ALPHA sampling at 12 locations across the 5-km grid square [24]. This analysis showed that site 7 overestimated the grid average partly due to its location, plus the existence of unexpected local emissions from animal processing by a gamekeeper. In contrast, analysis of the model and measurements showed that the most representative measured concentration was $0.3 \mu\text{g m}^{-3}$, which was very close to the FRAME estimate. Such local assessment studies are obviously not feasible at more than a few locations. Hence, a robust country scale assessment benefits greatly from analysis of many sites, as in Fig. 5.

Fig. 5 shows that, overall, FRAME provides larger NH_3 concentrations than the measurements. There are a number of possible reasons for this, including uncertainties in emissions, vertical diffusion scheme of the model, atmospheric conversion and removal processes, and the possibility that stations are more than the average distance from NH_3 sources within each grid square. Most of these points would be expected to be equally possible for all of the sites. However, in the case of emissions, it is possible that the emission factors for different source sector activities are differentially biased, and this will be reflected in the estimates for the different source sector dominated areas. Taking the regression between the measurements and model as the consequence of all the uncertainties, it is therefore of interest if sites

dominated by different source sectors fall above or below the line. In the case of sheep-dominated areas, the measurements are larger than the average for all the monitoring sites. Conversely, at all of the nonagricultural-dominated sites, the measurements are less than the average. At most of the cattle-dominated sites, the measurements are also less than the average, while for the mixed and pig plus poultry classes, the sites are distributed evenly. These findings suggest that sheep emissions may have been underestimated and nonagricultural sources and cattle overestimated relative to emissions from pig and poultry. The least certain of these comparisons are the nonagricultural sources, which are much less accurately mapped and include a wide diversity of sources that are not represented as dominant sources here. In addition to these source sector differences, there is also a systematic deviation for the background sites, with three quarters of the sites having larger concentrations than the average relationship. This may partly be due to emissions from wild animals and sheep in these background areas, but is most likely due to the existence of a “compensation point” concentration for NH_3 with seminatural vegetation [2,5,6]. This is not represented in the version of FRAME applied here, but is a subject of ongoing model development.

While the correlation for NH_4^+ aerosol is much closer than for NH_3 , it is still substantially above the 1:1 line. This is most likely due to insufficient wet scavenging of NH_4^+ aerosol, which is consistent with an underestimation of wet NH_x deposition by FRAME. Again, this is a subject of ongoing model development, where preliminary tests have shown that increasing the scavenging rate gives better agreement with the measurements for both NH_4^+ aerosol and NH_x wet deposition. It may be noted that there are no discernible differences for NH_4^+ aerosol between the sites dominated by different sectors. This is not surprising, since the NH_4^+ concentration responds to NH_3 emissions and atmospheric chemistry at a regional level.

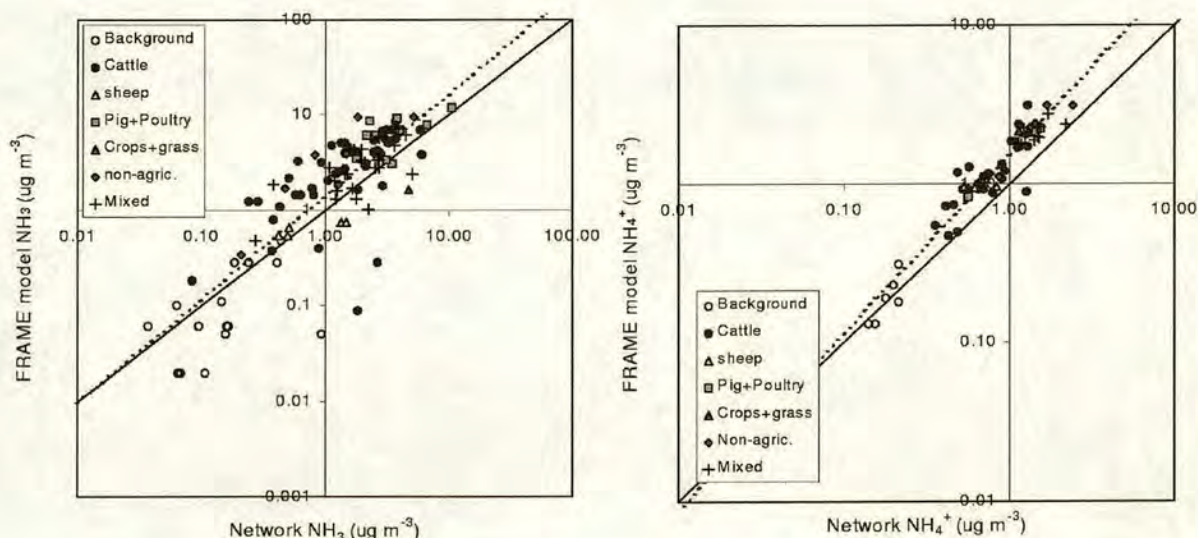


FIGURE 5. Comparison of measured NH_3 and NH_4^+ concentrations in the U.K. with estimates of FRAME classified by estimated dominant NH_3 source sector for the 5-km grids in which sampling sites occur. The regressions are: NH_3 , $\log(\text{FRAME}) = 1.0769 \log(\text{NAMN}) + 0.1379$; NH_4^+ , $\log(\text{FRAME}) = 1.1179 \log(\text{NAMN}) +$

Estimation of Dry Deposition

The FRAME model described here incorporates a simplified treatment of dry deposition according to land cover type. To provide more accurate deposition estimates, a more detailed inferential model is applied, which includes treatment of the ammonia compensation point for agricultural vegetation[22]. The regression between the NH₃ measurements and FRAME is used to scale the FRAME estimates to the network, and this is applied as input to the inferential model. The outputs of this model are maps of NH₃ dry deposition to five major land-cover types: forest, moorland (and low seminatural vegetation), agricultural grassland, arable, and urban. To estimate the budget of U.K. NH₃ dry deposition, these maps are combined according to percentage of land-cover occurrence in each 5-km grid-square, which gives a map of grid average NH₃ dry deposition. Fig. 6 shows as an example the comparison of the average grid square NH₃ dry deposition with that received by moorland/low seminatural vegetation.

Dry deposition NH₃ inputs on a grid-square basis are mostly in the range 0 to 10 kg N ha⁻¹ year⁻¹, which is similar to inputs as NH₄⁺ in wet deposition. The largest regional dry deposition is

estimated for Wales, where relatively large NH₃ emissions combine with a large percentage of land cover of moorland and seminatural vegetation. By contrast to the rather small values of average dry deposition, the NH₃ dry deposition received by moorland and low seminatural vegetation is much larger, in the range 0 to 40 kg N ha⁻¹ year⁻¹, and the distribution of this matches more closely to the pattern of estimated NH₃ concentrations. It should be noted that Fig. 6 shows the deposition that would be received by low seminatural vegetation if present, which explains why values are provided for the whole of the country.

The distinction between maps of dry deposition to grid squares and to receptors is an important one. While the former are useful to integrate total dry deposition for the country, the latter are what should be applied in summing deposition inputs for comparison with critical loads. The application of the grid average dry deposition field would give a substantial underestimation of critical load exceedance for seminatural vegetation because of the slower rates of NH₃ dry deposition to agricultural land. In many locations, the receptor-specific NH_x dry deposition estimates exceed critical loads for nitrogen deposition and acidification, even without counting other atmospheric inputs. It

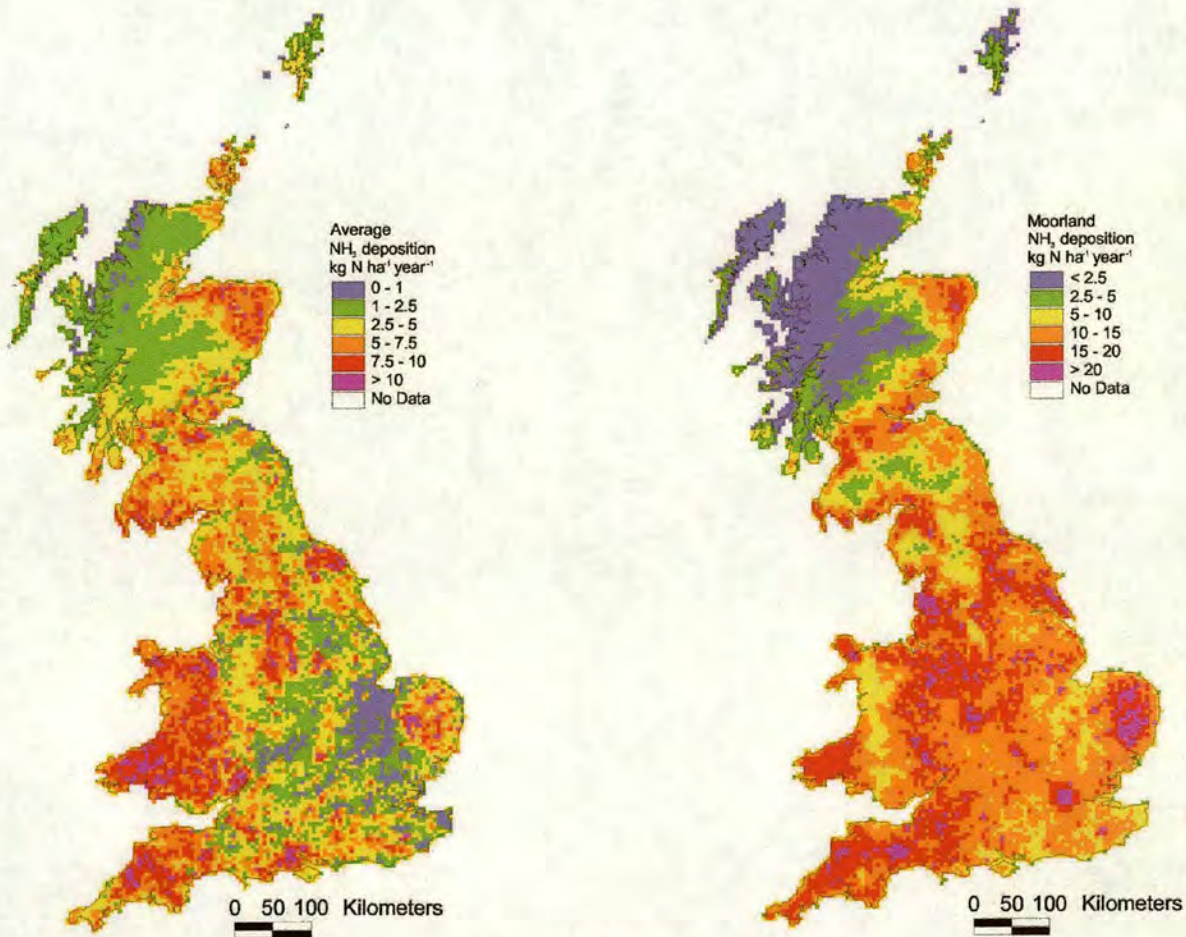


FIGURE 6. Estimated dry deposition of ammonia in Great Britain: a) average dry deposition to grid squares, b) dry deposition received by moorland/low seminatural vegetation where present.

is therefore clear that policies to reduce the effects of acidification and eutrophication must include measures to abate NH_3 emissions and deposition.

CONCLUSIONS

A combination of a monitoring network and modeling capability has been established to quantify the spatial patterns of gaseous NH_3 and NH_4^+ aerosol concentrations and deposition in the U.K. While monitoring of NH_4^+ aerosol representatively is possible with only a few tens of sites, the high spatial variability of NH_3 would require thousands of monitoring stations to characterize spatial patterns. The variability of NH_3 is related to its nature as a primary pollutant emitted in the rural landscape, with the result that meso- and local-scale sampling shows potentially as much variability as at the national scale. Precise site representativity may be investigated using sampling with many sites at a sub-5-km grid level, but is only feasible for a few locations. The U.K. network has therefore been established with many NH_3 sampling sites in order to build up a representative picture of NH_3 at the U.K. scale. While the sampling methods have been found to give reliable measurements for the full range of concentrations encountered, the use of over 80 sites proves to be adequate to reveal the major spatial differences in NH_3 across the U.K.. This large number of sites has the advantage that sites in areas dominated by different NH_3 source sectors can also be compared. The analysis here shows that NH_3 emissions from sheep may have been underestimated relative to those from cattle, pig, and poultry.

Combining the measurements with estimates from an atmospheric transport model provides the facility to estimate dry deposition inputs at a 5-km grid resolution. This level of detail is necessary since assessment of critical loads exceedance is made at this or even finer (1-km) scales. While maps of interpolated measured NH_3 concentrations are useful to envisage the main patterns, they are too uncertain to apply in mapping deposition at a 5-km resolution.

The model of NH_3 dry deposition makes the distinction between different land-cover types and simulates the larger inputs characteristic of seminatural compared with agricultural vegetation. This is important, since the receptor-specific estimates for seminatural land may substantially exceed critical loads, even in the absence of other sources of nitrogen deposition. The consequence is that policies to reduce the effects of acidification and eutrophication must include approaches to reduce NH_3 emissions and dry deposition. The U.K. National Ammonia Monitoring Network has been established to address spatial patterns with low-frequency (monthly) sampling. It is therefore well-placed to assess the long-term changes in NH_3 and NH_4^+ following the implementation of emission control policies.

ACKNOWLEDGMENTS

We gratefully acknowledge funding of the National Ammonia Monitoring Network and of the project "Acid Deposition Processes" by the U.K. Department of Environment, Food and Rural Affairs, together with underpinning funding from the Natural

Environment Research Council. We are grateful to Neil Cape and Roger Phillips for their helpful comments on earlier drafts of this article. The Ammonia Network would not be possible without the dedicated input of over 50 local site operators, to whom we express our thanks.

REFERENCES

1. Binkley, D. and Richter, D. (1987) Nutrient cycles and H^+ budgets of forest ecosystems. *Adv. Ecol. Res.* **16**, 1–51.
2. Sutton, M.A., Pitcairn, C.E.R., and Fowler, D. (1993) The exchange of ammonia between the atmosphere and plant communities. *Adv. Ecol. Res.* **24**, 301–393.
3. Fangmeier, A., Hadwiger-Fangmeier, A., van der Eerden, L., and Jaeger, H.J. (1994) Effects of atmospheric ammonia on vegetation—a review. *Environ. Pollut.* **86**, 43–82.
4. Asman, W.A.H., Drukker, B., and Janssen, A.J. (1988) Modelled historical concentrations and depositions of ammonia and ammonium in Europe. *Atmos. Environ.* **22**, 725–735.
5. Sutton, M.A., Asman, W.A.H., Ellerman, T., van Jaarsveld, J.A., Acker, K., Aneja, V., Duyzer, J.H., Horvath, L., Paramonov, S., Mitosinkova, M., Tang, Y.S., Achermann, B., Gauger, T., Bartnicki, J., Neftel, A., and Erisman, J.W. (2001) Establishing the link between ammonia emission control and measurements of reduced nitrogen concentrations and deposition. In *UNECE Ammonia Expert Group (Berne 18–20 Sept. 2000) Proceedings*. Menzi, H. and Achermann, B., Eds. SAEFL, Bern. pp. 57–84.
6. Asman, W.A.H., Sutton, M.A., and Schjoerring, J.K. (1998) Ammonia: emission, atmospheric transport and deposition. *New Phytol.* **139**, 27–48.
7. Duyzer, J.H., Nijenhuis, B., and Westrate, H. (2001) Monitoring and modelling of ammonia concentrations and deposition in agricultural areas of the Netherlands. *Water Air Soil Pollut.: Focus 1*, 131–144.
8. Asman, W.A.H. (1992) A detailed ammonia emission inventory for Denmark and some deposition calculations. In *Ammonia Emissions in Europe: Emission Coefficients and Abatement Costs*. Klaassen, G., Ed. IIASA, Laxenburg, Austria. pp. 159–168.
9. Singles, R.J., Sutton, M.A., and Weston, K.J. (1998) A multi-layer model to describe the atmospheric transport and deposition of ammonia in Great Britain. *Atmos. Environ. (Ammonia Special Issue)* **32**(3), 393–399.
10. Erisman, J.W., Vermetten, A.W.M., Asman, W.A.H., Waijers-Ijpelaan, A., and Slanina, J. (1988) Vertical distribution of gases and aerosols: the behaviour of ammonia and related components in the lower atmosphere. *Atmos. Environ.* **22**, 1153–1160.
11. Sutton, M.A., Miners, B., Tang, Y.S., Milford, C., Wyers, G.P., Duyzer, J.H., and Fowler, D. (2001) Comparison of low cost measurement techniques for long-term monitoring of atmospheric ammonia. *J. Environ. Monit.* **3**(5), 446–453.
12. Sutton, M.A., Tang, Y.S., Miners, B., and Fowler, D. (2001) A new diffusion denuder system for long-term, regional monitoring of atmospheric ammonia and ammonium. *Water Air Soil Pollut.: Focus 1*, 145–156.
13. Thijssen, T.R., Wyers, G.P., Duyzer, J.H., Verhagen, H.L.M., Wayers, A., and Möls, J.J. (1996) Measurement of ammonia with diffusion tube samplers. *Atmos. Environ. (Ammonia Special Issue)* **32**(3), 333–337.
14. Tang, Y.S., Cape, J.N., and Sutton, M.A. (2001) Development and types of passive samplers for NH_3 and NO_x . In *Proceedings of the International Symposium on Passive Sampling of Gaseous Air Pollutants in Ecological Effects Research*. *TheScientificWorld*, **1**, 513–529.

15. Sutton, M.A., Tang, Y.S., Miners, B.P., Coyle, M., Smith, R.I., and Fowler, D. (1998) Spatial and temporal patterns of ammonia concentration in the UK. Results of the National Ammonia Monitoring Network. Final Report to the DETR. Institute of Terrestrial Ecology, Edinburgh. 79 pp.
16. Buijsman, E., Aben, J.M.M., Van Elzakker, B.G., and Mennen, M.G. (1998) An automatic atmospheric ammonia network in the Netherlands: set-up and results. *Atmos. Environ. (Ammonia Special Issue)* **32**(3), 317–324.
17. Burkhardt, J., Sutton, M.A., Milford, C., Storeton-West, R.L., and Fowler, D. (1998) Ammonia concentrations at a site in S. Scotland from continuous measurements over 2 years. *Atmos. Environ. (Ammonia Special Issue)* **32**(3), 325–331.
18. Wyers, G.P., Otjes, R.P., and Slanina, J. (1993) A continuous flow denuder for the measurement of ambient concentrations and surface fluxes of ammonia. *Atmos. Environ.* **27A**, 2085–2090.
19. Dragosits, U., Sutton, M.A., Place, C.J., and Bayley, A. (1998) Modelling the spatial distribution of ammonia emissions in the UK. *Environ. Pollut. (Nitrogen Conference Special Issue)* **102**, S1, 195–203.
20. Fournier, N., Pais, V.A., Sutton, M.A., Weston, K.J., Dragosits, U., Tang, Y.S., and Aherne, J. (2002) Parallelisation and application of a multi-layer atmospheric transport model to quantify dispersion and deposition of ammonia over the British Isles. *Environ. Pollut.*, **116**, 95–107.
21. ApSimon, H.M., Barker, B.M., and Kayin, S. (1994) Modelling studies of the atmospheric release and transport of ammonia—applications of the TERN model to an EMEP site in eastern England in anticyclonic episodes. *Atmos. Environ.* **28**, 665–678.
22. Smith, R.I., Fowler, D., Sutton, M.A., Flechard, C., and Coyle, M. (2000) Regional estimation of pollutant gas deposition in the UK: model description, sensitivity analyses and outputs. *Atmos. Environ.* **34**, 3757–3777.
23. Dragosits, U., Theobald, M.R., Place, C.J., Lord, E., Webb, J., Hill, J., ApSimon, H.M., and Sutton, M.A. (2002) Ammonia, emission, deposition and impact assessment at a field scale: a case study of sub-grid spatial variability. *Environ. Pollut.*, **116**, 147–158.
24. Tang, Y.S., Dragosits, U., Theobald, M.R., Fowler, D., and Sutton, M.A. (2001) Sub-grid variability in ammonia concentrations in an upland landscape. In Air Surface Exchange of Gases and Particles. Edinburgh 2000. Poster Proceedings. CEH Edinburgh. pp. 48–57.

This article should be referenced as follows:

Sutton, M.A., Tang, Y.S., Dragosits, U., Fournier, N., Dore, A.J., Smith, R.I., Weston, K.J., and Fowler, D. (2001) A spatial analysis of atmospheric ammonia and ammonium in the U.K. In Optimizing Nitrogen Management in Food and Energy Production and Environmental Protection: Proceedings of the 2nd International Nitrogen Conference on Science and Policy. *TheScientificWorld* **1**(S2), 275–286.

Received:	August	8, 2001
Revised:	October	10, 2001
Accepted:	October	15, 2001
Published:	November	28, 2001

APPENDIX
Summary of Data from the U.K. National Ammonia
Monitoring Network (Netw) and Comparison with the FRAME Model

Site No	Site Name	National Grid Ref.	Netw. NH ₃	FRAME NH ₃	Netw. NH ₄ ⁺	FRAME NH ₄ ⁺	DS
1	Bush OTC	nt245635	2.54	2.77	0.71	1.02	5
2	Bush Cabin	nt247638	1.08	2.77			5
3	Inverpolly	nc187088	0.07	0.02	0.16	0.13	0
4	Penallt	so523095	1.45	2.69	1.15	1.70	1
5	Priddy	st525526	1.47	3.92	0.07	1.62	1
6	Holme Lacy	so554357	2.14	2.91	1.29	1.70	1
7	Glen Shee	no117693	2.66	0.28	0.36	0.54	1
7b	Gulabin Lodge	no110701	1.84	0.09	0.43	0.47	1
8	Stackpole	sr982947	2.26	1.04			6
8b	Orielton	sr954992	1.30	2.56	0.74	1.15	1
9	Brown Moss	sj559396	5.94	6.91			1
9b	Brown Moss 2	sj563390	3.50	6.91	1.15	2.36	1
10	Bure Marshes	tg334161	1.21	2.33	1.24	1.98	6
11	Mere Sands Wd.	sd447157	1.98	3.33	1.40	1.89	6
12	Halladale	nc902488	0.94	0.05	0.21	0.18	0
13	Aston Rowant.	su727979	1.69	1.7	1.54	2.26	6
14	Ellon Ythan	nj945304	1.53	4.64	0.46	0.74	1
15	Llyncllys Corn.	sj273237	1.34	5.01	1.07	1.85	1
16	Northallerton	se360930	3.66	4.75	1.51	1.94	6
17	Easingwold	se540675	4.52	6.06	1.22	2.22	6

APPENDIX (CONTINUED)
Summary of Data from the U.K. National Ammonia
Monitoring Network (Netw) and Comparison with the FRAME Model

Site No	Site Name	National Grid Ref.	Netw. NH ₃	FRAME NH ₃	Netw. NH ₄ ⁺	FRAME NH ₄ ⁺	DS
19	Shetland	hu500400	0.15	0.11	0.20	0.23	0
20	Drayton	sp165549	3.46	3.09	1.45	2.12	2
21	Glensaugh	no664799	0.29	1.24	0.52	0.92	1
22	Moor House	ny751334	0.24	0.28	0.64	0.92	0
23	North Wyke	sx659983	1.71	4.15	0.93	1.20	1
24	Rothamsted	tl123129	1.29	1.84	1.34	2.26	5
25	Sourhope	nt867218	0.51	0.55	0.53	0.95	3
26	Wytham Woods	sp452083	1.21	2.03	1.21	2.24	6
27	Alice Holt	su809379	1.24	1.58	1.14	1.81	6
28	Porton Down	su253365	1.72	4.34	1.18	1.78	6
29	Llydaw	sh695572	1.36	0.74	0.62	0.94	3
30	Strathvaich Dm.	nh348750	0.11	0.02	0.18	0.19	0
31	Eskdalemuir	nt235030	0.37	0.37	0.56	0.92	1
32	High Muffles	se776939	1.84	1.64	1.01	1.83	1
33	Stoke Ferry	tl700988	2.19	6.05	1.56	2.21	2
34	Yarner Wood	sx789788	0.52	2.15	0.90	1.08	1
35	Lullington Hth.	tq538016	0.64	1.44	1.29	3.10	1
36b	London, Vict.	tq291790	1.85	9.5	1.69	3.10	5
36c	London, Crom.	tq266791	5.25	9.5	2.42	3.10	5
37	5 Acres	sw794486	0.93	3.16	1.27	0.89	1
38	Sheffield	sk332870	0.84	3.8	1.44	2.39	5
39	Silsoe	tl088356	1.51	2.42	1.49	2.29	6
40	Sutton Bonntrn.	sk505268	5.15	2.41	1.72	2.75	6
41	Lagganlia	nh856037	0.16	0.06	0.21	0.31	0
42	Castle Cary	st609319	3.69	5.53	1.12	1.67	1
43	Tadcaster	se452455	2.10	3.15	1.22	2.21	6
44	Hillsborough	ij243577	3.22	5.07	0.64	1.00	1
45	Lough Navar	ih065545	0.43	1.08	0.41	0.72	1
46	Sibton	tm363722	2.67	3.4	1.49	2.00	6
47	Rum	nm408992	0.16	0.05	0.14	0.13	0
48	Wem Moss	sj473343	2.91	6.77			1
49	Frodsam	sj525795	3.17	3.4			2
50	Swettenham Mds.	sj804674	3.52	5.4			1
51	Wybunbury Moss	sj698502	3.06	5.59			1
52a	Fenn's Moss 1	sj490365	2.48	4.03			1
52b	Fenn's Moss 2	sj478368	1.85	4.03			1
52c	Fenn's Moss 3	sj498378	1.60	4.03			1
53	Little Budworth	sj584658	2.71	2.82			6
54	Bickerton Hill	sj498527	2.67	4.26			1
55	Ruabon	sj225489	0.58	1.44			5
56	Wardlow Hay Cop	sk177737	1.22	2.42			1
57	Stanford	tl858948	1.81	3.47			2
58	Redgrave+Lophm.	tm050797	2.76	5.71			6
59	Dunwich Heath	tm470680	1.23	1.32			6
60	Edinburgh	nt253734	1.49	3.97	0.87	1.11	5

APPENDIX (Continued)
Summary of Data from the U.K. National Ammonia
Monitoring Network (Netw) and Comparison with the FRAME Model

Site No	Site Name	National Grid Ref.	Netw. NH ₃	FRAME NH ₃	Netw. NH ₄ ⁺	FRAME NH ₄ ⁺	DS
61	Much Hoole	sd473231	3.87	9.31			2
62	Midge Hall	sd508231	2.72	5.98			6
63	Cardigan	sn185453	0.62	3.32	0.48	1.17	1
64	Pwllpeiran	sn798771	0.51	0.66			3
65	Allt a Mharcaidh	nh895024	0.09	0.06			0
66	Dennington	tm276669	4.05	7.05			2
67	Fressingfield	tm261759	6.63	7.87			2
68	Bedlingfield	tm173684	10.66	11.99			2
70	Cwmystwyth	sn771742	1.48	0.74	0.84	0.96	3
71	Myerscough	sd498399	3.73	8.27			1
72	Cardoun Burn	nx546658	0.19	0.28			0
73	Jenny Hurn	sk816986	1.80	1.31	2.23	2.34	6
74	Carlisle	ny468554	3.34	5.11	0.90	1.32	1
75	Westhay Moor	st455440	1.15	4.81			1
76	Pointon	tf128313	4.77	1.64	1.13	2.14	4
77	Carradale	nr798378	0.89	0.40108	0.48	0.50	1
78	Auchincruive	ns379234	6.03	3.79	0.69	0.93	1
78b	Auchincruive 2	ns384229	2.87	3.79			1
79	Coleraine	iC884211	2.49	5.42	0.78	0.87	1
80	Lyulphs Tower	ny403202	0.80	1.69	0.57	1.28	1
81	Pitmedden	nj883278	2.32	8.59	0.56	0.82	2
82	Brompton	se389988	3.92	7.06			6
83	Barcombe Mills	tq438149	1.05	2.02	1.34	2.11	1
84	Thursley Common	su910404	0.39	1.86			6
85	Savarnake	su055888	2.90	1.81			1
86	Lakes	sd337941	0.39	0.8			1
87	Thetford	tl944841	1.98	4.38			6
88	Sherwood	sk163905	0.45	0.49			0
89	Rannoch	nn603533	0.04	0.06			0
90	Coalburn	ny693782	0.21	0.34			5
91	Tummel	nn744611	0.06	0.1			5
92	Loch Awe	nm966115	0.08	0.18			1
93	Llynn Brianne	sn816484	0.27	0.48			6
94	Alice Holt (2)	su805427	0.48	1.7			5

Note: At some sites, more than one independent measurement system is applied (not shown here). Values in $\mu\text{g m}^{-3}$. DS = dominant source sector: 0, background; 1, cattle; 2, pig + poultry; 3, sheep; 4, crops + grass; 5, nonagricultural; 6, mixed.